Microwave curing of concrete repair

Shahriar Abubakri

A thesis submitted in partial fulfilment of the requirements of
Sheffield Hallam University
for the degree of Doctor of Philosophy

December 2018

"The greatest enemy of knowledge is not ignorance, it is the illusion of knowledge."

Stephen Hawking

To the memory of my father

and

To my mother

Declaration

I hereby declare that no portion of the work referred to this thesis has been submitted anywhere for any award apart from Doctor of Philosophy at Sheffield Hallam University. All sources of information in the thesis have been acknowledged.

Shahriar Abubakri December 2018

Abstract

Large number of concrete structures have approached or are approaching a state where repairs are necessary. During repair of concrete, curing is an important criteria and widely recognised to assure adequate performance of cement based repair materials. Curing is the process for promoting hydration of cement that leads to the strength development. Strength development of cement based repair materials is slow and often takes several days to develop fully. In addition, fresh concrete exposed to cold weather experience significant loss of strength, permeability and durability in long term due to frost damage. Thermal curing is an effective way to develop higher early age strength of cement based repair materials and it can be used to accelerate construction works, reopen roads soon after repair and maintain construction work in cold weather. However, most of the thermal methods are inefficient and rarely provide a controlled temperature increase to concrete and often are not suitable for site.

This project investigates the microwave curing of concrete repair as an effective method of thermal curing in order to accelerate curing. Initially, laboratory investigations are carried out to determine the important parameters of microwave and cement based repair materials such as power of microwave, duration of heating, temperature, type and volume of repair materials, and then, their relationships are determined empirically. These relationships were derived from laboratory investigations and led to the development of a Fixed Time Power Regulating (FTPR) algorithm which can be used for the automatic control of any microwave system to enable it to deal with endless variation of repair material formulations encountered on construction sites.

This research programme also deals with the effect of microwave curing on the properties of different commercial repair materials. This includes the effect of microwave curing on the hydration characteristics, porosity and pore structure, the bond between substrate and repair patch, strength, shrinkage and finally bond of steel rebar in patch repairs. Results show that microwave curing accelerates the heat of hydration and brings forward the peak time. It also increases the porosity of the bulk matrix and interfacial Transition Zone (ITZ) relative to normal curing. In addition, microwave curing prevents bond loss of concrete substrate with repair mortar applied at a sub-zero temperature (-5 °C) while microwave curing reduces the bond strength of plain (undeformed) steel bar embedded in repair materials by 10 to 40 %. Furthermore,

results also show that microwave curing reduces the shrinkage by 7 to 32% relative to normal curing.

Finally, this thesis also describes a pre-industrial prototype microwave system which has been developed by Fraunhofer IGB (Germany) based on the recommendations of the research. It also includes the results from field trials to validate the prototype and design equations by testing slab elements of four commercial repair materials and CEM II concrete. Slabs of dimensions 1 m x 1 m and depth up to 80 mm were cast and microwave cured to a temperature ranged between 41.9 to 76.5 °C for a predetermined time.

The results of the research show that microwave curing is an effective method of thermal curing for concrete repair. Relationships between the key parameters relating to the repair material properties and microwave energy parameters have been derived to enable design of microwave curing system.

Keywords: Concrete repair, microwave curing, heat of hydration, accelerated curing, temperature profile, porosity, bond strength, shrinkage, microwave prototype

Acknowledgements

First and foremost, I would like to express my sincere gratitude to my supervisor Professor Pal Mangat for his guidance and continuous support of this research, for his patience, motivation and immense knowledge.

I would like to express my gratitude to Dr Fin O'Flaherty, Dr Vincenzo Starinieri, Professor Paul Lambert and Dr Olalekan Ojedokun of the Centre for Infrastructure Management (CIM), Sheffield Hallam University for their guidance and support throughout this research project.

I would like to express my gratitude to Dr Konstantinos Grigoriadis, also co-author of several papers, for his advice and support during his time at Sheffield Hallam University.

I also express my appreciation for the valuable assistance given by the technical staff of the Construction Materials Laboratory.

I would like to acknowledge gratefully the funding provided by the European Union's Seventh Framework Programme for research on the MCure project to conduct research and technological development of microwave curing concrete repair. I express my gratitude also to the Materials and Engineering Research Institute (MERI), Sheffield Hallam University, for additional financial support during the completion of this thesis.

Last, but not least, I would like to thank my family. My wife Neelofar has been extremely supportive throughout this entire process and has made countless sacrifices that gave me the courage and determination to complete the thesis.

Shahriar Abubakri December 2018

Publications:

Part of the work presented in this thesis published in journal papers and conference proceedings. In addition, another paper is in preparation to be submitted in the near future. The publications are listed below:

Journal Publications

1. P.S. Mangat, K. Grigoriadis and S. Abubakri, Microwave Curing Parameters of In-Situ Concrete Repairs, Construction and Building Materials, 2016, 112, 856-866
2. K. Grigoriadis, P.S. Mangat and S. Abubakri, Bond Between Microwave Cured Repair and Concrete Substrate, Materials and Structures, 2017**,** 50 **(**125), 1-14
3. P.S. Mangat, S. Abubakri and K. Grigoriadis, Bond of Steel Reinforcement with Microwave Cured Concrete Repair Mortars, Materials and Structures, 2017, 50 (249) 1-16

Conference proceedings

1. P.S. Mangat, K. Grigoriadis and S. Abubakri, Microwave Curing of Concrete Bridge Repairs. In: Proceedings of 16th European Bridge Conference, Edinburgh, UK, 23-25 June, 2015.
2. P.S. Mangat, K. Grigoriadis and S. Abubakri, Temperature Development in Microwave Cured Repair Materials, In Proceedings of the 6th International Conference on Concrete Repair, Thessaloniki, Greece, 20-22 June, 2016. CRC Press, 273-279
3. P.S. Mangat, K. Grigoriadis, S. Abubakri, A. Javaid and C. Zhao, Microwave Curing System for In-situ Concrete Repair, In Proceedings of the 6th International Conference on Concrete Repair, Thessaloniki, Greece, 20-22 June, 2016. CRC Press, 267-272

In Preparation

1. P.S. Mangat, S. Abubakri, A. Javaid, C. Zhao and K. Grigoriadis, Field Trials with Microwave Prototype to Cure Repair Concrete, 2019 (In preparation)

Table of Contents

List of Figures

List of Tables

Abbreviations

ACI	American Concrete Institute
ASTM	American Society for Testing and Materials
ITZ	Interfacial transition zone
MCHW	Manual of Contract Documents for Highways Works
MIP	Mercury Intrusion Porosimetry
NaCl	Sodium Chloride
OPC	Ordinary Portland Cement
RC	Reinforced Concrete
w/p	water to powder ratio
w/c	water to cement ratio

Notations

a	Degree of hydration
c	Specific heat capacity of specimen ($Jkg^{-1}C^{-1}$)
d	Length of the bond steel bar (m)
D	Diameter of pores (nm)
E	Electric field (V/m)
ε	Complex permittivity (f/m)
ε_0	Permittivity of free space (f/m)
ε'	Dielectric constant (f/m)
ε''	Loss factor (f/m)
ε'_r	Relative dielectric constant
ε''_r	Relative loss factor
F	Maximum failure load (N)
f	Microwave frequency (Hz)
f_b	Bond strength (MPa)
f_c	Compressive strength (MPa)
k	Volumetric coupling coefficient
m	Mass (kg)
m_w	Mass of water (g)
m_c	Mass of container (g)
μ_0	Permeability of free space (H/m)
μ	Permeability (H/m)
σ	Electric conductivity (S/m)
ρ	Density (kg/m^3)
P	Microwave power absorbed per unit volume (W/m^3)
P_a	Microwave power absorbed in a load (W)
P_{max}	Output power of microwave (W)

Q	Heat (Joules)
Q_t	Cumulated heat of hydration at time t
Q_{total}	Cumulated heat of hydration at complete hydration
q	Heat production rate
r	Radius of steel bar (m)
t	Time (s)
T	Temperature (°C)
T_1	Initial temperature (°C)
T_a	Ambient temperature (°C)
T_f	Temperature at the end of microwave curing (°C)
T_m	Permissible temperature at the end of microwave curing (°C)
T_h	peak heat of hydration temperature (°C)
V	Volume of the mix (m^3)
V_s	Volume of solid matrix
υ_p	Loading rate (N/s)
γ	Surface tension of mercury (Nm^{-1})
ω	Angular frequency (s^{-1})
W_0	Weight of the cube at the start of microwave curing (g)
W_t	Weight of the cube at time t (g)
W_w	Initial weight of water present in cube (g)

Chapter 1

1. Introduction

1.1 Introduction

All around the world, many concrete structures have approached or are approaching a state where repairs are necessary. There are various reasons for concrete structures to disintegrate and fail which are described by Emmons [1]. According to Raupach et al. [2], the annual cost of repairing concrete structures is more than $20 billion in the USA alone.

Proper curing is widely recognised to assure adequate performance of concrete [3]. Curing is the process for promoting hydration of cement that leads to the strength development of concrete. Temperature is important to the curing process. Curing (strength development) gets slower in cold weather [4]. Fresh concrete exposed to freezing temperature experiences a significant loss at later ages of strength, impermeability and durability due to frost damage [5]. Examples of current methods for accelerated curing of concrete in cold weather include the use of type III cement [6], accelerator admixtures or heat application [7].

1.2 Accelerated curing of concrete repair

Curing of concrete can be accelerated by the application of thermal energy. The heat accelerates the hydration process and, therefore, develops early age compressive strength. Currently, there are several methods of heat curing such as discharge of steam or placing hot water pipes in fresh concrete, attaching electrical resistance wires to the form work, covering the concrete with insulation or using low voltage electric blankets.

These methods are normally expensive and, in some cases, they can only be used in a controlled environment such as pre-cast factories at industrial scale to be economical. In addition, most of these methods provide non-uniform heating to concrete. There is a real need to find a high efficiency and low cost technology that can be widely used on site to cure a wide variety of repair materials regardless of their composition, weather conditions and the patch repair position, size and shape.

Microwave heating is a high-performance method for curing concrete. Microwave heating is based on dissipation of internal energy associated with the excitation of molecular dipoles in an electromagnetic field. It provides a higher rate of compressive strength development and more uniform heating compared to other traditional methods such as steam curing. Generally, less than one hour of microwave curing is required to provide high early age compressive strength of concrete at relatively small power input [8, 9].

This research project investigates microwave curing of concrete repair. The project develops basic relationships between the key properties of concrete repair and the parameters of microwave energy for curing. Further investigations are carried out to determine the effect of microwave curing on the properties of repair such as internal temperature development, pore structure of microwave cured repair materials, the bond between substrate and repair and the bond between steel bar and microwave cured repair. The research has been conducted with microwave curing applied at ambient temperatures ranging between 20 °C and -5 °C. Finally, it also provides the results from field trials conducted using the prototype microwave system developed in the project. The work presented in this thesis provides a significant contribution to the knowledge of microwave curing of concrete repair by producing several journal and conference

papers. In addition, it was used to develop the prototype microwave system for curing repair.

1.3 Scope of research

Curing of concrete is needed to develop strength and durability. The curing process is normally slow and may take several days for concrete to be fully hardened. Application of heat accelerates hydration reaction and therefore, higher early age strength development can be achieved. Steam curing is the most common type of heat curing method. However, steam curing is an inefficient energy method and also it can be only used for pre-cast industry. Therefore, this research project introduces microwave curing as an effective and energy efficient method to cure concrete repair regardless of season on construction sites as well as for use with pre-cast industry.

1.4 Methodological approach

This research project investigates the effect of microwave curing on concrete repair as an efficient thermal curing method. The project adopts a predominantly experimental approach to develop the application of microwave curing for accelerated strength development of hydraulic cement based repair patches applied to substrate concrete. The relationship between the parameters of microwave energy application for curing and the properties of repair patch have been developed by analysing the test data on proprietary cementitious repair materials microwave cured at different powers and time period.

The analytical relationships developed from the test data have been used to design a prototype of the microwave system to conduct scaled up field trails. Tests on the repair materials have also been conducted to determine the effect of microwave curing on

important properties which control the performance of a repair patch applied to substrates. These include strength and shrinkage properties, the bond of patch repair materials with the substrate concrete and steel reinforcement. The application of microwave curing for cold weather repair has also been investigated in the experimental investigation. An analytical approach was taken to develop a Fixed Time Power (FTRP) algorithm from the experimental data obtained from the microwave cured repairs.

1.5 Aim and objectives of the Project

The aim of the project is to investigate the effect of microwave curing on the properties and durability of the commercial repair materials. Therefore, the project has the following objectives:

- Review the benefits of accelerated curing of concrete repair
- Review the current accelerated curing methods for concrete repair
- Identify and evaluate the important parameters of microwave and repair materials during microwave heating
- Investigate the effect of microwave curing on the heat of hydration, moisture loss and pore structure of repair materials
- Determine the effect of microwave curing on the bond between substrate and freshly applied repair at ambient temperatures of -5, 2, 10 and 20 °C.
- Determine the effect of microwave curing on the bond strength of reinforced concrete repair.
- Validate the pre-industrial prototype system by testing slab elements of several commercial repair materials.

1.6 Outline of thesis

This thesis has the following structure.

- Chapter 1 introduces the importance of concrete curing and the need for microwave curing technology as an effective method to accelerate curing of concrete repair.
- Chapter 2 presents a review of the accelerated curing of concrete and repair. It describes the current methods that can be used for accelerated curing. Limitations of these methods are highlighted. Microwave curing as an alternative method to cure concrete repair is introduced and the theory behind microwave heating is presented.
- Chapter 3 introduces the repair materials and equipment which are used throughout this study.
- Chapter 4 presents a series of laboratory tests that have been carried out to microwave cure repair materials. Relationships have been derived between key parameters of concrete repair and microwave energy input such as temperature, volume, microwave power and duration of microwave curing, etc. Based on the relationships derived from this chapter, a prototype microwave system has been developed. The optimal curing process determined from this chapter was further used to investigate the properties of microwave cured repair materials.
- Chapter 5 reports the investigation of the temperature development of microwave cured repair materials. Experimental investigations were carried out to determine the temperature profile across the depth of repair materials and at the top surface. Temperature development of microwave cured repair materials

was also investigated for cube specimens of 100 and 150 mm together with moisture loss of repair materials under microwave curing.

- Chapter 6 provides a brief literature review of porosity and pore structure of the cement based repair materials. It reports an experimental investigation on the effect of microwave curing on porosity and pore size distribution for different repair materials using mercury intrusion porosimetry both within the matrix and at the interfacial transition zone with the steel reinforcement.
- Chapter 7 presents the investigation to determine the effect of microwave curing on the bond strength between concrete substrate and repair materials applied at different ambient temperatures of -5, 2, 10 and 20 °C.
- Chapter 8 determines the bond strength of steel reinforcement with microwave cured concrete repair mortars. In addition, it also investigates the effect of microwave curing on compressive strength and shrinkage. The relationship between reinforcement bond strength and shrinkage, pore properties and strength of repair mortar is also investigated in this chapter.
- Chapter 9 introduces the prototype microwave system which has been developed based on the investigations presented in this thesis. In addition, it also provides results from field trials conducted to validate the equations used in the microwave prototype system design.
- Chapter 10 presents the conclusions and recommendations for future work.

Parts of the work reported in this thesis have been published in journal papers and conferences. In addition, another paper is in preparation to be submitted in the near future. The publications are listed at the beginning of the thesis.

Chapter 2

2. Literature Review

2.1 Introduction

This chapter presents a review on the curing of concrete and explains the principles of existing methods for accelerated curing of concrete. The limitations of current methods are highlighted. Finally, the background and theory of microwave heating are presented. The specific literature relevant to each individual chapter is reviewed in that particular chapter.

Concrete defects are due to many reasons such as chemical attack, freeze thaw and physical damage which are all described by authors and researchers such as Emmons [1], Raupach and Büttner [10], Smoak [11] and Grigoriadis [12]. They have described the process for repair which includes removing defects, selection of a proper repair material and preparing a sound surface of the substrate for repair application. The most common type of concrete repair is a patch repair which refers to the repair of relatively small areas in large surface elements of concrete [12]. The last stage of patch repair process is curing of repair which is important for its long-term performance.

2.2 Curing of concrete

Curing is the process for promoting the hydration of cement that leads to the development of microstructure and pore structure of concrete. Curing is achieved by controlling temperature and moisture movement from and into the concrete. Curing affects the strength and durability of concrete. Proper curing minimises evaporation of

water from the concrete and provides a source of external water to replace the water consumed during the hydration of cement [13]. Lack of proper curing leads to porosity and a weaker concrete which would provide rapid access to deterioration agents such as chlorides, carbon dioxide, moisture and oxygen into the concrete. The curing process starts immediately after placing and finishing of concrete. It should be continued for a reasonable period in order to achieve durability and strength. Proper curing also provides adequate and uniform temperature across the depth of concrete at an early age as it directly affects the rate of hydration and prevents thermal cracks.

The curing methods can be divided into the three main categories such as wet curing, membrane curing and accelerated curing. The wet and membrane curing keep concrete saturated by providing a source of water or minimize loss of water. Laboratory studies were conducted by Whiting and Snyder [14] to examine the effectiveness of different types of curing compounds in retaining water for hydration and their properties were compared. Results showed great variation. Specimens cured in water performed well compared to membrane cured ones. However, all specimens performed better than the specimens with no curing treatment.

The third category is accelerated curing which involves applying heat to the concrete or using admixtures such as sodium nitrite and potassium carbonate. There are methods that have been used since the 19th century along with other methods developed recently.

2.3 Accelerated curing of concrete repair

Proper curing is required for ensuring long-term durability and minimising restrained shrinkage of patch repair. Generally, 24 hours or more are required for cement based repair materials to develop sufficient compressive strength. In many patch repairs a

higher rate of compressive strength development is greatly desirable. For instance, a higher rate of strength development allows early removal of formwork and accelerates the construction process. Another example is the accelerated curing of repair to concrete pavements or runways, where severe restriction to traffic occurs until the repair develops sufficient compressive strength. The Specification for the Reinstatement of Openings in Highways [15], Manual of Contract Documents for Highway Works (MCHW) [16] and the Design Manual for Roads and Bridges [17] define a compressive strength of approximately 25 N/mm^2 for roads to be reopened to traffic after repair.

Repair in cold regions is another case when accelerated curing is very important to prevent frost damage at an early age and secure the quality of concrete. Cement hydration is slow at low temperature and if fresh concrete freezes there will be no water for the reaction. Therefore, the hardening of concrete is delayed. However, after thawing, due to the expansion of frozen fresh concrete, the concrete will set with large pores that affect its later strength. If freezing of fresh concrete takes place after it has developed sufficient strength, then it will resist the freezing temperature without damage. According to ACI 306R [4] the minimum strength of 3.5 MPa is required for fresh concrete to prevent frost damage. However, according to Koh et al. [5] even 5 MPa is not sufficient to prevent chloride ion penetration and freeze thaw damage. Frost damage is likely to occur when the temperature is defined as cold weather according to codes. The ACI 306R [4] defines cold temperature when 2 conditions are fulfilled. First, the average temperature for 3 continuous days is below +4 °C and secondly for any 12 hours period during those three days the maximum temperature is 10 °C or lower. Precaution needs to be taken when fresh concrete is exposed to the cold weather. General guidelines avoid placing concrete when the temperature is low. However, it is

not always feasible to delay maintenance work due to cold weather and it may be necessary to apply repair during cold weather.

Curing temperature is an important factor in the hydration, microstructure formation, bulk properties of Portland and blended cements which form the basis of repair materials. The curing temperature speeds up the chemical reaction of hydration producing a higher rate of strength development. In general, curing mortar and concrete at high temperature during placing and setting increases its early strength but may adversely affect the long-term strength [7]. However, a controlled rise in curing temperature can speed up hydration resulting in early age strength of concrete without causing any ill-effect on later strength.

2.4 Accelerated curing methods

Accelerated curing techniques are normally based on applying heat to the fresh concrete or using chemical accelerators. Thermal methods are mainly used in the precast concrete industry whereas accelerators are mainly used on site. The following section describes the most common methods of accelerated curing in concrete industries.

2.4.1 Low pressure steam curing

It is a method of steam curing concrete at a pressure of 70 to 100 KPa to achieve a high early strength in order to transfer concrete to the store or site at an early age. The steam curing is controlled to provide high temperature (40-70 °C) and high humidity. The curing period includes several stages that influence the quality of concrete. The stages are as follows:

- Initial delay prior to steaming (2 to 5 hours)
- Temperature rise period (2 to 3 hours)

- Maintain at the maximum temperature (6 to 12 hours)
- Temperature decrease period (2 to 3 hours)

Merritt and Johnson [18] investigated the effect of different parameters such as duration of curing, temperature, different cement and aggregates, water cement ratio under atmospheric steam curing. In general, steam curing gives high early strength and lower later age strength [7]. However, by using a proper delay period and curing regime high early strength of concrete can be achieved with steam curing without effecting the later age strength. According to Odom [19], with steam curing of concrete (21 hours), early age strength at 24 hours can be increased by 75% without affecting 28 days strength. Steam curing has been used in precast elements specially pre-stressed concrete sleepers and also precast pre-stressed girders in bridges [20].

There are some limitations of this method to accelerate curing of concrete. For instance, it provides non uniform heating across the depth of concrete. The surface of concrete will heat up earlier. Also, the location of the steam boiler and the position of concrete may result in curing temperature variations. For example, the steam leaves the boiler at 80-90 °C, and for an extensive network of steam pipes, it can go below 30 °C at the other side of the precast plant.

2.4.2 High pressure steam curing (autoclaving)

It is mainly used to manufacture smaller precast products such as concrete masonry blocks (hollow cored blocks) and small slabs and beams [21] with the thickness of 100 to 300 mm. Steam is applied at high pressure in closed chambers or vessels. A temperature of above 100 °C is produced and, therefore, it is not allowed to be in contact with the concrete surface, otherwise, it will result in drying of the concrete. High-pressure steam curing, normally involves steam at 150 °C to 180 °C under a

pressure of 500 KPa to 1000 KPa. Therefore, a curing chamber in form of a pressure vessel is used.

The main advantage of this method is the high early strength of concrete [7]. In addition, it provides high resistance to sulphate and other form of chemical attack and freezing and thawing [22] which may due to the reduction in porosity. However, there are limitations with this method mainly similar to the steam curing at low pressure. In addition, high pressure steam curing reduces bond strength with steel reinforcement, increases brittleness and reduces impact strength. Finally, steam curing methods are not suitable for site curing of repaired infrastructure [21].

2.4.3 Heating constituent materials

In this method, heat is applied to the constituents such as water, coarse aggregate and sand prior to mixing. This method has been used in Finland since the early 1980s [23]. Jonasson [24] showed that by heating only the mixing water, rate of hardening will increase. However, this method reduces the long-term strength of the concrete by 10 to 20 % [7].

2.4.4 Electrical curing

An electric current passing through fresh concrete raises its temperature. This method has been used in Sweden and Russia since 1932 [25]. In this method, 2 plate electrodes are placed on opposite faces of concrete and electrical power is connected to them. This method provides more uniform internal temperature compared to steam curing. However for cases when the method is practically difficult steel bars or nets are embedded in concrete to connect to the power supply. They can be used in walls, columns or piles. However, for such cases, the heat is not uniform as the density of the current varies from point to point in concrete. In addition, the high temperature

differential between steel bar and concrete may lead to reduced bond strength [25]. However, there are developments to the concept by adding conductive admixtures or fillers such as carbon fibre [26], graphite [27] or coins [28] to make concrete conductive. They have also been used to produce a conductive hardened concrete to apply heat, for example, to de-ice pavements [29] or airport runways [30]. However, depending on the size and volume of the concrete, it may require high voltage to produce sufficient heat which raises safety concerns. In addition, passing current may introduce corrosion in steel reinforced concrete.

2.4.5 Low voltage conductive polymer blanket curing

A conductive polymer technology has been developed by Sheffield Hallam University [31]. The material can be used as a blanket and by passing a low voltage (24V) current, it provides a high controlled temperature profile up to 120 °C. The consumed power is very low compared with traditional systems that operate at 110 or 240V. According to Mangat and Catley [31], this method provides not only high early strength (4 days) but also high later age strength (90 days) compared to normally cured concrete. The method can be used for precast concrete manufacture and on site. This method is currently used especially in cold weather to prevent frost damage to concrete. However, the equipment is relatively expensive.

2.4.6 Radio frequency heating

Lower frequency (below 300 MHz) than microwaves is used to increase the penetration of heat. This frequency can be used to heat insulator materials. Leivo [32] used a frequency of 27.12 MHz to cure fresh concrete with dimensions of 400 x 400 x 150 mm and applied a power of several kilowatts (<10 KW). The temperature of concrete rose to 50-60 °C in a few minutes and strengths of 30-40 MPa were achieved in 2-2.5 hours. However, there is no available data on later age strength. In addition, according to the

Leivo [32], there is a risk of short-circuiting the electromagnetic field or the field can be discharged through the surface of the specimen. Therefore, he concluded that it should not be used when steel reinforcement is present.

2.4.7 Admixtures

Compressive strength development of cement based materials can also be accelerated by adding chemical substances to the cement-water mix. Many organic and inorganic components have been reported to accelerate hydration of cement based materials. Accelerators may be defined as set admixtures and hardening admixtures or they may accelerate curing in both setting and hardening states. The British Standard BS EN 934-2:2009 [33] defines the minimum compressive strength for both set and hardened states at early and later age.

Antifreeze admixtures may be used in case of cold weather. They are similar to the admixtures which accelerate hydration of cement. In addition, antifreeze admixtures also reduce the freezing point of water in the fresh concrete. They accelerate hydration to a point where if the remaining water freezes, there would be sufficient empty pores to accommodate its expansion. Furthermore, they accelerate the development of strength to resist damage by the expansion of freezing water. Decreasing the freezing temperature of water is achieved by adding a solvent. For example, Karagol et al. [34] showed that adding calcium nitrate as antifreeze to concrete allows its exposure to even -10 °C up to 14 days without the need for additional precaution.

Most accelerators, however, are relatively new and their long-term durability is still not proven. Furthermore, some accelerators require very strict dosage control and it makes their applications expensive and very difficult to implement on site. Finally, there is no standard practice except in Russia where antifreeze admixtures have been accepted.

2.5 Energy efficiency of accelerated curing methods

Several conditions need to be fulfilled when selecting an accelerated curing method. The most important factor is the quality of repaired concrete. The selected method should not negatively affect the quality and durability of repair. Secondly, the method should be suitable for both in situ application and the precast industry. The method should be practical in cold weather to enable continuous work on repair to concrete structures throughout the year including in winter. It is also desirable for the developed technology to provide a higher energy efficiency compared to the traditional methods. Table 2.1 shows an estimation of energy consumption for some accelerated curing methods [35].

Table 2.1: Estimation of energy consumption for accelerated curing methods [35].

Type of accelerated curing	Energy (KW) consumed per m^3 of concrete	Initial cost of equipment	Maintenance cost of equipment	Remarks
Steam	160-180	High	High	-
Infra-red hot air	120-160	Moderate	Moderate	Evaporation of moisture from the surface is frequent
Hot water	140-160	Moderate	Moderate	-
Electrical curing				
Semi-direct	40-50	Low	Negligible	Has localised effects
Direct	30-60	Very low	Negligible	Has localised effects

There are two dominant factors for the cost of curing concrete, the capital cost (cost of equipment) and the running cost which is related to the consumption of energy. Methods stated in Table 2.1 normally require a long duration of curing up to 3 days and they need to maintain a high temperature. The effect is more severe in cold weather. According Korhonen [36] and Mironov and Demidov [37] winter weather can increase the construction cost by a factor of 1.5 to 2.

2.6 Bond strength of patch repair

According to the Matthews and Morlidge [38], 50% of concrete repairs exhibit signs of failure within 5 years. There are a number of reasons for repair to fail such as incorrect diagnosis of the fundamental problem, using inappropriate repair materials or poor workmanship including curing [39]. One of the important parameters to assess the durability of patch repair is the quality of the bond between the repair material and the substrate. The British standard BS EN 1504-10 [40] defines bond as the adhesion of the applied product or system to the concrete substrate. It is essential to have sufficient bond between the new applied repair and the substrate as it affects the reliability and durability of repair [41]. According to BS EN 1504-3:2005 Table 3 [42], the bond should be at least 2 MPa for structural and 0.8 MPa for non-structural repairs. To achieve sufficient bond, surface preparation is a key. There are several steps to achieve a sufficient bond that are described by Grigoriadis [12]. These steps include the removal of unsound or contaminated concrete, clean and prepare the surface with a certain roughness and provide compatibility with the substrate.

The bond tests are generally based on applying load on the composite specimens. Failure can occur either on the bond interface, substrate surface, repair surface or combinations of these. Several requirements need to be fulfilled by a standard test to determine the bond strength between repair and concrete substrate, such as [43]: ability to represent site conditions, high sensitivity to variation of bond strength, ability to reflect stress state of fairly typical service conditions and reproducibility of test result. However, currently, there is no test method that measures the property by fulfilling all requirements [43]. Many test methods have been developed based on an understanding and the degree of importance of each of the above requirements.

2.7 Microwave heating

2.7.1 Introduction

Microwave heating takes place when a material is exposed to the frequency range 0.3 to 300 GHz, which is a wavelength of 0.001 to 1 meter [44]. Microwaves carry energy that converts into heat inside the product when absorbed. Many factors affect the heating of a material inside a microwave field and this makes the heating mechanism very complicated. Microwave energy can be absorbed by materials with bipolar molecules e.g. water, reflected e.g. by metals, transferred e.g. by plastics or a combination of these mechanisms which is often the case in practice. When bipolar materials such as water are exposed to the magnetic field, molecules and atoms revolve at the frequency of the microwaves. The intense movement of molecules and atoms produces friction which generates heat. The principle is the same as rubbing hands together to keep warm. The main advantage of microwave heating is that it penetrates directly into the material which results in producing volumetric heating.

In conventional heating a material is heated by conduction or convection. These methods provide relatively slow heating since cement based materials are good heat insulators. These conventional methods result in a very hot surface and lower temperatures at the centre.

2.7.2 Microwave theory and background

Every material depends on its electromagnetic properties to interact in a unique way with an electromagnetic field [44]. A dielectric material such as concrete is characterised by two independent electromagnetic properties when exposed to an electromagnetic field. These are the complex magnetic permeability and the complex permittivity. Magnetic permeability is the resistance encountered when forming a

magnetic field in a vacuum. The complex permeability of most dielectric materials, such as solids and water is very close to the permeability of the free space which is $4\pi \times 10^{-17}$ Henry/meter. The complex permittivity is a parameter that needs to be considered as it determines the microwave absorption properties of the material. It depends on a real and imaginary part as:

$$\varepsilon=\varepsilon'-j\varepsilon'' \qquad (2.1)$$

where ε' is the real part, ε'' is the imaginary part of the complex permittivity and j is $\sqrt{-1}$.

If complex permittivity in Equation 2.1 is divided by permittivity of free space ε_0, the result will be dimensionless relative to the permittivity of free space.

$$\varepsilon/\varepsilon_0=\varepsilon'/\varepsilon_0- j\varepsilon''/\varepsilon_0 \qquad (2.2)$$

Substituting $\varepsilon_r=\varepsilon/\varepsilon_0$ in Equation 2.2 gives

$$\varepsilon_r= \varepsilon'_r -j\varepsilon_r'' \qquad (2.3)$$

Where ε_r is the relative complex permittivity, ε_r' is the real part of the relative complex permittivity which indicates how much energy can be stored in a material from an external magnetic field. ε_r'' is the imaginary part of the relative complex permittivity which is a measure of how a material dissipates electrical energy to heat and is usually called the dielectric loss factor. ε_0 is the permittivity of free space which is 8.854×10^{-12} F/m. Another parameter besides relative complex permittivity which is often seen in the literature is loss tangent (related to energy loss) which defined as follows:

$$tan\delta = \frac{\varepsilon''}{\varepsilon'} \qquad (2.4)$$

The loss tangent provides an indication of how well the material can be penetrated by an electric field and dissipates energy into heat.

2.7.3 Penetration depth

When microwaves penetrate a material, the amplitude of the wave diminishes due to power absorption. The field intensity falls exponentially with distance from the surface. According to Metaxas and Meredith [45], the penetration depth is defined as the depth at which the microwave magnitude decreases to e^{-1} of its original magnitude.

2.7.4 Power absorption

Power absorption of microwaves is directly related to the generated heat. According to Metaxas [45], absorption power can be calculated by the following equation:

$$P = 2\pi f \varepsilon_0 \varepsilon'' E^2 \qquad (2.5)$$

Where P is the power absorbed per unit volume (w/m^3), f is the frequency (Hz) of microwaves, ε_0 is the permittivity of free space, ε'' is the dielectric loss factor of the material and E is the electric field (V/m). This is a general equation to determine the absorption energy by any material. According to this equation, the absorbed energy depends on the frequency, which is fixed at 2.45 GHz for commercial ovens, dielectric loss factor and electromagnetic field. The problem with measuring the absorbed energy in practice is that these parameters are not constant and can change with frequency, moisture, temperature and properties of the materials which, in the case of concrete, are different as it sets and hardens. Therefore, it is extremely difficult to measure absorbed energy by a cement based material. Many researchers have studied the absorbed energy numerically and experimentally for different materials especially in food industries [46]. The following section describes the important parameters that influence the absorbed energy.

2.7.5 Factors affecting microwave power absorption

Microwave absorption depends on many factors such as shape, size [47, 48], dielectric properties, location of the specimen inside the oven [48, 49] and the oven system. Microwaves penetrate from all sides, therefore, shape is one of the important factors that influence the absorbed energy of a material when exposed to the magnetic field. Ayappa et al. [50] suggested avoiding corners and edges to reduce localised rapid heating of food samples. Zhang and Datta [51] numerically and experimentally investigated the effect of location of the load inside the oven. Results showed a significant difference in temperature for cylindrical potatoes exposed to 15 seconds of microwave energy.

The size and dimensions of the oven is another important parameter that manufacturers include in specifications of commercial microwave ovens. Persch and Schubert [52] investigated the efficiency of power absorption by a load to determine the effect of oven size and they concluded that a larger cavity leads to an increase in efficiency. The lower efficiency of a smaller oven is due to the increased reflection of the magnetron power [53]. This leads to the conclusion that even if a higher power capacity magnetron is used for a small cavity, it may not significantly increase the heating rate.

Non uniform heating of a load inside a microwave oven is another important parameter. Generally microwave ovens are considered to provide uniform heating inside a load, however, significant uneven heating can be produced. The significance of non-uniform heating will be important in concrete curing. There are two main factors that affect the uniformity of microwave heating. The first is the uniformity and magnitude of the electromagnetic field which is produced by the magnetron and guided by a waveguide. A larger volume of concrete (or repair) may be covered by different field magnetic intensity zones in the microwave cavity. The second factor is the properties of the

material exposed to the magnetic field. Improving the uniformity of the electromagnetic field does not always improve the uniformity of heating. The uniformity of internal temperature also depends on the shape of the load, size, location, the dielectric properties of the load, etc. Vadivambal and Jayas [54] reviewed various studies on the uniformity of microwave heating for food products. Teo et al. [55] conducted microwave curing of precast ferrocement for specimens of dimensions 600 x 900 by 20 mm depth and claimed to have developed a uniform temperature across the depth. However, a significant variation occurred across the top surface of specimen ranging from 40 to 62 °C.

One of the most effective methods to increase the uniformity of heating inside the load is to use a turntable inside a microwave oven. Geedipalli et al. [56] carried out a numerical study on modelling the heating uniformity provided by a rotating turntable in microwave ovens. It showed that the uniformity in temperature can be increased by up to 43% by using a turntable. The alternative method is using mode stirrers. A stirrer is a rotating metallic blade assembly near the feed port that is intended to improve the uniformity of heat [57].

The dielectric constant is an important parameter that has a direct effect on the power absorption of concrete. Wen and Chung [58] have investigated the effect of admixtures on the dielectric constant of cement paste with fibres. They used silica fume and latex as an admixture. The dielectric constant of cement paste varied from 19.6 to 63.2 depending on the admixtures and fibre content for a frequency of 10 KHz.

2.7.6 General output Power

The output power of a microwave oven is one of the most important parameters. Since 1990, manufacturers in the UK are required to measure the output power of microwave

ovens according to the BS 3999:1983 [59]. Since then there have been some modifications and the updated standard is BS EN 60705: 2015 [60]. It specifies the heating of 1 litre of water at the starting temperature of 10 °C for 123 seconds at the maximum power capacity of the oven. The maximum output power is then calculated from the following equation:

$$P = \frac{4187\, m_w\,(T_f - T_0) + 0.55 m_c (T_f - T_a)}{t} \qquad (2.6)$$

where P is the microwave power output (W); m_w is the mass of the water (g); m_c is the mass of the container (g); T_f is the final temperature of water (°C); T_0 is the initial temperature of the water (10 °C); T_a is the ambient temperature (°C) and t is the heating time (123 seconds).

2.7.7 Calculating the power output and power absorption by load

In practice, it is extremely difficult to measure absorbed power. It is very important to know the actual power absorbed by a load as it can be used to predict its temperature rise. Mudgett [61] proposed an empirical relationship between the load, volume and the power absorbed by the load as follows:

$$P_a = P_{max}(1 - e^{-kv}) \qquad (2.7)$$

where P_a is the power absorbed by the load (W), P_{max} is the output power of the microwave oven (W), V is the volume of the load in (m^3) and k is the volumetric coupling coefficient. According to this empirical relationship, applying a constant power to the load results in different absorbed power based on the volume.

Ma et al. [62] introduced a new practical method to determine the microwave energy absorption of materials. They used water, due to its sensitivity to microwave energy, as

the medium to absorb indirectly reflected microwave energy of the tested material. The method simply calculates the output power of a microwave oven by heating only water, based on Equation 2.6. Then, the test load together with the water in a container are exposed to the same microwave power. The difference in microwave power absorption by the water when it is heated alone and when it is heated together with the test load is calculated. The difference in microwave power is assumed to be absorbed by the load. The method is simple, practical and suitable for pure and mixed materials. However, it is only an indication to compare the relative ability of different materials in absorbing microwave energy.

2.8 Summary

This literature review chapter introduced the importance of the thermal curing of concrete to accelerate strength development especially in cold weather where concreting on site is not allowed under normal regulations. Different accelerated thermal curing methods, which are currently practised, were reviewed and their principles were explained. These methods are low and high pressure steam curing, heating constituent materials, electrical curing, low voltage conductive polymer blanket curing and radio frequency. Despite the wide range of methods, due to the limitations for each individual method, it was clear that there is a real need to develop a new technology or method to accelerate the strength development of repair materials that can be energy efficient and economically available for use on construction site regardless of weather, season and position of the repair. Furthermore, the theory and background of microwave heating were presented and it was considered as a high potential technology which can revolutionise the way concrete repairs are currently conducted.

Chapter 3

3. Materials and Equipment

3.1 Introduction

This chapter provides details of the repair materials and equipment that were used during the microwave curing investigations.

3.2 Repair materials

Various commercial (proprietary) repair mortar/concrete were used for this study. Brief details of each cement based repair material are given below.

3.2.1 Monomix

Monomix is a single component material provided as a 25 kg bag through the UK. It is a polymer-modified, fibre-reinforced, shrinkage compensated, Portland cement based repair material. It is a low density material and provides waterproof structural repair, rendering and profiling of vertical, horizontal and overhead surfaces. Table 3.1 shows the technical data and mechanical characteristics of Monomix repair material provided by the manufacturer [63].

Table 3.1: Technical data and mechanical characteristics of Monomix repair material provided by the manufacturer [63].

Technical data and mechanical characteristics		
Mixed density (Kg/m^3)	1725	
Water/Powder ratio	0.14	
Working life at 20 °C (Approx) (mins)	60	
Setting time at 20 °C (Approx) (mins)	225	
Compressive strength (MPa)	1 day	23.5
	7 days	41
	28 Days	48
Classification of compressive strength (MPa)	Class R3> 25	
Adhesive bond (MPa)	Class R4> 2.0	

3.2.2 Monopour PC6

Monopour PC6 is a single component material provided in a bag of 25 kg. It is a polymer modified cement based repair mortar, fibre-reinforced and shrinkage-compensated. The material is a micro concrete that can be used for large areas of concrete repair and heavy duty applications beneath base plates. Technical data and mechanical characteristics of Monopour PC6 are given in Table 3.2.

Table 3.2: Technical data and mechanical characteristics of Monopour PC6 repair material provided by the manufacturer

Technical data and mechanical characteristics		
Mixed density (Kg/m^3)	2225-2275	
Water/Powder ratio	0.124-0.14	
Working life at 20 °C (Approx) (mins)	60	
Compressive strength (MPa)	1 day	20-25
	7 days	50-55
	28 Days	65-70

3.2.3 Fastfill

Fastill is a single component material provided in a bag of 25 kg. It is a polymer modified, fibre reinforced Portland cement based fast setting repair mortar. The Fastfill repair mortar can be used to repair concrete in structures where accelerated curing is

required such as roads, runways, bridges, decks and footpaths. Technical data and mechanical characteristics of the material are shown in Table 3.3 [63].

Table 3.3: Technical data and mechanical characteristics of Fastfill repair material provided by the manufacturer

Technical data and mechanical characteristics		
Mixed density (Kg/m^3)	2150	
Water/Powder ratio	0.14	
Working life at 20 °C (Approx) (mins)	10	
Compressive strength (MPa)	1 hour	14.0
	2 hour	20.0
	4 hours	30.0
	1 day	40.0
	7 days	50.0
	28 days	60.0
Classification of compressive strength (MPa)	Class R4> 45	
Adhesive bond (MPa)	Class R4> 2.0	

3.2.4 Five Star

Five Star repair material is a preblended cementitious repair concrete. It is a shrinkage-compensated concrete with rapid hardening cement and pulverised fuel ash. This repair concrete can be used to repair bridge structures to HA model specification BD 27/86 [17]. It can repair concrete on beams and crossheads, car parks, buildings, balconies, stairs, concrete columns, walls, infill concrete and anchorage of bolts to large bolt pockets. The repair material is supplied in 25 kg bags. Table 3.4 shows the technical data and mechanical characteristics of Five Star repair concrete.

Table 3.4: Technical data and mechanical characteristics of Five Star repair concrete provided by the manufacturer

Technical data and mechanical characteristics		
Mixed density (Kg/m^3)	2200	
Water/Powder ratio	0.13	
Working life at 20 °C (Approx) (mins)	45-60	
Compressive strength (MPa)	1 day	16.0
	3 days	35.0
	7 days	45.0
	28 days	65.0

Classification of compressive strength (MPa)	>25
Adhesive bond (MPa)	1.5

3.2.5 HB40

HB40 is a single component, polymer-modified cement and fibre-reinforced repair material. It is a low-density material and can be used in structural concrete repair particularly where high, overhead build is required, repair of bridges and highway structures, carpark, bridge decks and columns. The repair material is supplied in a bag of 20 kg. Table 3.5 gives technical data and mechanical characteristics provided by manufacturer [64].

Table 3.5: Technical data and mechanical characteristics of HB40 Repair material provided by the Manufacturer

Technical data and mechanical characteristics		
Mixed density (Kg/m^3)	1500	
Water/Powder ratio	0.12-0.135	
Working life at 20 °C (Approx) (mins)	30-45	
Compressive strength (MPa)	3 days	30.0
	7 days	35.0
	28 days	43.0
Classification of compressive strength (MPa)	>25	
Adhesive bond (MPa)	1.5	

3.2.6 Pyrapatch

Pyrapatch is a prepacked product. It's a polymer-modified cement based, rapid setting concrete. Pyrapatch can be used in industrial floors, bridge decks, pavements both thin-bed and full-depth, car park decks and ramps, loading bays, coastal slipway and causeway repairs in tidal zones. The product is provided in a bag of 25 kg. Table 3.6 gives the technical data and mechanical characteristics provided by the manufacturer [64].

Table 3.6: Technical data and mechanical characteristics of Pyrapatch repair material provided by the manufacturer.

Technical data and mechanical characteristics		
Mixed density (Kg/m^3)	1500	
Water/Powder ratio	0.08-0.10	
Working life at 20 °C (Approx) (mins)	20-30	
Compressive strength (MPa)	3 hours	30
	6 hours	35.0
	1 Day	45.0
	7 days	55.0
	28 Days	60.0
Classification of compressive strength (MPa)	>25	
Bond strength (MPa)	1.2	

3.2.7 Weber Mortar

Weber Mortar is a polymer-modified, low resistivity, highway agencies class M patching mortar and render for cathodic protection. Weber mortar can be used for general purpose high strength concrete floors and other horizontal surfaces. It also can be used for thin bonded vertical repairs to concrete. This repair material is supplied in 25 kg bags. Table 3.7 gives the technical data and mechanical characteristics provided by the manufacturer [64].

Table 3.7: Technical data and mechanical characteristics of Weber Mortar repair material provided by the manufacturer.

Technical data and mechanical characteristics	
Mixed density (Kg/m^3)	2200
Water/Powder ratio	0.10
Compressive strength (MPa)	>45
Adhesive bond (MPa)	>2.0

3.2.8 CEM II Mortar

CEMII Mortar is designed with CEM II/A-L 32.5 R cement [65], coarse sharp sand (50% passing a 600 mm sieve) with a cement: sand ratio of 1:2, water to cement ratio of 0.5 and plastic density of 2200 kg/m^3. Similar mixes were also used with other w/c

ratios, however, for all of the tests w/c ratio of 0.5 is assumed unless the actual w/c is mentioned. Figure 3.1 shows the cumulative particle size distribution of the course sharp sand by sieve analysis [66].

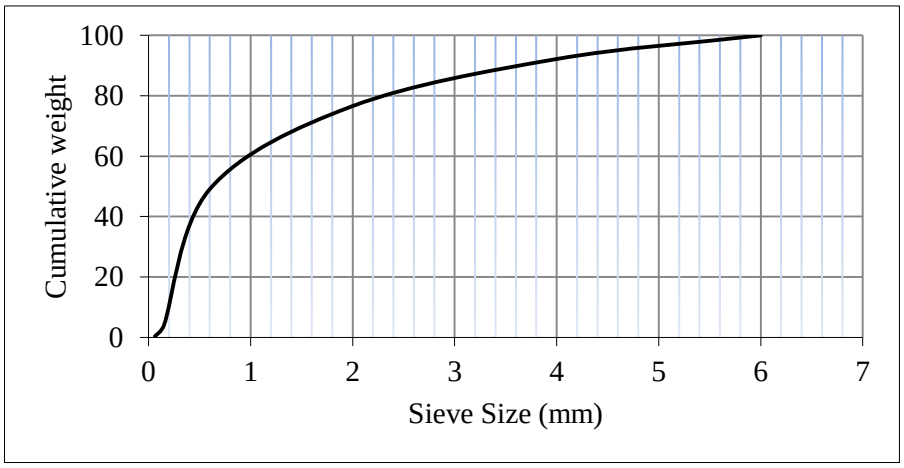

Figure 3.1: Cumulative particle size distibution of sharp sand

3.2.9 Sika MonoTop 613 DE

Sika Mono Top 613 DE is a Polymer-Modified Cement, Fibre-Reinforced mortar. This repair material is supplied in a bag of 25 kg. Density of fresh mix was 2100 kg/m^3. Technical data of Sike MonoTop 613 DE is presented in Table 3.8.

Table 3.8: Technical data and mechanical characteristics of SikaTop 613 DE

Technical data and mechanical characteristics	
Mixed density (Kg/m^3)	2100
Water/Powder ratio	0.125-0.135
Working life at 23 °C (Approx) (mins)	40-50
Compressive strength (MPa)	45-55
Flexural strength (Mpa)	7.0-9.0
Bond strength (MPa)	2.0-2.5

3.2.10 Sika MonoTop 412 DE

Sika Mono Top 412 DE is a fibre reinforced with plastics additives concrete repair. This concrete repair is supplied in a bag of 25 kg. Density of fresh mix is 2050 kg/m^3. Technical data of Sike Mono Top 412 DE is presented in Table 3.10.

Table 3.9: Technical data and mechanical characteristics of SikaTop 613 DE

Technical data and mechanical characteristics	
Mixed density (Kg/m^3)	2050
Water/Powder ratio	0.14
Working life at 20 °C (Approx) (mins)	60
Compressive strength (MPa)	53.3
Flexural strength	9.9

3.2.11 Stocrete GM P

Stocrete GM P is a Polymer-Modified Cement mortar with integrated corrosion protection. This repair material is supplied in a bag of 25 kg. Density of fresh mix was 1900 kg/m^3.

Table 3.10: Technical data and mechanical characteristics of StoCrete GM P

Technical data and mechanical characteristics	
Mixed density (Kg/m^3)	1900
Water/Powder ratio	0.11
Working life at +10 °C (mins)	60
Compressive strength (MPa)	20
Flexural strength	5
Bond strength (MPa)	> 0.8

3.2.12 Stocrete TG 204

Stocrete TG 204 is a Polymer-Modified Cementitious concrete repair product for the repair of concrete structures including reinforced concrete. The material has a good adhesive strength on the concrete substrate and claimed to have high protection against stress from frost/de-icing salt.

Table 3.11: Technical data and mechanical characteristics of StoCrete TG 204

Technical data and mechanical characteristics	
Mixed density (Kg/m^3)	2200
Water/Powder ratio	0.12
Working life at +23 °C (mins)	60
Compressive strength (MPa)	55
Flexural strength	10
Bond strength (MPa)	> 2.0

3.2.13 OPC Concrete

Ordinary Portland Cement (OPC) concrete designed with CEM II/A-LL 32.5 R cement conforming to BS EN 197-1, coarse sharp sand (50% passing a 600 mm sieve) and uncrushed river gravel (maximum size 20 mm) with w/c ratio of 0.50. The density of the fresh mix was 2350 kg/m^3. In addition, similar concrete mixes with w/c ratios of 0.40, 0.45, 0.50, 0.55 and 0.60 were used in order to test and calibrate the moisture detector of the prototype system.

3.3 Equipment

3.3.1 Commercial microwave ovens

Two commercial microwave ovens were used to cure repair material specimens in the laboratory investigations. Both microwave ovens were calibrated according to the BS EN and ASTM standards. The following section provides the specifications for both ovens.

3.3.1.1 *Microwave oven I (Logik)*

Microwave I is a commercial oven which can generate a power up to 900 Watts. It works with household electrical 240 Volts and frequency of the microwave is 2.45 GHz. It can be set to generate output power with increments of 10% up to 900 Watts. The microwave oven has a turntable glass to provide more uniform heating. Internal dimensions of the oven are 315 mm (W) x 347 mm (D) x 200 mm (H) and its external

dimensions are 483 mm (W) x 386 mm (D) x 281 mm (H). Table 3.12 provides the specifications of the microwave oven I provided by the manufacturer.

Table 3.12: Specification of Microwave Oven I (Logik)

Model	L25MDM13
Input Voltage (V)	230 - 240
Input Frequency (Hz)	~ 50
Microwave Output (Watts)	900
Microwave Frequency (MHz)	2450
Outside Dimensions (width x deep x height)	483 mm x 386 mm x 281 mm
Inside Dimensions (width x deep x height)	315 mm x 347 mm x 200 mm
Microwave input (Watts)	1400

3.3.1.2 *Microwave Oven II (Sharp R-2370)*

Microwave Oven II is a household oven that can generate power from 10 % to 100% of maximum nominal power of 1300 Watts. The frequency of microwave is 2.45 GHz. The internal dimensions of the oven are 350 mm (W) x 215 mm (D) x 370 mm (H) and external of 560 mm (W) x 414 mm (D) x 610 mm (H). Microwave oven II does not have a turntable. Table 3.13 presents the specification of microwave oven II.

Table 3.13: Specification of Microwave Oven II (Sharp)

Model	Sharp R-2370
Input Voltage (V)	230
Input Frequency (Hz)	~ 50
Microwave Output (Watts)	1300
Microwave Frequency (MHz)	2450
Outside Dimensions (width x deep x height)	560 mm x 414 mm x 610 mm
Inside Dimensions (width x deep x height)	350 mm x 215 mm x 370 mm
Microwave input (Watts)	2600
Weight approx (kg)	49

3.3.1.3 *Calibration of Microwave ovens*

Both microwave ovens were calibrated according to the BS EN 60705: 2012 [60] and ASTM F1317-98 [67] in order to determine their actual output power levels. The calibration was carried out by filling a plastic container with one litre water and placing it in the centre of the cavity and then applying full power of the microwave oven for 123 seconds. This included an additional 3 seconds to allow for the magnetron startup delay. The temperature rise due to the microwave energy was measured. The actual output power of the microwave oven was calculated from the following thermodynamic equation:

$$P = \frac{mc}{t}(T_2 - T_1) \qquad (3.1)$$

where m is the mass of a load (kg); c is the specific heat capacity of water (J/kg°C); t is time (s); T_1 is the initial temperature of water (°C) and T_2 is the final temperature of water (°C).

Multiplying the mass (m) of water (1 kg) by the specific heat (c) of water (4181 J/kg°C) and dividing by the time (t) which is 120 seconds gives a value of 34.9 (J/°C) which is substituted in Equation 3.1 to give:

$$P = 34.9(T_2 - T_1) \qquad (3.2)$$

The temperature of water was measured with a digital thermometer (probe) accurate to ± 0.5 °C. In addition, the temperature of water was also measured with a thermal camera (FLIR i7) accurate to ± 2 °C.

The investigation was carried out for 20, 40, 50, 60, 80 and 100 % of total power for both microwave ovens. The procedure was then repeated to obtain the average of three

measurements of the actual output power of each oven. The output power should be rounded to the nearest 50 Watts according to the BS EN 60705: 2012 [60]. However, due to the sensitivity of this investigation, the exact value of actual output power was rounded to one Watt.

3.3.1.3.1 Calibration of Microwave oven I

Figure 3.2 shows the calibration curve for microwave oven I, based on the digital thermometer and a thermal camera temperatures. Each point on the graph represents the average of 3 experimental results. The graph in Figure 3.3 is the average of thermometer and thermal camera readings to determine the relationship between the actual output power and nominal output power for microwave oven I. The data in Figure 3.3 are also presented in Table 3.14. The microwave power referred to in the thesis is the actual output power. The actual output power of microwave oven I is 66.7 % of the nominal power given by the manufacture.

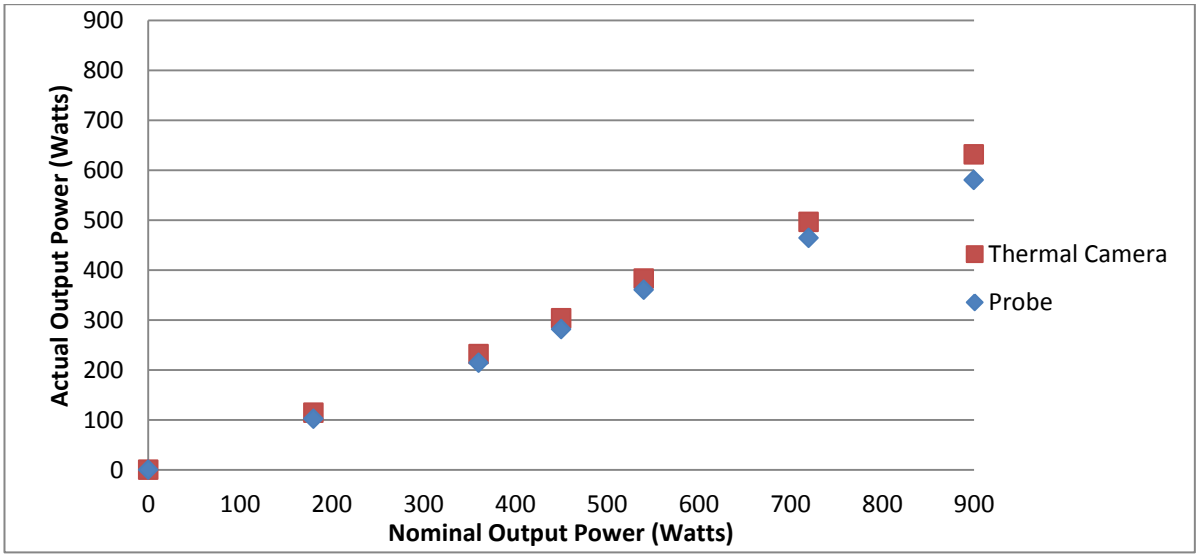

Figure 3.2: Actual output power versus nominal output power calibration curves for microwave Oven I determined using a digital thermometer probe and a Flir i7 Thermal camera

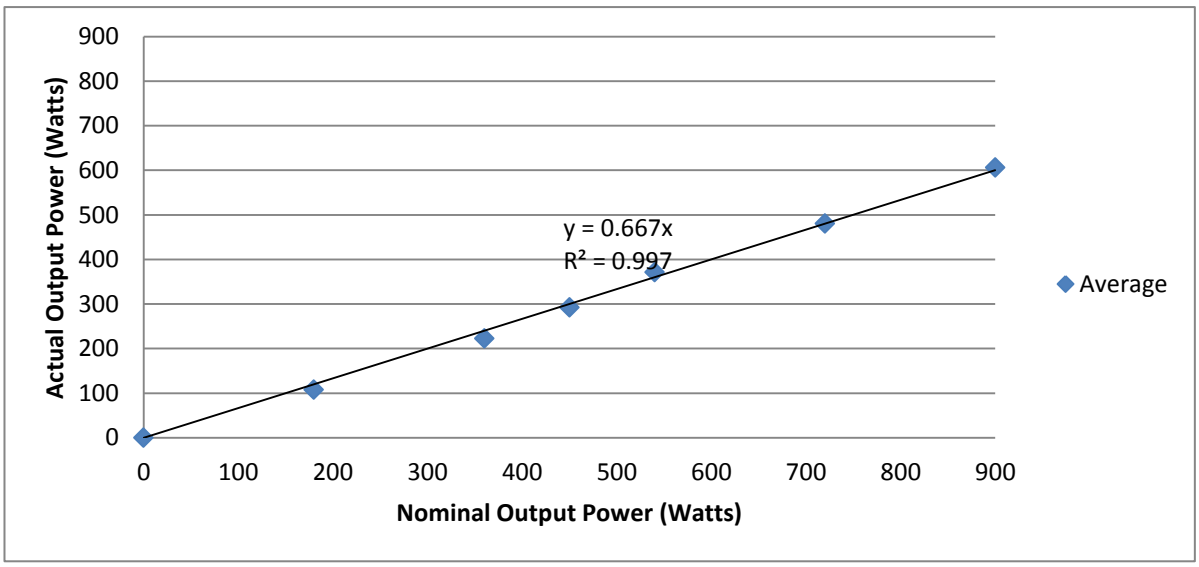

Figure 3.3: Actual output power versus nominal output power calibration curves for microwave oven I determined by averaging the thermometer and thermal camera

Table 3.14: The output power of microwave oven I

Power (%)	Nominal output power (W)	Actual output power (W)
100	900	600
90	810	540
80	720	480
70	630	420
60	540	360
50	450	300
40	360	240
30	270	180
20	180	120
10	90	60

3.3.1.3.2 Calibration of Microwave oven II

Figure 3.4 shows the calibration curve for microwave oven II based on the digital thermometer and thermal camera outputs. Each point on the graph represents the average of 3 experimental results. Figure 3.5 plots the average power calculated from the thermocouple and thermal camera readings to determine the relationship between the actual output power of microwave and nominal output power for oven II. The data in Figure 3.5 are also presented in Table 3.15. The microwave power is referred to in the thesis is the actual output power. The actual power of microwave oven II is 101.8% of the nominal power given by the manufacture.

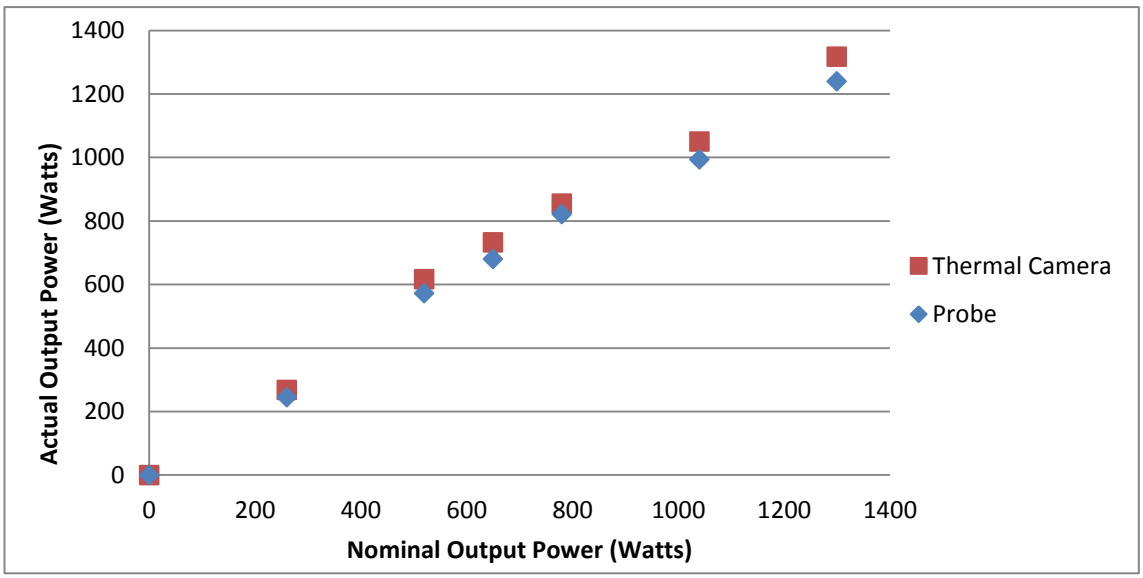

Figure 3.4: Actual output power versus nominal output power calibration curves for Microwave Oven II determined using a digital thermometer probe and a FLIR i7 Thermal camera

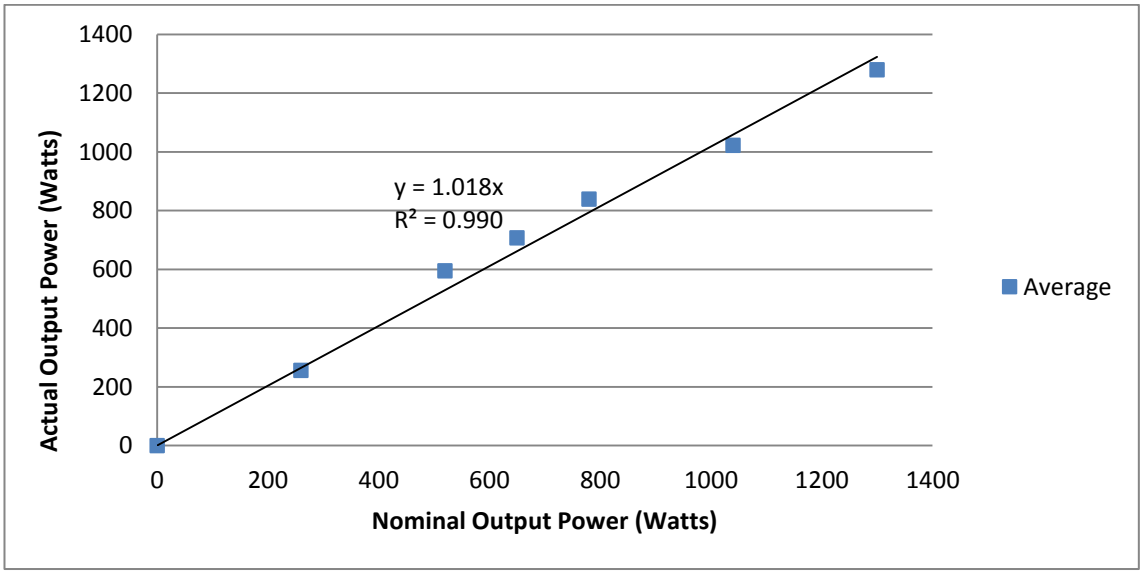

Figure 3.5: Actual output power versus nominal output power calibration curves for microwave oven II determined by averaging the thermometer and thermal camera

Table 3.15: The output power of microwave oven II

Power (%)	Nominal output power (W)	Actual output power (W)
100	1300	1323
90	1070	1089
80	940	957
70	810	825
60	780	794
50	650	662
40	520	530
30	350	356
20	260	264
10	130	132

3.3.2 Environmental Chambers

Two environmental chambers were used to replicate different ambient temperatures a Sanyo Atoms Chamber Type MTH-4400 PR and a customised environmental chamber suitable for scaled up tests. The second environmental chamber comprised of a large cold room approximately of 2 x 2 x 2 m which was used to provide an ambient temperatures in the range of -5 °C to +20 °C.

The number of cube specimens stored in any of these two environmental chambers had no effect on the temperature of the environmental chamber due to its size and power. These chambers were used to maintain different temperatures to replicate the site conditions including freezing temperatures. The time taken to increase the environmental chamber temperature from -5 to +20 °C is about 30 minutes.

3.3.3 Casting moulds

Standard steel moulds are commonly used in the field and laboratory investigations of concrete and mortar, including quality control. However, steel moulds are not suitable when mortar or concrete is exposed to microwave heating as they reflect microwaves which results in insufficient microwave energy being available for curing. Therefore, polystyrene moulds were used for this study and steel moulds were only used for quality control of the mixes. Polystyrene moulds transmit microwave energy without absorbing significant part of this energy. Any energy loss in the polystyrene mould has been neglected. Different polystyrene mould sizes such as 50, 75, 100 and 150 mm cubes and prism moulds of 75 x 75 x 300 mm were used during this study. The polystyrene mould sizes of 100 and 150 mm cubes are available globally and are often used by contractors to collect samples from construction sites. However, 50 and 75 mm polystyrene cube moulds and 75 x 75 x 300 prism mould were manufactured specifically for this study.

These polystyrene moulds have a thickness of 20 mm. The moulds were disposable after microwave curing and demoulding of specimens.

3.3.4 Temperature recording

Temperature development is fundamentally important in the process of thermal curing. During this study the following equipment was used to monitor and record the temperature of specimens.

3.3.4.1 *Thermocouples*

T-Type thermocouples (welded tip) was used to determine the internal temperature of specimens. They provide an accurate temperature reading of a point with instant response to the changes in temperature. This type of thermocouple can operate within a temperature range from -75 to +250 °C.

3.3.4.2 *Temperature recording Data logger*

Temperature data provided by the thermocouples were recorded through a datataker DT85G digital logger. The datataker can be used to view data in real time or takes data in the predefined interval and can store up to 10 000 000 data points.

3.3.4.3 *Thermal camera*

The surface temperature of the specimens was measured using a Flir i7 Thermal camera. The accuracy of the camera is 0.2% or ±2 °C and it takes pictures with a resolution of 140 x 140 pixels. Figure 3.6 shows the Flir i7 thermal camera. The camera can be set to provide an image of temperature distribution, maximum or minimum temperature range at a selected area and a spot point temperature. However, during this study, the camera was used to provide thermal images with temperature distribution across the top surface and also a spot point temperature at the centre of the cube surface.

Figure 3.6: Thermal camera used to monitor the surface temperature of slabs.

3.3.5 Shrinkage strain measurement

Shrinkage of the specimens was measured by recording length change of the prism specimens of dimensions 300 x 75 x 75 mm. Shrinkage pins (demec) were installed at two opposite faces of specimens after demoulding at 24 hours. The analogue Demec strain gauge with a length of 200 mm was used with a reference Gauge No 4690 and 1 division represents a strain of 0.79×10^{-5}.

Chapter 4

4. Microwave curing parameters of in-situ concrete repairs

4.1 Introduction

This chapter presents results from tests carried out to determine the relationships between microwave heating and repair material parameters. These parameters are related to the top surface temperature of the microwave cured specimens taken by a thermal camera. The relationships are essential to design and develop a microwave curing prototype system. The optimum microwave curing regime determined in this chapter is used throughout this study to further investigate the properties of microwave cured repair materials.

4.2 Literature review and background

4.2.1 Introduction

The idea to microwave cure concrete goes back to 1960. Alexander Watson [68] used a commercial microwave oven to apply 1 KW microwave energy (frequency of 2.45 GHz) to heat 6 cubes (100 mm) of concrete to 90 °C within one hour and then reduced power to maintain the temperature for another 1 or 2 hours. Microwave cured specimens showed a higher compressive strength at the end of microwave curing compared to the 24 hours normally cured specimens. However, a significant reduction in compressive strength was reported for specimens at 28 days age. In addition, a total weight loss of 150 to 300 g was observed for the six cubes that were exposed to microwave energy [68]. Loss of water can be explained by the high curing temperature that leads to its

escape as vapour. Wu et al. [69] used an automatic cooking microwave oven to cure OPC mortar specimens in 40 mm x 40 mm x 160 mm moulds for 15 to 120 minutes. The durations of 15 and 30 minutes of microwave curing were selected as optimum periods as the compressive strength increased by 43 % and 5 % at 3 and 28 days age, respectively. Results indicated no reduction of the long-term compressive strength of the OPC Mortar specimens. However, the temperature of specimens during and at the end of microwave curing was not reported.

Hutchinson et al. [70] conducted an experimental investigation to measure the percentage of hydration and the compressive strength of OPC mortar subjected to the microwave heating. Microwave power was set to 50 Watts and an additional volume of water (600 ml, 800 ml or 1000 ml) was placed next to the mortar specimens inside the oven. It was claimed that the power delivered to the mortar specimens was inversely proportional to the volume of water. Microwave heating accelerated the hydration process only during the first 24 hours. In addition, the compressive strength of specimens at 1, 7 and 28 days age was not influenced by microwave heating. Leung and Pheeraphan [71] conducted an experimental investigation of microwave curing of Portland cement mortar/concrete and determined their compressive strength at an early and later age. They showed that microwave heating of type III Portland cement, only for 45 minutes, developed an early age strength at 4.5 hours that was favourably comparable to the commercially available rapid hardening concrete or concrete containing accelerating admixtures.

Leung and Pheeraphan [9] conducted a series of tests to determine optimal process for microwave curing of concrete. They used discrete microwave power levels and used feedback temperature control in order to maintain temperature. Very high early age strength (4.5 hours) was recorded with no deterioration in later age up to 7 days.

Sohn and Johnson [72] investigated the effect of microwave curing on the 28 day strength of Portland cement type I mortar. They applied microwave heating to cylindrical specimens of 50 mm diameter and 100 mm length, at 30 minutes after water was added to the mix. Microwave heating was applied at the rate of 7 °C/min to reach 40, 60 or 80 °C and then maintained at the corresponding temperatures for 2 hours. Compressive strength at 28 days showed that heating to 40 °C gives strength of 95% and 102% for Type I Mortar and slag mortar, respectively compared to the normally cured specimens. However, heating to 80 °C was identified as incompatible with curing due to adverse effect on strength at later age. An investigation carried out by Lee et al. [73] lead them to conclude that 40 minutes microwave heating is optimal time for energy saving consideration. They achieved high early age strength for concrete by using steam or microwave curing. However, the later age (28 days) strength was slightly lower compared to the specimens cured normally.

4.2.2 Parameters of microwave curing of concrete

4.2.2.1 *Microwave power*

Commercial microwave ovens are manufactured with a power range of 1000 to 2000 Watts, representing low and heavy-duty microwave ovens respectively. Higher microwave powers result in the expansion of the concrete and overflowing of the slurry caused by the very rapid evaporation of water [74]. Microwave power is an important parameter in curing of mortar and concrete. The optimal microwave power for different mixes varies significantly based on the characteristics of the mix, including w/c ratio, cement content, cement type, additive and admixtures, etc.

Microwave power should be selected carefully in order to ensure concrete achieves the required temperature within a reasonable time and rate of temperature increase. This is

due to the fact that the temperature of microwave cured concrete has a direct effect on its early and later age compressive strength. Leung and Pheeraphan [75] reported a compressive strength of 5 and 35 MPa at 4.5 hours and 7 days age respectively for mortar specimens exposed to microwave power of 300 Watts. The corresponding compressive strength was 12 and 15 MPa at 4.5 hours and 7 days age respectively when exposed to 600 Watts. This indicates that higher microwave power significantly increases the early age compressive strength of mortar, however, at the same time, it significantly reduces the later age compressive strength.

The degree of increase in early age compressive strength of concrete should be defined based on the acceptance on the degree of reduction in long term compressive strength. Leung and Pheeraphan [75] used microwave power ranged from 300 to 600 Watts to microwave cure mortar specimens cast in cylinders of 76.2 mm diameter and 152.4 mm height. They compared the compressive strength at short term (4.5 hours) and long term (7 days) and concluded that microwave power of 400 Watts provides the best compromise considering both the early and later age compressive strength. This was based on the fact that lower power (300 W) gives the lowest compressive strength at 4.5 hours compared to the higher powers. On the other hand, its 7 days compressive strength was the highest compared to the other microwave powers. Furthermore, specimens which were microwave cured at 500 Watts gave the highest compressive strength at 4.5 hours and lowest compressive strength at 7 days compared to the specimens cured at lower powers.

Another approach is to consider using a fixed or variable power to microwave cure mortar. In case of fixed power, microwave power is constant throughout curing. However, in variable microwave power, depending on the temperature of the sample and time, power can be varied. Leung and Pheeraphan [9] reported a different curing

process chosen arbitrarily to provide a microwave curing temperature ranging from above 50 °C to about 85 °C. They used a power ranging from 412 (fixed) to a maximum power of 1200 Watts. In the case of using a fixed power, 412 Watts was continuously used for duration of 45 minutes. As a result, the temperature increased almost linearly and reached 85 °C at the end of 45 minutes of microwave curing. The other powers were used with a feedback temperature control to limit the maximum temperature to 50, 60 or 80 °C for a different duration of time. They concluded that using a variable discrete power provides the best combination for early and later age strength.

Rattanadecho et al. [76] investigated the acceleration of cement paste curing with microwave energy by using a continuous belt drier. The microwave power was generated from 14 compressed air-cooled magnetrons of 800 W each and it was applied to 15 cement paste specimens of dimensions 50 x 50 x 50 mm. Results showed that cement paste specimens achieved a temperature of about 64, 95 and nearly 120 °C with 1, 2 and 3 magnetrons respectively within 60 minutes. In addition, all microwave cured specimens achieved a higher compressive strength at one day age compared to the normally cured specimens.

4.2.2.2 *Duration of microwave curing*

Duration of microwave heating to cure concrete is another important parameter to ensure strength development of matrix within appropriate time. Traditional heat curing methods such as steam curing often require several hours pre-heating and additional several hours pre-cooling in the precast concrete. This is to make sure that concrete develops a uniform temperature across its depths during pre-heating and cooling periods. One of the biggest advantages of microwave heating is that it provides a uniform heating across the depth of the concrete and, therefore, does not require preheating stage.

In addition, microwave heating does not heat the room environment, it only heats the concrete specimens. These advantages of microwave heating reduce the duration of microwave curing and the power consumed during curing process compared to conventional heating.

Prolonged microwave curing of concrete results in an excessive temperature which adversely affects the long term compressive strength. In addition, it also results in consumption of unnecessarily high amount of energy. Furthermore, prolonging microwave curing introduces random surface cracking [77]. Typical duration of microwave curing reported by the majority of researchers [78, 79, 80] is less than 1 hour (typically 40-45 minutes) which is enough time to avoid excessive heating and also it is not too long for in situ curing of concrete repair.

4.2.2.3 *Water/ cement ratio*

Rattanadecho et al. [76] investigated the effect of different w/c ratio on microwave cured cement paste. Cement pastes with w/c ratio from 0.30 to 0.5 were exposed to three different microwave powers (using either 1, 2 or 3 magnetrons). Results showed that lower w/c ratio resulted in a higher temperature for all three powers. In other words, the specimens with higher cement content (lower w/c ratio) show a greater potential for absorbing microwaves. This is may due to the fact that a lower amount of water is heated for lower w/c ratio compared to the higher w/c ratio. In addition, it is also known that lower w/c ratio produces a higher heat of hydration which can also contribute to the increase in temperature under microwave curing [81].

4.2.2.4 *Initial delay time*

Initial delay time refers to the time from the moment of adding water into cement to the time of exposing it to microwave heating. In practice, concrete is mixed, placed and

surface finished before the application of microwave curing. This means that concrete is cured normally until the start of microwave curing. Therefore, it is common to delay the start of the microwave curing by letting concrete to cure normally for a short time.

Three phases of cement hydration process are considered when determining the delay time of microwave curing concrete. These phases are based on the relationship between the dielectric properties of concrete and the heat generation and transfer properties of microwave energy [82]. These three phases are known as the early, middle and final period [82]. The early period (dormant period) starts from the time when water is added to the mixture and it continues for several hours. This period can be referred to as the stage I or II in the hydration process of the cement which is discussed in Chapter 5. The middle period is referred to as the accelerated stage, known as stage III (discussed in Chapter 5). This stage is where calcium silicate hydrate begins to form. The final period is referred to as the deceleration stage. This is where the hydrated products start to form slowly and continue to form as long as water and unhydrated silicate is available.

Based on literature, researchers have used delay times to cover all these hydration periods, starting from 0 minutes (immediately after casting) [70, 79], 30 minutes after mixing [72, 80, 83, 84], 720 minutes [77] and as long as 1440 minutes after mixing [85, 86, 87]. However, among these three periods of hydration, the early period is the suitable period for microwave curing of concrete. This is due to the fact that during this period concrete contains both water molecules and cement which continue to react with each other [82]. This period of curing provides the best compromise between the rate of strength gain and the long term strength of concrete. Application of microwave curing during the middle and final phases of hydration, on the other hand, will be more disruptive to the internal structures formed by hydration and result in greater reduction in long term strength [88]. Leung and Pheeraphan [75] investigated the effect of delay

time from 20 to 61 minutes for mortar with water cement ratio of 0.50 by applying a microwave power of 400 Watts for duration of 45 minutes. Based on their results, the optimal delay time was 30 minutes. Similarly, the results of Makul and Agrawal [83] produced optimum compressive strength with a delay time of 30 minutes. A 30 minute delay time is commonly used by researchers investigating the effect of microwave curing on the properties of concrete [72, 80, 83, 84].

4.2.2.5 *Ambient temperature*

Ambient temperature is an important parameter in microwave curing of repair that may affect the temperature reached at the end of microwave curing. In general, the application of concrete repair in the laboratory is carried out at a temperature approximately 20 °C. However, in practice, for in situ repairs, the ambient temperature of repair varies depending on the seasons and geographical location. For example, in winter the temperature may fall to freezing. Dielectric properties of cement based repair materials, which determine the level of absorption of microwave energy may change with temperature which in turn it is likely to affect the rate of temperature increase in specimens.

Currently, there are no available data known to the author on the effect of ambient temperature, especially freezing temperature, on the effect of microwave curing on cementitious repair materials.

4.3 Experimental programme

4.3.1 Repair materials

The following repair materials were used for the investigation reported in this chapter:

- Five Star

- Monomix
- HB40
- Monopour PC6
- Fastfill
- Pyrapatch

A more detailed description of the repair materials is given in Chapter 3.

4.3.2 Microwave ovens

Two commercial microwave ovens were used to conduct the present study. Microwave oven I (logik L25MD13) and microwave oven II (Sharp R-2370) were used to cure the repair material specimens cast in polystyrene cube moulds of 100 and 150 mm dimensions. The specifications of both microwave ovens are given in Chapter 3.

4.3.3 Details of specimens, mixing and microwave curing

4.3.3.1 *Specimens prepared under ambient temperature*

Repair materials were mixed in a Hobart mixer and then cast in polystyrene cube moulds to provide three different volumes. These volumes were 1, 3.38 and 4.38 litres obtained from polystyrene moulds with internal dimensions 100, 150 mm and a combination of 100 and 150 mm cube moulds. Table 4.1 shows the details of all repair material mixes. It includes the name of repair material, type of microwave oven, microwave power, the weight of repair material (powder) and water in each mix, w/p ratio (water/powder), the volume of the mix, the size of the cube(s) and 28 days compressive strength. The required quantity of each repair material was cast in the cube moulds and compacted on a vibrating table. The specimens were kept in the laboratory (20 °C and 60% RH) for 30 minutes from the time when water was added to the powder. After the 30 minutes (delay time), specimens were placed inside a microwave oven and

cured for 45 minutes at power 60, 120, 132, 180 or 264 Watts. The temperature was measured at the centre of the top surface of each cube at 0, 10, 20, 30, 40 and 45 minutes from the start of microwave curing using a Flir i7 thermal camera.

Table 4.1: Details of repair material mixes.

Test series	Repair material	Mix number	Microwave oven	Power (W)	Weight of water (kg)	Weight of powder (kg)	w/p ratio*	Volume of mix (l)	Cube size (mm)	28 day strength** (MPa)
1	Monomix	1	Logik	60	0.21	1.52	0.14	1	100	42
		2	L25MDM13	120						
		3		180						
	Fastfill	1		120	0.26	1.88	0.14			60
	Monopour PC6	1		60	0.23	2.05	0.11			65-70
		2		120						
		3		180						
	Five Star	1		60	0.26	2.00	0.13			65
		2		120						
		3		180						
	HB40	1		60	0.17	1.33	0.13			≥ 25
		2		120						
		3		180						
	Pyrapatch	1		60	0.20	2.00	0.10			60
		2		120						
2	Monomix	1	Sharp	132	0.72	5.12	0.14	3.38	150	42
		2	R-2370	264						
	Monopour PC6	1		132	0.78	6.93	0.11			65-70
		2		264						
	Five Star	1		132	0.87	6.76	0.13			65
		2		264						
	HB40	1		132	0.59	4.51	0.13			≥25
		2		264						
3	Monomix	1	Sharp	132	0.93	6.64	0.14	4.38	100	42
		2	R-2370	264					+	
	Monopour PC60	1		132	1.01	8.98	0.11		150	65-70
		2		264						
	Five Star	1		132	1.12	8.76	0.13			65
		2		264						
	HB40	1		132	0.76	5.84	0.13			≥25
		2		264						

*w/p-water/powder ratio; **Manufacturer's compressive strength data.

4.3.3.2 *Specimens prepared under low temperatures*

The effect of different ambient temperatures of the fresh mix of a repair material on the microwave curing temperatures developed with time was investigated. The investigation simulated the application of repairs in different in situ conditions including cold weather. The constituent materials of each mix were "temperature conditioned" and mixed at three different ambient temperature ranges categorised as: very low (1.7-6.5 °C), low (8.9-10.0 °C) and medium range (15.8-18.3 °C) as shown in Table 4.2. The constituent materials were kept overnight in an environment chamber to condition them to the selected ambient temperature. The ambient temperature was maintained during mixing and for 30 minutes after casting one 150 mm cube specimen (3.38 L volume) for each mix. Materials Five Star, Monomix, and HB40 were tested using the Sharp R-2370 microwave oven at a power of 132 W. Temperature measurements at the centre of the top surface of the cubes were taken at 0, 10, 20, 30, 40 and 45 minutes from the start of microwave curing using a Flir i7 thermal camera.

Table 4.2: Details of the mixes prepared under low temperatures

Repair material	Mix number	Temperature range	Power	Volume (L)	Ambient temperature (°C)
Monomix	1	Very low	132	3.38	3.0
	2	Low			10.0
	3	Medium			17.1
HB40	1	Very low			1.7
	2	Low			8.9
	3	Medium			15.8
Five Star	1	Very low			3.2
	2	Low			9.9
	3	Medium			17.8
Monopour PC6	1	Very low			6.5
	2	Low			9.1
	3	Medium			18.3

4.4 Results and discussion

4.4.1 Top surface temperature during microwave curing

Figures 4.1 (a-f) show typical temperature distribution across the top surface of a 100 mm cube (HB40 repair material) at different times of microwave curing with 120 Watts power. The dark square edges represent the wall of polystyrene mould. The value on the top left of the thermal image represents the temperature at the centre of the cube. The two values in the lower left and right corners show the range of temperature across the image. For example, Figure 4.1 (b) shows the top surface temperature of the cube at 10 minutes after microwave curing. The top surface temperature ranged from 20 to 42 °C, representing the lower temperature at the polystyrene mould face and the hot zone respectively. In addition, the value at the top left corner (28.4 °C) is the temperature at the centre of the cube.

The temperature at the centre of the cube increased from 17.6 °C at time 0 minutes to 75.4 °C after 45 minutes of microwave curing. The increase in temperature due to microwave energy absorption is directly related to time which has been previously reported by other researchers [77, 89].

There is significant variation across top surface temperature during microwave curing. At 40 minutes of microwave curing, for example, the surface temperature is 68.4 °C at the centre whereas it increases towards 100 °C at the outer surface of the cube specimen. Similar variations were observed for all repair materials within all different volumes. It was observed that shortly after starting microwave curing, hot zones appeared mainly at the edges and corners of the polystyrene moulds.

Many researchers [69, 70, 72, 83, 85, 9] conducted experimental investigations and, based on localised temperature monitoring (e.g. by a single thermocouple), drew relationships between temperature, time and strength. For example, Sohn and Johnson [72] used a shielded type-K thermocouple to monitor temperature in cube specimens. The cubes were heated (by microwave) to 40, 60 and 80 °C and each temperature was maintained for 2 hours. They concluded that 40 °C curing gave the maximum 28 days strength. However, the significant variation of temperature developed in cube specimens of this investigation (Figure 4.1) indicates the unreliability of such precise conclusions about optimal temperature-strength relationships.

(a) At 0 minute (b) At 10 minutes (c) At 20 minutes

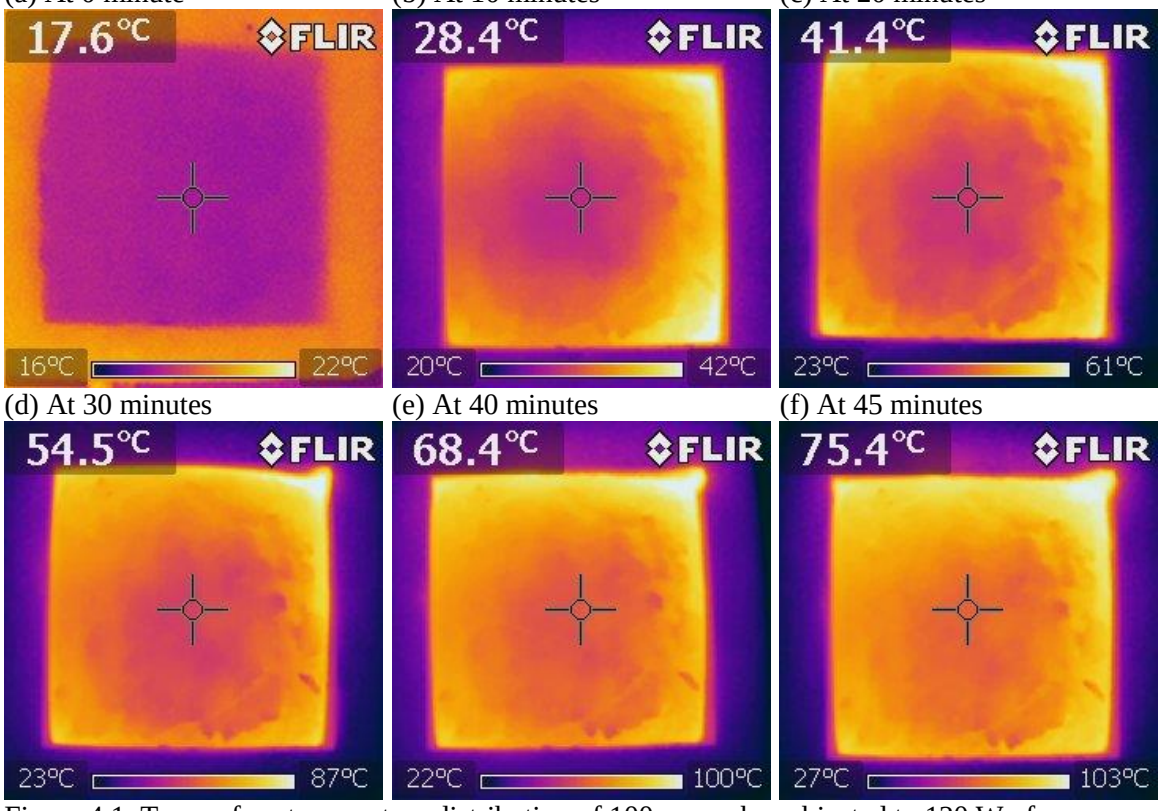

(d) At 30 minutes (e) At 40 minutes (f) At 45 minutes

Figure 4.1: Top surface temperature distribution of 100 mm cube subjected to 120 W of microwave power (HB40 Repair material)

4.4.2 Variation of top surface temperature during microwave curing

Figures 4.2 (a-f) shows temperature distribution for specimens of the six repair materials. Each thermal image represents a 100 mm cube of repair material exposed to

120 Watts. There is significant variation of mid surface temperature ranging from 56.1 to 99.9 ℃ at the end of 45 minutes of microwave curing. Repair materials Fastfill and Pyrapatch developed particularly high temperature (89.4 and 99.9 ℃ respectively). The corresponding temperature for repair material Five Star and Monomix are 56.1 and 59.7 ℃ respectively. Fastfill and Pyrapatch are described as fast setting repair materials by their manufacturers. This is the likely reason for their rapid temperature rise under microwave curing. On the other hand, Five Star repair material is described as rapid hardening by its manufacturer. However, it does not develop excessively high temperature at the end of microwave curing.

The absorption of microwave energy by repair materials is related to their dielectric properties. Dielectric properties are affected by admixtures, additives, water content and the change resulting from hydration [86]. Repair materials in this investigation contain different admixtures, additives and fineness of cement, which have an effect on temperature increase under microwave curing.

(a) Monomix (b) Fastfill (c) Monopour PC6

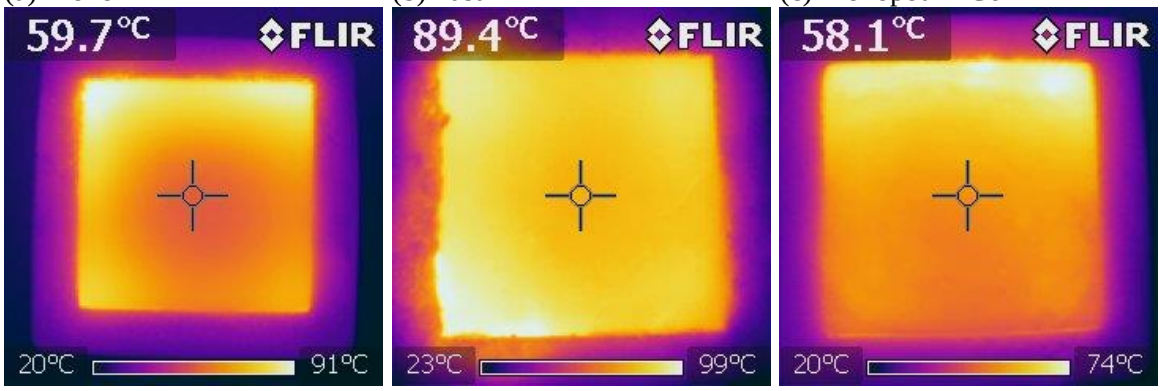

(d) Five Star (e) HB40 (f) Pyrapatch

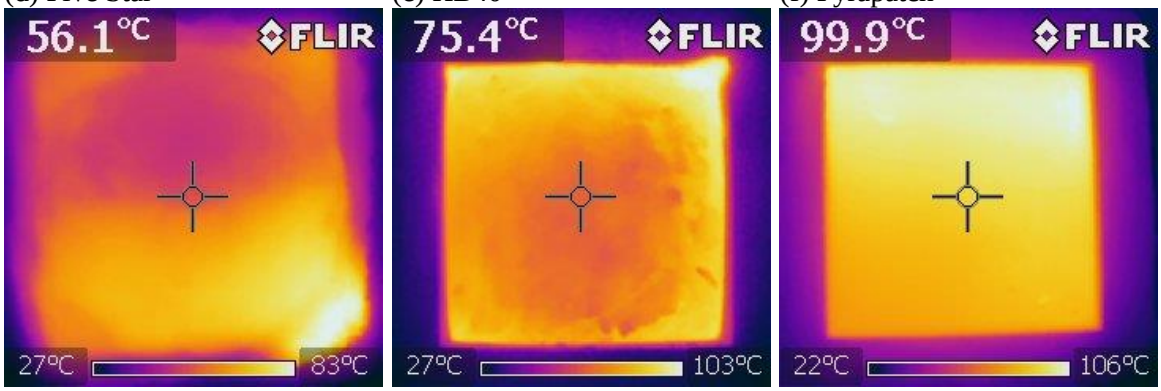

Figure 4.2: Top surface temperature of six repair materials after 45 minutes of microwave curing at 120 Watts (volume 1 litre)

4.4.3 Time-Temperature relationship

4.4.3.1 *Constant Volume (1 litre)*

The graphs in Figures 4.3 to 4.8 represent the top surface mid-point temperature-time relationship of the repair materials. One litre volume cubes of repair materials were microwave cured at different powers 60, 120 and 180 Watts. Microwave curing started 30 minutes after water was added to mix the powder. The specimens' temperature was approximately 20 °C at the start of microwave curing (except Fastfill which was 24 °C) and it increased linearly with time during microwave curing as shown in Figures 4.3 to 4.8 for the different repair materials.

The surface temperature increased at a different rate for the repair materials and applied power (Figures 4.3 to 4.8). Greater power results in a higher rate of temperature rise during microwave curing. For example, top surface mid-point temperature of Monomix increased linearly from 20 to 38 °C after 45 minutes of microwave curing at 60 Watts. The corresponding increase at 180 Watts power was from 20 to 85 °C after 45 minutes of microwave curing.

Effect of microwave power on temperature increase is well known and has been reported by other researchers [9, 70]. For example, Leung and Pheeraphan [9] reported temperature increase of mortar form approximately 25 °C to above 80 °C within 45 minutes of microwave curing at power of 410 Watts. The corresponding temperature increase at 800 Watts was from 25 °C to above 80 °C after only 20 minutes of microwave curing. This is due to the higher energy provided at higher power for the material to absorb.

The temperature increased rapidly for Fastfill and Pyrapatch repair materials (Figures 4.4 and 4.8) Which are fast setting repair materials. Fastfill underwent phase change and hardened during microwave curing after 20 minutes (Figure 4.4). Pyrapatch achieved 100 °C with only medium power (120 W) (Figure 4.8). The temperature rise of both materials is excessive. Materials with this kind of temperature-time relationship would not be suitable for in-situ microwave curing (except possibly at very low ambient temperature), which is suitable for normal, non-rapid setting repair materials which are cured to moderate temperatures.

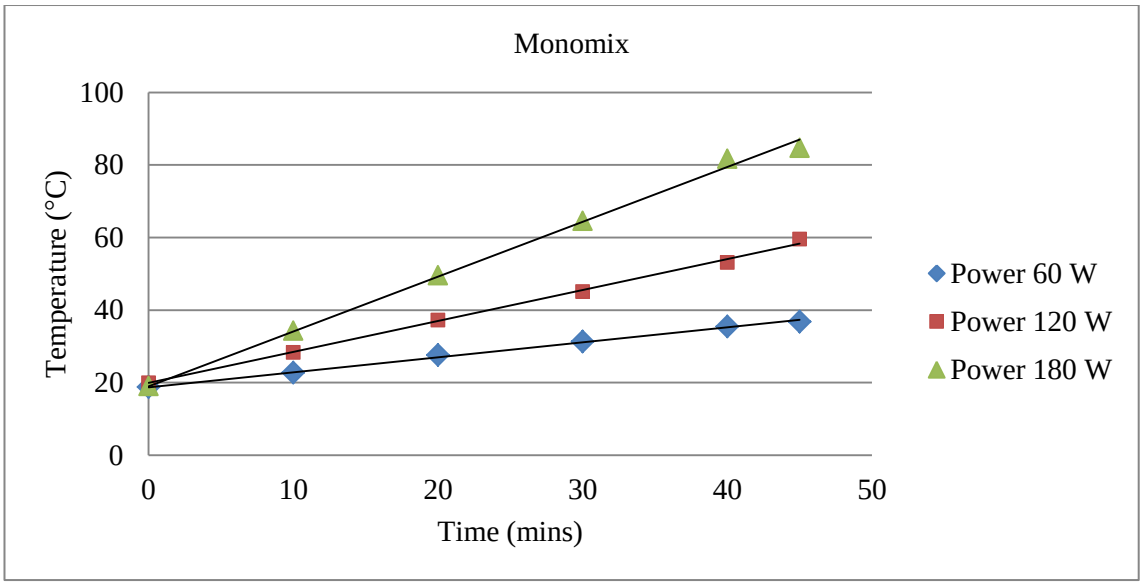

Figure 4.3: Top surface mid-point temperature-time relationship for Monomix (1 litre volume)

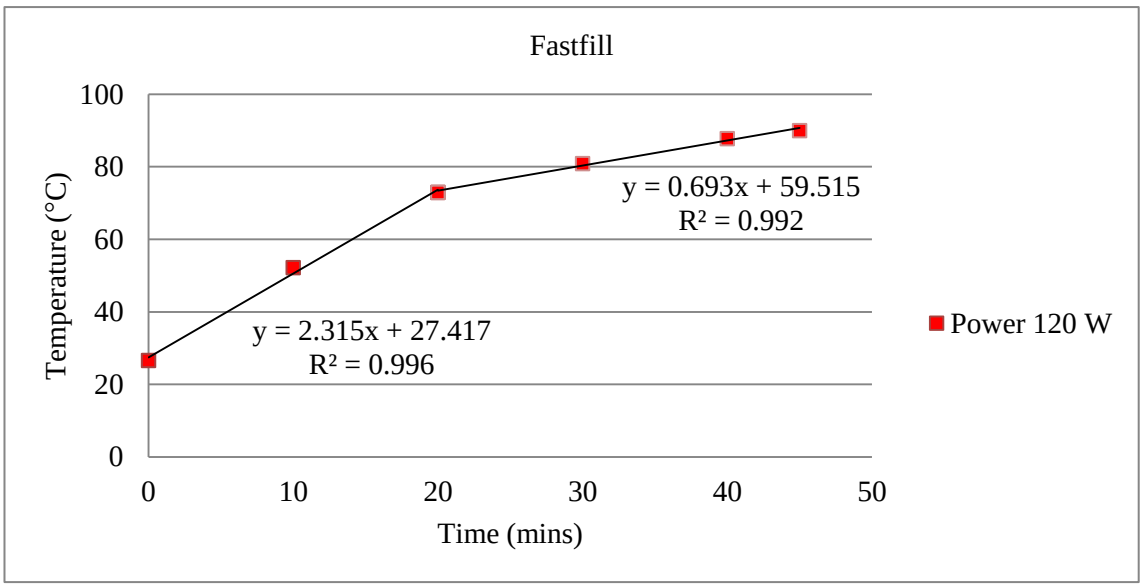

Figure 4.4: Top surface mid-point temperature-time relationship for Fastfill (1 litre volume)

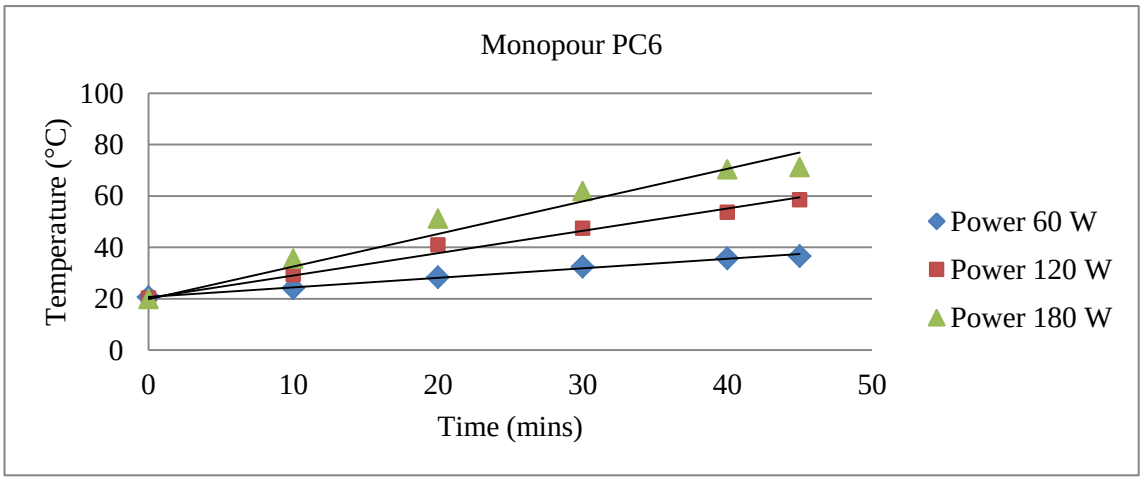

Figure 4.5: Top surface mid-point temperature-time relationship for Monopour PC6 (1 litre volume)

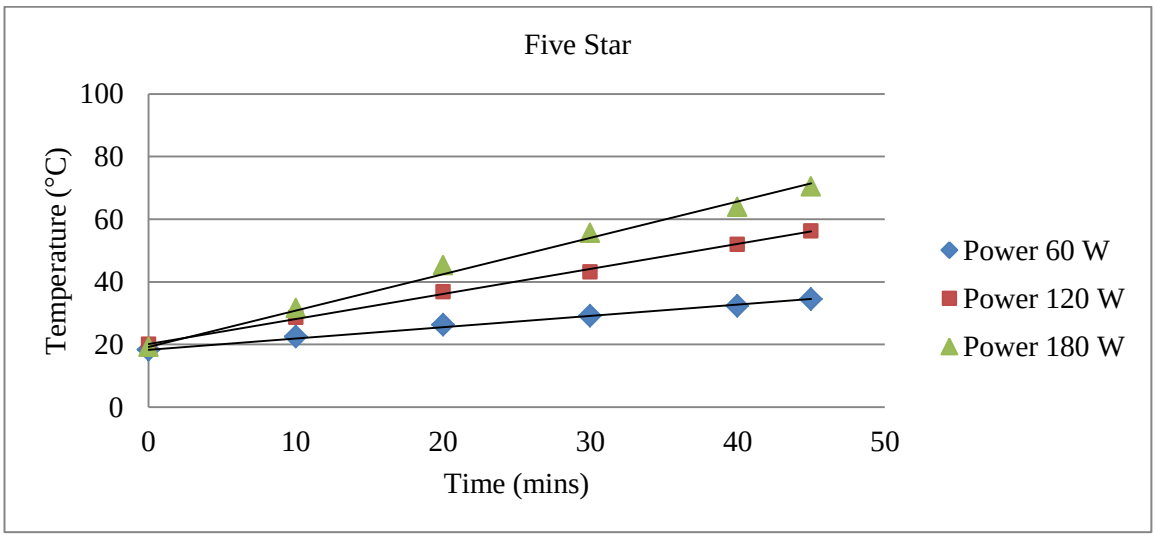

Figure 4.6: Top surface mid-point temperature-time relationship for Five Star (1 litre volume)

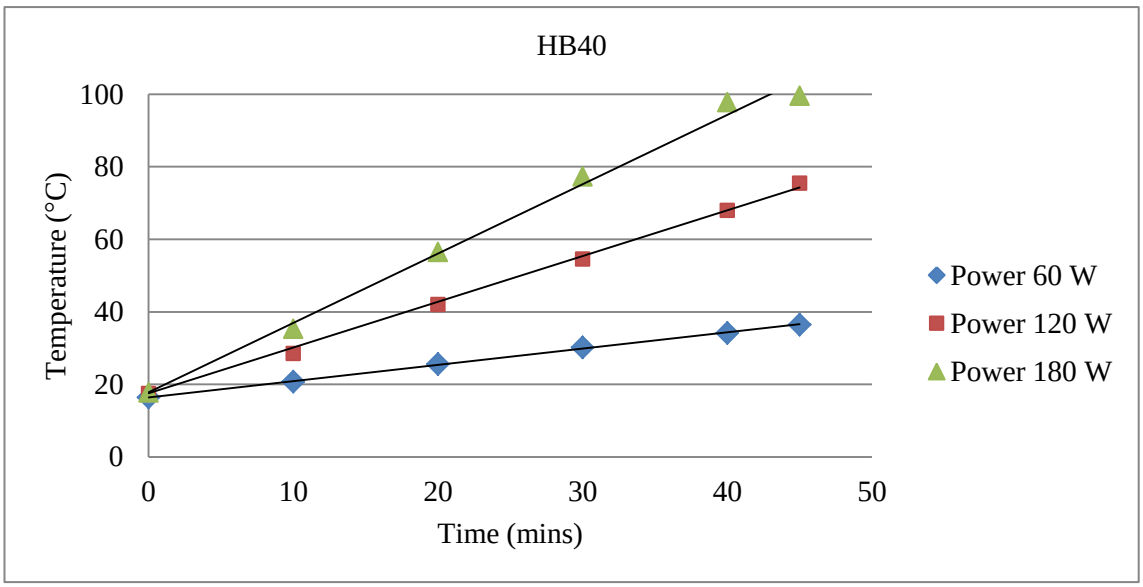

Figure 4.7: Top surface mid-point temperature-time relationship for HB40 (1 litre volume)

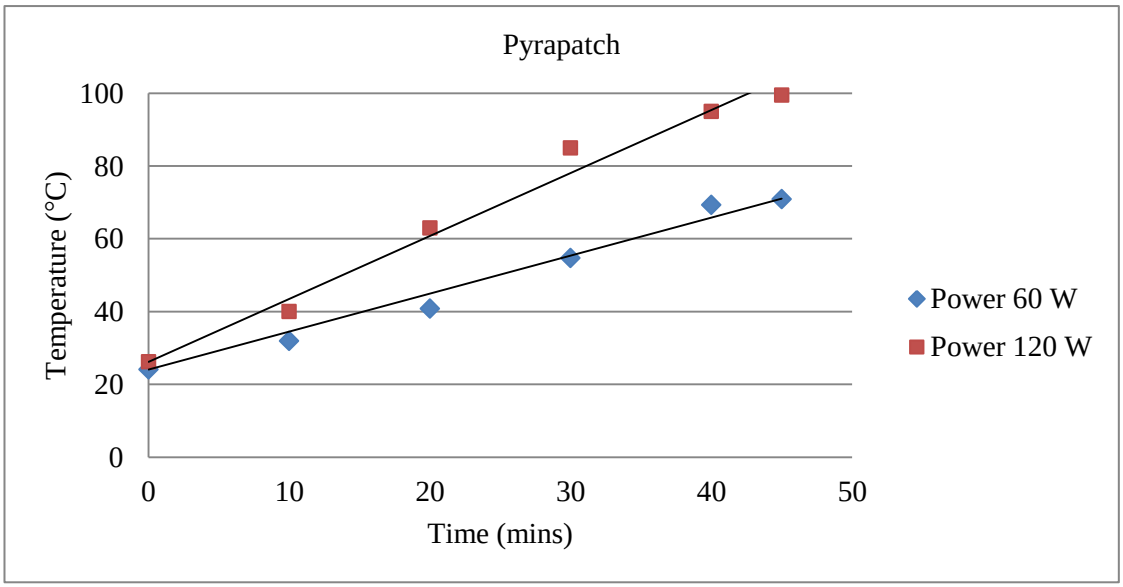

Figure 4.8: Top surface mid-point temperature-time relationship for Pyrapatch (1 litre volume)

4.4.3.2 ***Variable volume***

Table 4.3 presents the microwave curing temperatures at the beginning and end of 45 minutes of microwave curing for different volumes of repair materials applied at 120-132 Watts. A typical graph of time-temperature for three volumes of HB40 is shown in Figure 4.9 exposed to microwave power of 120-130 W over 45 minutes. Three volumes of 1, 3.4 and 4.4 litres were obtained from 100, 150 mm and a combination of 100 and 150 mm cubes. Temperature was taken at the top surface mid-point of each specimen.

In the case of combination of 100 and 150 mm cubes, the average mid-point temperature was calculated from both cubes. Temperature increased linearly for each volume and reached a maximum value at the end of microwave curing.

The surface temperature increased at different rate for the materials at power 120-132 W with greater volume resulting in a lower rate of temperature increase during microwave curing. For example, the top surface temperature of 1 litre HB40 increased linearly from 17.5 to 75.5 °C after 45 minutes of microwave curing. The corresponding increase for 3.4 litres was from 15.8 to 62.2 °C after 45 minutes.

The effect of volume on temperature increase is related to the energy required to heat the material and it is directly related to the volume (mass) of the material. This effect is discussed in more details in section 4.4.5.

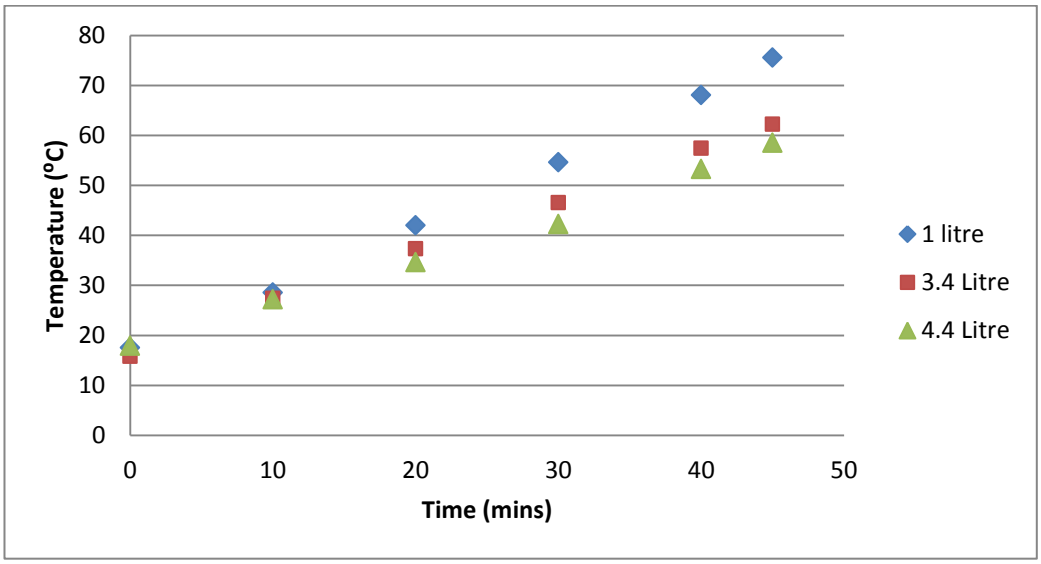

Figure 4.9: Time temperature relationship for HB40 with three volumes (microwave power 120-132 W)

Table 4.3: Summary of microwave curing temperatures developed for 1, 3.4 and 4.4 litres of rempair materials at 120-132 Watts in 45 mintues.

Material	Volume (litre)	Initial temperature (°C)	Final temperature (°C)	Temperature increase ΔT (°C)
Five Star	1.0	20.1	56.3	36.2
	3.4	17.8	39.0	21.2
	4.4	18.5	41.4	22.9
Monomix	1.0	19.9	59.5	39.6
	3.4	17.1	52.9	35.8
	4.4	16.8	52.3	35.5
Monopour PC6	1.0	20.3	58.6	38.3
	3.4	18.3	45.0	26.7
	4.4	17.8	42.6	24.8
HB40	1.0	17.5	75.5	58.0
	3.4	15.8	62.2	46.4
	4.4	17.9	58.5	40.6

4.4.4 Theoretical Relationship

The thermodynamic formula for absorbed microwave power relates the volume and temperature rise as follows [90]:

$$\frac{P_{abs}}{V} = \frac{c\rho(T_f - T_a)}{t} \qquad (4.1)$$

where P_{abs} is the microwave power (W); V is the volume (m^3); c is the specific heat capacity (J/kg^{o}C); ρ is the density (kg/m^3); T_f is the temperature at the end of microwave curing (^{o}C); T_a is the ambient temperature (^{o}C) and t is the microwave curing time (seconds).

This expression is applied to the data of this investigation (Table 4.3) at an applied microwave power of (120-132 W) over 45 minutes for materials Five Star, Monomix, Monopour PC6 and HB40. The ambient temperature of all tests ranged between 15.8 and 20.3 °C.

Equation 4.1 is re-written in the following form to present the results in Figure 4.10 :-

$$\Delta T = \frac{P_{abs}t}{c\rho}V^{-1} \qquad (4.2)$$

where $$\Delta T = T_f - T_a \qquad (4.3)$$

Figure 4.10 shows a linear relationship between ΔT and V for the constant power and microwave curing time for the experimental data of Five Star, Monomix, Monopour PC6 and HB40 . The slope of the graph in Figure 4.10 is a function of P_{abs}, t, c and ρ. The density ρ of Five Star, Monomix, Monopour PC6 and HB40 is 2200, 1730, 2280 and 1500 kg/m^3, respectively. The coefficient c (specific heat) accounts for the different constituents of the repair materials and their mix properties. It is affected by density(ρ) and the temperature of the mix during microwave curing.

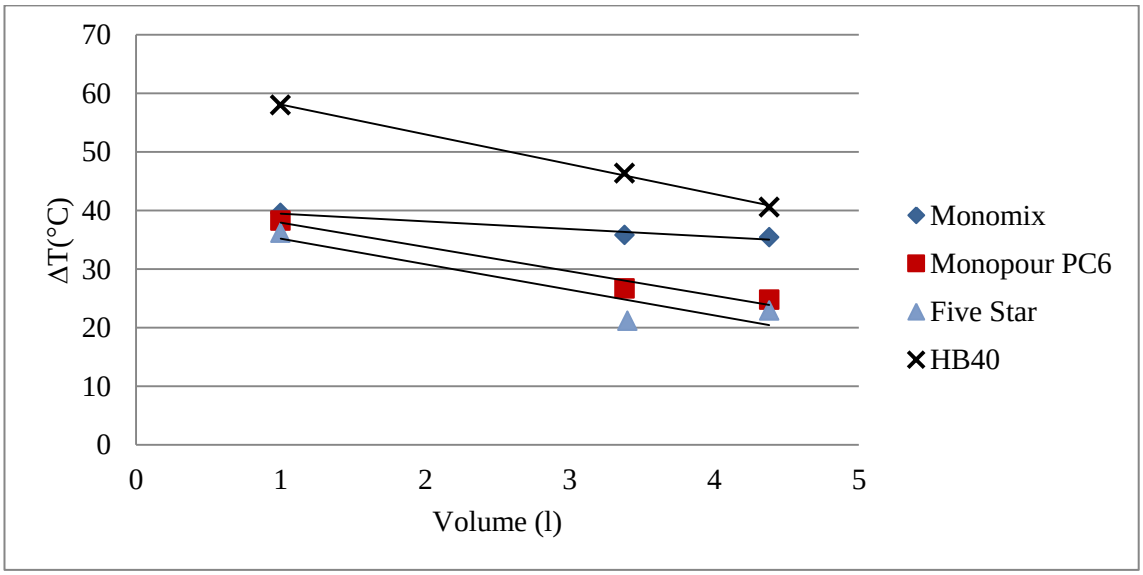

Figure 4.10: Volume-temperature rise relationship of repair materials at approximately 120 watts (120-132 W).

4.4.5 Rate of temperature increase with microwave power

Four repair materials Monomix, HB40, Five Star and Monopour PC6 are used in this analysis. The rapid setting Fastfill and Pyrapatch repair materials are excluded since

they developed very high temperatures and are not suitable for microwave curing under these conditions.

Figure 4.11 shows the relationship between slope (dT/dt) and microwave power for the repair materials, obtained from Figures 4.3, 4.5 to 4.7. It is clear that there is a linear relationship between this slope (α) and microwave power for all repair materials. This relationship will provide input to develop an algorithm for the automatic control of power of the microwave prototype developed in the project.

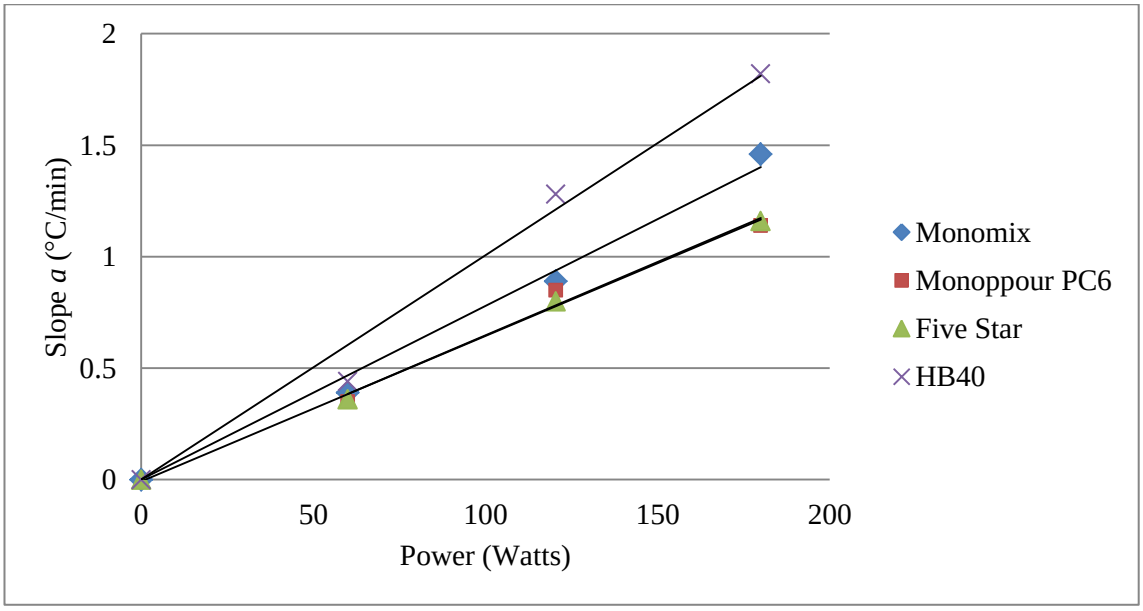

Figure 4.11: Slope α versus power relationship for four repair materials (volume 1 litre).

4.4.6 Effect of w/p ratio on temperature development

The data in Table 4.4 present the water to repair material powder (w/p) ratio, density and the temperature rise at the end of microwave curing for all mixes. The water to powder ratios recommended by the repair material manufacturers were used for each mix. The fresh material density is also provided by the manufacturers.

Based on the data there is no clear trend between these parameters. For example, both Monomix and Monopour PC6 have w/p ratios 0.14 and 0.11 respectively, but the temperature developed after 45 minutes of microwave curing are similar (39.6 °C and 38.2 °C, respectively). Monomix and HB40, on the other hand, have similar w/p ratios (0.14 and 0.13 respectively) and densities (1730 and 1500 kg/m^3, respectively) but they developed significantly different temperatures after 45 minutes of microwave curing. The lower density material developed a higher temperature as would be expected from Equation 4.1.

The rate of temperature rise (Table 4.2) is high for repair materials Fastfill (1.41 °C/min), Pyrapatch (1.64 °C/min) and HB40 (1.28 °C/min). Fastfill and Pyrapatch are rapid setting materials unsuitable for microwave curing. HB40 is a lightweight material (density=1500 kg/m^3) which is the cause for its high temperature rise rate. The temperature rise rate of the remaining repair materials is similar at 0.89, 0.85 and 0.8 °C/min.

Table 4.4: Summary of microwave curing temperature developed in 1 litre of repair materials at 120 Watts in 45 minutes.

Repair material	Water/Powder ratio	Density kg/m^3	ΔT (°C)	dT/dt (°C/min)
Monomix	0.14	1730	39.6	0.89
Monopour PC6	0.11	2280	38.2	0.85
Fastfill	0.14	2140	46.3 (17.1)*	2.32 (0.68)*
Five Star	0.13	2260	36.2	0.80
HB 40	0.13	1500	57.8	1.28
Pyrapatch	0.10	2200	73.8	1.64

*Fastfill has two slopes. The value in bracket refers to the 2nd slope

4.4.7 Effect of ambient temperature on the microwave curing temperature

A summary of results which include the temperature rise (ΔT), the rate of temperature increase (dT/dt) and maximum temperature after microwave curing for 45 minutes at 132 W, is given in Table 4.5 for all repair materials prepared at different ambient

temperatures. Figure 4.12 shows the time-temperature relationships under microwave curing of HB40 repair material prepared at different ambient temperatures of 1.7 °C, 8.9 °C and 15.8 °C (HB40 repair material mixes 1, 2 and 3 respectively, Table 4.5). The graphs are typical of repair materials Monomix, HB40, Five Star and Monopour PC6 (Table 4.5) which shows a linear increase in temperature with time.

The results in Table 4.5 for Monomix, Five Star and Monopour PC6 show that the temperature rise ΔT achieved after 45 minutes of microwave curing is greater at lower temperature, resulting in a higher rate of temperature rise dT/dt at lower ambient temperatures. For example, the temperature rise of Monomix at ambient temperature of 3 °C is 0.88 °C/min compared with 0.80 °C/min at 17.1 °C ambient temperature. The corresponding rates for Monopour PC6 repair material are 0.74 °C/min and 0.59 °C/min for ambient temperatures of 3.2 and 17.8 °C. However, this trend is reversed for repair material HB40 which heats more rapidly at higher ambient temperatures (see Figure 4.12 and Table 4.5).

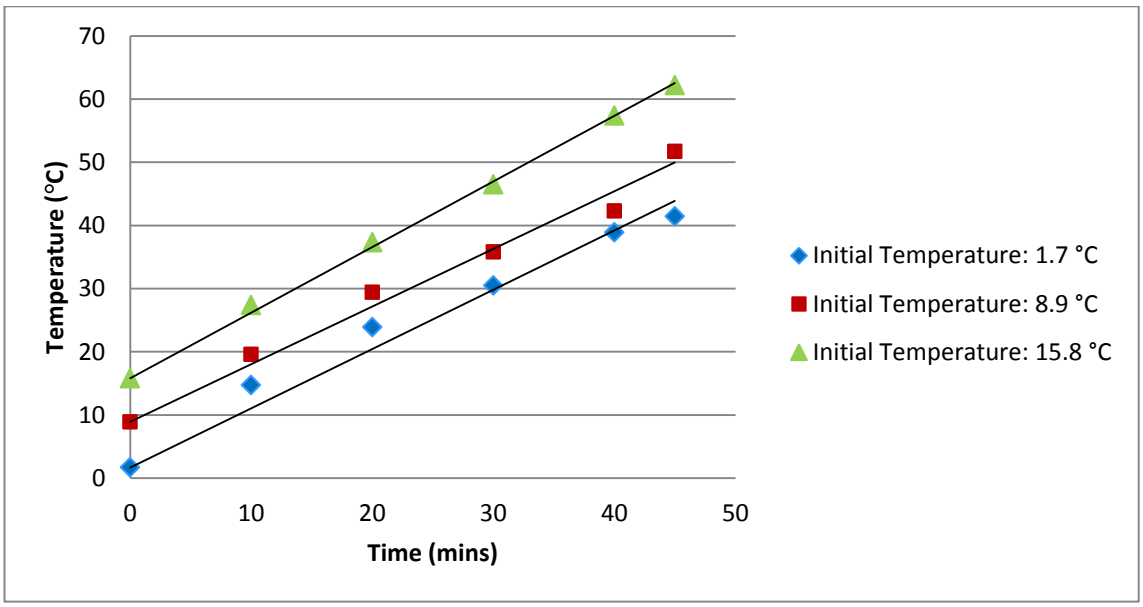

Figure 4.12: Time-temperature profile of HB40 prepared at 1.7, 8.9 and 15.8 °C and microwave cured for 45 minutes at 132 Watts

Table 4.5: Summary of microwave curing temperatures developed at different ambient temperatures

Repair material	Mix number	Power	Volume (L)	Ambient temperature (°C)	Maximum temperature (°C)	ΔT (°C)	dT/dt (°C/min)
Monomix	1	132	3.38	3.0	42.5	39.5	0.88
	2			10.0	47.2	37.2	0.83
	3			17.1	52.9	35.8	0.80
HB40	1			1.7	41.4	39.7	0.88
	2			8.9	51.7	42.8	0.95
	3			15.8	62.2	46.4	1.03
Five Star	1			3.2	30.5	27.3	0.61
	2			9.9	35.0	25.1	0.56
	3			17.8	39.0	21.2	0.47
Monopour PC6	1			6.5	39.9	33.4	0.74
	2			9.1	43.8	34.7	0.77
	3			18.3	45.0	26.7	0.59

4.4.8 General relationship between microwave curing parameters of repair materials

The basic parameters of microwave curing which are power, time and volume are related to the temperature rise provided by microwave curing as shown in Figure 4.13. The data in Figure 4.13 represent all tests listed in Table 4.1 for repair materials Five Star, Monomix and Monopour PC6 and volumes of cubes 1, 3.38 and 4.38 litres. The best fit relationship is given by the equation:

$$\Delta T = \frac{Pt}{\sqrt{V}} \qquad (4.4)$$

Where ΔT is the temperature rise due to microwave curing (°C); P is the microwave power (W); t is the microwave curing time (s); V is the volume of the repair material (dm^3).

Equation 4.4 can be used to design the microwave curing prototype. It can be used to calculate the maximum power rating required to deliver the range of parameters ΔT, t and V specified for in-situ curing of repair.

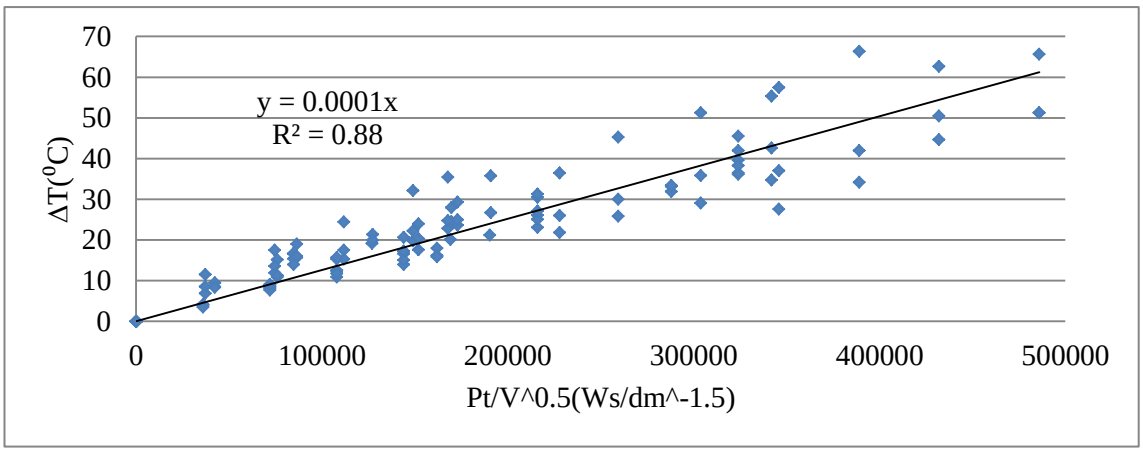

Figure 4.13: General relationship between microwave curing parameters of repair materials Monomix, Five Star and Monopour PC6.

4.4.9 Permissible microwave curing temperature

Temperature of the cement based repair materials at the end of microwave curing is an important parameter that affects their compressive strength at early and later age. Therefore, an acceptable compromise between the rate of strength gain and the long term strength of concrete need to be considered. Based on the literature, temperatures from 40 to 80 °C are considered appropriate at the end of microwave curing [9, 72], nevertheless, temperatures as high as 200 °C are reported [77]. A temperature less than 40 °C does not increase the early age strength of concrete significantly and will not be beneficial except in cold weather. On the other hand, a temperature higher than 70 °C is not only less effective in increasing strength but will also have detrimental effect on the durability of concrete [72]. It is also commonly accepted that higher curing temperature increases the rate of moisture loss which leads to severe shrinkage and cracking problems.

Curing temperature limits need to be integrated into the microwave curing system to control the properties of the repair materials. These limits are based on the permissible temperature of the repair patch at the end of microwave curing, the heat of hydration

which also contributes to the temperature of repair after microwave curing (Figure 4.14) (this will be discussed in Chapter 5) and the factor of safety accounting for microwave curing temperature variations (hot spots). This can be done by adopting the following equations to determine the permissible temperature:

$$\boldsymbol{T_m + \Delta T_h \leq \frac{70}{\gamma_T}} \qquad (4.5)$$

$$\boldsymbol{\Delta T_h = T_h - T_m} \qquad (4.6)$$

where T_m is the permissible temperature at the end of microwave curing (^{o}C); T_h is the cumulative temperature at the end of peak heat of hydration, which equals $T_m + \Delta T_h$; γ_T is the factor of safety accounting for microwave curing temperature variations (hot spots).

The temperature at the hot spots reported here is likely to have been exaggerated by the edge effects of the polystyrene moulds. More accurate information will be obtained from the larger scale trials (Chapter 9) with the microwave prototype. In addition, the prototype has a magnetron of higher specifications than the laboratory ovens, which provides more uniform heating. Consequently, the value of γ_t is likely to be small. Most concrete repairs are relatively small (thin) and, therefore, their volume will not cause excessive heat of hydration. The acceleration of hydration by microwave curing, however, can lead to high temperature before the repair hardens thereby raising durability concerns. The upper limit set by durability considerations regulates the maximum microwave curing temperature T_m. The temperature increase relative to the ambient (T_a), $\Delta t=T_m-T_a$, available for microwave curing at low ambient temperature is high and, therefore, exceeding the durability upper limit temperature is unlikely. A microwave curing temperature limit of about 40 °C is assumed based on the factors discussed above.

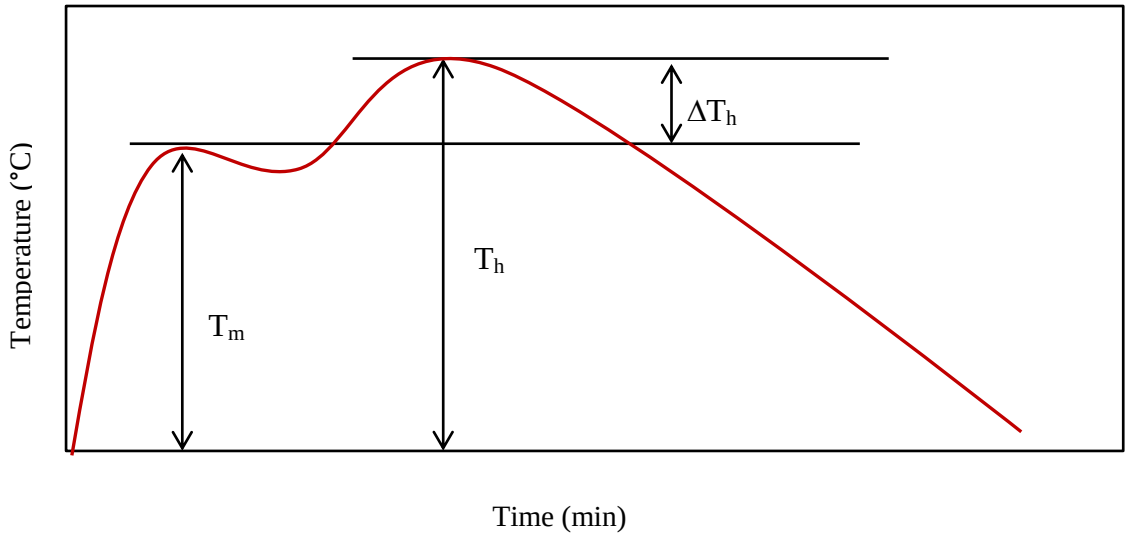

Figure 4.14: Typical temperature increase of a microwave cured repair mortar

4.4.10 Basis for Fixed Time Power Regulating (FTPR) Algorithm of microwave control system

Microwave curing system should be equipped with a control system that provides heating to any concrete repair material in a repair patch of a given volume at a temperature that avoids over heating the repair patch. Figure 4.15 shows an ideal temperature-time profile of a repair patch microwave heated to achieve a target temperature (T_t = 40 °C) within a target period (t_t = 45 minutes), based on the permissible microwave curing temperature (Section 4.4.9) of 40 °C. The duration of 45 minutes of microwave heating would be practical for site curing. The aim of the control system is to adjust the power to generate a temperature-time profile as shown in Figure 4.15. The non-linear temperature-time profile has been determined as optimum for early strength development of concrete mixes [9]. The rate of temperature increase is high at the beginning and is lowered towards the end of microwave curing. The lower rate of temperature increase towards the end of microwave heating provides a more uniform heat distribution and minimises the risk of hot zones.

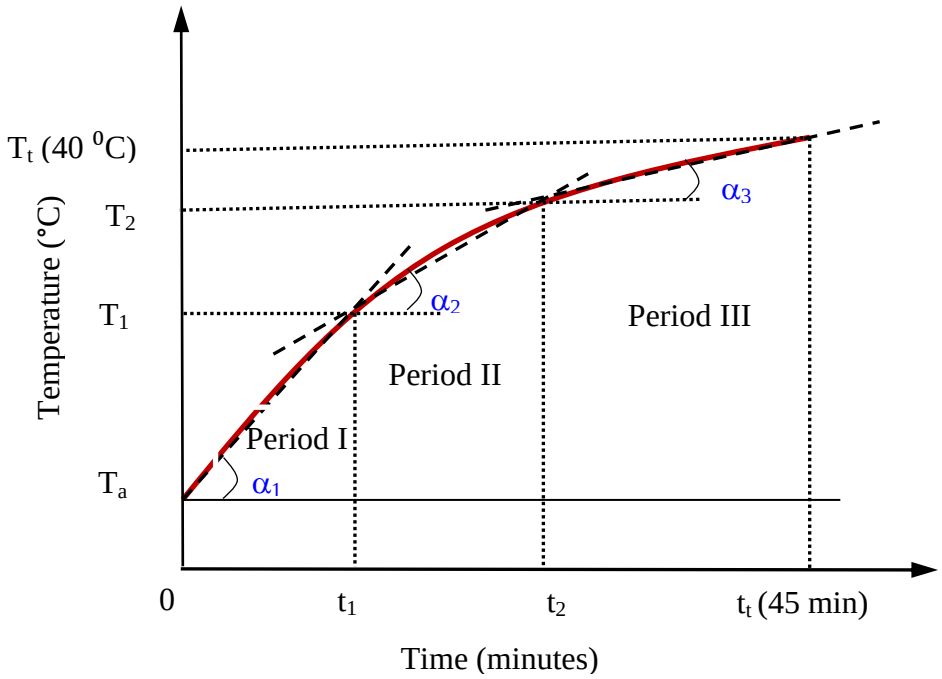

Figure 4.15: Non-linear Temperature versus time relationship of repair under microwave curing, divided into 3 linear periods

For simplicity, the non-linear temperature profile in Figure 4.15 can be replaced by 3 (or more) linear temperature-time profiles as shown in Figure 4.15, representing 3 different decreasing rates of temperature rise (Periods I to III). The target temperatures at the end of periods I, II and III are T_1, T_2 and T_t, which are fed into the control system together with their respective times of t_1, t_2 and t_t. The target values of T_t and t_t have been selected as 40 °C and 45 minutes respectively in the analyses.

Microwave heating of a repair patch of given volume at a microwave power which avoids over heating of the repair material results in a linear temperature-time relationship as shown in Figure 4.16. The slope α of the temperature-time relationship in Figure 4.16 increases linearly with an increase in the microwave power in accordance with the experimental data of four repair materials plotted in Figure 4.11.

A schematic diagram showing the linear relationship of slope α with power is shown in Figure 4.17. The slope in Figure 4.17 is represented by symbol β. Figures 4.16 and 4.17 are supported by experimental data plotted in Figures 4.3 to 4.8 (Section 4.4.3) and Figure 4.11 (Section 4.4.6).

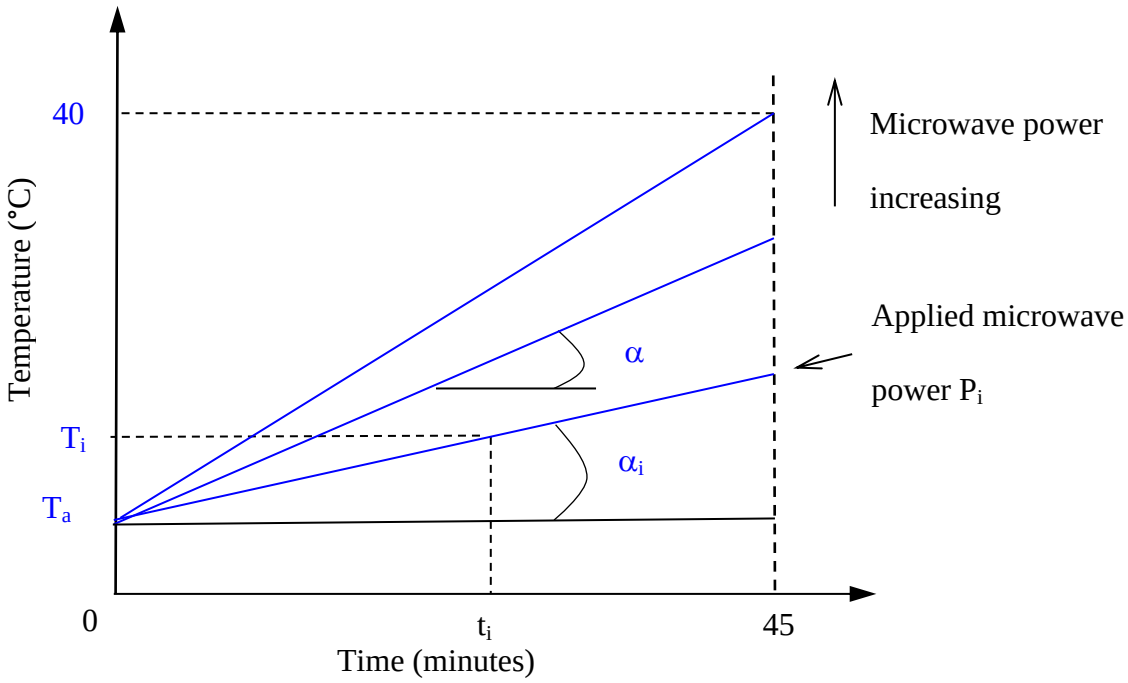

Figure 4.16: Temperature versus time relationship of repair under microwave curing with increasing power input

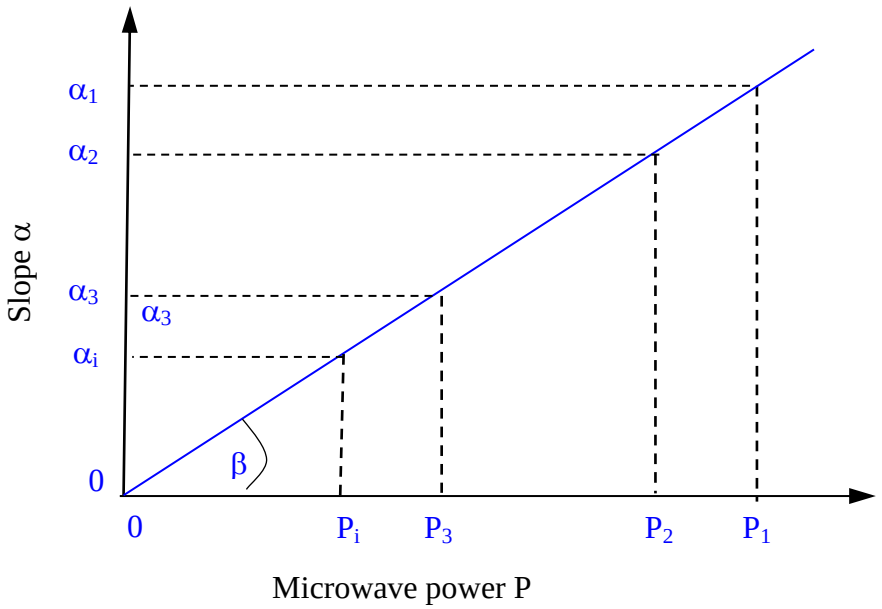

Figure 4.17: Slope α of the temperature-time relationship versus microwave power

The aim of the control system is to provide adequate microwave power to achieve a curing temperature of 40 °C (target temperature) in the repair after 45 minutes (target curing time). This will be achieved by an iterative process providing three decreasing rates of temperature increase (Period I, II, III) shown in Figure 4.15.

At the start of curing (time 0, Figure 4.16), apply an initial microwave power P_i for an initial incremental time t_i. Measure the temperature T_i of the repair surface (by remote sensing) at the initial incremental time t_i. The values of t_i and T_i will enable characterisation of the linear temperature-time relationship of the repair patch cured at microwave power P_i by determining the slope α_i from Figure 4.16 as follows:

Calculation for Period I:

$$\alpha_i = \frac{T_i - T_a}{t_i} \qquad (4.7)$$

where T_a is the ambient temperature.

Since the slope α versus Power relationship of the repair materials is known to be linear (Figure 4.11), the known values of α_i and P_i provide a point on the linear graph of slope α versus power P for the repair patch in Figure 4.17. The graph can now be used to calculate the slope β of the α versus power relationship of the repair patch of Figure 4.17 as follows:

$$\beta = \frac{a_i}{P_i} = \frac{T_i - T_a}{t_i P_i} \qquad (4.8)$$

The temperature-time graph of Figure 4.16 at microwave power P_i in the Period I is re-drawn in Figure 4.18. The target curing temperature of the repair patch at the end of Period I is T_1 °C at time t_1 minutes.

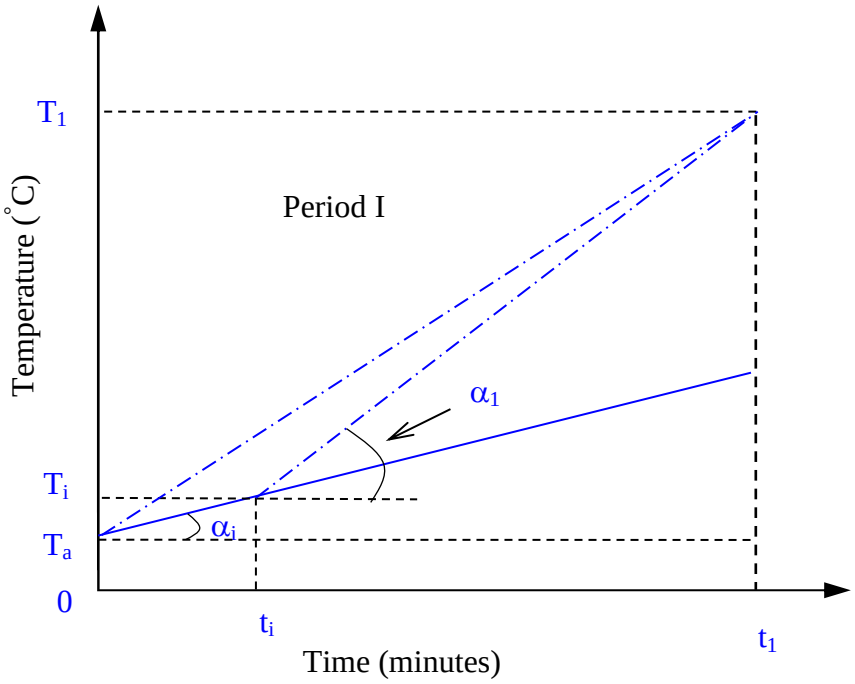

Figure 4.18: Temperature versus time relationship of curing patch in the first curing period of t_1 minutes

The corrected slope α_1 of the temperature-time relationship required to achieve the target temperature T_1 at time t_1 is calculated as follows:

$$\alpha_1 = \frac{T_1 - T_i}{t_1 - t_i} \qquad (4.9)$$

Hence the corrected microwave power input P_1 required after the initial curing period t_i in order to achieve the target temperature T_1 of the repair after time t_1 is calculated from Figure 4.17 as follows:

$$\beta = \frac{\alpha_1}{P_1} \qquad (4.10)$$

Substituting from equations 4.8 and 4.9 gives

$$P_1 = \left(\frac{T_1 - T_i}{t_1 - t_i}\right)\left(\frac{t_i P_i}{T_i - T_a}\right) \qquad (4.11)$$

The three stages of Temperature-time profile in Figure 4.15 which show the temperature-time curing profile of the repair patch over the total 45 minutes period, is presented in Figure 4.19.

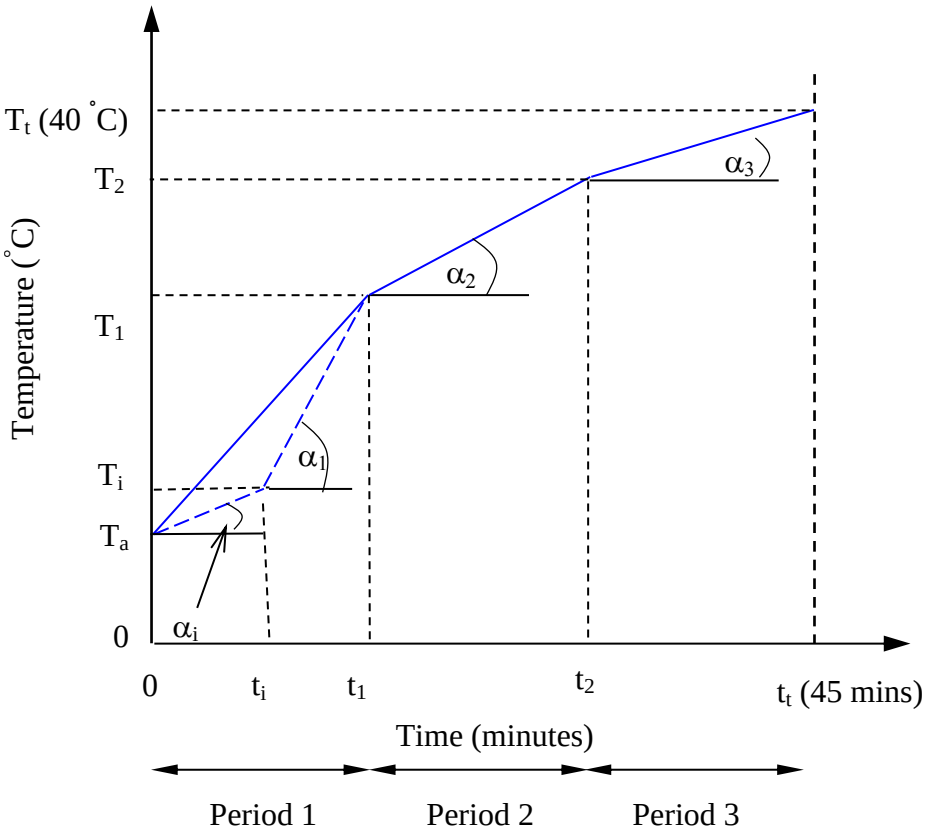

Figure 4.19: Temperature-time curing profile of the repair over 45 minutes

Calculation for Period II:

From Figure 4.19,

$$\alpha_2 = \frac{T_2 - T_1}{t_2 - t_1} \qquad (4.14)$$

From Figure 4.17,

$$\beta = \frac{\alpha_2}{P_2} \qquad (4.15)$$

Substituting for a_2 and β from equations 4.14 and 4.8 gives:

$$P_2 = \left(\frac{T_2 - T_1}{t_2 - t_1}\right)\left(\frac{t_i P_i}{T_i - T_a}\right) \qquad (4.16)$$

Calculation for Period III:

Similarly from Figure 4.19,

$$\alpha_3 = \frac{T_t - T_2}{t_t - t_2} \qquad (4.17)$$

and

$$P_3 = \left(\frac{T_t - T_2}{t_t - t_2}\right)\left(\frac{t_i P_i}{T_i - T_a}\right) \qquad (4.18)$$

Equations 4.11, 4.16 and 4.18 has provided the basis for the Fixed Time Power Regulating (FTPR) algorithm developed to regulate power in order to achieve the target microwave curing temperature in a fixed time period. This algorithm has been incorporated in the control system of the microwave prototype (Chapter 9).

Additional temperature measurements at incremental intervals during periods I, II and III can improve the accuracy of achieving temperature-time profile. The control system

can continuously adjust power supply after each temperature measurements according to the above procedures.

Solved example:

An example is given to show the application of the fixed time power regulating (FTPR) algorithm of the microwave system. In this example, the aim is to determine the rate of temperature increase with time and the microwave power required to achieve a target temperature in a pre-determined period (45 minutes) of microwave curing. A general non-linear Temperature-Time relationship is assumed to provide optimum microwave curing as shown in Figure 4.15. It provides a decreasing rate of temperature increase in three phases (Figure 4.15), which is simplified into linear relationships of period I, II and III.

Now, assume that initially a power of 10 W is applied to a given volume of repair patch for 1 minute, and as a result, the temperature of the repair patch increases from 20 ºC to 20.5 ºC.

T_a = 20 ºC

T_i = 20.5 ºC

P_i = 10 W

Calculation for Period I:

The slope of the initial temperature-time relationship, α_i, is given by Equation 4.7 as:

$$\alpha_i = \frac{T_i - T_a}{t_i} \quad ^\circ C/min \qquad (4.7)$$

$\alpha_i = \frac{20.5-20}{1}$ $\alpha_i = 0.5\ ^0C/min$

Therefore, the slope of the α versus power P relationship, β, is given by Equation 4.8 as:

$$\beta = \frac{a_i}{P_i} = \frac{T_i - T_a}{t_i P_i} \qquad (4.8)$$

$\beta = \frac{0.5}{10} = \frac{20.5-20}{1x10}$ °C/Wmin

$\beta = 0.05$ °C/Wmin

Now, we need to determine the target temperatures at the end of periods I, II and III.

Assume temperature increase in three periods as follows:

Target temperature at the end of Period I = T_1 °C

Target temperature at the end of Period II = T_2 °C

Target temperature at the end of period III = T_t °C

Ambient Temperature is 20 °C and the target temperature at the end of microwave curing is 40 °C, therefore, temperature increase in 45 minutes is 20 °C. The target temperature increases at the end of period I, II and III are assumed to be as follows:

X = 1.5 Y

Y = 1.5 Z

X + Y + Z = 20 °C

1.5 Y+ Y + $\frac{2}{3}$ Y = 20

3.16 Y = 20

Y = 6.32 °C Target temperature increase at the end of Period II

X = 9.47 °C Target temperature increase at the end of Period I

Z = 4.21 °C Target temperature increase at the end of Period III

Calculation for Period I:

$T_1 = 20 + X$ $T_1 = 29.47\ ^{o}C$

$$\alpha_1 = \frac{T_1 - T_i}{t_1 - t_i} \quad (4.9)$$

$\alpha_1 = \frac{29.47 - 20.5}{15 - 1}\ ^{o}C/min$ $\alpha_1 = \frac{8.97}{14}\ ^{o}C/min$ $\alpha_1 = 0.64\ ^{o}C/min$

$$\beta = \frac{\alpha_1}{P_1}\ ^{o}C/Wmin \quad (4.10)$$

$$P_1 = \left(\frac{T_1 - T_i}{t_1 - t_i}\right)\left(\frac{t_i P_i}{T_i - T_a}\right) \quad (4.11)$$

$P_1 = 0.64\ x\ 20$ $P_1 = 12.8\ W$

This means that, after initial power of 10 Watts for the first 1 minute, a power of 12.8 Watts needs to be applied for the next 14 minutes in order to achieve a temperature of 29.47 ºC at the end of period I (15 minutes duration).

Now, we need to calculate the rate of temperature increase in period II from 29.47 ºC to 35.79 ºC (ΔT of 6.32 ºC) in 15 minutes.

Calculation for Period II:

$T_2 = 35.79\ ^{o}C$

$T_1 = 29.47\ ^{o}C$

$t_2 = 30$ mins

$t_1 = 15$ mins

$$\alpha_2 = \frac{T_2 - T_1}{t_2 - t_1} \quad (4.14)$$

$\alpha_2 = \frac{35.79 - 29.47}{30 - 15}$ $\alpha_2 = 0.42\ ^{0}C/min$

Hence the rate of temperature increase during period II is 0.42 ºC/min. The power to achieve this temperature increase is calculated form Equations 4.15 and 4.16.

$$\beta = \frac{\alpha_2}{P_2} \qquad (4.15)$$

$$P_2 = \left(\frac{T_2 - T_1}{t_2 - t_1}\right)\left(\frac{t_i P_i}{T_i - T_a}\right) \qquad (4.16)$$

$P_2 = \left(\frac{35.79-29.47}{30-15}\right)\left(\frac{10}{0.5}\right)$ $P_2 = 8.43\ W$

Calculation for Period III:

Similarly, the rate of temperature increase and power required to achieve a target temperature is calculated using equations 4.17 and 4.18.

T_t= 40 ºC

T_2 = 35.79 ºC

t_t = 45 mins

t_2 = 30 mins

$$\alpha_3 = \frac{T_t - T_2}{t_t - t_2} \qquad (4.17)$$

$$P_3 = \left(\frac{T_t - T_2}{t_t - t_2}\right)\left(\frac{t_i P_i}{T_i - T_a}\right) \qquad (4.18)$$

$\alpha_3 = \frac{T_t - T_2}{t_t - t_2}\ ^0C/min$ $\alpha_3 = \frac{40-35.79}{45-30}\ ^0C/min$ $\alpha_3 = 0.28\ ^0C/min$

A temperature increase rate of 0.28 ºC/min is required in period III to achieve a target temperature (40 ºC). The power required is calculated from equation 4.18.

$$P_3 = \left(\frac{T_t - T_2}{t_t - t_2}\right)\left(\frac{t_i P_i}{T_i - T_a}\right) \qquad (4.18)$$

$$P_3 = \left(\frac{40-35.79}{45-30}\right)\left(\frac{10}{0.5}\right) \qquad P_3 = 5.6\,W$$

Depending on the accuracy required and hence the frequency of temperature measurements taken during periods I, II and III by the microwave control system, multiple iterations can be performed using the above procedure. This can allow adjustment to the applied power to achieve the target temperature accurately.

4.5 Conclusions

Based on the results presented in this chapter the following conclusions can be made:

- Microwave curing is suitable for normal, non-rapid setting repair materials, avoiding excessively high temperatures.
- Considerable variation of temperature occurs on the surface of microwave cured cubes. The hot areas are at the edges of the mould, sometimes showing melting of the polystyrene mould. Elements with larger surface areas have more uniform temperature.
- Variation of temperature on the surface of microwave cured specimens should be taken into account in the cumulative total temperature of the microwave cured material when selecting the permissible microwave curing temperature.
- The following equations provide the limits for the permissible microwave curing temperature:

$$\boldsymbol{T_m + \Delta T_h \leq \frac{70}{\gamma_T}}$$

$$\boldsymbol{\Delta T_h = T_h - T_m}$$

where T_m is the permissible temperature at the end of microwave curing (^oC); T_h is the peak heat of hydration temperature ($T_h = T_m + \Delta T_h$) (^oC); ΔT_h is the increase in temperature after the end of microwave curing due to heat of hydration; γ_T is the factor of safety accounting for microwave curing temperature variations (hot spots).

- The temperature during microwave curing increases linearly with time and power input under the recommended limits of microwave curing temperature which is obtained from the above equation.

- The rate of temperature increase with microwave curing time (slope α=dT/dt) increases linearly with the applied power under the recommended limits of curing temperature (40-45 °C). The rapid setting materials are an exception unless the curing temperature T_m remains below the curing temperature limit.
- An empirical relationship between microwave power and the parameter *t*, *V* and temperature is proposed based on the experimental results as follows:

$$\Delta T = \frac{Pt}{\sqrt{V}} \qquad (4.4)$$

Where ΔT is the temperature rise due to microwave curing (°C); *P* is the microwave power (W); *t* is the microwave curing time (s); *V* is the volume of the repair material (dm^3).

- Fixed Time Power Regulating (FTPR) algorithm of microwave control system is developed to regulate power in order to achieve the target microwave curing temperature in a fixed time period.

$$P_1 = \left(\frac{T_1 - T_i}{t_1 - t_i}\right)\left(\frac{t_i P_i}{T_i - T_a}\right)$$

$$P_2 = \left(\frac{T_2 - T_1}{t_2 - t_1}\right)\left(\frac{t_i P_i}{T_i - T_a}\right)$$

$$P_3 = \left(\frac{T_t - T_2}{t_t - t_2}\right)\left(\frac{t_i P_i}{T_i - T_a}\right)$$

Chapter 5

5. Temperature development in microwave cured repair materials

5.1 Introduction:

This chapter presents experimental results of an investigation to determine the temperature development in microwave cured repair materials. Six proprietary repair materials and a CEM II mortar were studied. It also reports on the moisture loss of the repair materials under microwave curing up to 24 hours after casting.

5.2 Literature review and background

5.2.1 Introduction

A chemical reaction of hydration takes place when cement is mixed with water, which leads to the formation of the binding material. The hydration reactions are complex and not yet fully understood especially in concrete repair materials which incorporate different types of cements and replacement materials, different admixtures and polymers which influence the chemical reactions and alter the properties of the cementitious materials. In addition, most repair materials are proprietary formulations whose constituent details are not available in the public domain.

The most common type of cement used in concrete and repair materials is Portland cement. It is made up of lime (CaO), silica (SiO_2), alumina (Al_2O_3) and iron oxide (Fe_2O_3) [91, 92]. The final compounds of Portland cement are tricalcium silicate ($3CaOSiO_2$), Dicalcium silicate ($2CaOSiO_2$), tricalcium aluminate ($3CaOAl_2O_3$) and

tetracalcium aluminoferrite ($4CaOAl_2O_3Fe_2O_3$). These are simplified by abbreviation to C_3S (alite), C_2S (belite), C_3A (aluminate) and C_4AF (aluminoferrite).

A series of chemical reactions take place with each compound when Portland cement comes in contact with water. The hydration of cement can be affected by several factors such as the type of cement, water to cement ratio, supplementary cementitious materials and the temperature.

5.2.2 Hydration reactions of Portland cement

The first hydration reactions occur with the two types of calcium silicates (tricalcium silicate and dicalcium silicate) which are stoichiometrically very similar and the only difference is the amount of calcium hydroxide formed as can be seen from equations 5.1 and 5.2.

$$2C_3S + 6H \longrightarrow C_3S_2H_3 + 3CH \quad (5.1)$$

$$2C_2S + 4H \longrightarrow C_3S_2H_3 + CH \quad (5.2)$$

The hydration reaction of calcium silicates C_3S and C_2S results in a calcium silicate hydrate which is also known as C-S-H. C-S-H makes up about 50% to 67 % of the volume of the hydrated paste and, therefore, dominates its behaviour. The calcium silicate hydrate particle size is so small that they can be studied only by electron optical techniques. The extremely small size of hydrated products results in a very high surface areas of cement paste.

Calcium hydroxide is a well-crystallized material with large enough crystals to be seen with the naked eye and they only grow where free spaces (voids) are available in concrete. They occupy about 20-25% of the paste volume. Calcium hydroxide may vary in morphology which is affected by the admixtures and by the temperature of hydration.

The next reactions of hydration are of tricalcium aluminate, C_3A, which reacts with the sulphate ions supplied by the gypsum in cement. Gypsum predominantly affects paste set times by delaying the hydration of C_3A. Equation 5.3 shows the reaction of tricalcium aluminate with gypsum which results in the formation of calcium sulphoaluminate, commonly known as ettringite.

$$C_3A + 3CSH_2 + 26H \longrightarrow C_6AS_3H_{32} \qquad (5.3)$$

The reactions of tricalcium aluminate contribute little to the strength of cement paste.

The final reactions are the hydration of tetracalcium aluminoferrite (C_4AF) which forms the same sequence of hydration products as C_3A. The reactions are slow and there are no rapid hydrates to cause a flash set.

The rate of reaction for the above compounds of cement, during the first few days, are in the approximate order $C_3A > C_3S > C_4AF > C_2S$. This is a reasonable assumption, however, it is not entirely true. For example during the hydration reaction of Portland cement, C_3A and C_4AF both compete for sulphate ions from the gypsum reactions, and the more reactive C_3A consumes more sulphate than does C_4AF.

5.2.3 The heat of hydration

The hydration of cement is an exothermic reaction due to the breaking and creating of chemical bonds during hydration and it releases energy in the form of heat. The heat of hydration can be helpful as it provides activation energy which can result in high early age strength especially in cold weather. The quantity of the heat (ΔH) from each reaction can be calculated or measured experimentally. Theoretical calculation of the heat of hydration is possible if the composition of cement compounds and their ΔH for the reaction are known. The resulting temperature can be calculated when the amount of

heat and the heat capacity of the paste is known, assuming there is no heat loss to the surrounding. The heat released from hydration can be used to map the progress of hydration.

The heat released from hydration can be studied with different methods, mainly using a calorimeter. Figure 5.1 shows a typical graph of the rate of heat for plain concrete during the hydration process [93]. The heat generated during the hydration process can be classified into five stages as shown in Figure 5.1.

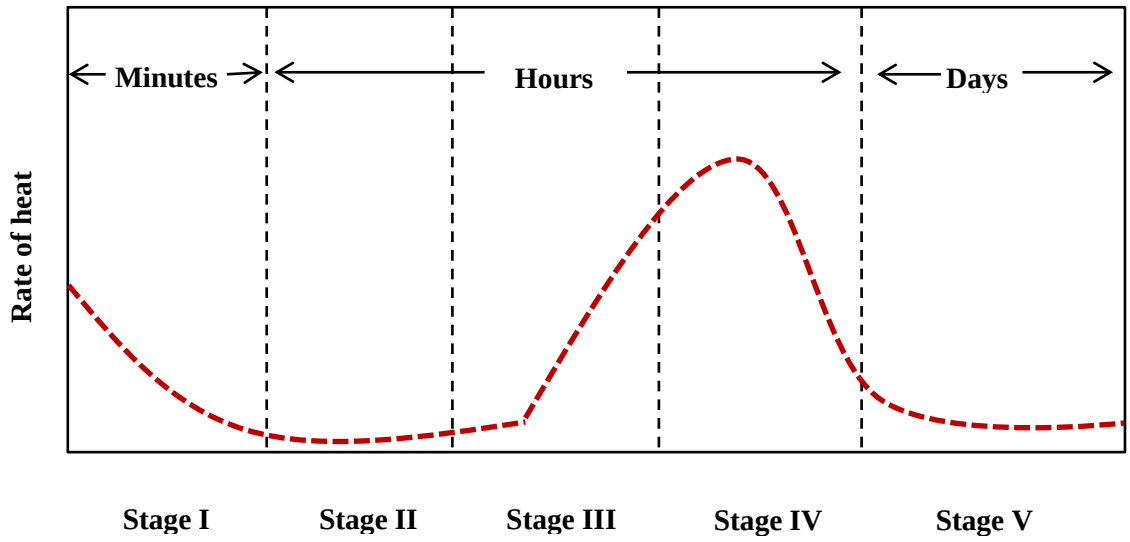

Figure 5.1: Stages during hydration process of plain concrete [93]

5.2.3.1 *Stage I, Pre-induction stage*

Heat is released instantaneously when water is added to the cement. It reaches a maximum value and then the temperature drops. The ettringite produced after initial hydration reactions reduces the rate of reaction in the later part of stage I. Stage I expires within few minutes after adding water to the cement and temperature rises rapidly. This stage has little effect on concrete strength.

5.2.3.2 *Stage II, Induction or dormant stage*

The concrete remains in the plastic state during this stage and there is no strength development. The duration of this stage approximates 1 to 3 hours. Transportation of the fresh concrete mix generally takes place during this period.

5.2.3.3 *Stage III, Acceleration stage*

At the end of the dormant period, there is a sudden rapid increase in the rate of hydration and heat evolves from approximately three to twelve hours after mixing. The initial set of cement usually occurs on the lower side of stage 3, where the rate of hydration is still increasing. The final set generally occurs soon after the maximum exothermic peak is reached [94]. First, the alite (C_3S) and belite (C_2S) in the cement start to hydrate and the release of heat is accelerated. The silicate setting begins and the release of heat accelerates. The silicate reaches a high rate of hydration at the end of this stage. Concrete strength is developed, final setting has finished and early hardening has begun. This stage is very important as it has a direct influence on the later age properties of concrete.

5.2.3.4 *Stage IV, Deceleration stage*

The rate of heat generation further decreases and shifts to a diffusion-controlled process. The thickness of hydrated particles increases and the surface area of unhydrated particles decreases. The layer of cement hydrates acts as a diffusion area to govern the permeability of water and dissolved ions. Ettringite is converted to monosulfate phase which is sometimes noted as the heat contribution of C_3A hydration.

5.2.3.5 *Stage V, Steady state*

The thicker layer of hydrates around the cement particles reduces the rate of hydration remarkably. It is difficult in this stage for hydrates to be precipitated because the space

originally filled by water is covered with hydrated cement. At this stage, the hydration is completely controlled by the diffusion process. This stage is reached after 36 hours. The slow formation of hydration products occurs and continues as long as water and unhydrated silicate are present.

5.2.4 Parameters that affect heat of hydration

The heat of hydration is related to the type of cement, the particle size, the size distribution or fineness, the w/c ratio, chemical admixtures and the curing temperature. Sidney and Young [95] carried out tests with different types of cement such as type I, II, III and IV. Cement type III produces the highest temperature rise, whereas cement type IV provides the lowest temperature rise. The difference in temperature rise is related to their chemical composition and fineness of the cement. The compounds of cements, such as C_3S, C_2S and C_3A, have a different effect on the temperature rise. For example, Lerch and Bogue [96] showed that increasing C_3A content from 0% to 20% increased the heat evolved. They also showed that increasing C_3S content from 16% to 62% increases the heat evolved.

The effect of the fineness of the cement on the temperature rise is due to the increase in specific surface area with increasing fineness [97]. Specific surface area and temperature also affects the workability [98]. The finer cement creates higher specific area and, therefore, higher hydration rate and reduced workability. RILEM 24-CEA 1981 [99] reports that higher water/cement ratio (w/c) results in a higher heat evolution. The heat evolution increased by increasing w/c from 0.30 to 0.70.

Supplementary cementitious materials normally result in slow hydration, slow setting and low heat of hydration temperature [100, 101, 102]. Fly ash with low calcium content is known to reduce the heat of hydration. For example, Nocuń-Wczelik [103]

have shown that the addition of class C fly ash not only reduced the peak heat of hydration but also postponed it. However, some high calcium class C fly ashes may react very quickly with water and release heat similar to OPC [104].

The use of chemical admixtures is a common method for changing the hydration rate and therefore, the heat evolution of concrete. Retarders are common admixtures used in construction to delay the setting and hardening of concrete. On the other hand, accelerators are used to accelerate the hydration and, therefore, higher early age strength development.

The initial (environmental) temperature is another factor that affects the heat evolution of cementitious repair materials. According to the Arrhenius law, increasing the temperature leads to an increase in the reaction rates and, therefore, curing temperature plays an important role in the hydration and microstructure formation of cementitious materials [105, 106]. In practice, concrete repairs are exposed to different climate temperatures, deliberately applied external heat during curing in addition to the heat of hydration. Copeland and Kantro [107] reported an increase in the initial rate of hydration of alite (C_3S) and belite (C_2S) at higher temperature. Kjellsen and Detwiler [108] carried out an experimental investigation on the hydration reaction kinetics of Portland cement mortar cured at incremental temperatures between 5 °C to 50 °C. They reported a higher degree of hydration for higher temperature applied at early age. However, the degree of hydration was levelled at 91 days age. The higher environmental temperature accelerates the hydration at an early age while it decelerates at a later age. Similar results were also reported by Mukesh et al. [105] from a study of the rate of heat evolution during the hydration of Portland cement with different percentages of fly ash and calcium hydroxide at temperatures of 35 and 45 °C. They concluded that the hydration is accelerated with the rise of temperature. A study carried

out by Escalante and Sharp [106] showed that higher initial temperature of OPC accelerates hydration and, therefore, results in higher heat evolution. The lowest heat evolved was for an initial temperature of 10 °C while the highest was recorded for the maximum initial temperature of 60 °C. This knowledge on heat of hydration indicates that early age microwave curing should have significant impact on the heat of hydration of repair materials. It should be noted that achieving a temperature above 70 °C is likely to impact long-term durability of repair such as the risk of sulphate attack due to delayed ettringite formation (DEF) which is often the case for steam curing and for mass concrete. Consequently, the temperature of microwave cured repair materials should be controlled to remain below 70 °C [109] which has been already considered during developing the permissible microwave curing temperature (Chapter 4, Section 4.4.9).

5.2.5 Measurement of heat of hydration

Heat of hydration measurement can provide valuable information about the reactions which occur in the early stages of cement hydration. It can be used to characterise the setting and hardening behaviour of cement and relate it to the properties of the concrete. A large amount of heat evolves within the first few days with the greatest rate of heat generally liberated within the first 24 hours. There are several methods to measure the heat of the hydration [110]. Calorimeter test methods are the most commonly used methods to determine the heat of hydration over time. Calorimeter tests can be classified into three types known as adiabatic, semi-adiabatic and isothermal calorimetry.

Adiabatic refers to a process occurring without the gain or loss of heat. The heat generated during hydration is measured by perfectly insulating a specimen to prevent heat loss or gain and measuring the temperature rise due to hydration as a function of

time. Different test methods and devices have been developed to measure such hydration heat. However, their principle is the same, which is basically to insulate the specimen perfectly and then measure the temperature rise. However, in practice, it is almost impossible to achieve an adiabatic environment, therefore, there will be a heat loss. For example, RILEM TC 119-TCE [111] defines adiabatic as the condition which allows a temperature loss not greater than 0.02 K/h.

The Semi-adiabatic method is similar to the above with the difference of allowing a small amount of heat loss to the environment. This makes the method simple and more practical. Due to the permitted heat loss, the heat of hydration measured by this method is less than that measured by adiabatic methods. However, the heat loss is limited to less than 100 J/hK [111]. This method has been specified in a BS EN 196-9:2010 [112].

The Isothermal hydration method maintains a constant temperature in the system. A calorimeter measures the rate of the heat of hydration generated from the specimen. The temperature of the surrounding environment is kept constant and equal to the temperature of cement. This method was first introduced by Woods et al. [113] and it has been specified in National Standards [114, 115] and the state of the Art Papers PD CEN/TR 1663:2014 [116]. This method uses an isothermal heat conduction calorimeter which consists of a thermostatic heat sink upon which two heat flow sensors are placed. The specimen and reference are connected through the heat flow sensors to a thermostatic heat sink and the difference between two specimens is the output of the calorimeter.

5.2.6 Degree of hydration

The degree of hydration is important as it confirms the fraction of cement that has reacted with water. However, determining the degree of hydration experimentally is

very difficult. Hence, it has been the subject of research [117, 118] to determine the heat of hydration and to relate it to the degree of hydration. Copeland et al. [119] stated that there is an approximately linear relationship between non evaporable water and the heat of hydration, which can be used to estimate the degree of hydration.

The degree of the hydration, which varies from 0 to 1, representing no hydration at all to full hydration, can be calculated as follows [120, 121] :

$$a(t)= \frac{Q(t)}{Q(total)} = \frac{1}{Q(total)} \int_0^t q(t)dt \qquad (5.4)$$

Where a(t) is the degree of hydration at time t; Q_t is cumulated heat of hydration at time t; Q_{total} is cumulated heat of hydration at complete hydration and q is heat production rate.

The challenge in this experiment is to determine the total heat of hydration after complete hydration. The complete heat of hydration for Portland cement can be calculated from the chemical composition of cement as proposed by Bogue [122], however, it is not valid when admixtures or other supplementary constituents are used in the mix, as is normally the case with concrete repair materials.

5.3 Test programme

Two series of tests were carried out to determine temperature development in repair materials during microwave curing and subsequently under laboratory air curing (20 °C, 60 % RH) for up to 24 hours after mixing to determine the effect of a short period of microwave curing on the heat of hydration characteristics. The first series comprised of 100 mm cubes of repair materials with a thermocouple located at the centroid to determine temperature development of seven repair mortars. The second series

comprised of 150 mm cubes of two selected repair materials, which were microwave cured to similar temperature over a similar curing period as the specimens of series 1. The internal temperatures in the 150 mm cubes were determined at different distances from the top surface of the cube. In addition, the water loss of 100 mm cube specimens (series I) was determined during microwave curing and up to 24 hours age.

5.3.1 Repair materials

The following seven repair materials were used in the investigation on microwave curing.

- Five Star
- HB40
- Monomix
- Monopour PC6
- Weber Mortar
- FastFill
- CEMII Mortar (cement/ sand ratio of 1:2 and water/ cement ratio of 0.5).

A description of each repair material is presented in Chapter 3 (Section 3.2). The repair material powders were used as supplied at water/powder ratios recommended by the manufacturers. Details are given in Table 5.1.

Two microwave ovens I and II were used for microwave curing the 100 mm and 150 mm cube specimens of repair materials respectively. Details of the microwave ovens are given in Chapter 3 (Section 3.3.1).

5.3.2 Preparation of cube specimens and curing

Cube specimens were prepared for two series of tests (Table 5.1). Series I tests comprised of 100 mm cubes with a thermocouple installed at the centroid to monitor the

hydration temperature. Specimens from this series were also used to monitor moisture loss during microwave curing and subsequently up to 24 hours. The second series (Series II) comprised of 150 mm cubes with thermocouples installed at four locations along the centroidal axis at a depth of 37.5 mm, 75 mm, 112.5 mm and 150 mm from the top surface. The fourth location (150 mm from top surface) was at the bottom surface of the cube.

Table 5.1: Details of the test Series.

Series	Repair material	w/p*	Cube size (mm)	Microwave Power (W)	Test summary
I	Five Star	0.13	100	60	Temperature development during microwave curing and after up to 24-hour age. These specimens were also used to measure moisture loss during microwave curing and subsequently up to 24 hours age.
	Monomix	0.14			
	Monopour PC6	0.13			
	HB40	0.13			
	Weber	0.10			
	Fastfill	0.14			
	CEM II	0.5(w/c)**			
II	Five Star	0.13	150	132	Temperature development with depth during microwave curing and subsequently up to 24 hours age.
	CEM II	0.5(w/c)**			

* water/powder, ** water/cement

5.3.2.1 ***Series I***

100 mm polystyrene cube moulds (20 mm wall thickness) were used to prepare two cube specimens for each repair material. A "T" type thermocouple was located at the centroid of each cube by securing it to a wooden coffee stirrer stick as shown in Figure 5.2. The tip of the thermocouple was positioned at the centroid of the cube, approximately 5 mm away from the stirrer stick.

The repair materials were mixed in proportions according to the manufacturers' recommendations. The cube specimens were cast, compacted by vibration, and then placed in the laboratory environment (approximately 20 °C and 60% RH) for 30

minutes from the start of mixing. One of the two cubes prepared for each repair material provided the control (normally cured) specimen which was cured in the ambient environment (20 °C, 60 % RH) up to 24 hour age from the start of mixing.

The second cube specimen for each repair material was exposed to microwave curing at a power of 60 Watts at 30 minutes from the start of mixing. Figure 5.3 shows a typical cube specimen inside the microwave oven at the start of microwave curing. Microwave energy was applied to the cube until the centre of its top surface reached a temperature of approximately 40-45 °C which was selected as the target temperature. The top surface and the internal temperature of the cubes were recorded with a Flir i7 thermal camera and a thermocouple at the centroid respectively before the start of microwave curing and then at every 10 minutes until the end of microwave curing. The cube was removed from the microwave oven upon reaching the target temperature and then placed in the laboratory environment along with the normally cured control specimen. The weight of each cube specimen was also measured during the curing period at each increment of time when temperature was recorded. After the end of microwave curing, the internal temperature (thermocouple at the centroid) of the cube was continuously recorded for 24 hours using the Data Taker DT85G digital logger (Figure 5.4). The weight of the cubes was measured at the end of 24 hours.

A different time period of microwave curing was required for the different repair materials to achieve the target temperature of 40-45 °C at a constant power of 60 W. Table 5.2 shows the microwave curing period applied for all repair materials exposed to 60 Watts.

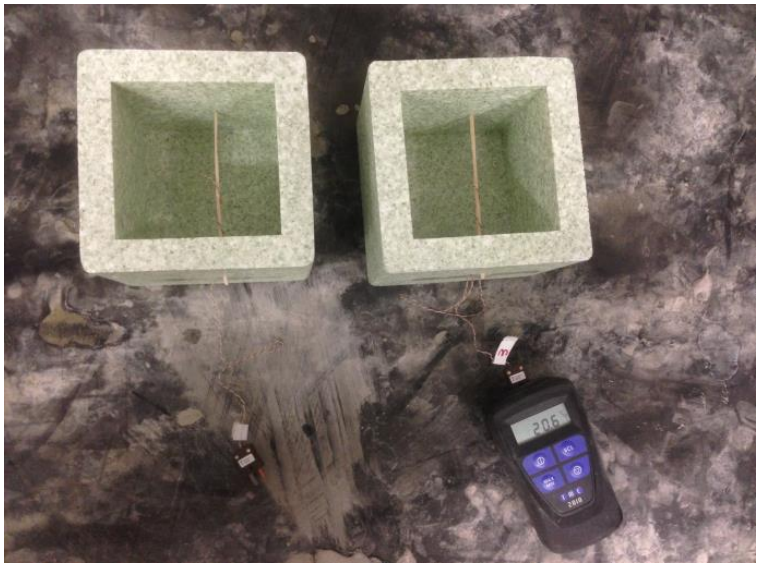

Figure 5.2: Polystyrene mould with support for T-type thermocouple

Figure 5.3: Specimen placed inside microwave oven

Figure 5.4: Set up for monitoring internal temperature

Table 5.2: Microwave curing period for 100 mm cubes of different repair materials

Repair Materials	Microwave Power (Watts)	microwave curing period (mins)	Top surface temperature (°C)
Five Star	60	50	39.9
Monomix		40	40.7
Monopour PC6		40	41.8
HB40		40	44.1
Weber Mortar		45	41.5
Fastfill		15	40.7
CEM II		50	42.1

5.3.2.2 ***Series II***

Series II specimens were cast in 150 mm polystyrene cube moulds (wall thickness of 20 mm) for Five Star and CEM II mortar. T-type thermocouples were located along the centroidal axis of each cube at different depths of 37.5, 75.0, 112.5 and 150 mm from the top surface of the specimens. Figure 5.5 shows the location of the thermocouples inside cube moulds. The temperature at each location was taken at 60 seconds interval using a Data Taker DT85G digital logger. The control specimens were normally cured in the laboratory (20 °C, 60 %RH) for 24 hours after the start of mixing. Microwave cured specimens of both materials were exposed to 130 Watts of microwave energy at 30 minutes after the start of mixing. The temperatures of top surface and at the centroid

of the cube were recorded with a Flir i7 thermal camera and thermocouples respectively before the start of microwave curing and then at every 15 minutes until the end of microwave curing. The maximum top surface temperature achieved at the end of microwave curing for specimens of Five Star and CEM II materials was 43.2 °C and 43.1 °C respectively. At the end of microwave curing, the specimens were placed in the laboratory environment (20 °C, 60 %RH) up to 24 hours age and the internal temperatures were monitored throughout this period.

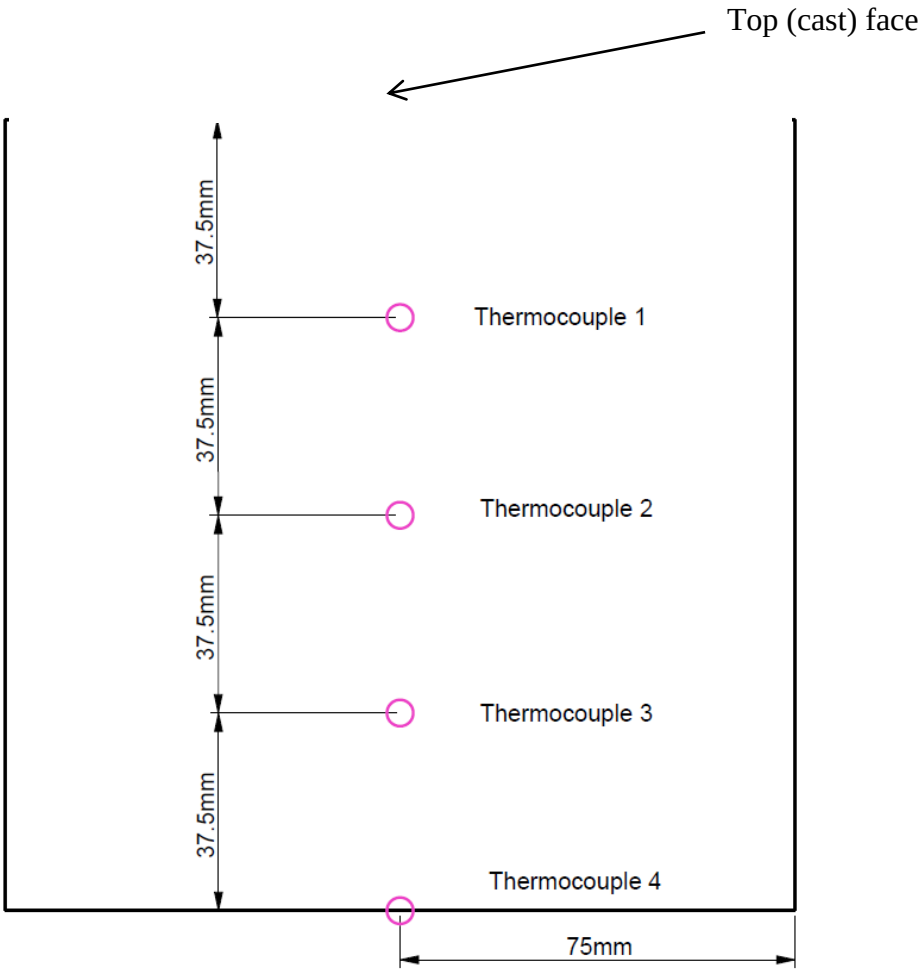

Figure 5.5: Location of thermocouples inside a 150 mm cube specimen.

5.3.3 Determination of moisture loss

The water loss of the specimens during 24 hours after the start of mixing was calculated by recording the mass loss of a specimen during the microwave curing period and

subsequently up to 24 hours. Moisture loss of the normally cured control specimens was also monitored at similar time intervals. The weight of water added to the mix was recorded and the weight loss of specimens during microwave curing was assumed to be due to the evaporation of water. The water loss was calculated as follows:

$$\text{Water loss \%} = \frac{W_0 - W_t}{W_w} \text{ x } 100 \qquad (5.5)$$

where W_0 is the weight of the cube at the start of microwave curing (30 minutes after starting mixing); W_t is the weight of the cube at time t after the start of microwave curing and W_w is the initial weight of water present in the cube.

In addition to the above equation, the weight loss of cube was also determined as follows:

$$\text{Weight loss \%} = \frac{W_0 - W_t}{W_0} \text{ x } 100 \qquad (5.6)$$

Where W_0 is the weight of the cube at the start of microwave curing (30 minutes after starting mixing) and W_t is the weight of the cube at time t.

5.4 Results and discussion

5.4.1 Results of Series I

5.4.1.1 *Surface temperature during microwave curing*

Figure 5.6 (a-f) show typical temperature distributions across the top surface of the cube specimen for Five Star repair material during 50 minutes of microwave curing. The dark square is the polystyrene mould and the cross point at the centre of the thermal image is the location of the thermal camera temperature which is shown at the top left corner of the thermal image. This temperature is used as the top surface temperature plotted in Figure 5.7 for all repair materials. Similar to the results in previous chapter, temperature increases linearly in Figure 5.7 during microwave curing for all materials except Fastfill. The repair materials show slightly different rates of temperature rise, which is related to their dielectric properties. Dielectric properties of repair materials depend on many parameters such as w/c ratio [123], temperature, the electric field inside the microwave cavity, constituents of repair materials and the fineness of powders. However, Fastfill repair material exhibits a completely different time-temperature relationship. This is because Fastfill is a rapid hardening repair material which hardened in 10 minutes of microwave curing and then its time-temperature relationship became much steeper.

Figure 5.8 shows the top surface temperature distribution for all repair materials at the end of microwave curing. The temperature at the centre of the surface ranges from 39.9 to 44.1 °C which is within the target range of 40-45 °C. Temperature variation on the surface is due to the non-uniformity of microwave heating.

(a) at 0 minutes (b) at 10 minutes (c) at 20 minutes

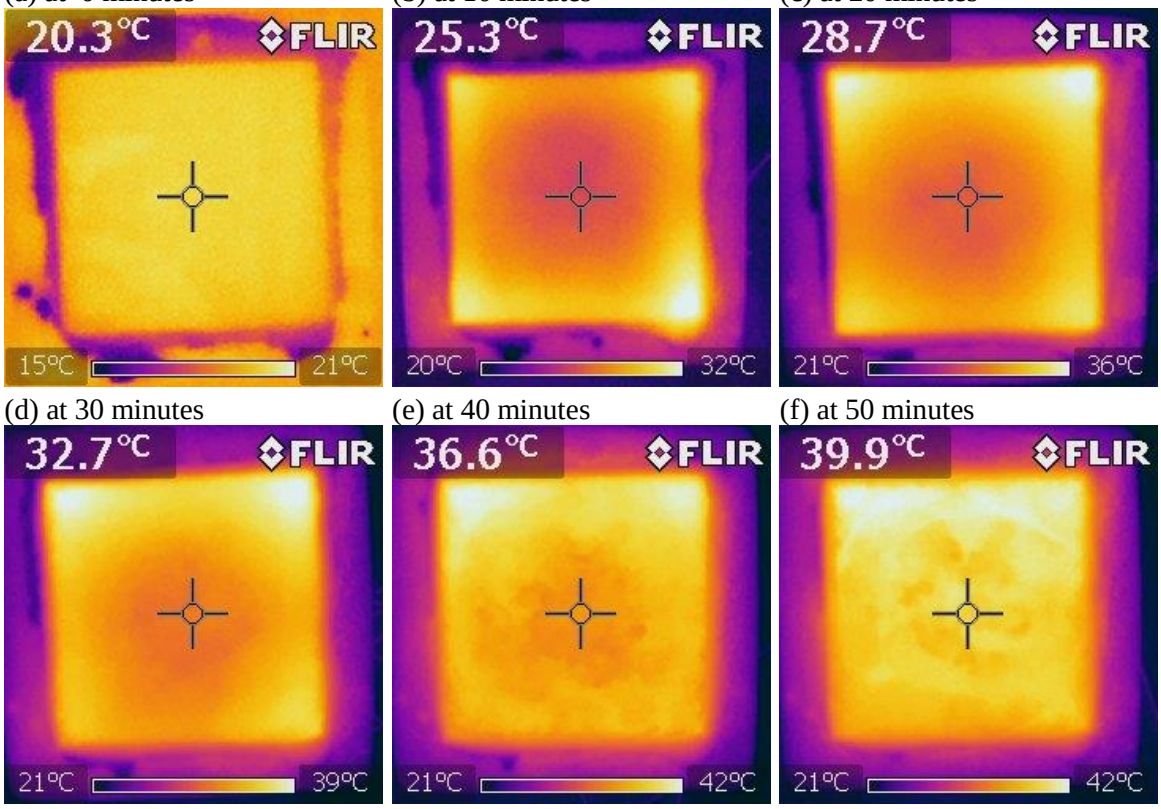

(d) at 30 minutes (e) at 40 minutes (f) at 50 minutes

Figure 5.6: Top surface temperature distribution with time of Five Star repair material exposed to 60 Watts of microwave power

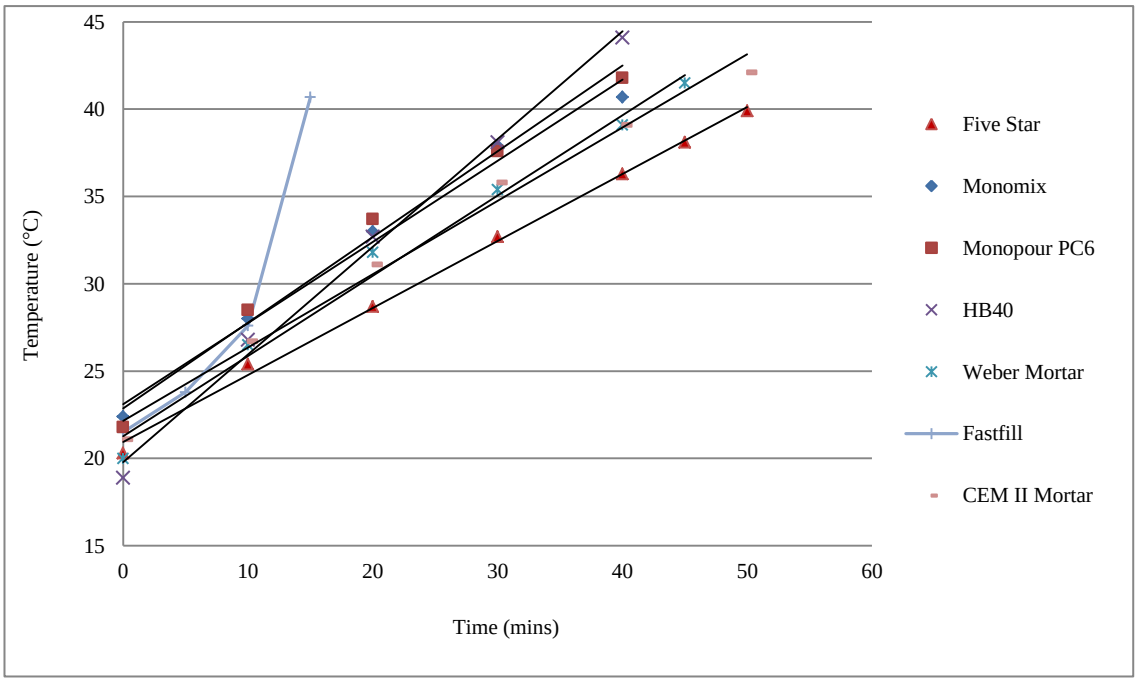

Figure 5.7: Temperature rise with time of different repair materials during microwave curing at 60 W.

(a) CEM II (b) Weber (c) Monopour PC6

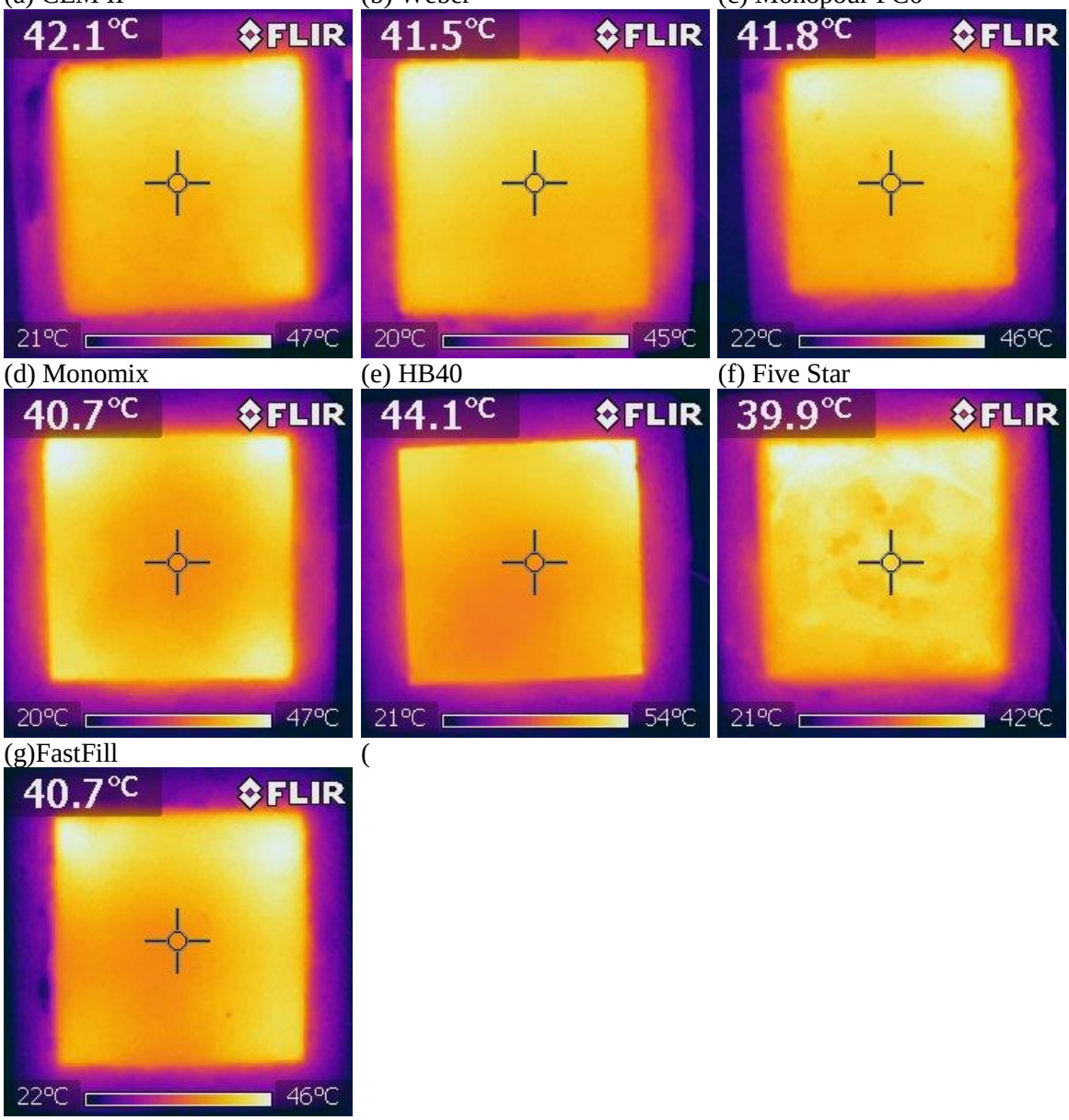

Figure 5.8: Top surface temperature distribution of repair materials at the end of microwave curing at 60 Watts.

5.4.1.2 *Internal temperature during microwave curing*

Temperature development at the centroid of the 100 mm cube specimens (series I), during microwave curing, was monitored from thermocouples for both microwave and normally cured specimens. A typical graph showing the temperature at the centroid of the cube is given in Figure 5.9 for repair material Five Star, which is typical of all repair

materials. In addition, the temperatures at the centre of the top surface, taken with the thermal camera, are plotted for the microwave cured specimens in Figure 5.9.

The internal temperature of the normally cured specimen (20 °C, 60 % RH) in Figure 5.9 is constant and stayed unchanged at 22.5 °C during the microwave curing period of up to 50 minutes. That is the time which refers to the dormant period of hydration (stage II) as seen previously (Figure 5.1). However, for microwave cured specimens, the internal temperature increased linearly and reached 57.5 °C at the end of microwave curing.

A comparison between the internal and top surface temperature of microwave cured specimens shows that the top surface temperature is lower than the internal. The difference starts getting bigger as microwave curing time goes beyond 10-20 minutes for the different repair materials. At the end of 50 minutes, the interior temperature reached 57.5 °C, while the top surface temperature only reached 39.9 °C. The hot spot surface temperature is up to 42 °C (Figure 5.8 f) which is significantly less than the internal temperature.

Table 5.3 presents the internal and top surface temperature at the end of microwave curing for all repair materials. The differences between the top surface and internal temperature ranged from 10.0 °C to 23.7 °C for all repair materials (except Fastfill) at the end of microwave curing. Fastfill is an exception due to its rapid setting and hardening. These differences in centroid and top surface temperature can be due to convective heat loss from the top surface of the specimen. In addition, evaporation of water from the exposed top surface may affect temperature due to drying of the surface. This effect will be discussed further in Section 5.4.5.

Higher internal temperature for microwave cured specimens is not in agreement with analytical simulations done by researchers especially in the food industry [124, 125, 126] nor with the results of Series II tests (Section 5.4.3.1). The analytical studies have simulated temperature profiles at different depths mainly in foods and the results showed a decrease in microwave penetration with depth and a higher top surface temperature. Most of these analytical studies assumed a maximum thickness of 20-30 mm which is much less than the 100 mm cubes discussed here. The simulations exposed solids on one or two sides [127] to high power for a few minutes, whereas the concrete cubes were exposed to microwaves on all faces at low power for 40-50 minutes. This aspect is also discussed in Section 5.4.3 in the content of Series II tests.

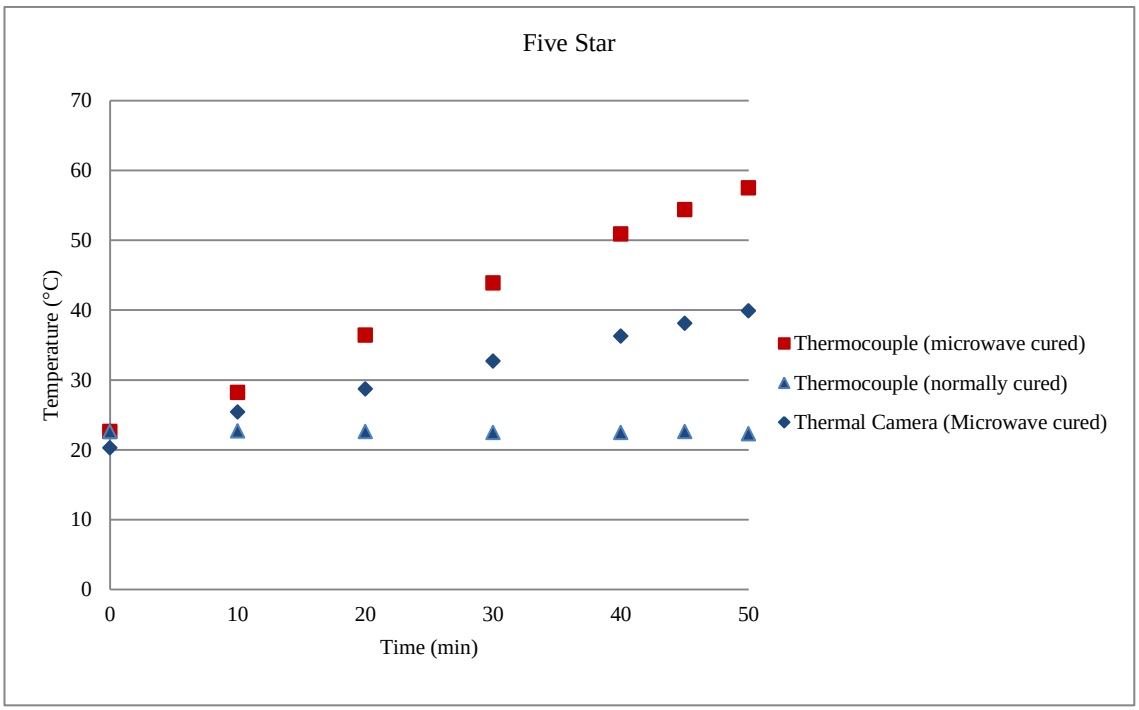

Figure 5.9: Temperature-time relationship of Five Star (specimen: 100 mm cube).

Table 5.3: Temperature of microwave cured specimens (100 mm cubes) at the end of microwave curing

Repair Materials	Temperature at the end of microwave curing (°C)			Water content of fresh cube (g)	Moisture loss (%)[2]
	Surface (thermal camera)	Centroid (thermocouple)	Temperature difference (ΔT_1)[1]		
Five Star	39.9	57.5	17.6	253.67	3.04
Monomix	40.7	59.8	19.1	222.62	2.35
Monopour PC6	41.8	51.8	10.0	230.18	2.08
HB40	44.1	67.8	23.7	186.44	2.39
Weber Mortar	41.5	51.5	10.0	207.85	2.58
Fastfill	40.7	46.4	5.7	305.97	0.70
CEM II Mortar	42.1	53.0	10.9	268.16	2.44

[1] Temperature difference between surface and centroid at the end of microwave curing.
[2] Based on equation 5.8

5.4.1.3 *Internal temperature profile shortly after microwave curing*

Immediately after microwave curing, the internal temperature at the centroid of the 100 mm cubes continued to rise for all repair materials. Figure 5.10 shows a typical temperature profile for microwave and normally cured specimens of repair material HB40 for the duration of 70 minutes from the start of microwave exposure. The microwave heating stopped at 40 minutes and the internal temperature continued to rise gently to reach a maximum value. The temperature increased linearly during microwave curing and continued to increase at a similar rate for about 4 minutes after the microwave stopped. Then the rate of temperature rise levelled off until the maximum temperature of 71.1 °C was achieved at 60 minutes after starting microwave curing (20 minutes after microwave stopped). The internal temperature at the centroid of the normally cured cube specimen, however, stayed unchanged during this period.

Figure 5.11 shows the internal temperature profile for microwave and normally cured 100 mm cube specimens of CEMII mortar for the duration of 70 minutes from the start of microwave exposure. The microwave heating stopped at 50 minutes and the internal temperature continued to rise gently, similar to the HB40 material, to reach a maximum

value. Again, the temperature increased linearly during microwave curing and continued to increase at the similar rate for a few minutes after the microwave stopped. Then the rate of temperature rise levelled off until the maximum temperature of 55.4 °C was achieved at 60 minutes after starting microwave curing (10 minutes after microwave stopped). The internal temperature of the normally cured specimen, however, stayed unchanged during this period.

Similar results were observed for all repair materials. Table 5.4 gives the maximum internal temperature at the centroid of the 100 mm cube specimens and the time when it is achieved for microwave cured specimens of all repair materials. Table 5.4 shows that the maximum temperatures were achieved after 4 to 60 minutes from the time when microwave was stopped. The likely reason for the continuous rise of temperature after the microwave stopped was accelerated hydration caused by high temperature (see Section 5.4.1.4) and by redistribution of temperature from the hot zones which were observed at the end of microwave curing and subsequently became uniform.

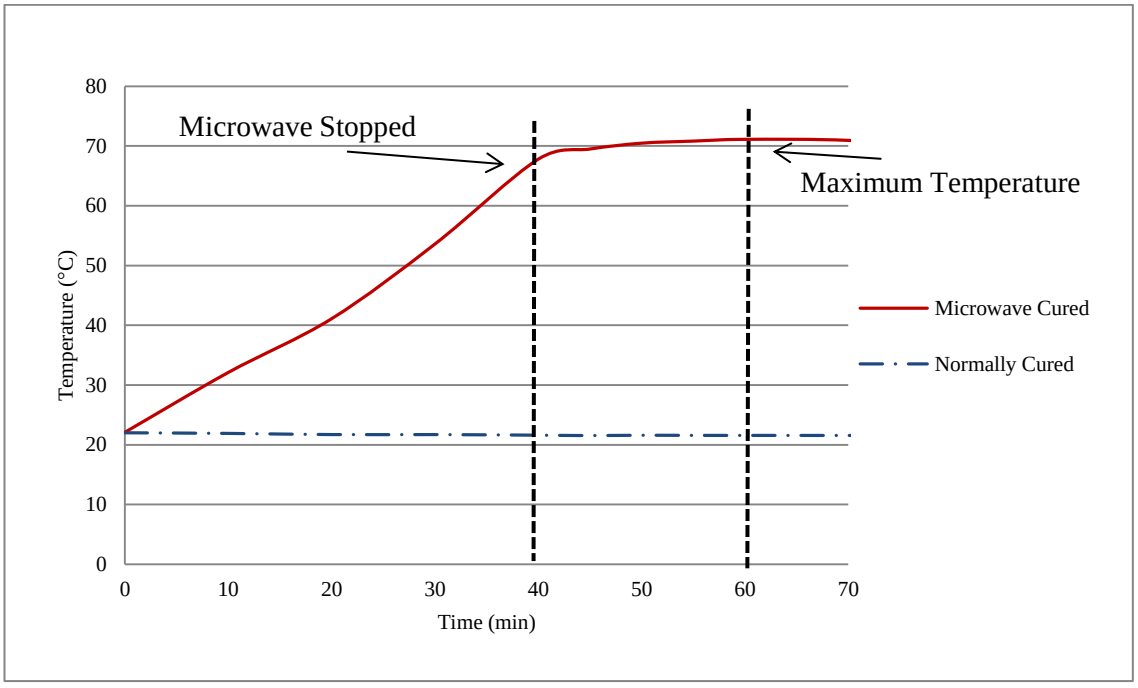

Figure 5.10: Internal temperature of microwave and normally cured HB40 repair material (100 mm cube).

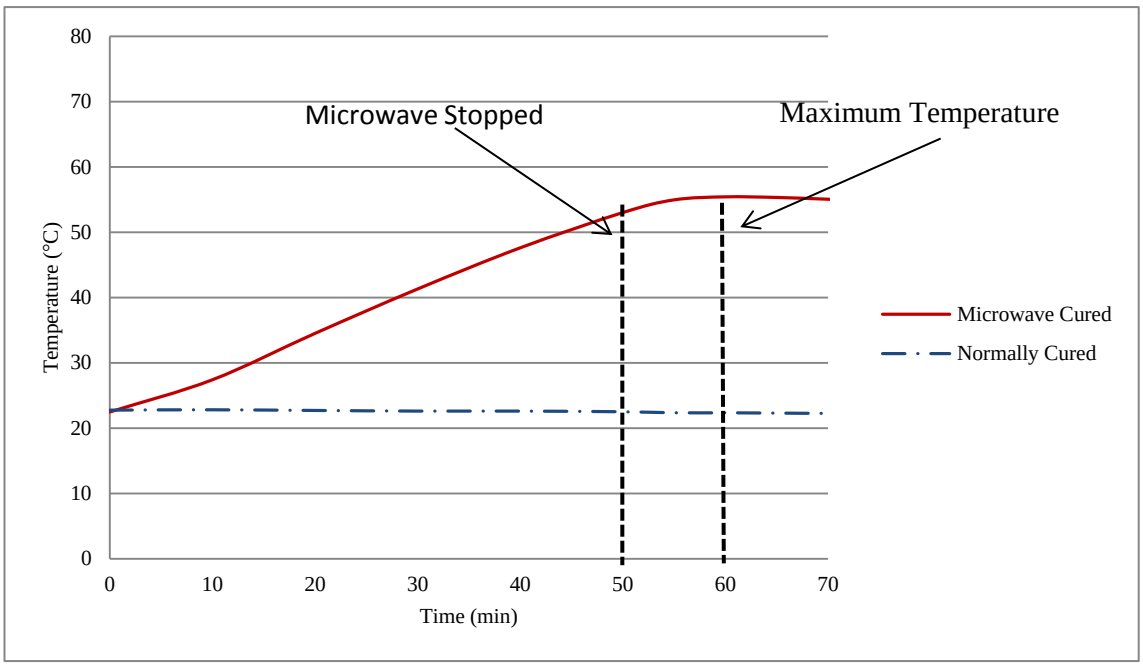

Figure 5.11: Internal temperature of microwave and normally cured of CEM II mortar (100 mm cube).

Table 5.4: Time period and internal temperature at the end of microwave curing and at maximum temperature (Series I, 100 mm cube).

Repair Material	At end of microwave curing		At maximum temperature		Temperature difference (ΔT_2)
	Time (mins)[1]	Temperature (°C)[2]	Time (mins)[1]	Temperature (°C)[2]	
Five Star	50	57.5	55	58.2	0.7
Monomix	40	59.8	100	65.5	5.7
Monopour PC6	40	51.8	50	53.8	2.0
HB40	40	67.8	60	71.1	3.3
Weber	45	51.5	49	52.1	0.6
Fastfill	15	46.4	30	65.3	18.9
CEM II Mortar	50	53.0	60	55.4	2.4

[1] From the start of microwave curing
[2] Internal temperature taken by thermocouples

5.4.1.4 *Internal temperature development during 24 hours*

Figures 5.12 to 5.18 show the internal temperature profiles for normally and microwave cured specimens (at centroid of 100 mm cubes) for all repair materials during 24 hours after commencing mixing. All normally and microwave cured specimens achieved their peak of hydration temperature during the 24 hours. The time to achieve the peak heat of hydration depends on the type of cement blend and admixtures [128, 129], therefore, the

different repair materials achieved their peak heat of hydration at different times and temperatures.

Microwave curing impacts the heat of hydration, as shown in Figures 5.12 to 5.18, by reaching the peak temperature much earlier than normally cured repair materials. The internal temperature continued to increase for some time after microwave heating stopped. The peak heat of hydration temperature for Fastfill repair material occurred at the end of microwave curing (Figure 5.12) and remained constant for nearly 15 minutes. The normally cured specimen of Fastfill repair material (Figure 5.12) had a very similar heat of hydration temperature profile due to its rapid hardening properties. On the other hand, the microwave cured Weber repair material shows two peak temperatures (Figure 5.17). The first peak was after the end of microwave heating and the second peak of 32.5 °C was due to the hydration heat, which occurred at approximately 800 minutes after the start of mixing. The normally cured sample of Weber repair material reached the maximum heat of hydration temperature of 32.3 °C, similar to the microwave cured sample, at approximately 1350 minutes after the start of mixing.

The peak heat of hydration under microwave curing for the repair materials occurred between the end of microwave curing and before the peak of hydration temperature was reached in their normally cured specimens. This is due to the acceleration of hydration caused by high temperature [7]. The peak heat of hydration almost merged with the end of microwave curing period in some materials such as Fastfill (Figure 5.12) and HB40 (Figure 5.16). For instance, the hydration temperature of the microwave cured rapid hardening Fastfill peaked at about 15 minutes after the end of microwave curing (60 minutes after start of mixing) whereas the hydration temperature of the corresponding normally cured Fastfill peaked at 80 minutes (Figure 5.12) after the start of mixing.

Other materials such as Monopour PC6, Five Star and CEM II reached their peak heat of hydration during the cooling down period after microwave curing. In each case, the normally cured specimens reached their peak hydration temperature later than the microwave cured specimens. Table 5.5 provides the details of maximum temperature and the time taken from the start of microwave curing to reach these temperatures for all repair materials. The time difference Δt between reaching the peak hydration temperature and end of microwave curing ranges between 4 and 60 minutes. However, in the case of Weber repair material the second peak hydration temperature of after microwave curing occurred after 800 minutes (Figure 5.17).

Figures 5.14, 5.16 and 5.18 show that the normally cured materials have a short dormant period (200 to 300 minutes) before hydration temperature starts rising. This relates to the peak hydration temperature of the corresponding microwave cured specimens occurring soon after the end of microwave curing. On the other hand, Figures 5.13, 5.15 and 5.17 show that the normally cured materials have a long dormant period (600 to 900 minutes) before hydration temperature rise. In these cases the peak hydration temperature of the corresponding microwave cured specimens occurs during the cooling down period after microwave curing. This reflects the composition of the repair materials when cement replacement materials or retarder have prolonged the dormant period.

The results presented here are in agreement with other researchers who investigated the effect of temperature on heat of hydration [106, 130] of different cements cured at elevated temperature with conventional heat. For example, Hill et al. [130] reported the peak of heat evolved and the time it occurs for OPC hydrated at various temperatures (20, 40 and 90 °C) by means of isothermal conduction calorimetry. They reported that

increasing temperature results in a higher peak of heat of hydration and it occurs earlier. For example, OPC hydrated at 20 °C shows a peak of heat of above 3.5 W/kg and it occurs at about 12 hours. The corresponding peak of heat is 11 W/kg and it occurs at about 5 hours for OPC hydrated at 40 °C. However, under conventional thermal curing used by the researchers [106, 130], heat was applied throughout the experiment (approximately 24 hours) to keep the elevated curing temperature constant whereas microwave heating in this investigation was applied only for a short time (up to 50 minutes). For example, normally cured CEM II mortar shows a maximum internal temperature of 26.7 °C at 630 minutes after casting. The corresponding temperature for microwave cured CEM II mortar is 55.4 °C at 90 minutes after casting. This is a significant result which indicates that even a short time of microwave curing actually can have a similar effect on the peak of hydration and the time it occurs.

Table 5.5: Details of the maximum temperature and the occurring time during the maximum heat of hydration.

Repair Materials	Microwave curing period (min)	Peak hydration: Microwave cured			Peak of hydration: Normally cured	
		Time (min)[1]	Maximum temperature (°C)	Time difference (Δt) (min)[2]	Time (min)[1]	Maximum temperature (°C)
Five Star	50	55	58.2	5	1200	24.9
Monomix	40	100	65.5	60	650	32.6
Monopour PC6	40	50	53.8	10	1350	27.3
HB40	40	60	71.1	20	600	34.0
Weber Mortar	45	49	52.1	4	1350	32.3
CEM II Mortar	50	60	55.4	10	600	26.7
Fastfill	15	30	65.3	15	50	59.3

[1] Time from start of microwave curing.
[2] Time difference for microwave cured specimens between reaching the peak temperature and the end of microwave curing.

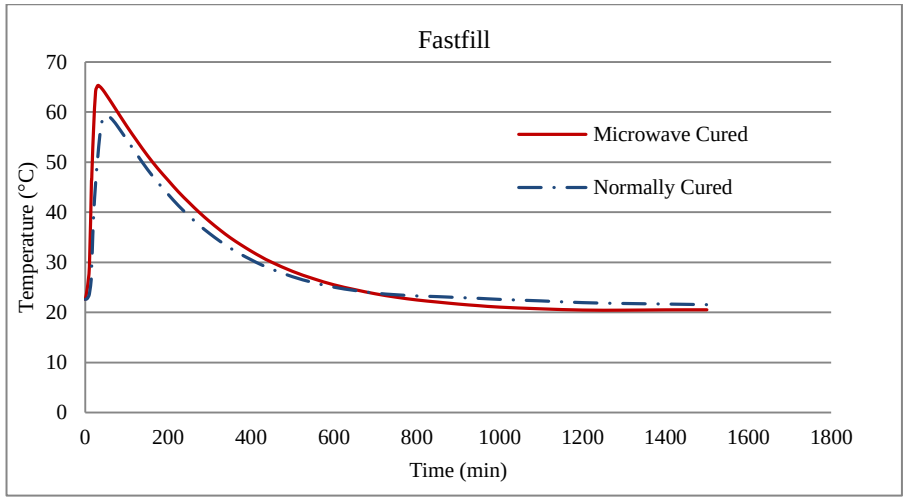

Figure 5.12: Internal temperature of microwave and normally cured Fastfill repair material.

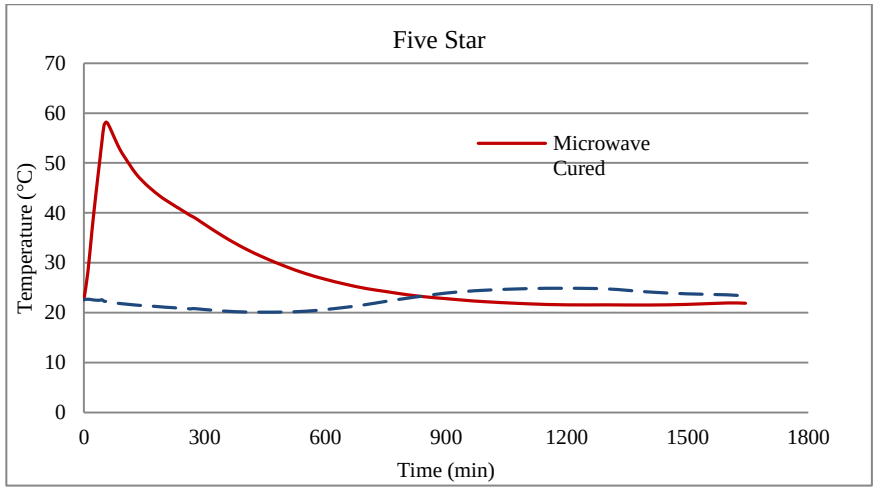

Figure 5.13: Internal temperature of microwave and normally cured Five Star repair material.

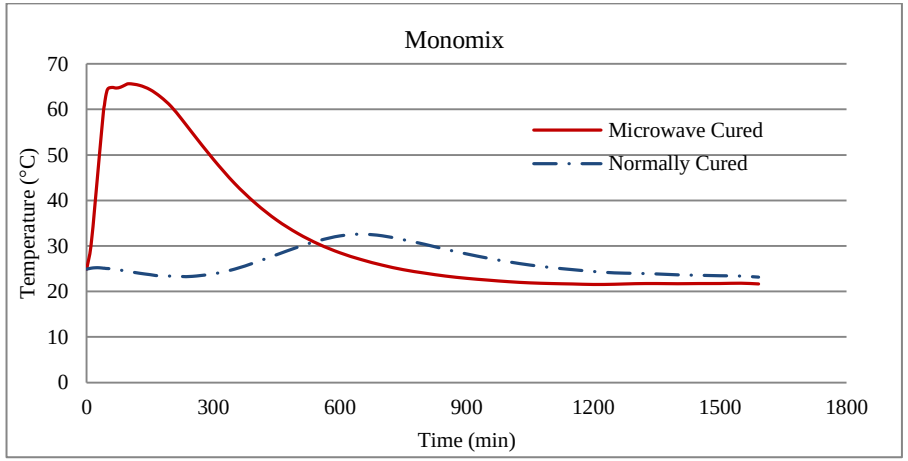

Figure 5.14: Internal temperature of microwave and normally cured Monomix repair material.

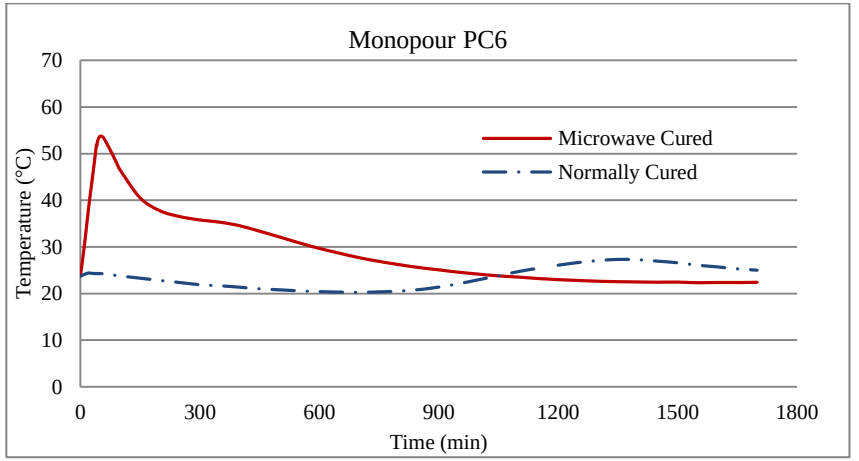

Figure 5.15: Internal temperature of microwave and normally cured Monopour PC6 repair material.

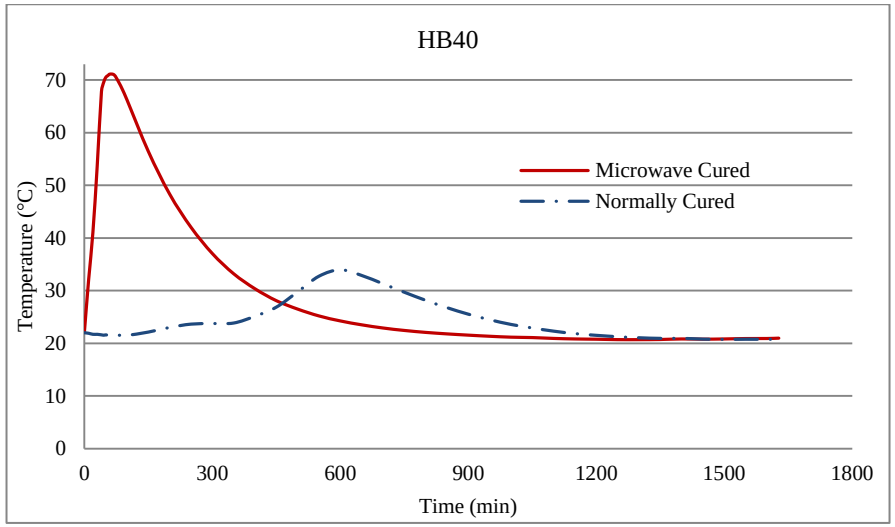

Figure 5.16: Internal temperature of microwave and normally cured HB40 repair material.

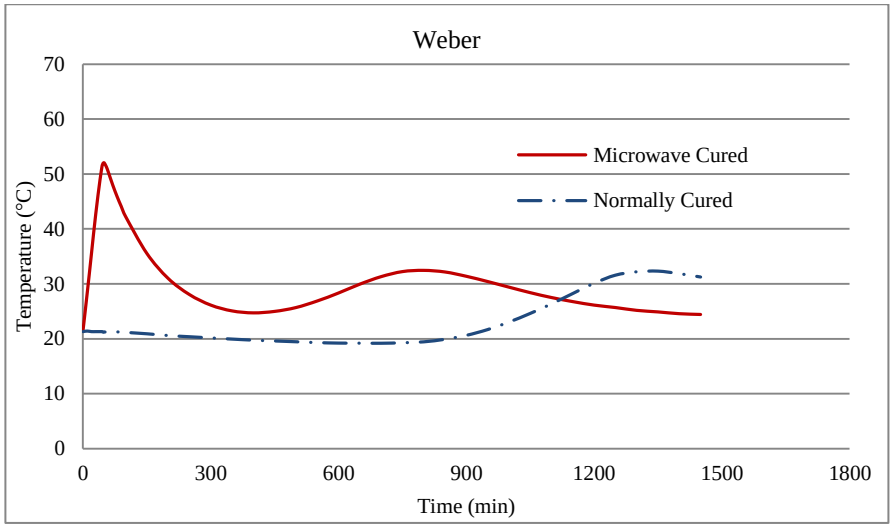

Figure 5.17: Internal temperature of microwave and normally cured Weber Mortar repair material.

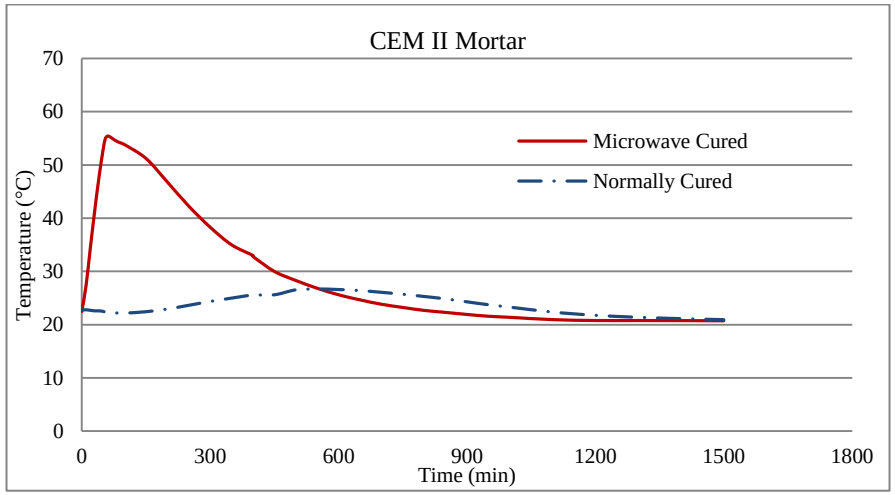

Figure 5.18: Internal temperature of microwave and normally cured CEM II Mortar.

5.4.2 Discussion of Series I results

The tests reported represent semi-adiabatic conditions of hydration of small volumes (100 mm cubes) of repair mortars cast in insulative polystyrene moulds. A short period of early age microwave curing of the cubes results in the acceleration of the hydration process and brings forward the peak hydration time relative to the control specimens which were continuously exposed to ambient conditions (20 °C, 60 %RH). The occurrence of the peak hydration temperature in some repair materials almost coincided with the end of the microwave curing period.

The maximum internal microwave curing temperature at the end of microwave curing ranged between 46.4-67.8 °C while the surface temperature ranged between 39.9-44.1 °C (Table 5.3). The corresponding maximum temperatures achieved by the microwave cured cube specimens occurred at the peak hydration time and ranged between 52.1 and 71.1 °C (Table 5.4).

It is clear that the internal temperatures both at the end of microwave curing and at the time of peak hydration exceed the surface temperature of 40-45 °C which was set as the target temperature. The target temperature was set to satisfy the criteria for early strength development and durability. An adequate factor of safety was provided to prevent temperature rise beyond 70 °C to prevent long term durability problems [7]. However, the internal temperatures monitored with the thermocouples have considerably exceeded the target surface temperatures and entered the durability risk zone [7]. However, these results are based on test samples of very small volume in insulative polystyrene moulds, which do not represent large repair patches on site. The next section of this chapter reports an investigation of larger specimens (150 mm cubes)

of two selected repair materials to gain more information on internal temperature development.

5.4.3 Results of Series II tests

5.4.3.1 *Internal and surface temperature development during microwave curing*

Figures 5.19 and 5.20 show the internal temperature at different depths for microwave cured CEM II and Five Star repair materials. The 150 mm cube specimens were exposed to 130 W of microwave energy for 45 minutes to reach microwave curing temperature of 43.1 °C and 43.2 °C respectively at the top surface. These are similar to the curing temperatures of the 100 mm cubes of these materials reported in the previous section, which were 42.1 °C and 39.9 °C respectively.

The internal temperature recorded by thermocouples is similar (21 °C) at all depths before the start of microwave heating (at 0 minutes, Figures 5.19 and 5.20). The top surface temperature recorded at time 0 by the thermal camera is lower (17 °C), similar to the room temperature. At the end of microwave curing, the CEM II repair material achieves a temperature range 43.2 to 50.0 °C from the top surface to the bottom of the specimen, respectively. The lower temperature of 43.2 °C at the top surface is due to the loss of heat by convection to the room temperature and due to the drying of the surface by evaporation of water. The maximum temperature of 50 °C occurs at the bottom surface (thermocouple 4) which is insulated by the polystyrene mould base. The remaining internal temperatures at the positions of thermocouples 1, 2 and 3 are fairly similar at each monitoring time. Similar temperature profiles were observed for the Five Star material during microwave curing as shown in Figure 5.20. The temperature

increased linearly with time and at the end of microwave curing it ranged from 43.1 to 48.7 °C across the depth of the specimen.

The temperature recorded at the centroid of the specimen (thermocouple 2) in CEM II mortar is slightly higher (2.7 °C) than the top surface (thermal camera) temperature while it is almost the same for Five Star repair material. These results indicate that monitoring the top surface temperature of 150 mm cubes by the thermal camera provides a reasonably accurate representation of the internal temperature of the cube except at the insulated base.

A comparison of Figure 5.20 (for 150 mm cubes) and Figure 5.9 (for 100 mm cube) representing Five Star repair material show a greater difference between the thermal camera and centroid temperature for the 100 mm cube specimens than the 150 mm cubes. At the end of microwave curing after 45 minutes to 50 minutes the thermal camera temperature for both cube sizes is similar at about 40 °C. However, the internal temperature at the centroid is much greater in the 100 mm cube (over 55 °C) while the thermal camera (surface) and internal temperature are similar for the 150 mm cube. This indicates that the volume of material is an important factor in creating the differential in the surface and internal temperature. Therefore, in practical repairs which are normally of a relatively larger volume and surface area, the top surface temperature will provide a reliable representation of the internal temperature under microwave curing. This will be verified further in the field trials reported in Chapter 9. In addition, the insulation provided to the five faces of the cube by the polystyrene mould is likely to be more effective in the small volume of the 100 mm cube thereby causing high internal temperature.

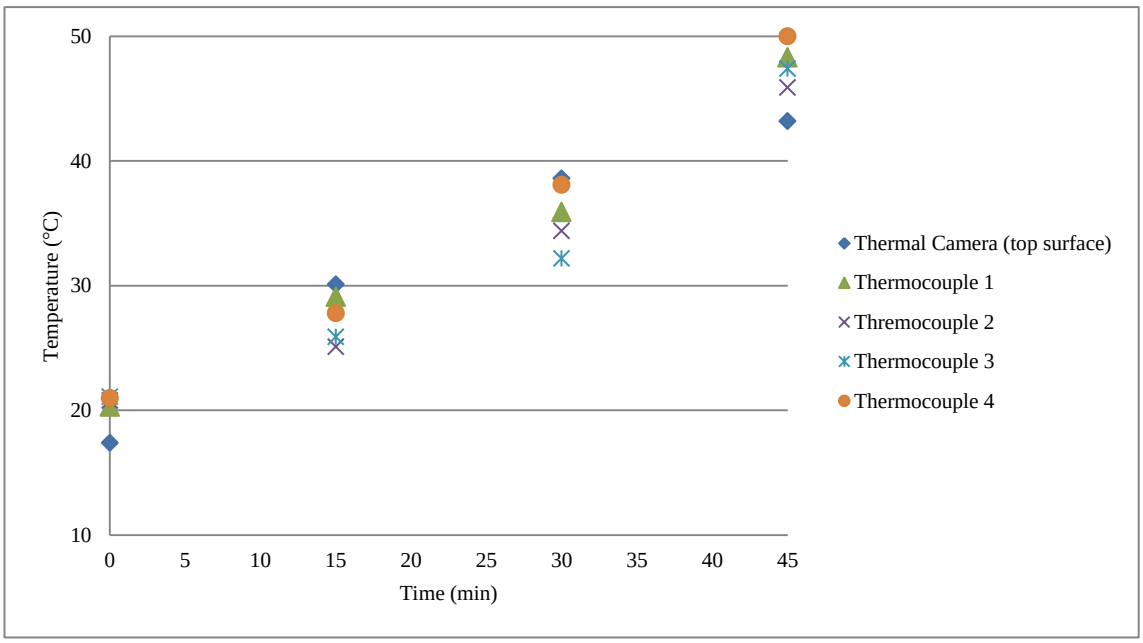

Figure 5.19: Temperature development during microwave curing for CEM II repair material (150 mm cube)

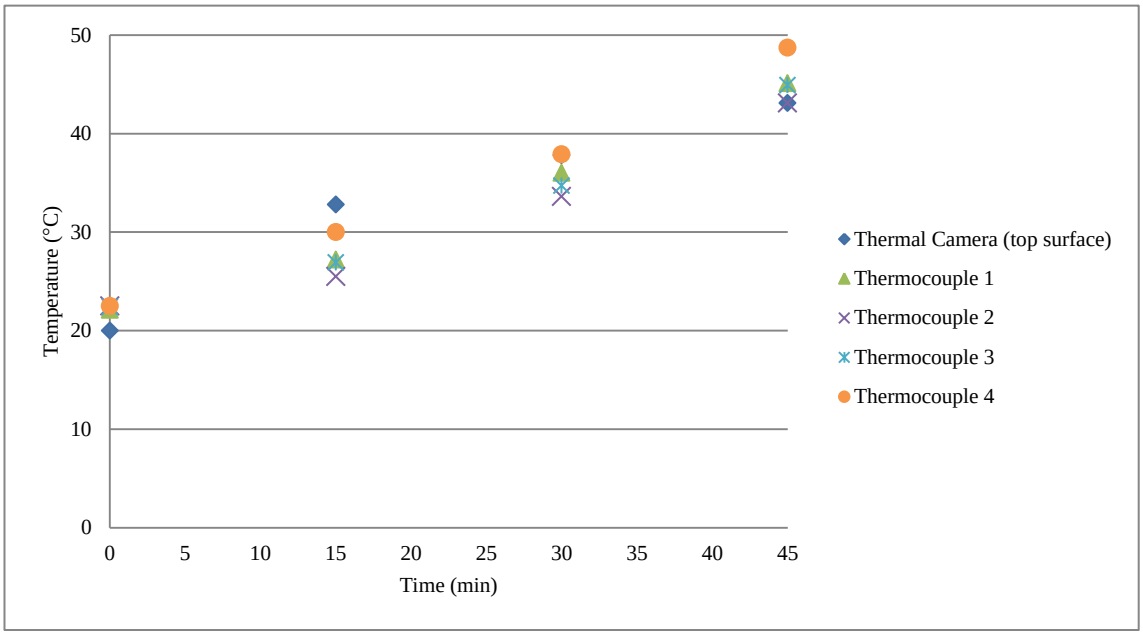

Figure 5.20: Temperature development during microwave curing for Five Star repair material (150 mm cube)

5.4.3.2 *Temperature profile during 24 hours*

Figures 5.21 to 5.24 show the internal temperature of CEM II and Five Star repair materials during 24 hours after commencing mixing. Normally cured specimens for both CEM II and Five Star repair materials show one hump at about 754 and 774 minutes, respectively (Figures 5.22 and 5.24). This is due to the heat of hydration

reaching 37.8 °C for CEM II and 45.1 °C for Five Star repair materials (Table 5.6). Specimens for both repair materials were placed in the laboratory environment (approximately 20 °C) and this indicates an increase in temperature of 17.8 and 25.1 °C for CEM II and Five Star repair materials respectively. However, the microwave cured specimens experienced higher humps in much shorter time resulting in maximum internal temperatures of 73.1 °C for CEM II and 78.2 °C for Five Star repair material (Figures 5.21 to 5.24). The higher temperatures achieved with microwave curing compared with normal curing are the cumulative effect of microwave heating and heat of hydration. The difference in the maximum heat of hydration temperature and the maximum microwave curing temperature of microwave cured specimens for CEM II and Five Star repair materials is 29.9 °C and 35.1 °C respectively. A comparison with the corresponding values of 17.8 °C and 25.1 °C for normally cured specimens shows that early age microwave curing produced greater heat of hydration temperatures. In addition, early age microwave curing for a short period accelerates the hydration process and the peak temperatures are reached much sooner than normally cured materials (Table 5.6).

Table 5.6: Details of time and temperature at peak heat of hydration.

Repair Material	Microwave curing		Maximum temperature and time after starting microwave curing				
	Period (min)	temperature (°C)	Microwave cured			Normally cured	
			Maximum temperature (°C)	Time (min)	Time difference (Δt) (minutes)*	Maximum temperature (°C)	Time (min)
Five Star	45	43.1	78.2	245	200	45.1	774
CEM II	45	43.2	73.1	165	120	37.8	754

*Time difference between reaching peak hydration temperature and end of microwave curing.

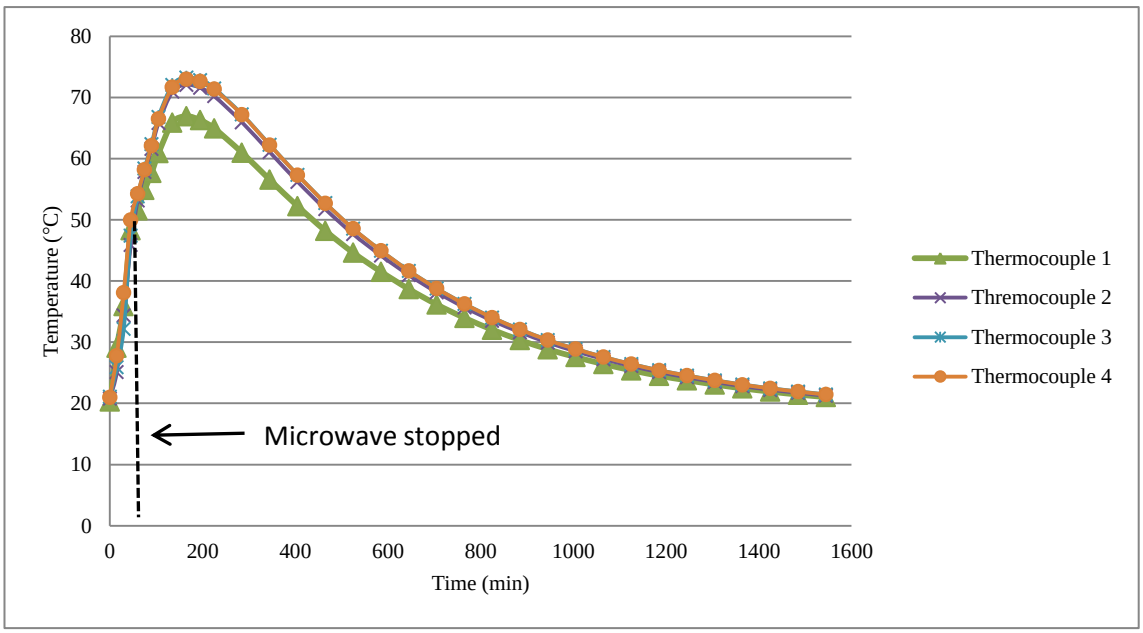

Figure 5.21: Internal temperature of microwave cured CEM II Mortar.

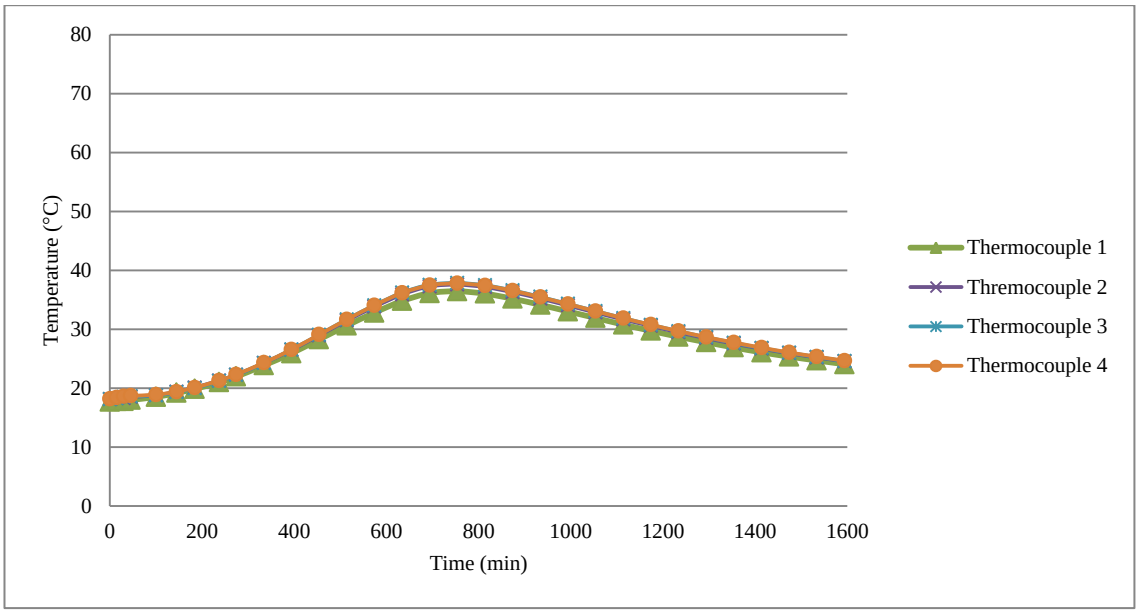

Figure 5.22: Internal temperature of normally cured CEM II Mortar.

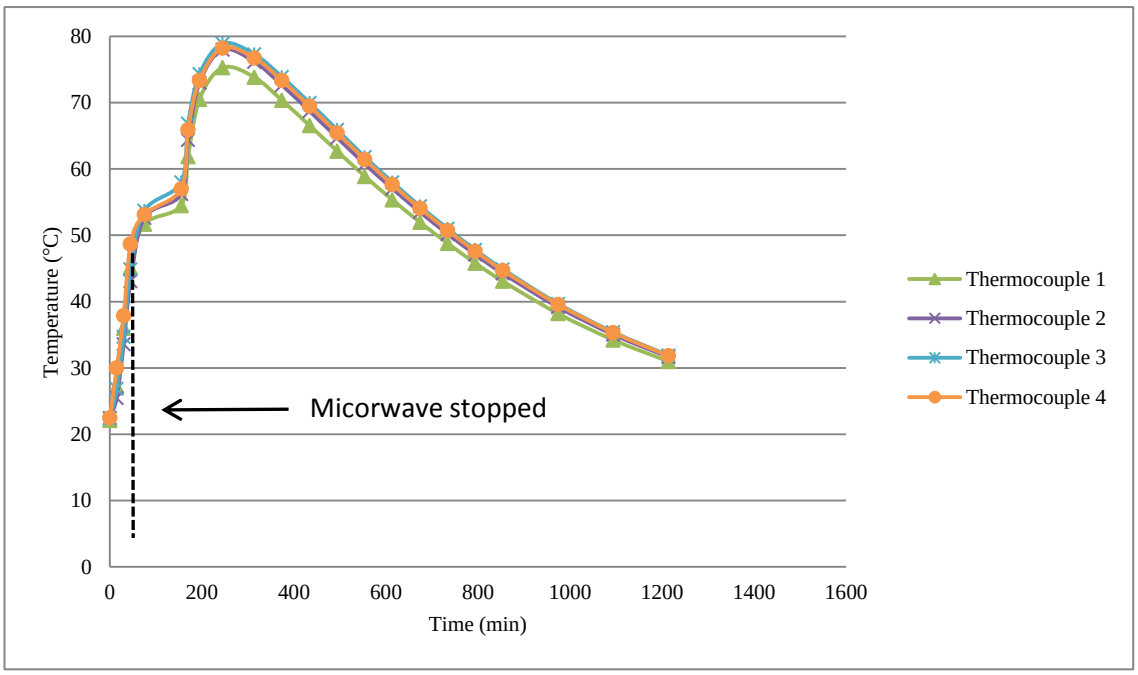

Figure 5.23: Internal temperature of microwave cured Five Star repair material.

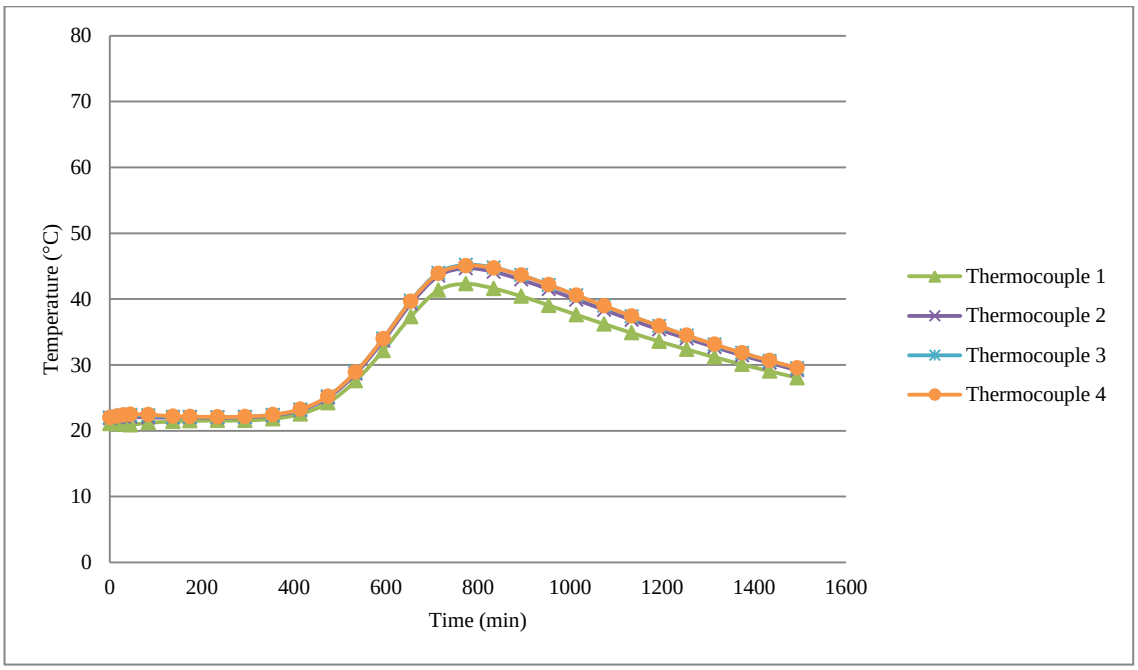

Figure 5.24: Internal temperature of normally cured Five Star repair material.

5.4.4 Influence of specimen size (volume) on the heat of hydration

5.4.4.1 *Normally cured*

A comparison between the 100 mm (1 litre) and 150 mm (3.4 litres) normally cured cube specimens shows that increasing the size of specimen results in additional heat of hydration. For example, the 100 mm cube of CEM II mortar achieves the peak heat of hydration temperature of 26.7 °C at 630 minutes from commencing mixing (Figure 5.18). The corresponding results for the 150 mm cube specimen were 37.8 °C at 784 minutes (or 754 minutes after microwave started) (Figure 5.22). The corresponding values for Five Star are similar with the 100 mm cube showing a peak temperature of 24.9 °C at 1230 minutes (Figure 5.13) compared with 45.1 °C at 804 minutes (Figure 5.24) for 150 mm cube. This is in agreement with the results reported by Lee et al. [131] from adiabatic tests on OPC concrete cylinders of 6, 30 and 50 litre volumes. Their results showed that the higher volume results in higher adiabatic temperature rise. For example, OPC concrete achieved a temperature rise of below 50 °C for 6 litre volume and 60 °C for 30 litre volume. The higher temperature is due to the effect of volume on the heat of hydration. The effect of volume on the heat of hydration is well documented and it is an important issue when considering a mass concrete application. However, in the case of patch repairs the volume/surface ratios are small since repair patches have a low thickness and relatively large surface area. Consequently, heat of hydration is unlikely to be a problem.

5.4.4.2 *Microwave cured*

The effect of microwave curing on temperature rise during and after microwave exposure of the 100 mm and 150 mm cubes of the CEM II and Five Star repair materials is shown in Figures 5.25 to 5.28. The internal temperature at the centroid of the cubes is recorded in these figures. Figure 5.25 shows that the internal temperature at

the centroid of the 100 mm cube of CEM II mortar was 53.0 °C at the end of microwave curing and it continued to rise to reach a maximum value of 55.4 °C after 10 minutes (60 minutes after the start of microwave curing). However, Figure 5.26 shows that the corresponding temperature for the 150 mm cube was 45.9 °C at the end of microwave curing and it continued to rise at a lower rate reaching a maximum value of 73.1 °C at 165 minutes after the start of microwave curing. The corresponding results for the Five Star material in Figures 5.27 and 5.28 show a similar trend for the 100 mm and 150 mm cubes with the peak heat of hydration occurring at 58.2 °C after 55 minutes and 78.2 °C after 245 minutes respectively for the two cubes series. A comparison of the time of peak hydration temperature reached by the normally and microwave cured specimens shows the acceleration of hydration by microwave curing. The peak times are 600 and 60 minutes respectively for 100 mm cubes compared with 754 and 165 minutes for 150 mm cubes. The peak hydration temperature occurs much closer to the end of microwave curing for 100 mm cubes. The reason for that is a higher internal temperature at the centroid for 100 mm cube (53 °C) compared to the 43 °C for 150 mm cube specimen.

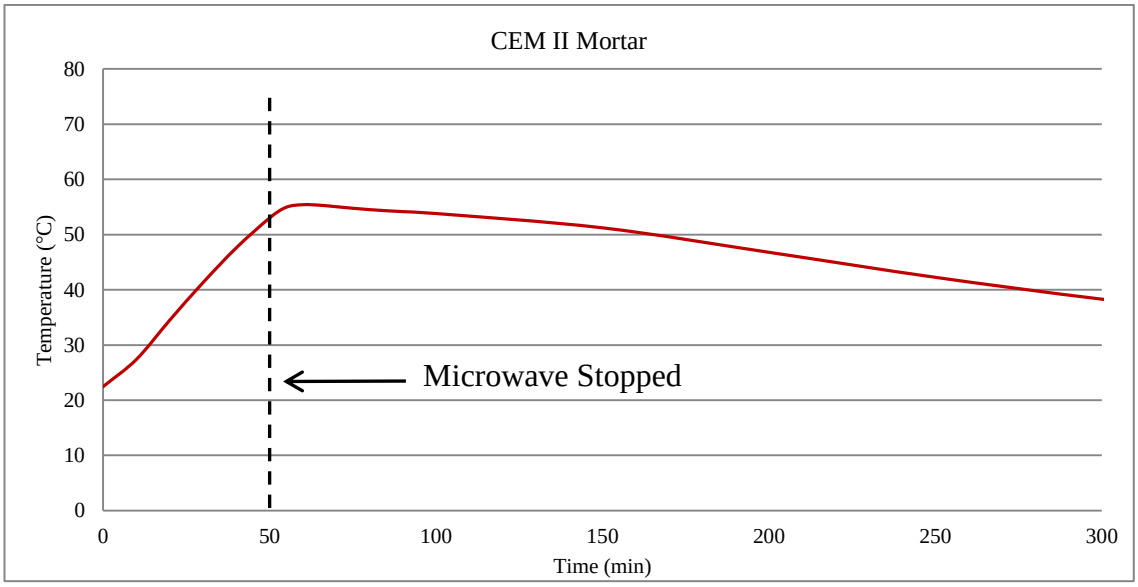

Figure 5.25: Internal temperature of microwave cured of CEM II mortar (100 mm cube) up to 300 minutes.

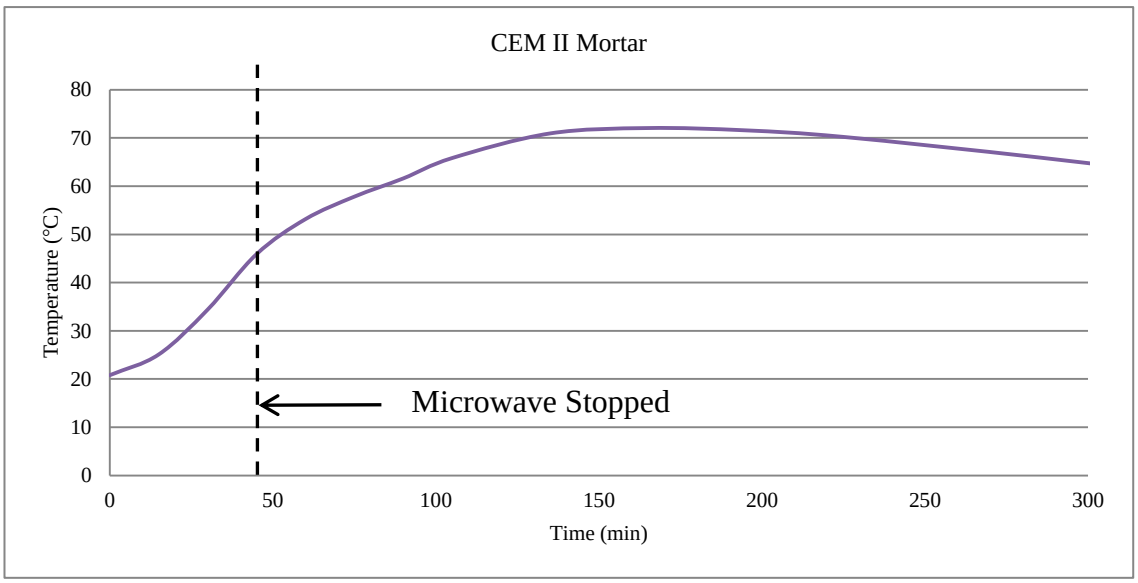

Figure 5.26: Internal temperature of microwave cured of CEM II mortar (150 mm cube) up to 300 minutes.

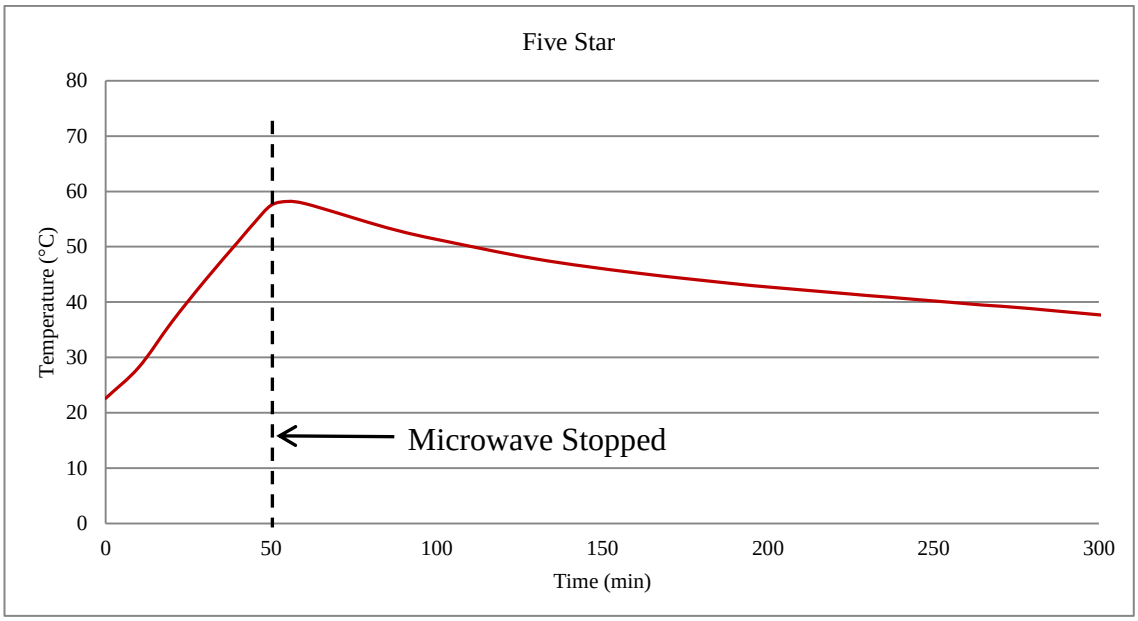

Figure 5.27: Internal temperature of microwave cured of Five Star repair material (100 mm cube) up to 300 minutes.

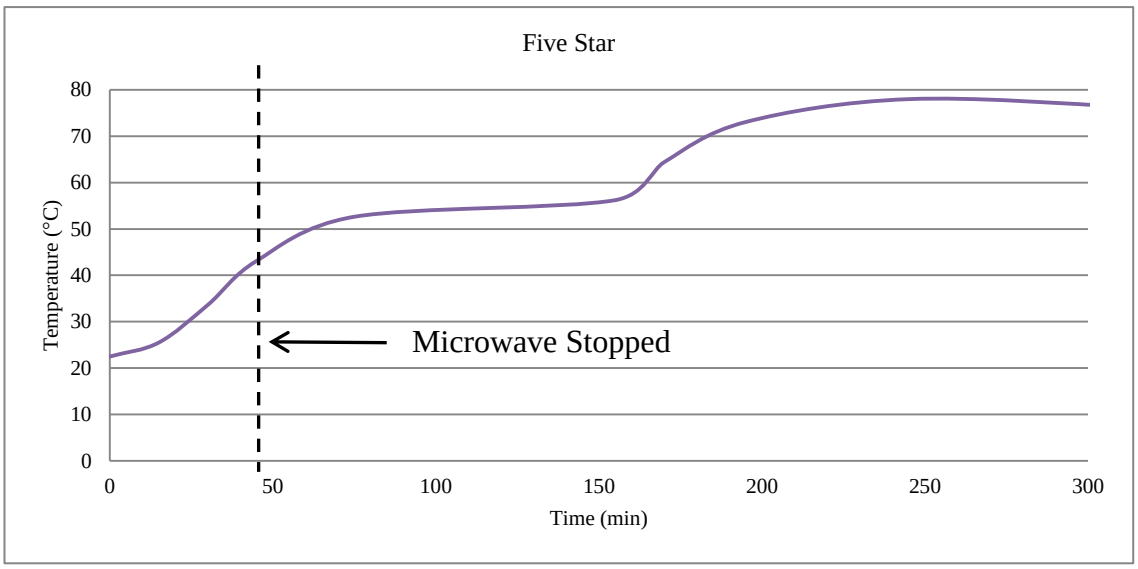

Figure 5.28: Internal temperature of microwave cured of Five Star repair material (150 mm cube) up to 300 minutes.

5.4.5 Effect of microwave curing on water loss

The temperature of repair material, environmental temperature, humidity and the speed of air are primarily responsible for the loss of water in freshly applied concrete repairs. A higher loss of water is expected at a lower humidity, higher environmental temperature and a higher temperature of the mix [132]. In the case of microwave curing, the fresh repair material is subjected to microwave heating at the early stage when it is most vulnerable to moisture loss. In order to decide on the need for preventative measures such as curing membranes or providing covers during curing, an evaluation of moisture loss due to microwave curing under unprotected conditions has been carried out. Therefore, water loss of each repair material was measured during microwave curing and at 24 hours after casting. The procedure and calculation of water loss is based on the weight of water added to the mix and then monitoring the weight of specimens during and after microwave curing as described in Section 5.3.3. The 100 mm cube specimens were kept in the polystyrene mould with the top surface uncovered

during microwave curing and subsequently under ambient temperature exposure at 20 °C, 60 % RH up to 24 hours age in order to represent the worst case of water loss in practice.

Table 5.7 gives the data for water loss of normal and microwave cured repair materials up to 24 hours age. The relationships used to calculate the data for the various columns in Table 5.7 are given at the bottom of the table.

Table 5.7: Details of water loss for normally and microwave cured 100 mm cube specimens at the end of microwave curing period and at 24 hours

Material	Type of curing	At start of microwave curing (0 minutes)		At the end of microwave curing		At 24 hours		Water loss (%)		Weight loss (%)	
		Mass of cube (g)	Mass of water (g)	Mass of cube (g)	Mass of water (g)	Mass of cube (g)	Mass of water (g)	At end of microwave curing	At 24 hours	At end of microwave curing	At 24 hours
Column		1	2	3	4	5	6	7	8	9	10
Five Star	Microwave	2204.78	253.67	2197.08	245.96	2162.58	211.43	3.04	16.65	0.35	1.91
	Normal	2190.64	252.02	2189.14	250.50	2165.88	227.26	0.60	9.82	0.07	1.13
Monomix	Microwave	1812.76	222.62	1807.53	217.39	1792.52	202.38	2.35	9.09	0.29	1.12
	Normal	1793.30	220.23	1792.38	219.31	1778.14	205.07	0.42	6.88	0.05	0.85
Monopour PC6	Microwave	2000.80	230.18	1996.02	225.40	1973.12	202.50	2.08	12.03	0.24	1.38
	Normal	1003.14	230.45	1002.16	229.47	981.32	208.63	0.43	9.47	0.10	2.18
HB 40	Microwave	1620.59	186.44	1616.13	181.98	1604.11	169.96	2.39	8.84	0.28	1.02
	Normal	1627.20	187.20	1626.71	186.70	1610.67	170.70	0.27	8.81	0.03	1.02
Weber	Microwave	2286.35	207.85	2280.98	202.48	2259.10	180.60	2.58	13.11	0.23	1.19
	Normal	2288.99	208.09	2288.17	207.27	2271.28	190.38	0.39	8.51	0.04	0.77
Fastfill	Microwave	2183.59	268.16	2181.70	266.27	2173.65	258.22	0.70	3.71	0.09	0.46
	Normal	2203.86	270.65	2203.14	269.93	2194.89	261.68	0.27	3.31	0.03	0.41
CEM II	Microwave	2195.03	305.97	2187.56	298.50	2148.32	259.26	2.44	15.27	0.34	2.13
	Normal	2179.61	303.74	2178.26	302.39	2146.41	270.54	0.44	10.93	0.06	1.52

Relationships to calculate each column:

Col 2 = $(\frac{W}{P} \text{x Col 1})$

Col 4 = $\text{Col 2} - (\text{Col 1} - \text{Col 3})$

Col 6 = $\text{Col 2} - (\text{Col 1} - \text{Col 5})$

Col 7 = $\frac{\text{Col 1} - \text{Col 3}}{\text{Col 2}} \text{x } 100$

Col 8 = $\frac{\text{Col 1} - \text{Col 5}}{\text{Col 2}} \text{x } 100$

Col 9 = $\frac{\text{Col 1} - \text{Col 3}}{\text{Col 1}} \text{x } 100$

Col 10 = $\frac{\text{Col 1} - \text{Col 5}}{\text{Col 1}} \text{x } 100$

5.4.5.1 *Water loss during microwave curing*

Figures 5.29 to 5.35 show the graphs of water loss due to evaporation of water for normally and microwave cured repair materials during the microwave curing period. Normally cured specimens show a linear increase of water loss with time. An insignificant water loss, ranging between 0.27 % and 0.60 %, occurs in normally cured specimens at the time corresponding to the end of the microwave curing period. The microwave cured specimens exhibit a non-linear increase in water loss with time reaching a maximum at the end of microwave curing. The water loss is several times higher under microwave curing. The linear temperature increase with time under microwave curing, as shown in Figure 5.7, is the cause of higher water loss with time. As temperature increases the rate of water evaporation increases.

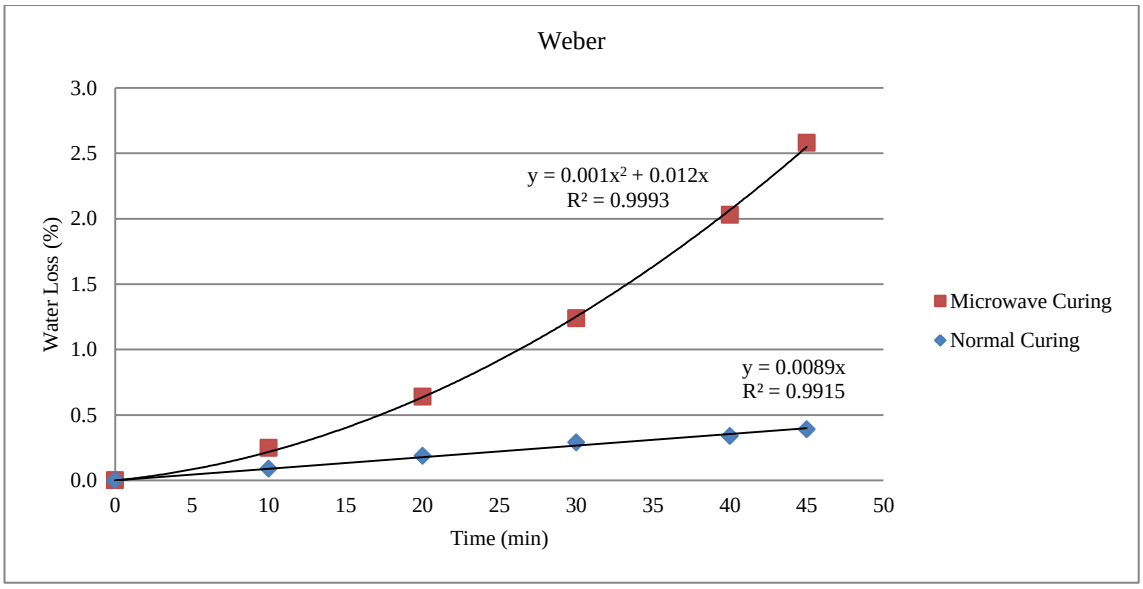

Figure 5.29: Water loss of both normally and microwave cured Weber repair material during 45 minutes (microwave curing period 45 minutes).

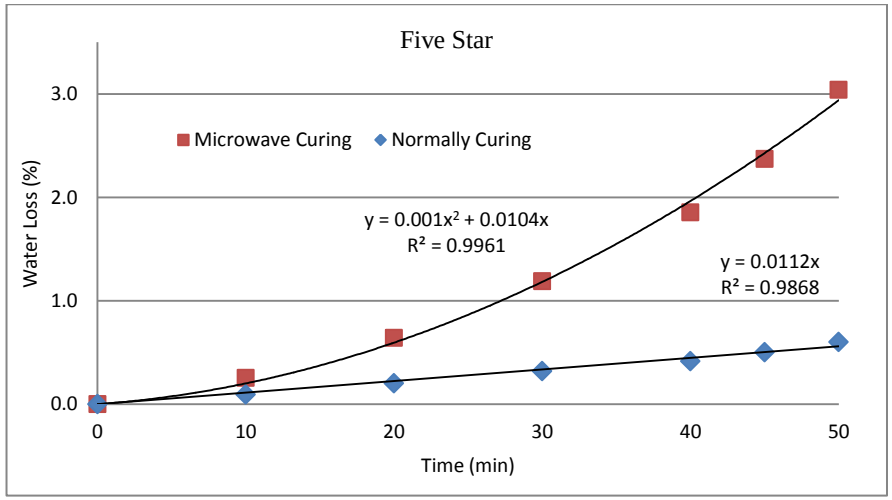

Figure 5.30: Water loss of both normally and microwave cured Five Star repair material during 50 minutes (microwave curing period 50 minutes).

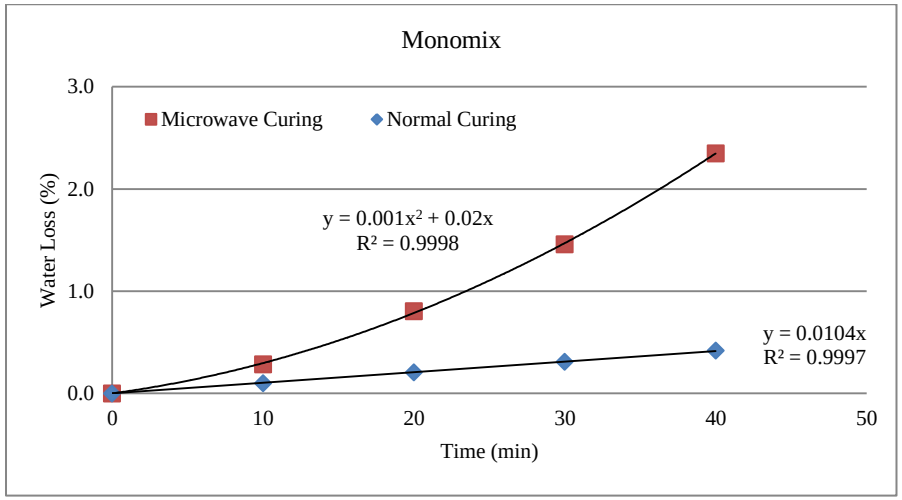

Figure 5.31: Water loss of both normally and microwave cured Monomix repair material during 40 minutes (microwave curing period 40 minutes).

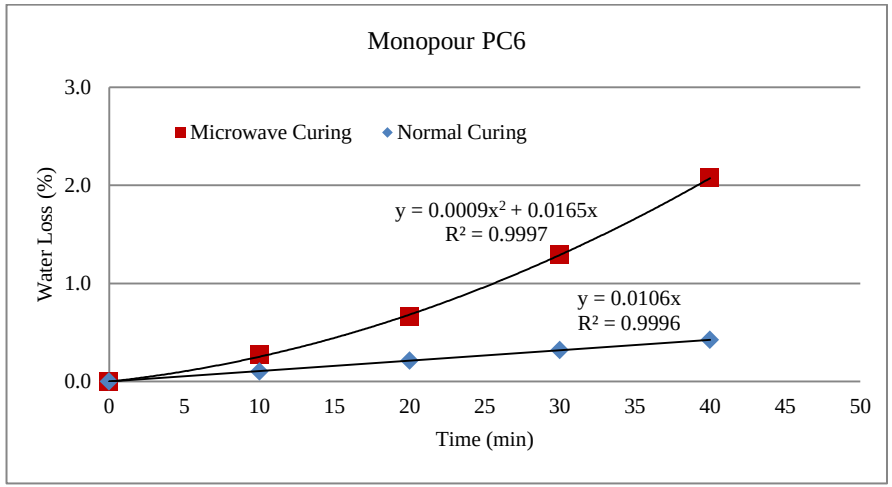

Figure 5.32: Water loss of both normally and microwave cured Monopour PC6 repair material during 40 minutes (microwave curing period 40 minutes).

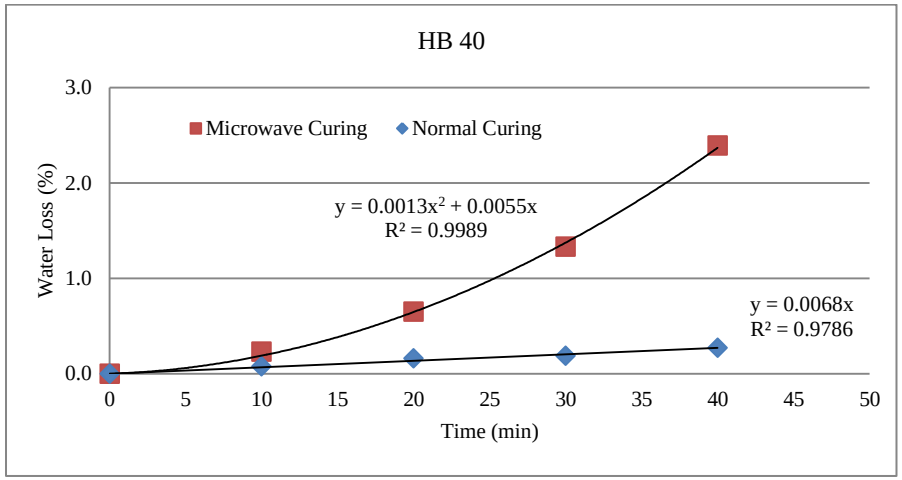

Figure 5.33: Water loss of both normally and microwave cured HB40 repair material during 40 minutes (microwave curing period 40 minutes).

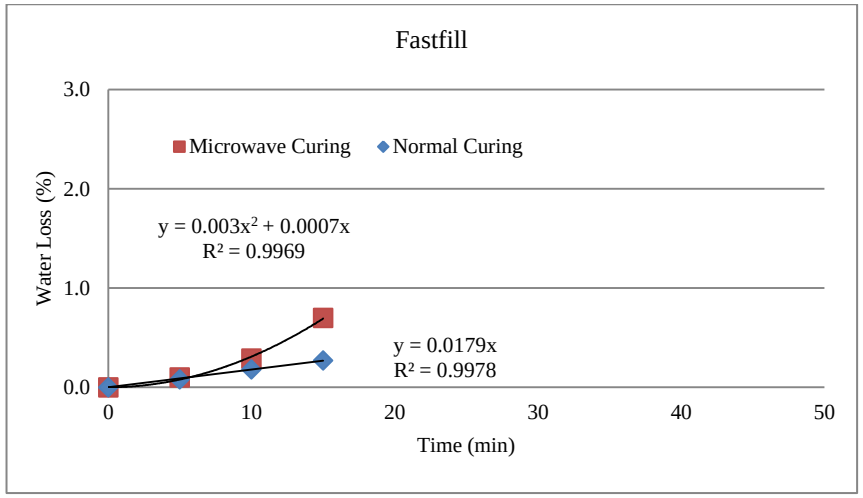

Figure 5.34: Water loss of both normally and microwave cured Fastfill repair material during 15 minutes (microwave curing period 15 minutes).

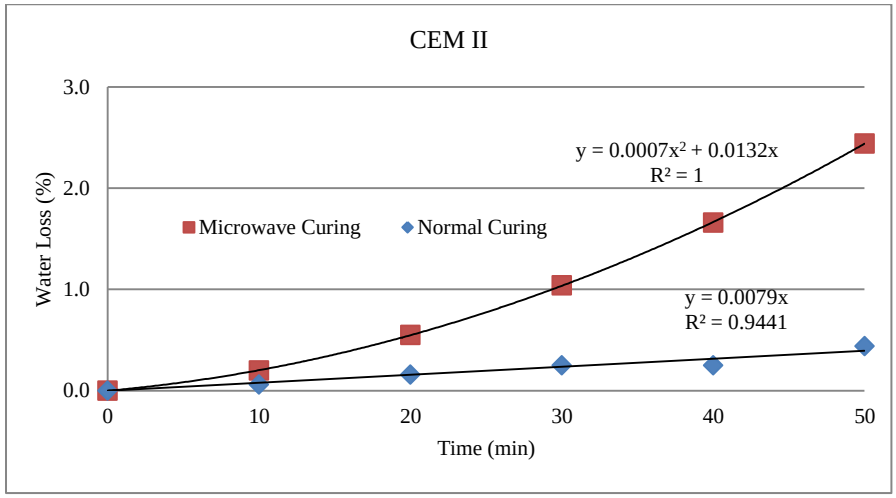

Figure 5.35: Water loss of both normally and microwave cured CEM II repair material during 50 minutes (microwave curing period 50 minutes).

5.4.5.2 *Water loss at the end of microwave curing*

Figure 5.36 shows the water loss at the end of the microwave curing period for the normally and microwave cured specimens of all repair materials. Water loss for microwave cured specimens is much higher than normally cured specimens. Water loss for normally cured specimens ranged between 0.27 to 0.60 %, while for microwave cured specimens it ranged between 0.7 to 3.04%. Fastfill repair material experienced the lowest water loss for both microwave and normally cured specimens. Fastfill is a rapid setting material and it could only be exposed to microwave energy for 15 minutes due to a rapid increase in temperature. It is likely that within the 30 minutes after commencing mixing and before the start of microwave curing, the free water in Fastfill was mostly consumed due to the early hydration and, therefore, no free water was available to evaporate during microwave curing.

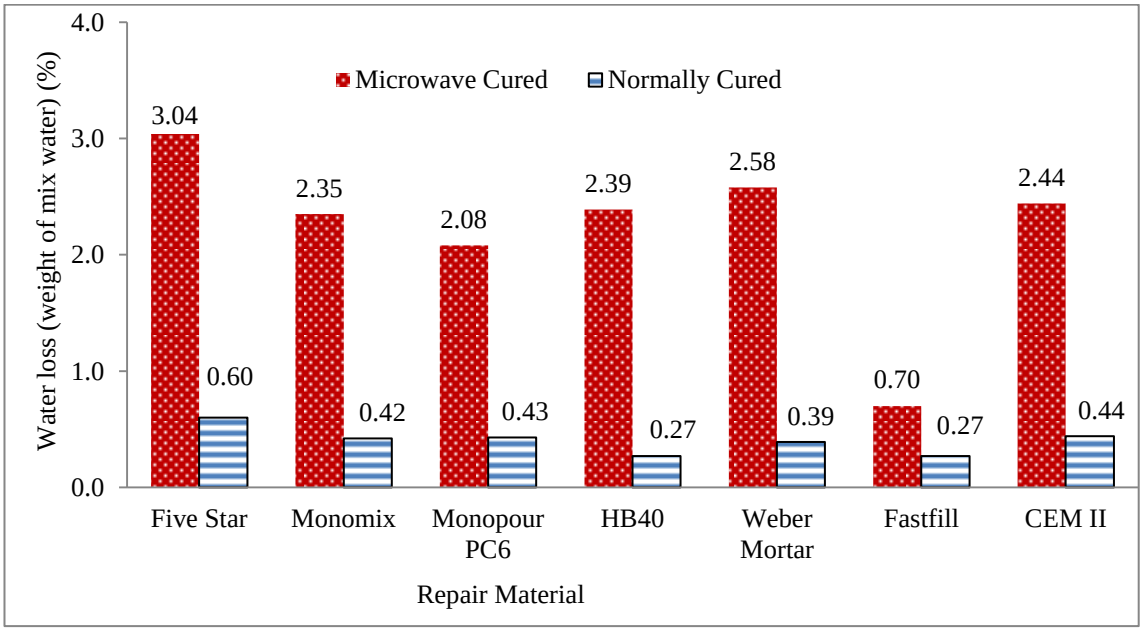

Figure 5.36: Water loss (% by weight of mix water) at the end of microwave curing

5.4.5.3 *Water loss after 24 hours*

The graph in Figure 5.37 shows the water loss of normally and microwave cured cubes for all repair materials at 24 hours after commencing mixing. All specimens were stored in the laboratory air (20 °C, 60 % RH) after the microwave curing period. The graph shows that microwave cured specimens experienced higher water loss for all repair materials. For example, normally cured Five Star repair material shows a water loss of 9.82 % which increased to 16.65% under microwave curing, resulting in a 70% increase in water loss. Repair materials such as Fastfill and HB40 show an insignificant increase in water loss between normal and microwave curing compared to the other repair materials.

A comparison between Figures 5.36 and 5.37 shows that water loss under normal and microwave curing is much higher after 24 hours than at the end of microwave curing. For example, Monopour PC6 shows a water loss of 0.43 % and 2.08 % respectively for normal and microwave curing at the end of microwave exposure time while the corresponding water loss increased to 9.47 and 12.03 % for normal and microwave curing at the end of 24 hours.

It is clear from Figure 5.37 that both microwave and normally cured repair materials experience a high water loss during 24 hours after commencing mixing. This highlights the importance of preventing water loss at early age. Microwave cured repair materials show a higher water loss than the normally cured ones due to their higher temperature both during microwave curing and afterwards during the peak hydration period whereas normally cured samples show modest temperature rise (Figures 5.12 to 5.18) during this period. For example, Figure 5.13 shows that the peak temperature at the end of microwave curing took more than 1000 minutes (16.7 h) to reach room temperature. Moisture loss increases at higher temperature.

Water loss effects the physical and durability properties of the repair and, therefore, it is always desirable to seal or cover the repair surface as soon as possible to prevent water loss.

Water loss from the specimens has occurred due to evaporation from the top surface as the other faces of the cubes were sealed with the polystyrene mould. Hence, the top surface zones of the specimens will have a lower water content than the lower parts of the specimens during the hydration period unless a high degree of bleeding occurs in the mortar, which is not investigated here.

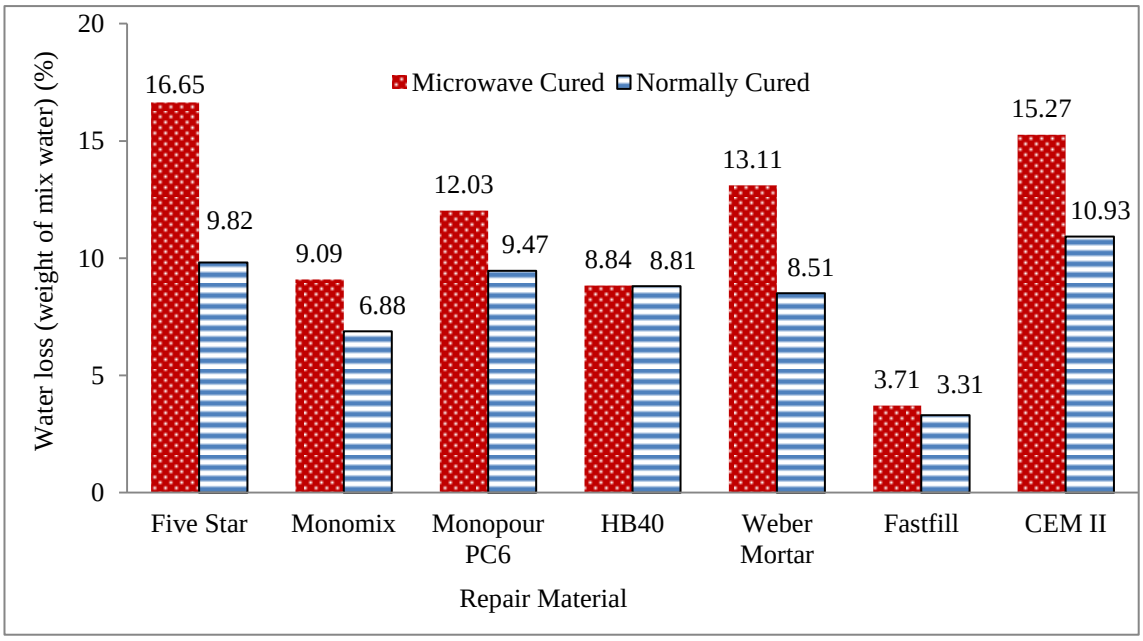

Figure 5.37: Water loss (% by weight of mix water) at 24 hours after casting

5.5 Conclusions

The following conclusions can be drawn from the results presented in this chapter:

- Different durations of microwave curing at a constant power of 60 W are required for different repair materials to reach a common target temperature of curing (40-45 °C). The time depends on the composition of materials and is significantly lower for rapid setting materials.
- The internal and top surface temperatures of 150 mm size cubes of repair materials are similar at the end of microwave curing.
- A short period of microwave curing of fresh material accelerates the heat of hydration reactions of concrete repair materials. It brings forward the time to reach the peak hydration temperature and increases the magnitude of temperature. For example, HB40 repair material microwave cured for 40 minutes after mixing achieves a peak hydration temperature (combination of microwave heating and heat of hydration) of 71.1 °C at 60 minutes. The corresponding values are 34.0 °C at 600 minutes for normally cured HB40 repair material.
- Microwave curing impacts the heat of hydration temperature by bringing it forward. As a result it influences the permissible microwave curing temperature to ensure it does not exceed the limit which affect durability.
- Microwave curing of repair materials results in higher water loss than the normally cured specimens. For example, Five Star repair material shows a water loss of 16.65 % at the end of microwave curing relative to 9.82 % under normal curing.

Chapter 6

6. Pore structure of microwave cured repair materials

6.1 Introduction

This chapter introduces the importance of pore structure of cement based repair materials. It describes the terminology used in pore characterization and the principal of different methods used to determine the porosity and pore structure of such materials. Then, the mercury Intrusion Porosimetry (MIP) test method, a widely used technique to characterise pore structure of cement based materials, is used to investigate the effect of microwave curing on the pore structure and pore distribution for six repair materials and a CEM II mortar.

6.2 Literature review and background

6.2.1 Introduction

A chemical reaction of hydration takes place when water is mixed with cement. The hydration reaction of cement results in a product consisting of a porous system. The hydration of cement produces three forms of water present in the hydration products, such as combined water, gel water and capillary water. Capillary water produces a series of channels through the concrete matrix. However, this water maybe partly consumed through continuing hydration or removed by evaporation which produces capillary pores. In addition, inadequate compaction of fresh concrete or intentionally introduced air voids also introduce more pores in concrete.

Pore structure is one of the most important parameters that directly affect the physical, mechanical and durability properties of cement based materials [133, 134, 135]. These properties include strength, elasticity, shrinkage, permeability and durability to freeze-thaw, etc. The influence of porosity on the properties of concrete depends on different parameters of pore structure such as the total porosity, the size and spatial distribution of pores, pore size distribution, pore shape and also pore connectivity. These parameters influence properties of the material in different ways. For example, total porosity relates to compressive strength and elasticity of concrete while permeability and diffusivity of concrete are influenced by total pore volume, size, shape and connectivity of pores. The volume and spacing of the entrained air in concrete control its durability to freeze-thaw cycles. Shrinkage is influenced by the total surface area of pores as shrinkage is largely a function of changes in surface energy at the pore walls which results in moisture migration. The degree of porosity and connectivity of pores is the cause of durability problems in cement based materials due to the ingress and movement of harmful substances. Deleterious ions such as CO_2, Cl^- in solution with water can penetrate through pore spaces and affect the durability of concrete. For example, chloride ions can diffuse through the pore water of reinforced concrete and attack the passive film which protects the reinforcing steel from expansive corrosion, and therefore has a direct impact on the durability of reinforced concrete.

There have been many studies to determine the effect of porosity and pore structure of cement based materials on their properties and behaviour. Nevertheless, it is still one of the most important challenges faced by concrete researchers because of the complexity of microstructure of concrete compared to the other porous materials. The complexity is due to the several factors mentioned by Aligizaki [136] which include the following: Firstly, the range of the pore sizes is very wide, ranging from a few nanometres up to

millimetres. Secondly, Porosity includes the entrapped or deliberately entrained air and the pores vary in shape, connectivity and distribution. Thirdly, the pore structure of concrete is tortuous and complex and spatially not homogeneous. This is due to the different pore structure of cement paste, coarse and fine aggregate as they have their own individual pore structure. Fourthly, pores are filled with pore water which is a highly concentrated potassium and sodium hydroxide solution [137, 138]. Continuous removal of water from the pores due to continuing hydration and evaporation leave solid deposits in these pores and reduce their actual sizes and affect pore spacing. Fifthly, the fragile microstructure of cement paste can be damaged during testing by techniques such as mercury intrusion porosimeter which introduces mercury in the pores under very high pressure. Finally, many drying techniques damage the structure of pores.

All these challenges make it difficult to accurately characterise the pore structure of cement based materials. Nevertheless, practical test methods are available for this purpose.

6.2.2 Type of pores

The different types of pores which can be observed by the external accessibility of fluid or gases are shown in Figure 6.1. The pores can be simply categorised as closed, open and ink-bottle pores. Closed pores refer to the pores that are trapped and there is no connection between them leading to the exterior of the specimen as seen in Figure 6.1 (a) [139]. These pores influence the properties of cement based materials such as bulk density, strength, and thermal conductivity. However, they do not influence the penetration of gases or liquids. Open pores are the pores that connect through channels and they may also be called through or blind pores. Through pores begin on one

location of the surface and end in a different location of surface (Figure 6.1 (d)). Blind pores are open to the surface only at one end (Figure 6.1 (b)). Finally, ink-bottle refers to the larger pores that are connected to the outside through a narrower channel (Figure 6.1 (c)).

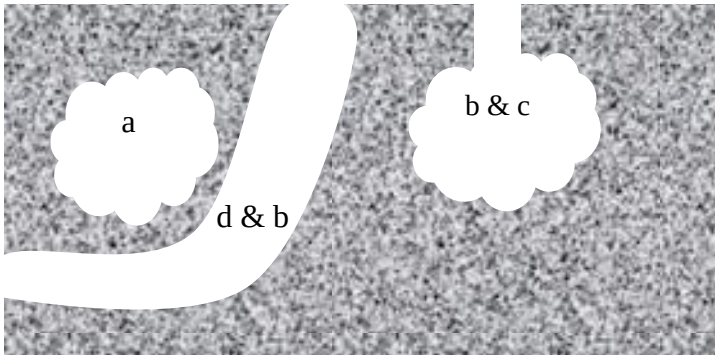

Figure 6.1: Pore types (a) close pore (b) open pore (c) ink-bottle pore (d) through pore

6.2.3 Classification of pores

Cementitious mortars are generally a mix of cement paste with fine aggregate (less than 4 mm) and concrete is a combination of cement paste with fine aggregate and coarse aggregate (larger than 4 mm). Fine and coarse aggregates introduce additional pore structure to the material. The categories of pores in cement paste are gel pores, capillary pores, hollow-shell pores and voids or bubbles. These types of pores are normally based on their size and geometry and are classified as follows:

6.2.3.1 *Gel pores*

Gel pores are formed within the main cement hydration product and they are responsible for strength and microstructure of cement paste. Gel pores have a size range of 1.5 to 4.1 nm [140]. Continuous hydration results in increasing hydration products,

which fill capillary pores and at the same time increase the volume of gel pores (pores inside hydration products). There is a reduction in total porosity as hydration proceeds. Gel pores have no relationship with freeze-thaw resistance. This is because gel pores are too small to permit nucleation of ice crystals as their size is only an order of magnitude greater than the size of a water molecule. The affinity of water molecules to the gel surface limit the movement of water in gel pores and, therefore, it does not contribute to the permeability of paste.

6.2.3.2 *Capillary pores*

The spaces that may fill with water in cement paste and interconnected channels are called capillary pores. They have a size range of 10 to 50 nm for a mature cement paste and they can be large as 10 μm for aggregates [141]. Capillary pores depend on water cement ratio and the degree of hydration. As hydration proceeds, capillary pores are gradually filled with hydration products and subsequently, the capillary pore volume decreases continuously until, at some point, the pores may transform into disconnected space by a percolation transition [142]. The disconnection of capillary pores has a significant effect on the permeability of fluids [143]. The size of capillary pores is ranged from a very small to large values and they are of a very irregular shape. The size of pores is defined as the diameter of the cylindrical pore or the distance between sides of a slit-shaped pore. Capillary pores ranging from 5 to 50 nm are referred to as small capillary pores and they influenced by mineral admixtures such as silica fume, ground granulated blast furnace slag [144] and limestone [145] used in cement based materials. According to Wu Zhongwei [146] pores smaller than 50 nm are beneficial to durability. Capillary pores larger than 50 nm are believed to be more influential in determining the strength of the material [7, 141].

Capillary pores are assumed to have a major effect on the transportation of liquids in concrete. In addition, water stored in capillary pores is also responsible for damage due to freeze-thaw cycles inside the capillary pores.

6.2.3.3 *Hollow-shell pores*

The attention to the hollow-shell pores and their importance in pore structure were drawn by Kjellsen et al. [147]. They discovered the hollow spaces between the anhydrous hydrating cement core and the already formed hydration products. These pores are closed and generally have the shape of relicts of cement particles. It has been considered that the presence of the hollow shell may result in a weak physical interaction between the anhydrous cement grain and the surrounding shell of hydration products.

6.2.3.4 *Voids*

The final type of pores are known as voids or bubbles. They may refer to entrapped or entrained air voids which are typically isolated from other entrapped air and have little influence on permeability. Entrained air voids are intentionally introduced and uniformly distributed by the addition of admixtures to the concrete mixture. Their size ranged from 50 μm to less than 1 mm. Entrapped air voids are unintentionally introduced air during mixing and placing and their size is relatively large, typically 1 to 10 millimetres or more.

Air entrained voids protect concrete from frost damage by limiting the hydraulic pressure in the cement paste pores during the initial stages of freezing and preventing the growth of microscopic bodies of ice [136].

In addition to these types of pores, there can be also micro cracks at the aggregate-mortar interface due to shrinkage. The shrinkage cracks are mainly around 1.5 -2.0 nm size and do not influence the strength of concrete adversely.

6.2.4 Pore structure parameters

The most common terminologies that are used by researchers to characterise the pore structure of cement based materials are total porosity, surface area of pores, pore size distribution, critical pore diameter, pore connectivity and tortuosity. Generally more than one parameter is required to study the effect of pore structure on concrete properties. For example, total porosity is an important parameter related to strength, however, other parameters such as pore size distribution and pore connectivity are required to determine the permeability of cement paste. Several parameters that are commonly used by researchers are as follows:

6.2.4.1 *Total porosity*

Total porosity can be referred to as the porosity or effective (intruded) porosity of the specimen depending on the test method used to determine the porosity. However, it is common that intrudable porosity is misleadingly termed as total porosity. Total porosity represents the total volume of pores and voids within the cement based materials. The value of total porosity is dimensionless. It is well known that there is an inverse relationship between porosity and strength of cement based materials [7, 134, 141, 148, 149]. However, it is not always easy to determine the total porosity and often, depending on the test technique, it may determine only effective porosity. Effective porosity is based on the volume that an external fluid or gas can access through capillary pores. It does not include closed pores. Accordingly, it is very important to clearly state the technique used to determine the porosity. For example, if porosity is

measured with techniques such as absorption, then, only open pores can be detected and measured. While with other methods such as optical microscopy both open and closed pores can be detected and measured. Nevertheless, as far as durability is concerned, the effective porosity is an important parameter. This is due to open pores allowing transport of deleterious liquids and gases.

6.2.4.2 *Pore size*

Pore size defines the size of the pores referred to the diameter of the cylindrical pore or the distance between sides of a slit-shaped pore. The size can range from nanometre to centimetre and is measured either by direct methods such as optical microscopy or indirect methods such as gas adsorption. The geometry of pores in most cases is assumed to be cylindrical. The size of pores may be defined by measuring each single pore individually or by representing the entire pore system, depending on the adapted test technique.

6.2.4.3 *Threshold Diameter*

Threshold diameter refers to the minimum diameter of channels that are essentially continuous through the paste at a given age [150]. It provides the possibility that large pores which exist in the concrete can have access to the exterior only through the smaller channels of the continuous pore system. Pore distribution plot is normally used to reveal the threshold pore diameter. It is the limiting diameter which allows transport of fluids in the matrix. The value of the threshold diameter is normally determined as a pore diameter that there is relatively little mercury intrusion and immediately below that, there is a great increase in mercury intrusion. However, there is not an agreement among the researchers on how to exactly determine the threshold pore diameter. This is due to the fact that it is difficult to determine what value can be considered as little

mercury intrusion. In general, the inflection point in cumulative porosity is determined as threshold diameter, however, determining the inflection can leads to errors as it can be a range of probable pores depending on individual researcher to decide.

6.2.4.4 *Critical pore diameter*

Critical pore diameter corresponds to the steepest slope of cumulative porosity curve and can be determined by the highest point on the corresponding logarithmic differential pore volume [151]. Critical pore diameter is smaller than threshold diameter, nevertheless, critical pore diameter sometimes misleadingly referred to as the threshold pore diameter [152].

6.2.4.5 *Pore size distribution*

Pore size distribution is also another important parameter of porosity. Mehta and Monteiro [141] have suggested that pore size distribution is a better criterion for evaluating the characteristics of hydrated cement paste rather than the total capillary porosity. The pore connectivity and accessibility are undoubtedly important as it determines the ability to transport gas and liquid mainly water with substances dissolved in it through the matrix. Hence it affects durability.

6.2.5 Mercury Intrusion porosimetry (MIP)

Mercury intrusion porosimetry (MIP) is the most widely used method to characterise the porosity of cement based materials [153].

In 1921, E. Washburn [154] laid a theoretical foundation for the technique and proposed an equation that is true for any non-wetting liquid. Later in 1945, Ritter and Drake [155] introduced the technique by building a mercury intrusion porosimeter and testing

a variety of porous materials. However, mercury intrusion porosimetry was not commercially available until the 1960s and it has greatly developed thereafter. It has been used by many researchers to determine the pore structure parameters such as effective porosity, pore size distribution, specific surface area of pores, the density of solids and powders.

It has been widely used by researchers [150, 151, 156, 157, 158, 159, 160, 161] as an effective method to compare the porosity and pore size distribution of cementitious materials for many years. MIP is based on the principle that a non-wetting liquid can penetrate open pores in a solid under external pressure. This method can measure large pore sizes from 1000 μm by applying a lower pressure and small pores up to 0.003 μm by applying a higher pressure. It provides other information such as pore size distribution and, therefore, the threshold pore size can be determined.

Mercury Intrusion Porosimetry is relatively easy and simple to conduct compared to the other methods such as scanning electron microscopy and low-temperature calorimetry and less expensive. Therefore, it has been used to characterise the microwave cured repair materials in this project. The following section provides more details of the MIP process.

6.2.5.1 *Theory of the mercury intrusion porosimetry*

Mercury intrusion porosimetry is based on the principle that a none-wetting liquid creates a contact angle with the surface of the cement based material and bridges across the pore (capillary) diameters (Figure 6.2). The pressure required for the mercury to penetrate into pore depends on their diameter. As the pore diameter decreases, greater pressure is required to force mercury into pores (Figure 6.2). The pressure applied through the pore cross-section area is represented by the Equation 6.1.

$$P = \frac{F}{A} \qquad (6.1)$$

F=PA (Applied force through the mercury)

Where P is the pressure required to intrude mercury into the pore (N/mm^2); F is the force required to intrude the pore (N) and A is the cross-section area of the pore (mm^2).

In order to force the mercury into the pores, there must be some internal force to act in the opposite direction to the applied pressure on mercury in order to maintain equilibrium. This reaction force is the product of the surface tension of the mercury (γ) and the cosine of the angle of contact (θ) between the mercury and the capillary acting along the perimeter of the pore (πD).

The equilibrium equation is:

$$PA = (\pi D)\,\gamma\cos\theta \qquad (6.2)$$

$$P\pi D^2/4 = (\pi D)\,\gamma\cos\theta \qquad (6.3)$$

$$D = \frac{4\gamma\cos\theta}{P} \qquad (6.4)$$

Where D is the diameter of pores; γ is the surface tension of the mercury; θ is the contact angle between mercury and the capillary pore surface and P is the applied pressure.

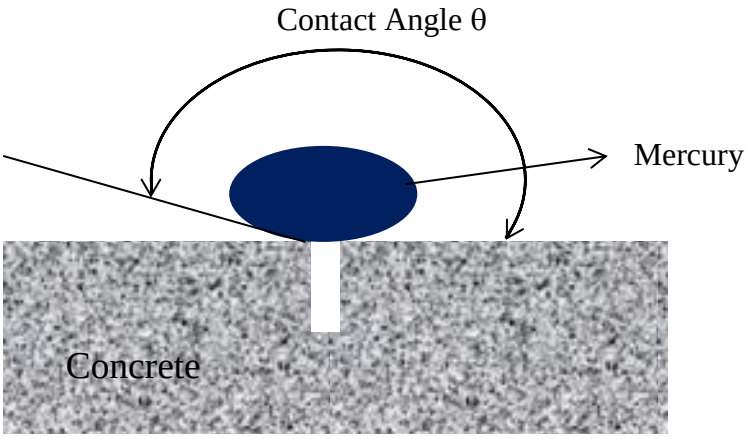

Figure 6.2: Intrusion of mercury into a pore.

The relationship in Equation 6.4 is called Washburn equation in honour of E.L. Washburn [154] who first recognised its vital role in pore size determinations. The surface tension and contact angle values of mercury used in Equation 6.4 are 0.840 N/m and 140°, respectively. The equation assumes a cylindrical pore geometry whereas, in reality, the pore geometry is much more complex. This is a basis of some concern for materials that have complicated pore geometry not accurately reflected by MIP.

6.2.5.2 *Limitations of MIP*

Consider a pore system with diameters ranged from d_1 to d_4 (Figure 6.3 (a)) where d_1 is the largest pore and d_4 is the smallest pore size ($d_1>d_2>d_3>d_4$). During MIP mercury first intrudes d_1 and then by increasing pressure, it will intrude the smaller pores until finally fills d_4 at the end. However, in reality, this is not always the case. The pores are not connected in such an idealised order. There may be larger pores connected through smaller pores. For instance, consider a pore structure with pores from d_1 to d_4 (Figure 6.3 (b)). Assume these pore sizes are representing as $d_1>d_4>d_2>d_3$. For mercury to intrude d_4, it needs first to penetrate d_3 which has a much smaller pore size. But as soon mercury penetrate d_3, with the same pressure it will penetrate d_4 too. The total volume

of mercury penetrating into the pore with diameter d_3 and d_4 will be represented as a single pressure. This effect is called ink bottle effect and it is one of the limitations for using MIP [162]. However, the presence of the ink-bottle can be determined during extrusion of mercury.

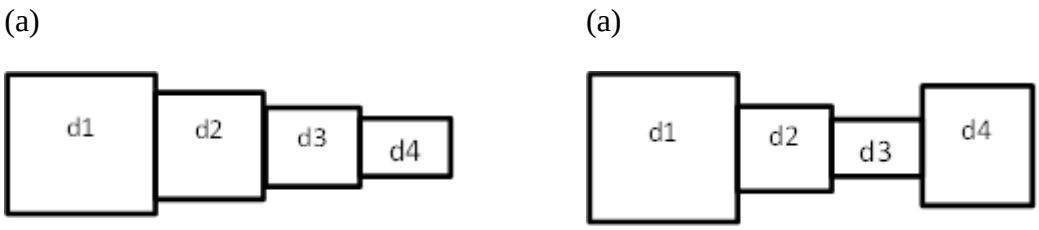

Figure 6.3: Pore structure with different pore structure (a) assumption and (b) likely to be a reality.

Mercury intrusion Porosity assumes that pores are connected and mercury can have access to fill them. However, in reality, total pores are not completely connected and there are closed pores (Figure 6.1(a)) which mercury cannot access. This is another limitation of MIP test [162]. However, for the purposes of this research MIP is suitable for investigating the relative pore properties of materials.

6.2.6 Effect of heat curing on pore size and pore size distribution

Curing conditions, especially curing temperature of cement based repair materials, have an important effect on the pore size and pore distribution. Sellevold [157] carried out MIP tests to determine the porosity of hardened cement paste steam cured at 97 °C for 10 days. The results compared to similar specimens cured at room temperature for at least 1 year showed higher porosity for steam cured specimens. However, it can be argued that the specimens are at different ages (10 days and 1 year) and porosity normally decreases with age due to continuing hydration. On the other hand, continued hydration of steam cured concrete will be small.

Knut et al. [163] investigated the pore structure of plain cement pastes hydrated at three different temperatures as 5, 20 and 50 °C and they carried out MIP test after 70% of

hydration had taken place. MIP results showed an increase in porosity by increasing temperature. For example, cement paste cured at 5 °C showed effective porosity of 33.2 %. The effective porosity increased to 35.7 % for the corresponding cement paste cured at 50 °C. In addition, their pore size distribution curves were very similar except that the volume of pores of radius 20-100 nm increase with increasing temperature.

Goto and Roy [158] carried out an investigation to determine the porosity of pastes of type 1 Cement with different w/c ratios by curing specimens in a $Ca(OH)_2$ saturated solution at 27 and 60 °C. Specimen cured at 60 °C showed a higher porosity. However, porosity measured by evaporated water (difference in weight of sample when saturated and dried) showed a reduction of porosity by curing at 60 °C [158]. The reason for the difference with the two methods can be attributed to the MIP technique that did not measure pores larger than 7.5 μm in radius. Khatib and Mangat [164] reported increased porosity for specimens exposed to air at 45 °C for 14 days relative to specimens cured at 20 °C and 55% RH.

Ballester et al. [165] investigated the effect of heat on microstructure and mechanical properties in fresh cement based materials. Cement and mortar specimens heat cured under IR radiation to a uniform temperature of 40-80 °C within four hours showed that porosity increased with curing temperature. Ballester et al. [165] also showed that specimens heat cured under IR radiation, if soaked by immersion in distilled water for 5 minutes after 24, 48 and 72 hours of curing, resulted in a decrease of porosity. The properties of thermal cured cement based materials also depend on the wet and dry curing conditions. It is essential that after application of thermal curing, water is supplied to the specimen. Khatib & Mangat [164] also determined the effect of

superplasticizers on reducing the porosity of specimens exposed to different temperatures.

Fall et al. [166] carried out an investigation on the pore structure of Portland cement with 7% slag cured for 160 days at 20 and 50 °C. Results showed a significant impact of curing temperature on the pore size distribution and porosity. Results showed that higher temperature curing leads to a refinement of pore structure at w/c of 0.5.

6.3 Experimental investigation

6.3.1 Repair materials

Six commercial repair materials and CEM II mortar were used to study the effect of microwave curing on pore size and pore size distribution. The repair materials used are as follows:

- Five Star
- Monomix
- Monopour PC6
- Weber Mortar
- Fastfill
- HB40
- CEM II Mortar: Portland limestone cement (CEM II/A-L32.5 N) [65], coarse sharp sand (50% passing a 600 μm sieve) with a ratio of 1:2 were used. The mix was designed with w/c ratio of 0.5 and the plastic density of 2200 kg/m^3.

The repair materials were mixed according to the manufacturer's recommendations. A more detailed description of the repair materials is given in Chapter 3.

6.3.2 Apparatus

6.3.2.1 *Microwave oven*

Two commercial microwave ovens were used to conduct the present study. Microwave oven I (Logik Model L25MDM13) was used to conduct series 1 investigation. In this series, 100 mm cubes were microwave cured at 10% of the maximum microwave oven power resulting in a power of 60 Watts.

Microwave oven II (Sharp) was used to microwave cure repair material specimens with embedded reinforcement (bond specimens) identified as Series II. These specimens were exposed to 10% of the microwave oven power, giving 132 Watts.

Both microwave ovens were calibrated according to BS EN 60705 [167] and ASTM F1317 [168].

6.3.2.2 *Mercury Intrusion Porosimetry*

The PASCAL 140/240 porosimeter was used to measure the porosity of test samples. Figure 6.4 shows both porosimeters connected to a computer to monitor the test process. The instrument is controlled through hardware installed on each porosimeter or it can be connected to a PC and controlled remotely. The diameter of pores was calculated according to the Washburn equation (Equation 6.4 described in Section 6.2.5.1). The surface tension of mercury (γ) is 0.48 N.m^{-1} and the contact angle (θ) is assumed to be 140 °.

Figure 6.4: Front panel of mercury intrusion porosimeter

6.3.3 Details of specimens, casting, curing and preparation for MIP

6.3.3.1 *Series I*

Two specimens were cast in 100 mm polystyrene cube moulds for each repair material. The specimens were cast in the laboratory environment (20 °C and 60% RH) and cured in the laboratory air without any cover to represent the worst possible case of moisture loss (representing site application) during 24 hours after microwave curing.

Thirty minutes after commencing mixing, one cube per mix was placed uncovered (in the polystyrene mould) in the laboratory environment to cure for 24 hours. This specimen is referred to as the normally cured specimen. The second cube specimen per mix was exposed to 60 Watts of microwave energy after 30 minutes of mixing. Microwave curing was applied until the centre of the top surface of the cube reached approximately 40 to 45 °C (target temperature). The temperature of the top surface was recorded with a Flir i7 Thermal camera before the start of microwave curing, then every 10 minutes. The microwave oven was stopped briefly and the specimen removed from

the oven to monitor the temperature. Subsequently, the specimen was moved back for further microwave heating. When the centre of the top surface of the cube reached the target temperature, it was removed from the microwave oven and placed in the laboratory environment (20 °C and 60% RH) and left to cure uncovered for 24 hours. These specimens are referred to as microwave cured specimens. Both normally and microwave cured specimens were de-moulded 24 hours after casting and cured in water for 27 days.

Based on the previous results reported in Chapter 4 (Section 4.4.2), it is known that each repair material has a different capacity to absorb microwave energy, therefore, different durations of microwave exposure were used to achieve the target temperature with a constant power of 60 W. The microwave curing times were estimated from previous research results (Chapter 4) and a few trials were carried out to determine the accurate duration of curing time. Table 6.1 shows the duration of microwave curing that was used for the current study.

Table 6.1: Duration of microwave curing to achieve a target temperature of 40-45 °C.

Repair material	Duration of microwave curing (mins)
Five Star	50
Monomix	40
Monopour PC6	40
HB40	40
Weber Mortar	45
CEM II	50
Fastfill	15

The 100 mm cube specimens were removed from water at the age of 28 days and placed in an oven to dry at +105 °C for 3 days. Then they were removed from the oven and kept in the laboratory environment (20 °C) and wrapped airtight in a plastic sheet to cool off. The cubes were then crushed in a compression testing machine under a loading

rate of 10 kN/s. MIP test samples were collected near the centre of the crushed cubes, placed inside a plastic sample bag and kept airtight inside a desiccator until the MIP test was carried out. Figure 6.5 (a) shows a typical test specimen inside a sample bag and Figure 6.5 (b) shows a desiccator used to store MIP test specimens.

(a) (b)

Figure 6.5: MIP specimens inside plastic bag (a) and then kept inside a desiccator (b)

6.3.3.2 ***Series II***

Series II investigates the effect of microwave curing on the porosity of the repair materials at the reinforcement interface commonly known as Interfacial Transition Zone (ITZ). Porosity of the ITZ has a direct impact on the bond strength of the steel. Therefore, the current investigation will determine the effect of microwave curing on the porosity at the steel interface. Bond specimens of steel reinforcement (similar to the specimens used for pull out tests in Chapter 8) were prepared as follows:

A plain mild steel bar with a diameter of 10 mm and length 255 mm was cleaned with acetone, dried and then placed horizontally across the entire length of a 100 mm polystyrene cube mould by drilling two opposite vertical faces of the mould. The steel bar was located along the centroidal axis of the cube and extended 30 and 85 mm beyond the two opposite faces of the mould. A plastic sleeve was inserted on the steel bar inside the mould to provide a 50 mm unbonded length within the cube as shown in Figure 6.6 (a). Four specimens for each material were cast and vibrated as shown in

Figure 6.6 (b). Two of the four specimens were kept in the laboratory (20 °C and 60 %RH) and covered with a plastic sheet. These specimens are referred to as normal cured specimens. The other two specimens were exposed to microwave energy at 30 minutes after adding water to the mix to achieve a target temperature of 40-45 °C at the end of microwave curing.

Data in Table 6.2 show the repair materials, power and the duration of microwave exposure for each repair material in series II. At the end of microwave curing, specimens were covered with a plastic sheet and placed in the laboratory (20 °C, 60 %RH) where the normally cured specimens had remained since. These specimens are referred to as microwave cured specimens. Both normally and microwave cured specimens were de-moulded at 24 hours age and cured in the laboratory air (20 °C, 60% RH) for 42 days. The curing condition of these specimens is the same as used in Chapter 8 and it is different from the specimens of Series I. At 42 days age, the specimens were subjected to the tensile split test to split the cube at the middle along the steel bar. Figure 6.7 (a) shows a typical reinforcement bond specimen subjected to the tensile split test and Figure 6.7 (b) shows a typical sample after splitting at the middle. Tensile splitting provides access to the surface of the undamaged mortar matrix close to the steel bar.

Mortar samples with a weight of 1-2 g were collected for MIP testing near the middle of the bond specimens representing the bulk mortar for all repair materials. In addition, mortar samples were also collected from the interface with the steel bar for materials Monomix and HB40. The specimens were prepared for MIP testing by placing them in an oven at 60 °C for three days. They were then cooled and were immersed in acetone for four hours before placing them inside a desiccator for a minimum of 24 hours until they were tested. Figure 6.8 shows a typical specimen for MIP testing.

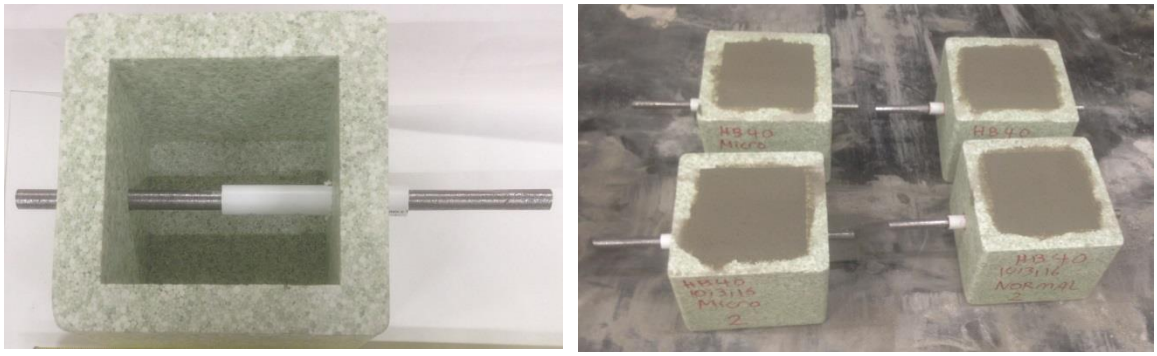

Figure 6.6: Preparation of the polystyrene mould for casting, (a) inserting a steel bar with sleeve and (b) four specimens after casting.

Table 6.2: Details of microwave curing of Series II specimens.

Repair material	Location of MIP sample	Power (Watts)	Duration of Microwave Curing (mins)	Microwave curing temperature*
Five Star	Middle	132	30	44.0
Monomix	Middle		20	42.0
HB40	Middle		20	41.0
CEM II	Middle		30	42.0
Monomix	Surface		20	42.0
HB40	Surface		20	41.0

*average temperature of 2 cubes

(a) (b)

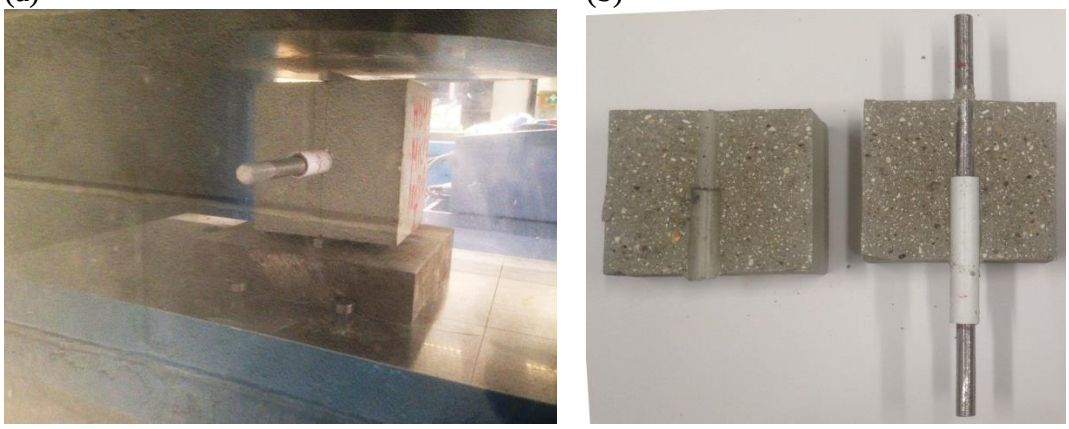

Figure 6.7: Crushing specimens for MIP testing, (a) cube specimen subjected to tensile splitting and (b) specimen after splitting.

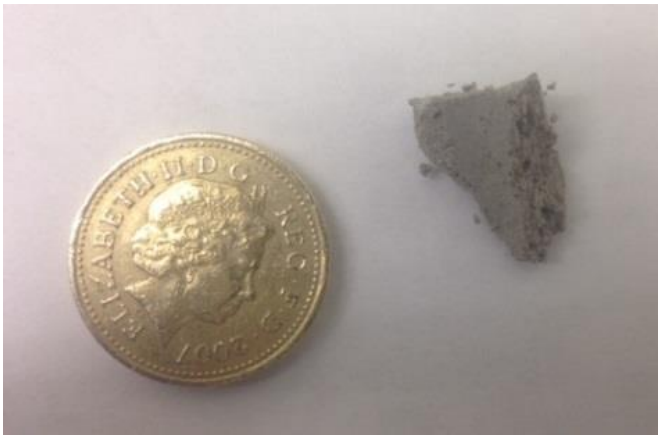

Figure 6.8: A typical specimen for MIP testing collected from the interface with steel bar representing ITZ.

6.4 Results and discussion

6.4.1 Series I

6.4.1.1 *Microwave curing temperature*

Table 6.3 provides the top surface temperature of microwave cured specimens at the end of microwave curing. Temperatures were taken from the centre of the top surface of the 100 mm cube specimens using a thermal camera. The duration of microwave curing for each repair material was controlled to achieve a midpoint top surface temperature of the cube of about 40 - 45 °C. Results presented in Table 6.3 show that specimens achieved a temperature range from 39.9 °C (Five Star) to 44.0 °C (HB40). The different duration of curing time is related to the composition of each repair material, which is discussed in Chapter 4.

Table 6.3: Duration of microwave curing to achieve a target temperature of 40-45 °C.

Repair material	Microwave curing	
	Duration (mins)	Peak temperature at the end (°C)
Five Star	50	39.9
Monomix	40	40.7
Monopour PC6	40	41.8
HB40	40	44.1
Weber	45	41.5
Fastfill	15	40.7
CEM II	50	42.1

6.4.1.2 *Effective Porosity*

Table 6.4 shows the effective porosity (intruded mercury) of Series I investigation for all repair materials (microwave and normally cured). The MIP test samples were collected close to the centroid of the cube specimen. Results show a significant variation between porosity of the repair materials. The porosity ranged from a low value

of 8.3% (Normally cured Monopour PC6) up to a value of 29.1% for microwave cured HB40. Repair materials Monomix and HB40 represent the highest porosity, which corresponds to the low density of the materials (1725 and 1500 kg/m^3 respectively). Both repair materials are described as polymer modified by manufacturers without more detail. Results presented by Calderón et al. [169] showed that replacing the sand by polymer waste aggregate in mortar by 0, 25, 50, 75 and 100% gives a fresh density of 2113, 1910, 1690, 1440 and 1200 kg/m^3 respectively while increasing the porosity. Repair material Monopour PC6 and Fastfill are also described as polymer modified but they have normal density of 2250 and 2150 kg/m^3 respectively which is in the same range as the repair materials Five Star (2200 kg/m^3) and Weber mortar (2200 kg/m^3).

The effect of microwave curing on porosity can be significant depending on the composition of the material. Based on the experimental results, the effect of microwave curing on effective porosity can be divided into three categories: Category I: repair materials in which microwave curing increases porosity. This includes materials Monopour PC6 and HB40 whose porosity increased by 16 and 9 % respectively compared to the normally cured specimens. Category II: repair materials in which microwave curing resulted in a denser structure. Materials Five Star, CEM II and Fastfill experienced a reduction in porosity by 18, 19 and 24 % respectively under microwave curing relative to normal curing. Category III: the third category is repair materials in which microwave curing has no significant effect on the effective porosity. It is represented by Monomix and Weber repair materials whose porosities are within 1% of the normally cured materials.

It is clear that microwave curing may have different effects on the porosity of repair materials based on their binders. For example, the reduction in porosity for repair materials in category II (Five Star, CEM II and Fastfill) under microwave curing is

possibly due to the well-documented phenomena of greater formation and growth of hydration products in the pore space due to thermal curing, resulting in a decrease of pore volume(s) [7]. The reduction of porosity in microwave cured Five Star, which contains pulverised fuel ash (according to the manufacturers' data), is in agreement with the results of other researchers [160, 170, 171, 172]. For example, Almari [170] reported that specimens containing pulverised fuel ash, cured at 20, 35 and 45 °C, showed a significantly lower effective porosity under 45 °C curing. Goto and Roy [158] also reported a decrease in porosity for pastes of type I cement with water cement ratios of 0.35, 0.4 and 0.45 cured at 60 °C compared to 27 °C.

Almari [170] also reported that specimens with ground granulated blast furnace slag (ggbs) showed similar porosity at 20 and 45 °C. This similar porosity under 20 and 45 °C is in agreement for repair materials Monomix and Weber.

It is clear that the effect of microwave curing on the porosity of repair materials depends on their composition. Without full knowledge of the formulation of the repair materials it is difficult to relate more fully the effect of microwave curing on porosity. It is also clear that the heat applied by microwave curing is the primary cause of influencing the pore structure, similar to conventional heat.

Table 6.4: Effect of microwave curing on effective porosity

Repair material	Porosity (%)		Increase %
	Microwave Cured	Normally Cured	
Five Star	13.6	16.6	-18
Monomix	29.0	28.6	1
HB 40	29.1	26.6	9
Monopour PC 6	9.6	8.3	16
Weber	11.4	11.4	0
Fastfill	10.8	14.2	-24
CEM II	17.0	20.9	-19

6.4.1.3 *Pore size distribution*

Figures 6.9 to 6.15 present the differential pore volume distribution graphs for all repair materials, both under normal and microwave curing. To assist the reader in comparing both normally and microwave cured materials, the scale used for the ordinate (Y axis) is based on the maximum value of the differential volume of each repair material. These graphs are plotted to estimate the critical pore diameter. Critical pore diameter corresponds to the maximum peak in the pore size distribution graph, above which no connected path can form throughout the sample [173]. Generally, it is accepted that the smaller the critical pore diameter, the finer the pore structure.

The shape of the pore size distribution curves of both normal and microwave cured specimens appear to be similar with the obvious difference being a shift in the position of the critical pore diameter and the corresponding differential pore volume. For example, normally cured Five Star shows a critical pore diameter of 0.1 μm and the differential volume is 80.72 mm^3/g. The corresponding critical pore diameter under microwave curing is similar at 0.1 μm, however, the differential volume is reduced to 61.6 mm^3/g. In the case of Monopour PC6, for example, both the critical pore diameter and differential volume have shifted (increased) under microwave curing.

Another significant observation is that the repair materials exhibit a multi-modal pore size distribution graph, unlike CEM II mortar. Multi-modal graphs represents more than one peak of differential volume at different pore diameters. Microwave curing shows a similar multi-modal pore size distribution graph to normal curing, however, the peaks are at different pore diameters. In other words, microwave curing resulted in shifting peaks toward either smaller or larger pores. For example, normally cured Monomix

shows two peaks at pore diameters 0.90 and 0.019 μm. The corresponding peaks under microwave curing moved to 1.34 and 0.023 μm respectively.

CEM II shows only one peak which is similar to the trend reported by Kong et al. [174]. They reported the distribution of pore diameter for mortar with CEM I 42.5 under normal and microwave curing to 40 °C. Their results showed a similar trend to CEM II in Figure 6.15, with one peak. However, the peaks (both in normal and microwave cured specimens) in their study appeared at a smaller pore diameter relative to the CEM II presented in Figure 6.15. This is possibly due to one of the two reasons. First, the type of cement of their study is CEM I with high compressive strength (42.5 MPa) compared to the CEM II used in this study which has a lower compressive strength (32.5 MPa). Second, CEM II used in this study is a Portland limestone cement (6-20 % lime based on BS EN 197-1). The presence of limestone up to 20 % is likely to increase porosity up to 5-10% [175].

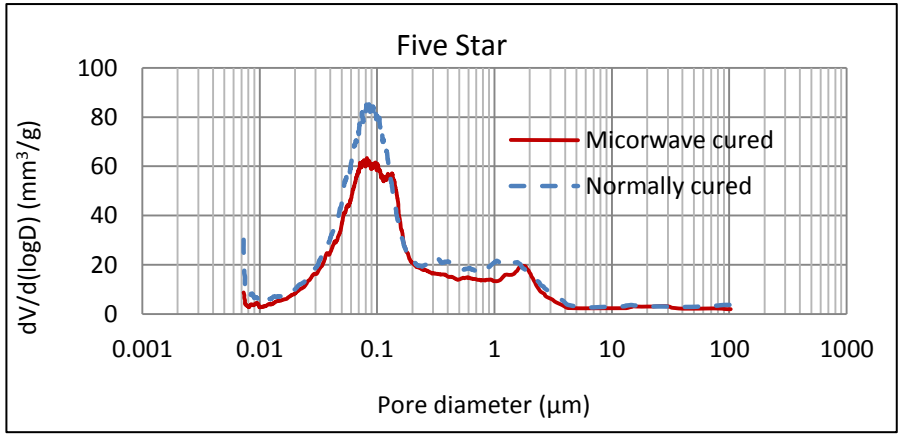

Figure 6.9: Pore distribution for Five Star repair material normal and microwave curing.

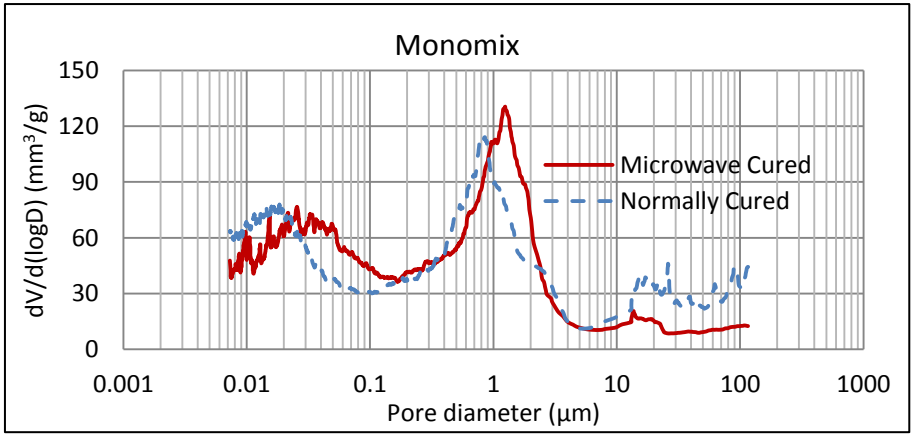

Figure 6.10: Pore distribution for Monomix material normal and microwave curing.

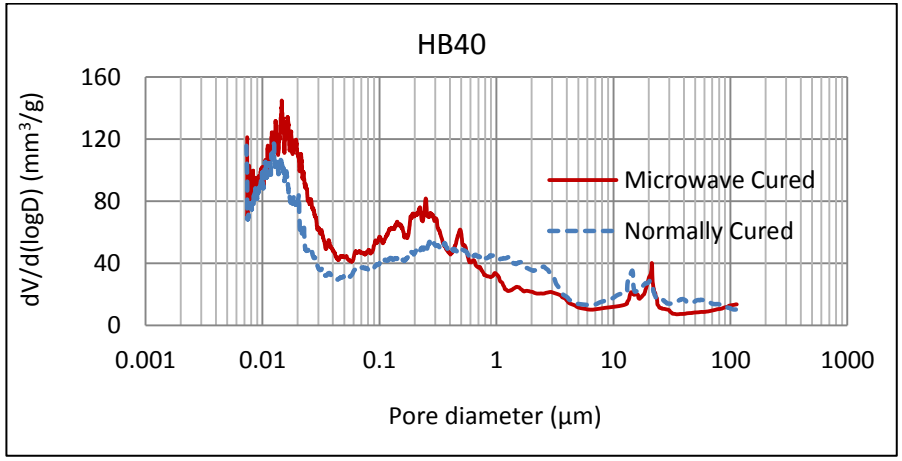

Figure 6.11: Pore distribution for HB 40 repair material normal and microwave curing.

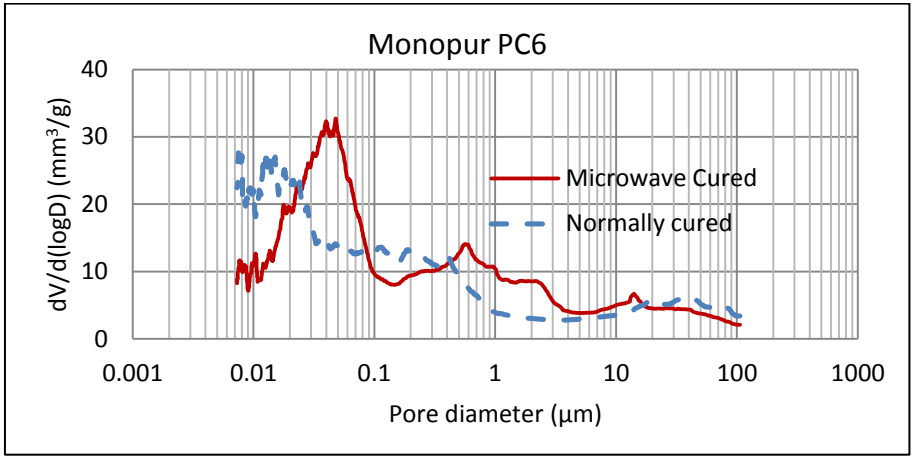

Figure 6.12: Pore distribution for Monopour PC6 Mortar normal and microwave curing.

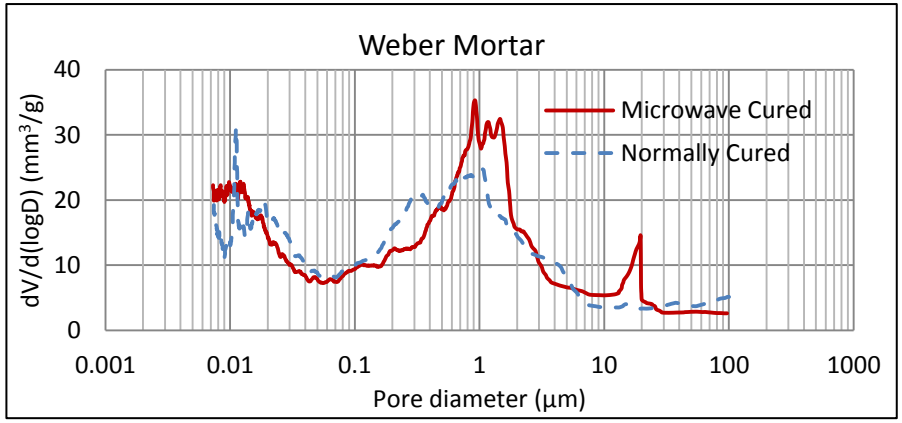

Figure 6.13: Pore distribution for Weber Mortar normal and microwave curing.

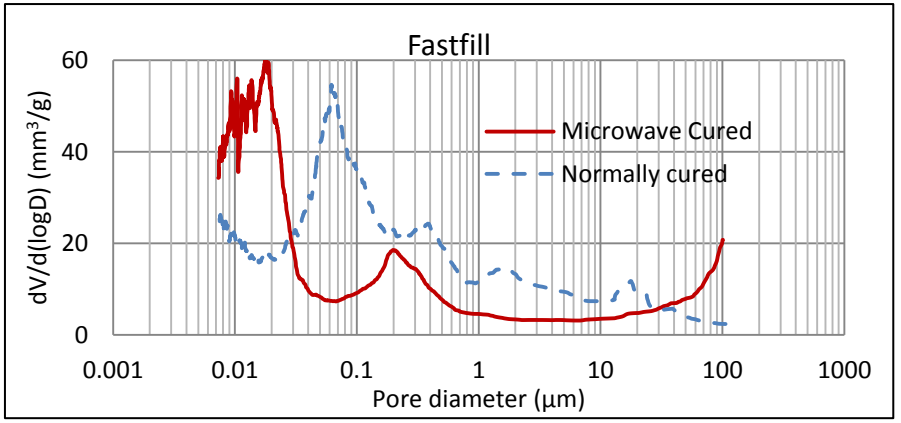

Figure 6.14: Pore distribution for Fastfill Mortar normal and microwave curing.

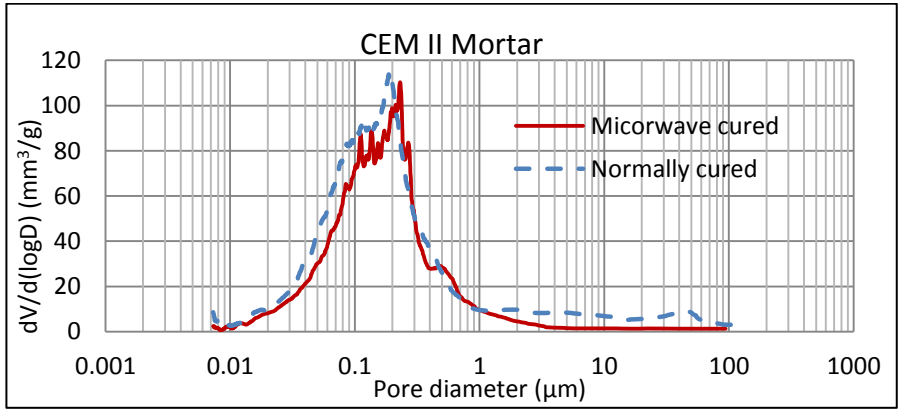

Figure 6.15: Pore distribution for CEM II Mortar normal and microwave curing.

6.4.1.4 *Effect of microwave curing on the volume of large and small pores:*

Figure 6.16 and the data in Table 6.5 present the influence of microwave curing on the volume of large (capillary) and small (gel) pores for all repair materials. The data can be collected from the pore size distribution curves provided in Figures 6.9 to 6.15 or alternatively, the cumulative intrusion distribution curves, which are the output data of the MIP equipment. The total intruded pore volume for each repair material is provided while differentiating the intruded volume of large pores (>50 nm) and small pores (<50 nm). In general large pore sizes (>50 nm), which refer to capillary pores, are more influential in determining the strength and permeability of mortar and small pores (<50 nm) play an important role in the drying shrinkage and creep properties of concrete [141].

The results show that microwave curing decreases the cumulative intruded pore volume of pore sizes larger than 50 nm for materials Five Star, HB40, Fastfill and CEM II. For example, normally cured Five Star repair material shows a differential pore volume of 65.4 mm^3/g of large pores (>50 nm) which decreases to 54.0 mm^3/g under microwave curing. In addition, microwave curing affects the cumulative volume of pore sizes smaller than 50 nm. For example, microwave curing reduces the cumulative intruded volume for pore size smaller than 50 nm for materials Five Star, Monomix, Monopour PC6 and CEM II and it increases it for materials HB40, Weber and Fastfill.

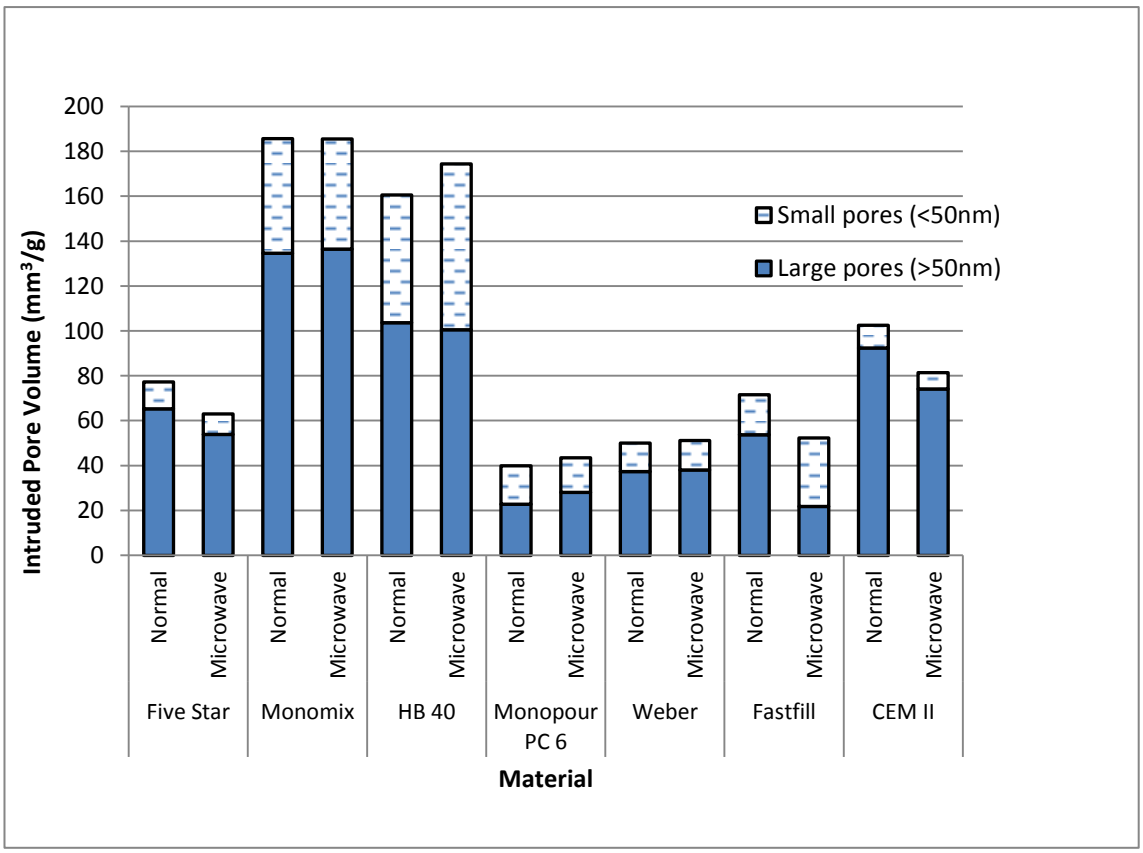

Figure 6.16: Influence of microwave curing on large (>50 nm) and small pores (<50 nm)

Table 6.5: Cumulative intruded pore volume of large and small pores in repair materials subjected to normal and microwave curing

Material	Curing regime	Total cumulative Intruded Volume (mm^3/g)	Large pores (>50nm) (mm^3/g)	Small pores (<50nm) (mm^3/g)
Five Star	Normal	77.4	65.4	12.0
	Microwave	63.1	54.0	9.1
Monomix	Normal	185.7	134.6	51.1
	Microwave	185.6	136.5	49.1
HB 40	Normal	160.6	103.7	56.9
	Microwave	174.4	100.6	73.8
Monopour PC6	Normal	40.0	22.8	17.2
	Microwave	43.6	28.1	15.5
Weber	Normal	50.0	37.3	12.7
	Microwave	51.2	38.2	13.0
Fastfill	Normal	71.6	53.8	17.8
	Microwave	52.4	21.8	30.6
CEM II	Normal	102.6	92.5	10.1
	Microwave	81.4	74.2	7.2

6.4.2 Results of Series II

6.4.2.1 *Effective Porosity*

Table 6.6 presents the effective porosity of all repair materials used in the "bond" specimens with embedded rebar (microwave and normally cured). The MIP test samples were taken at locations representing the bulk material of the cube (denoted as "bulk" in Table 6.6) and the ITZ at the embedded steel surface (denoted as "surface" in Table 6.6). The bulk material was taken close to the middle of the cube but clear from the steel rebar and the ITZ sample was taken at the steel surface (Figure 6.8).

The effective porosity of the materials ranges from 10.37 % (normally cured Five Star bulk) to 35.05 % (microwave cured HB40 surface). The Five Star and CEM II show low porosity ranging from 10.37 % (normal curing Five Star) to 13.88 % (microwave curing CEM II). However, the other two repair materials, Monomix and HB40 show higher porosity, both in bulk and surface under both normal and microwave curing. Both Monomix and HB40 are lightweight materials and their composition causes the high porosity, similar to their data of Series I tests. The differences in the porosity results of these materials in Series I and II tests are discussed in Section 6.4.3.

Table 6.6: Porosity results of Series II

Repair material	Location	Porosity (%)		Increase %
		Microwave Cured	Normally Cured	
Five Star	Bulk	11.98	10.37	15.5
Monomix	Bulk	27.95	27.92	0.1
HB 40	Bulk	33.74	28.49	18.4
CEM II	Bulk	13.88	13.44	3.3
Monomix	Surface	31.16	28.42	9.6
HB 40	Surface	35.05	27.85	25.9

6.4.2.1.1 Bulk porosity

Results presented in Table 6.6 show that microwave curing increases the effective porosity of the bulk material, relative to normal curing (20 °C and 60% RH), for all repair materials. For example, the porosity of the bulk Five Star sample increased from 10.37 to 11.98% under microwave curing. The corresponding increase for HB40 was from 28.49 to 33.74%. The increase in effective porosity under microwave curing is very small for Monomix (27.92 to 27.95%) and CEM II (13.44 to 13.88%). The results for CEM II are similar to the results from Kong et al. [174] who reported a porosity of just below 15% for a cement mortar under normal curing (20 °C, 95% RH) which increased to just above 15% under microwave curing.

The increase in effective porosity is due to the microwave heating applied at early age, similar to the increase in porosity due to conventional heating reported by the other researchers [176, 177, 178, 179]. For example, Kjellsen et al. [179] showed an increase in porosity from 10.93 % to 15.11 % for plain cement paste cured in water at 20 °C and 50 °C respectively, by using backscattered electron image analysis.

6.4.2.1.2 ITZ porosity

Data presented in Table 6.6 show that the effective porosity in the ITZ increased for both Monomix and HB40 under microwave curing relative to normal curing. The ITZ porosity of Monomix increased from 28.42 (normal curing) to 31.16% (microwave curing). The corresponding values for HB40 are 27.85 and 35.05% under normal and microwave curing respectively.

A comparison between normally cured specimens taken from "bulk" and "ITZ" show similar porosity. For example, normally cured Monomix shows an effective porosity of 27.92 and 28.42 % for specimens taken from "bulk" and "ITZ" respectively. The

corresponding values for HB40 are 28.49 and 27.85 % for bulk and ITZ respectively under normal curing. On the other hand, microwave curing increases the effective porosity at the ITZ (relative to bulk) significantly for both Monomix and HB40. For example, microwave cured Monomix repair material shows an effective porosity of 27.95% at bulk which increased to 31.16% at ITZ. The corresponding increase for HB40 is from 33.74 % to 35.05 % at bulk and ITZ respectively under microwave curing.

Increased porosity in the ITZ relative to bulk porosity has been previously reported. For example, Horne et al. [180] reported an increase in porosity at both the steel and aggregate interface with cement paste in reinforced concrete. It was based on a microscopic investigation of porosity representing micro-thickness of the ITZ whereas, the present investigation uses MIP analysis on larger samples which represent a greater mean distance from the steel interface compared to Horne et al. [180]. The results of Horne et al. [180] indicate an exponential reduction in porosity with increasing distance from the steel surface.

6.4.2.2 *Pore size distribution*

Figures 6.17 to 6.22 show the pore size distribution for repair materials investigated in Series II. The results show that microwave curing significantly affects the critical pore size for Monomix and HB40 repair materials at both the bulk and ITZ locations. For example, normally cured Monomix shows two peaks at 0.77 and 0.0315 μm pore sizes with volumes of 155 and 148.8 mm^3/g respectively. The corresponding peaks under microwave curing occur at pore dimeters 2.45 and 0.0279 μm with volumes of 179.1 and 84.175 mm^3/g respectively. Shifting the peaks toward the larger pore diameters results in a coarser microstructure of the repair material under microwave curing.

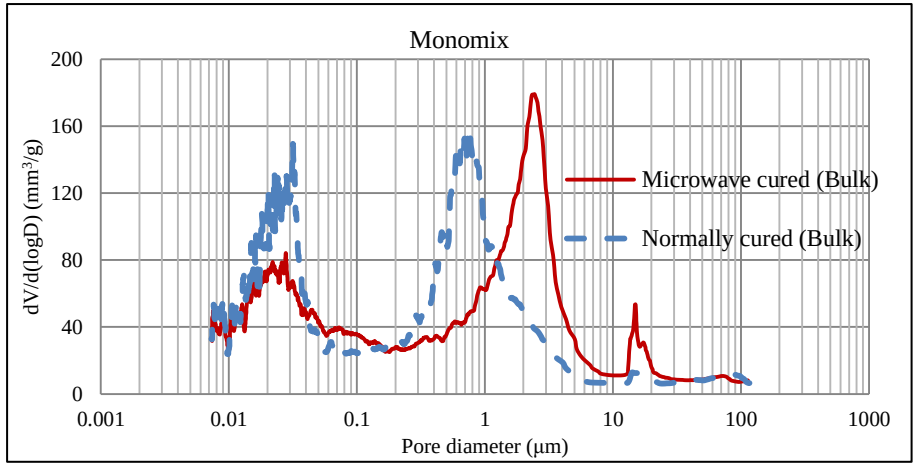

Figure 6.17: Pore volume distribution curve for normally and microwave cured Monomix bulk samples

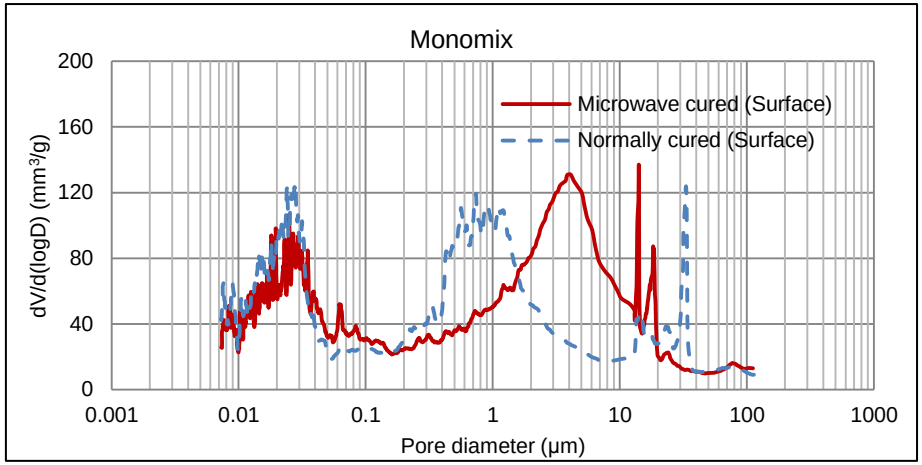

Figure 6.18: Pore volume distribution curve for normally and microwave cured Monomix ITZ samples

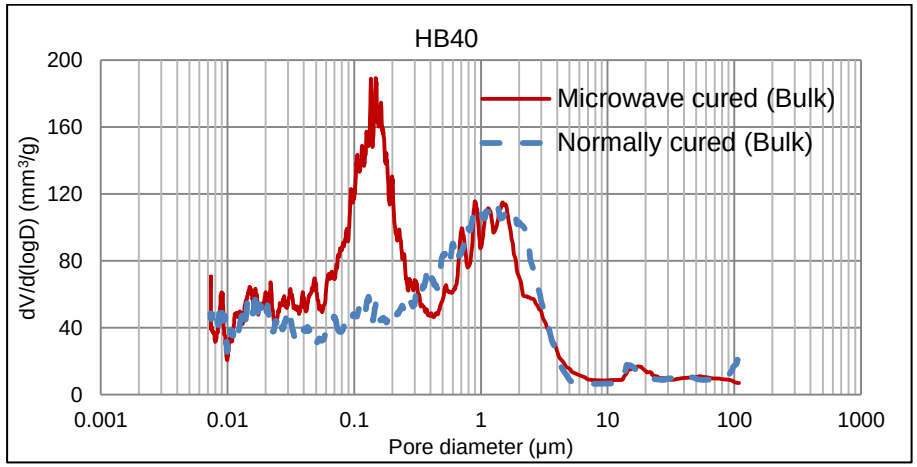

Figure 6.19: Pore volume distribution curve for normally and microwave cured HB40 bulk samples

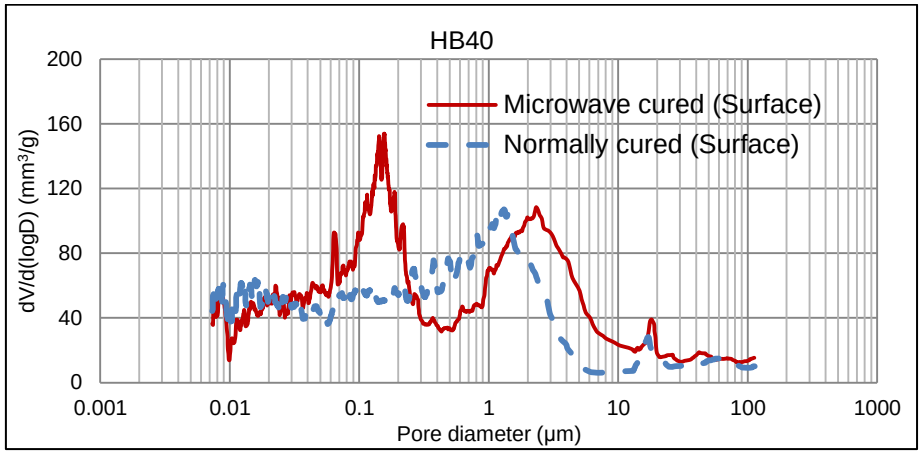

Figure 6.20: Pore volume distribution curve for normally and microwave cured HB40 ITZ samples

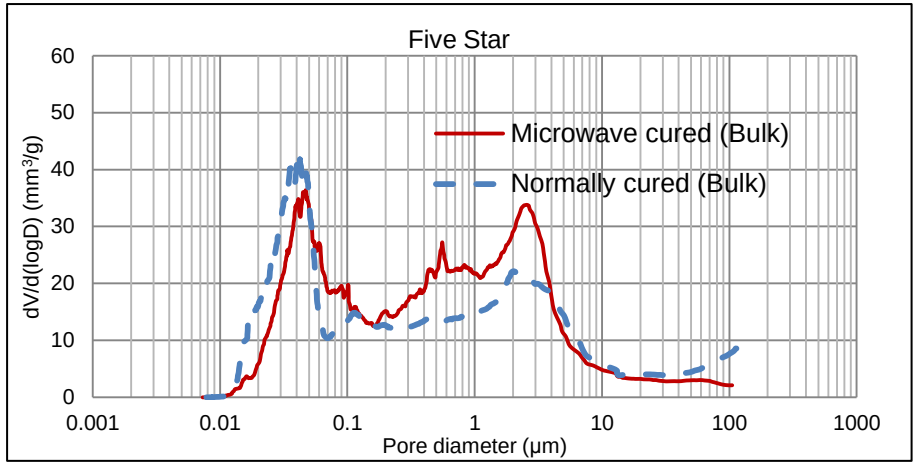

Figure 6.21: Pore volume distribution curve for normally and microwave cured Five Star bulk samples

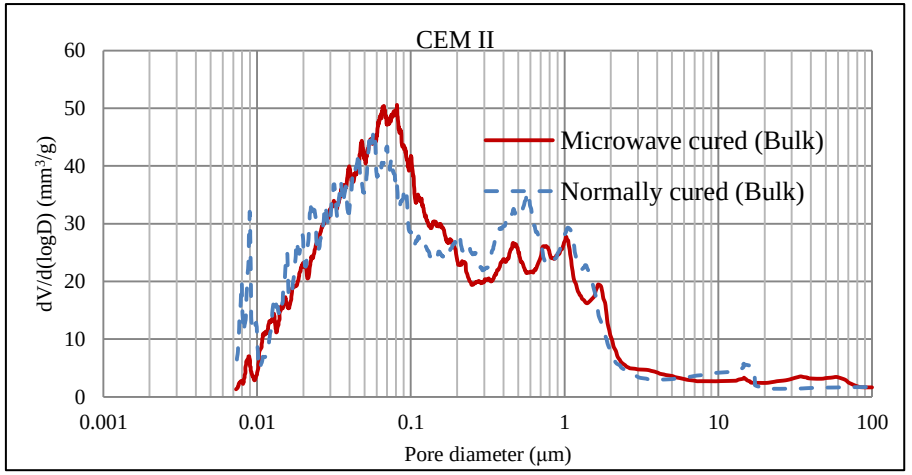

Figure 6.22: Pore volume distribution curve for normally and microwave cured CEMII bulk samples

6.4.2.3 *Effect of microwave curing on the volume of large and small pores:*

Figure 6.23 and corresponding data in Table 6.7 show the cumulative intruded pore volume for normal and microwave cured repair materials which has been determined from Figure 6.17 to Figure 6.22. The intruded volumes for pore sizes larger than 50 nm and smaller than 50 nm are given. Results show that microwave curing produces a greater volume of pores larger than 50 nm for all repair materials relative to normal curing. For example, the cumulative intruded volume of pores larger than 50 nm for normally cured Monomix is 124.31 mm^3/g compared with 145.65 mm^3/g under microwave curing. The trend is similar for the other repair materials for both bulk and ITZ specimens. However, the difference for CEMII is insignificant, increasing from 50.63 to 52.30 mm^3/g. Microwave curing also provides a lower volume of pores smaller than 50 nm compared with normal curing with the exception of HB40 bulk sample, but not the "ITZ". For example, the pore volume for Five Star decreases from 13.05 to 10.39 mm^3/g under microwave curing. However, the difference for CEMII, again, is less significant, decreasing from 18.81 to 17.08 mm^3/g under microwave curing.

The decrease in volume for pore size smaller than 50 nm is responsible for decreasing shrinkage under microwave curing which will be discussed in Chapter 8. Similarly, the increase in volume for pore size larger than 50 nm is responsible for decreasing compressive (and bond) strength under microwave curing. These two aspects are discussed in Chapter 8.

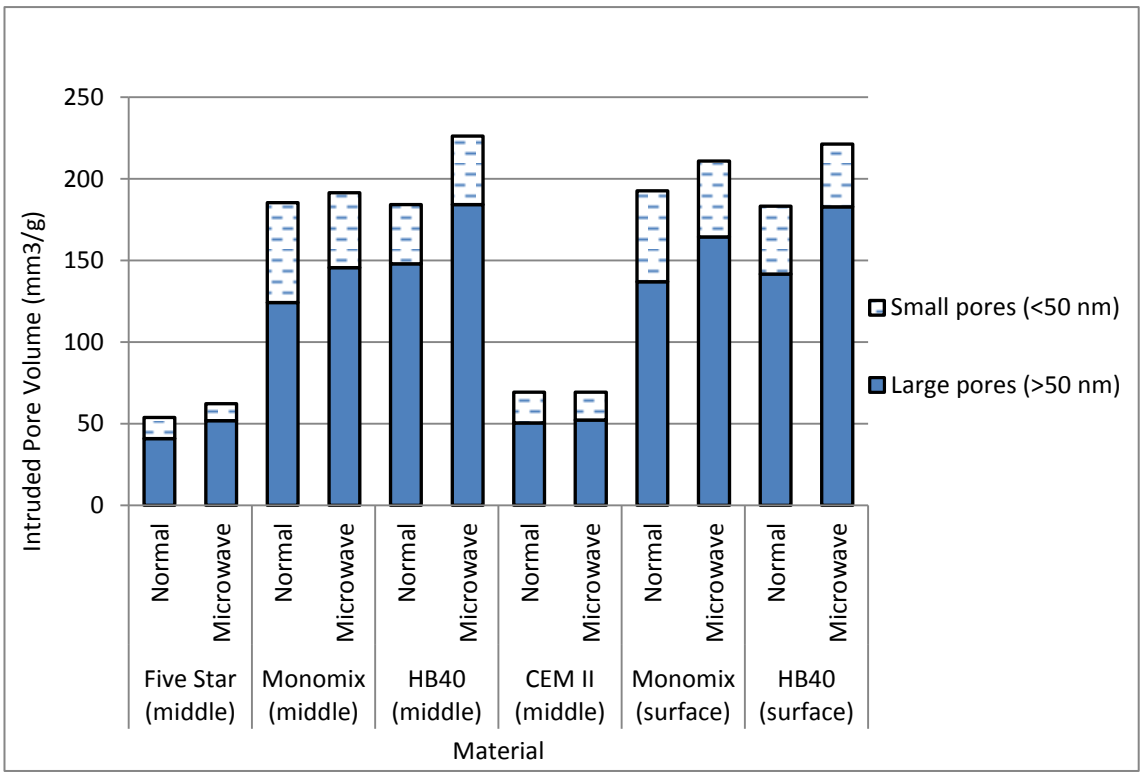

Figure 6.23: Influence of microwave curing on large and small pores

Table 6.7: Effect of microwave curing on large and small pores

Material	Location	Curing regime	Cumulative intruded volume (mm^3/g)	Large pores (>50 nm) (mm^3/g)	Small pores (<50 nm) (mm^3/g)
Five Star	Middle (bulk)	Normal	53.96	40.91	13.05
		Microwave	62.26	51.87	10.39
Monomix	Middle (bulk)	Normal	185.48	124.31	61.17
		Microwave	191.71	145.65	46.06
HB40	Middle (bulk)	Normal	184.28	148.00	36.28
		Microwave	226.31	184.3	42.01
CEM II	Middle (bulk)	Normally	69.44	50.63	18.81
		Microwave	69.38	52.3	17.08
Monomix	Surface (ITZ)	Normal	192.73	136.98	55.75
		Microwave	211.13	164.5	46.63
HB40	Surface (ITZ)	Normal	183.45	141.83	41.62
		Microwave	221.41	182.98	38.43

6.4.3 Comparison of effective porosity in Series I and II

Data in Table 6.8 present the effective porosity of the bulk materials (specimens taken at the core) for Series I and II under normal and microwave curing. Results show that repair materials in Series I tests have higher effective porosity compared to Series II for both normal and microwave cured repair materials. For example, microwave cured CEM II in Series I has an effective porosity of 17.0 % compared with 13.88% in Series II, showing an increase of over 18%. Material HB40 is an exception as both normally and microwave cured specimens in Series II show higher effective porosity compared to the Series I.

Specimens in Series I also show a decrease in intruded pore volume of the bulk material for large pores (>50 nm) under microwave curing compared to normal curing (Table 6.5). However, it is reversed for specimens in Series II (Table 6.7). For example, Five Star repair material in Series I shows an intruded pore volume of 65.4 mm^3/g for large pores (50> nm) under normal curing and it reduced to 54.0 mm^3/g under microwave curing. The corresponding intruded volume for normally cured Five Star in Series II is 40.91 mm^3/g and it increased to 51.87 mm^3/g under microwave curing. Monomix repair material in Series I is exception.

The difference in porosity in Series I and II discussed above is due to the early (first 24 hours) curing condition of repair materials. Series I specimens were cured uncovered in air during the first 24 hours after casting and then cured in water for 27 days. The repair material specimens in Series II were covered (wrapped in polyethylene) during the first 24 hours after casting and then cured in air (20 °C and 60% RH) while wrapped with polyethylene sheets (Chapter 8). The specimens of Series II were cured at a higher level of humidity during the first 24 hours although the humidity levels were reversed after

24 hours when Series I specimens were cured in water and Series II wrapped in air. The first 24 hours curing has the dominant influence resulting in low porosity of Series II specimens. The reduction of porosity in Series II is lower for microwave cured specimens, ranging from 3.6 % to 18.4 % (excluding HB40) compared with 2.4% to 37.5% for normal curing.

The curing of Series 1 samples in water for 27 days has not overcome the initial disadvantage of exposed air curing during the first 24 hours. The results show that early age moist curing, including prevention of moisture loss during microwave curing, is the dominant factor in producing low porosity material.

The effect of moist and air curing at early age has been previously reported by Khatib and Mangat [164]. They reported an increase of porosity up to 25% for specimens cured at 45 °C in air compared to the specimens cured at the same temperature but initially moist cured. The availability of moisture during early curing produces more hydration products resulting in the filling of pores which reduce the pore volume and provide a finer pore structure. In the case of specimens which were exposed to air, evaporation of moisture led to the availability of less water for hydration and, therefore, resulting in a coarser pore structure [164]. Similar results were also reported by Ballester et al. [165]. They argued that exposure to the higher temperature results in a higher porosity, nevertheless, the porosity allows retaining a larger amount of water (if available) during curing, which facilitates the hydration reactions [165].

Table 6.8: Comparison of porosity of the bulk material for Series I and II

Repair material	Density (kg/m^3)	Porosity (%)				Decrease %	Decrease %
		Series I		Series II			
		Microwave Cured	Normally Cured	Microwave Cured	Normally Cured	Microwave cured	Normally cured
Five Star	2200	13.6	16.6	11.98	10.37	11.9	37.5
Monomix	1725	29.0	28.6	27.95	27.92	3.6	2.4
HB 40	1500	29.1	26.6	33.74	28.49	-15.9	-7.1
CEM II	2200	17.0	20.9	13.88	13.44	18.4	35.7

6.5 Conclusions

The following conclusions can be drawn from this chapter.

- Microwave curing increases the porosity of the bulk matrix and ITZ relative to normal curing under ambient conditions. For example, HB40 shows a porosity in the bulk materials of 28.49 % under normal curing and 33.74% under microwave curing. The corresponding porosity at the ITZ is 27.85% and 35.05% respectively.
- Microwave curing reduces the intruded pore volume of small (gel) pores (<50 nm) of repair mortars relative to normal curing.
- Early age wet curing (after microwave curing) and prevention of moisture loss during microwave curing are the dominant factors for producing low porosity repairs.

Chapter 7

7. Bond between microwave cured repair and concrete substrate

7.1 Introduction

This chapter presents experimental results of an investigation to determine the effect of microwave curing on the bond strength between the repair patch and concrete substrate applied at ambient temperatures 20, 10, 2 and -5 °C. Three proprietary repair materials and CEM II mortar were selected for this investigation. In addition to the bond strength, it also investigates the effect of microwave curing on compressive strength of repair patch and substrate.

7.2 Background

In general, concrete repair is classified as structural and non-structural (cosmetic) [181]. Structural repair is expected to share load while non-structural repair does not share load. The most common type of repair is a patch repair which covers a relatively small area in large surface elements of the structure. They have long been used to repair damaged concrete structures in order to restore or increase the strength, provide water tightness, improve appearance and the durability of concrete. The durability of patch repair is a serious concern as according to Matthews and Morlidge [38] 50% of concrete repairs exhibit signs of failure within 5 years. Furthermore, most structure owners are dissatisfied with repairs within 10 years of application [182, 183].

One of the most important parameters to assess the durability of patch repair is the quality of bond of the repair material to the substrate. The British standard BS EN 1504-

10 [40] defines bond as the adhesion of the applied product or system to the concrete substrate. It is fundamental in concrete repair to have sufficient bond between the new applied repair and the substrate as it affects the reliability and durability of repair [41]. According to BS EN 1504-3:2005 [42], the adhesive bond should be at least 2 MPa (Class 4) or 1.5 MPa (Class R3) for structural repair and 0.8 MPa for non-structural repairs. This is due to the fact that the adhesion of the repair material applied on the concrete substrate is essential to achieve successful and long-term durability of the repair.

Bond failure may occur in the substrate, repair interface, the new repair patch or in a combination of these locations [184]. Bond failure at the interface indicates a true failure in bond. Failure in either the substrate or the repair patch indicates that the bond strength is greater than the material strength. Sprinkel and Ozyildirim [184] classified the bond strength of concrete repair from "poor" to "excellent" as shown in Table 7.1. It can be used as a general guideline to classify the bond strength and evaluate the quality of repair.

Table 7.1: Bond strength classification provided by Sprinkel and Ozyildirim [184]

Bond strength (MPa)	Classification
0-0.7	Poor
0.7-1.4	Fair
1.4-1.7	Good
1.7-2.1	Very good
≥2.1	Excellent

7.3 Test programme and materials

7.3.1 Experimental programme

The effect of microwave curing on the bond strength between the concrete substrate and various repair materials was determined in the laboratory investigation. Concrete cubes

were cast and then cut in half (100 x 100 x 50 mm) to produce the substrate prisms. The substrate prisms were then placed at the bottom of polystyrene moulds and filled with a repair material to form a 100 mm "composite" cube of equal halves of substrate and repair material. The repair materials were mixed and applied at ambient temperatures 20, 10, 2 and -5 °C (corresponding to Series 1, 2, 3 and 4 respectively) and the specimens remained exposed to the corresponding temperature for 24 hours after repair application. Specimens were de-moulded and cured in water for 27 days and then the splitting tensile test was carried out. Table 7.2 presents the details of the experimental programme.

7.3.2 Repair materials

The repair materials are single component bagged materials and only require the addition of water. The following three repair materials and CEM II mortar were used to apply a repair to the concrete substrate half-cube specimens.

- Five Star
- Monomix
- Monopour PC6
- CEM II Mortar (cement/ sand ratio of 1:2 and water/ cement ratio of 0.5).

A description of each repair material is presented in Chapter 3. The materials were mixed in proportions according to the manufacturers' recommendations using a Hobart mixer.

7.3.3 Microwave curing and temperature conditioning equipment

Microwave oven II (Sharp R-2370) was used for microwave curing composite cubes. Details of the microwave oven are given in Chapter 3, Section 3.3.1.2.

A Sanyo Model MTH 4400 PR ATMOS environmental chamber was used to condition the concrete substrate specimens, repair material constituents and the composite cubes, before and for 24 hours after repair to ambient temperature of either 20, 10, 2 or -5 °C (Series 1, 2, 3 or 4 respectively, Table 7.2).

Table 7.2: Experimental program

Test Series	Repair temperature (°C)*	Number of substrate cubes	Substrate strength** (MPa)	Repair Material	Number of composite (repaired) cubes		Number of cubes for quality control
					Normally cured	Microwave cured	
1	20	4	48.5	Five Star	4	4	3
		4	48.5	Monomix			3
		4	48.5	Monopour PC6			3
		4	49.5	CEM II			3
2	10	4	49.5	Five Star	4	4	3
		4	49.5	Monomix			3
		4	49.5	Monopour PC6			3
		4	49.5	CEM II			3
3	2	4	49.5	Five Star	4	4	3
		4	52.0	Monomix			3
		4	52.0	Monopour PC6			3
		4	52.0	CEM II			3
4	-5	4	58.0	Five Star	4	4	3
		4	58.0	Monomix			3
		4	48.5	Monopour PC6			3
		4	48.5	CEM II			3

* Temperature of the repair during and for 24 hours after mixing and casting. Subsequently cured in water at 20 °C.

**28 day compressive strength

7.3.4 Details of specimens, mixing and microwave curing

7.3.4.1 *Substrate specimen preparation*

Substrate concrete cubes were cast in 100 mm steel moulds according to the BS EN 12390-2 [185]. Oven dried coarse sharp sand (50% passing a 600 μm sieve) and uncrushed river gravel with the maximum size of 10 mm along with Portland limestone cement CEM II/A-L [65] were used to cast the substrate cubes. The ratio of Cement/sand/aggregate was 1:1.4:2.4. The concrete substrate was designed according to the BRE guide [186] with w/c ratio 0.4 to achieve a high strength concrete of 48.5-58.0 MPa. Due to the requirement for a large number of substrate cubes and also the limitation of equipment, the substrate concrete cubes were prepared by casting 6 separate mixes for 10-12 cubes each. Three cubes were used to determine the strength of the mix at 28 days age for quality control according to the BS EN 12390-3 [187]. All substrate mixes were prepared in the laboratory environment at 20 °C, 60 % RH using a Cretengle Multi Flow Mixer. The specimens were compacted on a vibrating table and special care was taken to keep the trowelled face of the cubes smooth and level. They were covered with a plastic sheet and kept under laboratory conditions (20 °C, 60% RH) for 24 hours. Subsequently, they were de-moulded and cured in water at 20 °C for 27 days. The cube specimens were temporarily removed from the water after 27 days (±1 day) and cut in halves using a diamond blade masonry saw with running cooling water. Cube specimens were cut in such way that the cutting face was parallel to the trowelled face of the cubes. The cut faces were then grit blasted for one minute.

The eight sawn and grit blasted substrate cube-halves of dimensions (100 x 100 x 50 mm prisms) per mix (Table 7.2) were placed in a water tank (temperature 20 °C) until the application of the repair. The half-cubes of substrate and the repair materials were

conditioned to the ambient "repair temperatures" given in Table 7.2 before repair application (Section 7.3.4.2).

7.3.4.2 *Temperature conditioning and composite cube preparation*

The ingredients of each repair material mix and the approximately 28 days old substrate concrete halves (100 x 100 x 50 mm prisms) were kept in the environmental chamber overnight prior to mixing in the laboratory. The environmental chamber was set at 20, 10, 2 and -5 °C respectively representing the "repair temperature" for Series 1, 2, 3 and 4 in order to regulate the temperature of the repair mix constituents and the substrate cube-halves to the "repair temperatures" given in Table 7.2. Mixing and casting of the repair material were carried out in the laboratory environment (20 °C, 60% RH) after 24 hours of "conditioning". The repair material constituents and the half-cubes of the substrate were removed from the environmental chamber immediately prior to mixing the repair material. The substrate half-cubes were dried with an absorbent towel to achieve a saturated surface dry condition before the application of repair. The substrate cubes were carefully placed level in the polystyrene cube moulds (100 mm) with the grit blasted surface facing upward to receive the repair material. At the same time, the repair material was mixed.

Immediately after mixing, a total of 8 composite cubes (100 mm) were cast in the polystyrene moulds for each repair material of each Series. Soon after casting and compacting, the composite cubes were placed in the environmental chamber set at the ambient temperatures 20, 10, 2 and -5 °C respectively for Series 1, 2, 3 and 4. Four composite cubes (100 mm) were kept inside the environmental chamber, (covered with plastic sheet), throughout the 24 hours and they are referred to as representing normal curing at 20, 10, 2 and -5 °C respectively. The other four cubes were removed from the

environmental chamber 30 minutes after water was added to the mix and placed in the microwave oven at 132 Watts for 45 minutes (40 minutes for Monomix repair material) to achieve curing temperatures within the optimum range of 40-45 °C. Four specimens were placed in the microwave oven at each time. Figure 7.1 shows the arrangement of specimens inside the microwave oven. These specimens are referred to as microwave cured specimens. Immediately after microwave curing, the specimens were covered and returned to the environmental chamber where the control samples of composite cubes made with each repair material had remained since the application of repair.

Both normally and microwave cured specimens were removed from the environmental chamber after 24 hours and de-moulded except Series 4 (-5 °C) which were de-moulded at 48 hours. Subsequently, the specimens were cured in water at 20 °C. The specimens were removed from water at 28 days age (the substrate was 56 days old) and subjected to the tensile split test on the bond surface to determine the splitting tensile strength of the repaired surface. After splitting, each half cube was also crushed in order to determine the compressive strength of the prisms.

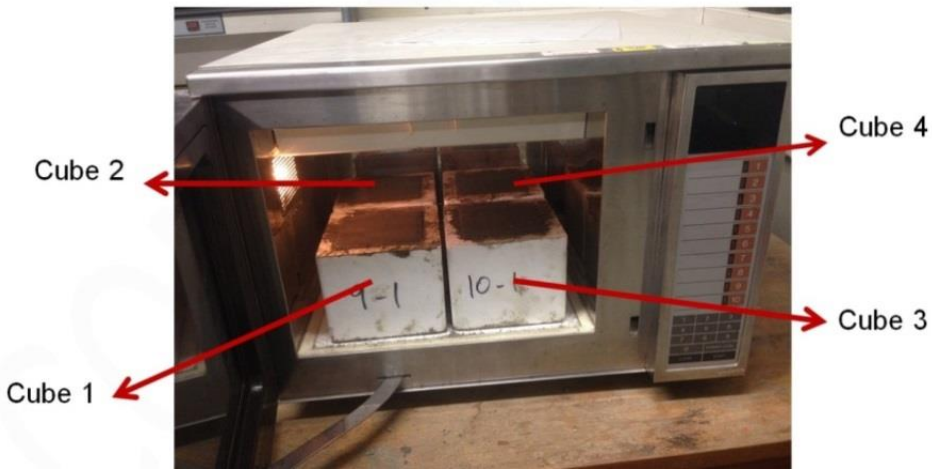

Figure 7.1: Arrangement of repaired specimens inside commercial microwave oven

7.3.5 Testing

The tensile split test was carried out in accordance with BS EN 12390-6: 2009 [188] to determine the bond strength between the concrete substrate and the repair materials. A schematic diagram of the test method with a stress diagram across the interface is shown in Figure 7.2(a-b). The "repaired" cubes were located within the splitting test rig as shown in Figure 7.2 a and the whole assembly was placed between the loading platens of the compression test machine. A compressive load was applied through the platens and increased gradually until splitting failure of the specimens. The applied load (P) produces a vertical compressive stress and a horizontal tensile stress at the interface of the repair as follows [188, 189, 190]:

$$\sigma_{y\,\max} = \frac{6P}{\pi L^2} \qquad (7.1)$$

$$\sigma_{x\,\max} = \frac{2P}{\pi L^2} \qquad (7.2)$$

Where, σ_{ymax} is the maximum local compressive stress at the interface of the repair (MPa); σ_{xmax} is the maximum horizontal tensile stress at the bonded interface of the composite cube (MPa); P is the compressive load on the cube at failure (N); L is the height of the composite cube (mm). The bond strength of the repaired substrate reported in this chapter was calculated with equation (2) at the maximum load (P). The splitting tensile test and a compression test was carried out for all test Series (Table 7.2) in the laboratory environment (20 °C and 60% RH) at 28 days age of the repair.

A compression test was performed on the 100 x 100 x 50 mm prisms of the repair and substrate material, which separated after the tensile split test. The crushing load was applied in the same direction as the splitting load.

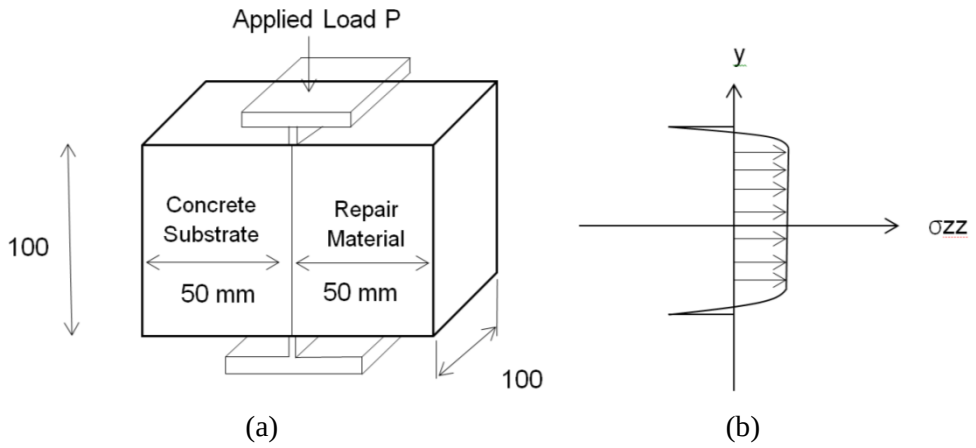

Figure 7.2: (a) Schematic diagram for splitting tensile test, (b) Stress diagram across the interface (b).

7.4 Results and discussion

7.4.1 Temperature distribution

Top surface temperatures of cubes were recorded during 45 minutes of microwave curing. Figure 7.3 shows a typical top surface temperature distribution of 4 cubes of the Five Star repair material at the end of 45 minutes of microwave curing at 132 Watts. The temperature range of the midpoint top surface is 36.2 °C to 40.3 °C (Figure 7.3). In addition, there are also significant temperature variations across the top surface of four cubes at the end of microwave curing. The variation on the midpoint of the top surface of the four cubes and variation across the top surface of each individual cube is attributed to the properties of microwave heating which are discussed in Chapter 4 and the location of each specimen inside the oven.

Figure 7.4 shows a typical graph of top middle surface temperature during 45 minutes of microwave curing for Five Star repair material. Temperature increases were similar for all repair materials and as observed in Chapter 4. Typical temperature variation between the four specimens was up to 12%.

Cube 1

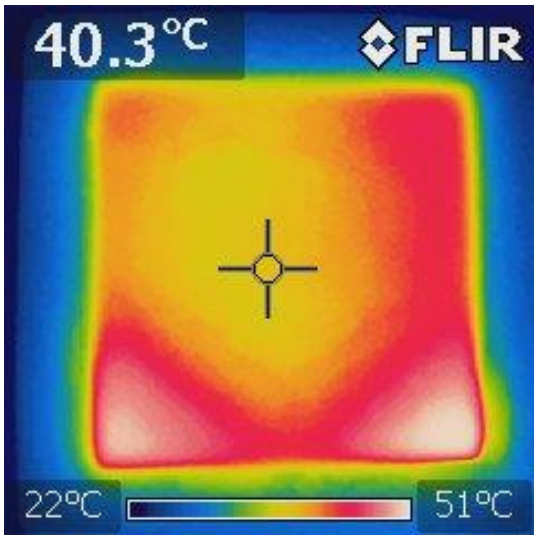

Cube 2

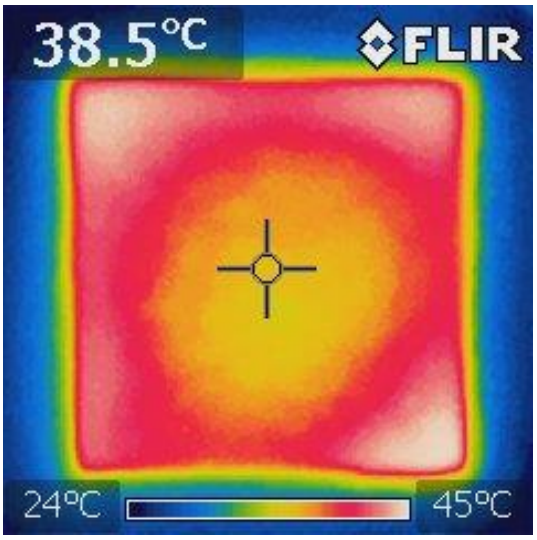

Cube 3

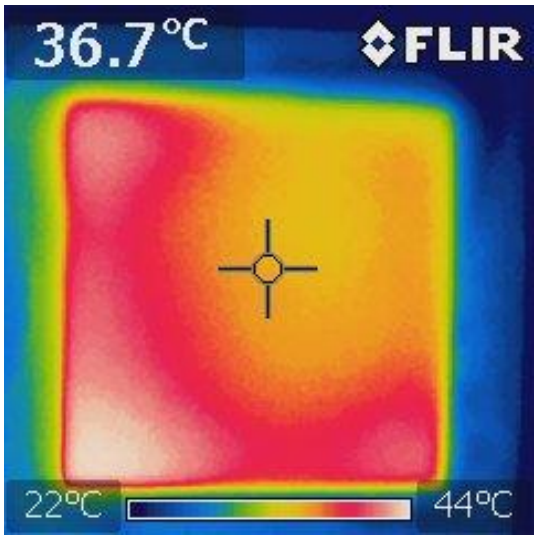

Cube 4

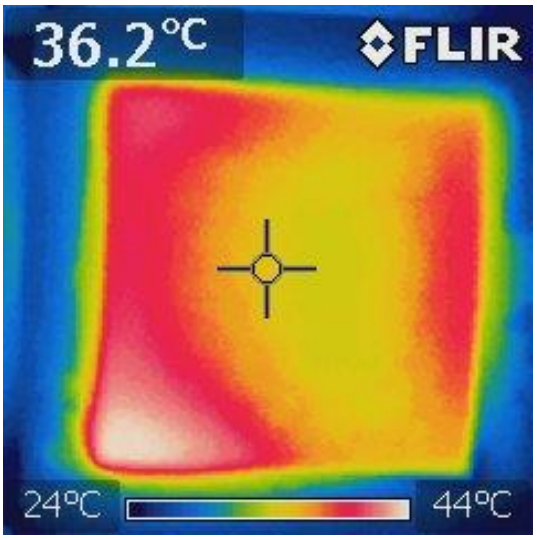

Figure 7.3: Image of top surface temperature distribution of four cubes of Five Star repair material (Series 2) at the end of 45 minutes of microwave curing at 132 Watts. (Figure 7.1 shows the positions of each specimen inside microwave oven).

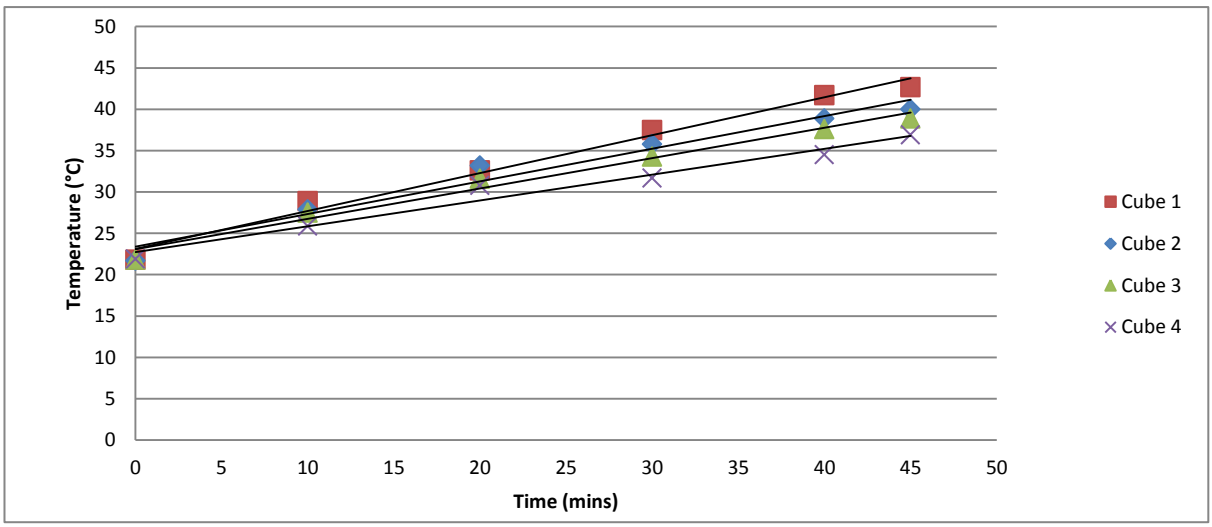

Figure 7.4: Top surface temperature of four cubes of Five Star repair material, microwave cured at 132 Watts for 45 minutes (Series 1).

7.4.2 Failure mode

Failure in the tensile split test may occur in different modes depending on the relative strength of the repair, the interface and the substrate. Failure can occur in the substrate, repair patch or the interface depending on the weakest zone. All specimens which were subjected to the tensile split test in this investigation (both normally and microwave cured) exhibited failure at the bond interface between the substrate and the repair material. Figure 7.5 shows typical examples of the two-half composite cubes after the tensile split test. This indicates that the results provide a true bond strength, with the interface between the substrate and repair being the weakest zone compared with the adjacent substrate and repair material. The failure surfaces are clear and undamaged.

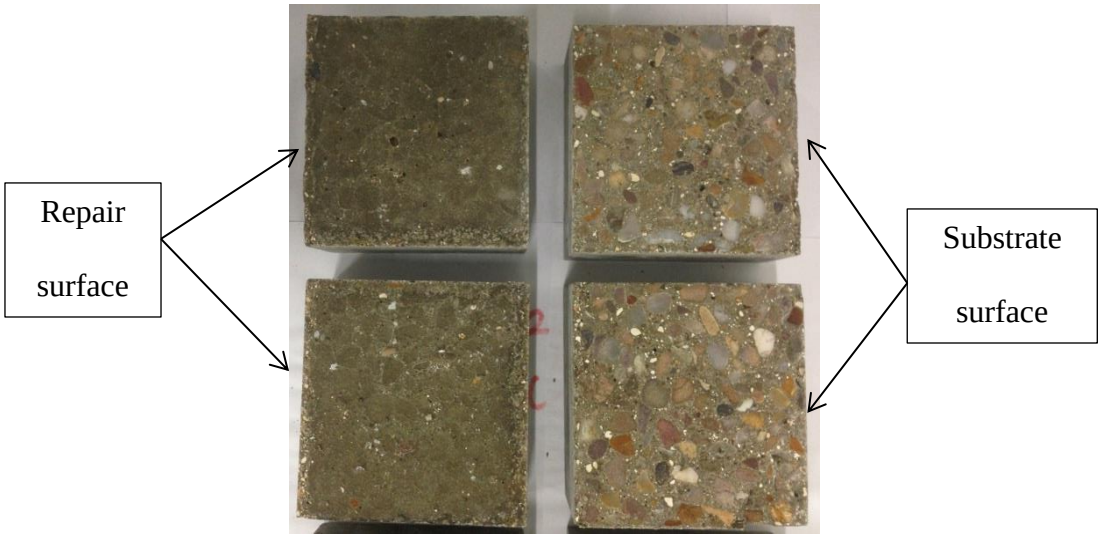

Figure 7.5: Typical examples of failure at the bonded surface between substrate and repair material subjected to split tensile test (CEM II mortar microwave cured (Series 3)).

7.4.3 Bond Strength

Figure 7.6 and the corresponding data in Table 7.3 show the results of bond strength for microwave and normally cured repair materials applied at ambient temperatures of 20, 10, 2 and -5 °C. Due to the similarities between the results for temperatures 20, 10 and 2 °C, they are analysed in one section, whereas, results for temperature -5 °C are analysed in a separate section since these samples were exposed to freezing at an early age.

Table 7.3: Bond strength results of normally and microwave cured "composite" cubes

Series	Repair temperature (°C)	Repair material	Normally cured		Microwave cured		Temperature after microwave curing*** (°C)	Bond strength increase (%)
			Bond strength* (MPa)	SD** (MPa)	Bond Strength* (MPa)	SD** (MPa)		
1	20	Five Star	2.30	0.15	2.50	0.28	39.6	9
	20	Monomix	2.25	0.33	2.15	0.27	47.4	-4
	20	Monopour PC6	2.55	0.44	2.75	0.42	45.8	8
	20	CEM II	1.40	0.25	1.40	0.16	41.1	0
2	10	Five Star	1.95	0.34	2.15	0.21	37.9	10
	10	Monomix	2.05	0.16	1.90	0.22	42.7	-7
	10	Monopour PC6	2.30	0.51	2.25	0.16	41.0	-2
	10	CEM II	1.85	0.22	1.65	0.12	38.9	-11
3	2	Five Star	2.15	0.17	2.15	0.01	35.9	0
	2	Monomix	2.65	0.20	2.70	0.18	40.0	2
	2	Monopour PC6	2.60	0.26	2.10	0.07	40.0	-19
	2	CEM II	1.90	0.30	1.90	0.07	40.9	0
4	-5	Five Star	0.75	0.19	2.45	0.31	34.6	227
	-5	Monomix	0.70	0.13	1.30	0.17	38.7	86
	-5	Monopour PC6	0.80	0.18	1.95	0.34	37.6	143
	-5	CEM II	1.15	0.24	2.15	0.28	38.2	87

* 28 day strength
** Standard deviation
*** Average (of 4 cubes) top surface middle point temperature of repaired cubes at the end of microwave curing

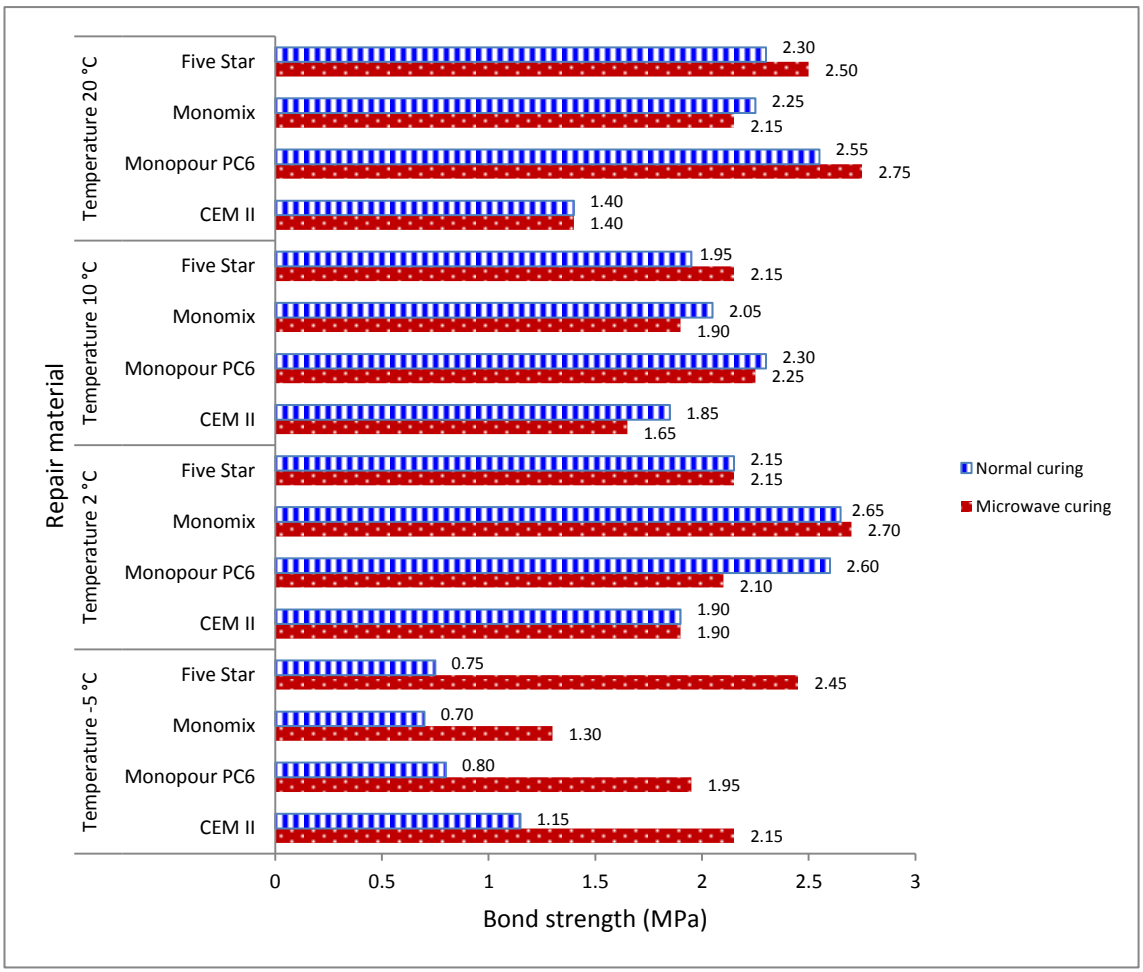

Figure 7.6: Comparison graph of average bond strength for Series 1, 2, 3 and 4 tests

7.4.3.1 *Bond strength at repair temperature 20, 10 and 2 °C*

The results presented in Figure 7.6 and the data in Table 7.3 show that microwave curing applied under the repair temperatures of 20, 10 and 2 °C did not significantly affect the interfacial bond strength at 28 days age relative to normally cured repair. In total, eleven of the twelve repair material results exhibit a change in bond strength between -11 to 10 % with an average decrease of 0.5 %. The remaining repair material (Monopour PC6 cured under ambient temperature 2 °C) shows a decrease of 19% under microwave curing, which is inconsistent with its trends at 20 °C, and 10 °C curing where it shows +8 % and -2% variation respectively.

The bond strength for normally and microwave cured proprietary materials Five Star, Monomix and Monopour PC6 applied at ambient temperature 20 °C ranged between

2.15 to 2.75 MPa. The corresponding range of average bond strength for repair applied at 10 and 2 °C are 1.90-2.30 MPa and 2.10-2.70 MPa respectively. A comparison between these bond strengths with the classification of concrete overlays provided by Sprinkel and Ozyildiring [184] in Table 7.1 shows that they mostly fall within the "excellent" range for both microwave and normally cured repair materials.

The bond strength of CEM II mortar applied under ambient temperature 20, 10 and 2 °C ranged between 1.4 and 1.9 MPa for both normally and microwave cured specimens. These indicate a lower bond strength compared to the other three proprietary materials. Repair materials are formulated for patch repair to provide high bond strength regardless of their compressive strength. This becomes more apparent from their compressive strength data presented in Section 7.4.4 which vary greatly between 21 and 67 MPa while their bond strength remains within the range given above.

7.4.3.2 *Bond Strength at repair temperature -5 °C*

Results in Table 7.3 show that exposing freshly cast "composite" cubes to freezing temperature at an early age has significantly reduced the bond strength of subsequently normally cured specimens. This loss is attributed to the damage due to freezing temperature at an early age. However, microwave curing provides significantly higher bond strength for all repair materials. The bond strength for normally cured repair materials ranges from 0.70 to 1.15 MPa and it increases to 1.30 to 2.15 MPa under microwave curing. This increase in bond strength with microwave curing of repair materials is due to the application of heat at early age that prevented early damage due to the freezing temperature.

A comparison between the bond strength of normally cured repair materials applied at "repair" temperatures 20, 10, 2 with those applied at -5 °C shows that the bond strength

is severely affected at repair temperature -5 °C. For example, normally cured Five Star repair material exhibits a bond strength of 2.30, 1.95 and 2.15 for repair applied at temperature 20, 10 and 2 °C respectively. The corresponding bond strength of repair applied at -5 °C reduced to 0.75 MPa due to freezing at early age. However, early age microwave curing of repair applied at -5 °C gave a bond strength of 2.75 MPa.

A comparison of the bond strength of microwave cured repair materials applied at repair temperature -5 °C with the classification of bond provided by Sprinkel and Ozyildirim [184] (Table 7.1) shows that, with the exception of Monomix repair material, all other repair materials fall within the "very good" and "excellent" category of bond strength. The corresponding normally cured repair materials fall within the "fair" category.

The bond strength of microwave cured Monomix repair material applied at -5 °C is significantly lower than its bond strength when applied at 20, 10 and 2 °C. The bond strength of microwave cured Monomix decreased from the range of 1.9-2.7 MPa to 1.3 MPa under -5 °C repair application. Monomix is a lightweight repair material and its constituents are responsible for this reduction.

7.4.4 Compressive Strength of prisms

Figure 7.7 and the data in Table 7.4 show the compressive strength of the 100 x 100 x 50 mm prisms produced after the tensile split test. It should be noted that the compressive strength of prisms is less than the compressive strength of cubes due to their size effect and height/width ratio. The two compressive strengths can be comparable if correction factors are applied to the prism strength [7]. The correction factor is influenced by the strength [191], shape and size of the test specimens [192, 193]. However, the aim of this investigation was to study the effect of microwave curing relative to normal curing rather than evaluating the absolute cube strength.

The following section provides the analysis of the compressive strength in two separate sections. Section 7.4.4.1 analyses compressive strength for specimens "repaired" at ambient temperatures of 20, 10 and 2 °C and Section 7.4.4.2 analyses the compressive strength of specimens "repaired" at -5 °C.

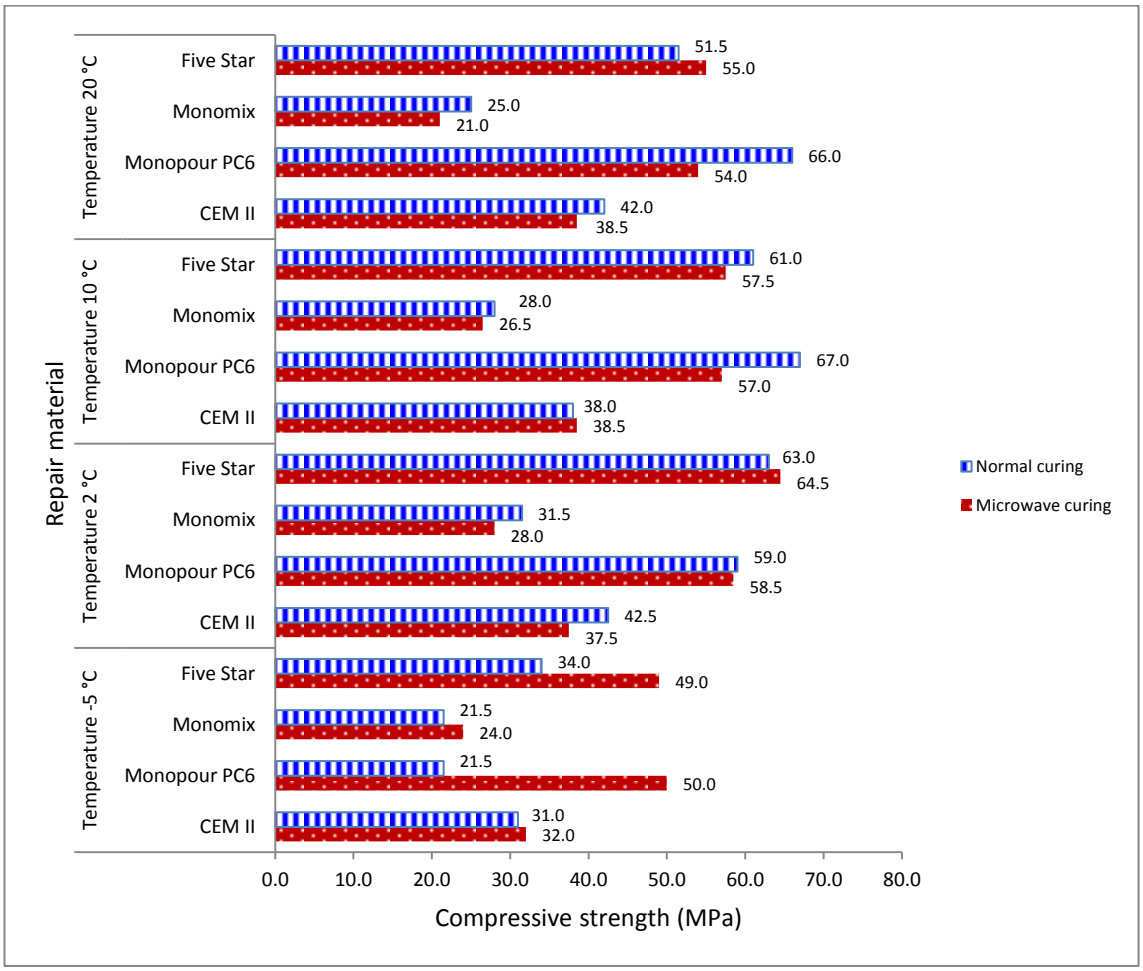

Figure 7.7: Comparison graph of prism compressive strength for repair temperature 20, 10, 2 and -5 °C.

Table 7.4: Compressive strength of repair applied at repair temperatures 20, 10, 2 and -5 °C

Series	Repair temperature (°C)	Repair material	Normally cured		Microwave cured		Temperature after microwave curing*** (°C)	Compressive strength increase (%)
			Compressive strength (MPa)	SD** (MPa)	Compressive strength (MPa)	SD** (MPa)		
1	20	Five Star	51.5	2.34	55.0	3.57	39.6	7
	20	Monomix	25.0	3.10	21.0	2.97	47.4	-16
	20	Monopour PC6	66.0	4.05	54.0	3.47	45.8	-18
	20	CEM II	42.0	1.84	38.5	5.21	41.1	-8
2	10	Five Star	61.0	1.56	57.5	5.71	37.9	-6
	10	Monomix	28.0	4.47	26.5	1.68	42.7	-5
	10	Monopour PC6	67.0	6.10	57.0	2.22	41.0	-15
	10	CEM II	38.0	2.48	38.5	2.84	38.9	1
3	2	Five Star	63.0	6.90	64.5	2.36	35.9	2
	2	Monomix	31.5	2.16	28.0	2.79	40.0	-11
	2	Monopour PC6	59.0	8.86	58.5	6.65	40.0	0
	2	CEM II	42.5	3.39	37.5	4.46	40.9	-12
4	-5	Five Star	34.0	2.23	49.0	5.08	34.6	44
	-5	Monomix	21.5	3.28	24.0	3.37	38.7	12
	-5	Monopour PC6	21.5	2.01	50.0	4.54	37.6	133
	-5	CEM II	31.0	6.11	32.0	2.41	38.2	3

*28 day prism strength
**Standard deviation
***Average (of 4 cubes) top surface middle point temperature of repaired cubes at the end of microwave curing

7.4.4.1 *Compressive strength of prisms at "repair" temperatures 20, 10 and 2 °C*

Figure 7.7 and the data in Table 7.4 show the compressive strength for both microwave and normally cured repair materials applied at 2, 10 and 20 °C. The variation in the 28 day compressive strength of microwave cured repair materials applied at ambient temperatures 20, 10 and 2 °C, relative to the normal curing ranged between +7 to -18%. There is no clear trend between compressive strengths and the variation was randomly distributed for each of the four repair materials. The average was a reduction in compressive strength of microwave cured specimens relative to normal curing of 6.75% for the twelve mixes of series 1, 2 and 3, which is similar to other reported results [76]. This reduction is due to the short period of high temperature curing at early age provided by microwave exposure, similar to the effect of high temperature curing by conventional methods on the long term strength of concrete. Concrete develops less dense products of hydration under higher temperature curing, leading to lower long term strength [7]. However, the average reduction of 6.75% under microwave curing is less than the typical reduction in 28 day strength of 10-15% observed under steam curing [171] and 10-20% reduction observed with the hot-mix method when either the constituents are heated prior to mixing or steam is injected in the mixer [7]. The lower reduction in long term strength with microwave curing is likely to be due to lower temperature of curing (about 40 °C) and, therefore, denser hydration products compared with curing temperature of 60-70 °C produced in concrete by steam curing and heating of mix constituents.

7.4.4.2 *Compressive strength of prisms cured at "repair" temperature -5 °C*

Figure 7.7 and the data in Table 7.4 show the compressive strength for normally and microwave cured repair applied at -5 °C for all repair materials. Microwave curing

provided significantly higher compressive strength than normal curing for repairs applied at -5 °C. The increase was 12, 44 and 133 % for 3 out 4 repair materials. The CEM II mortar showed a modest increase of 3%. However, the 28 day compressive strength of repairs applied at -5 °C was less than the repairs applied under higher "repair temperatures" of 2-20 °C, thereby indicating some effect of freezing. For example, the strength of microwave cured Five Star repair material decreased form the range 55.0-64.5 MPa to 49 MPa. The corresponding reductions for Monopour PC6 and CEM II mortar were 54-58.5 MPa to 50 MPa and 37.5-38.5 MPa to 32 MPa respectively. Monomix repair material shows insignificant reduction in compressive strength from 21-28 MPa to 24 MPa. Monomix has a lower density of 1730 kg/m^3 than Five Star, Monopour PC6 and CEM II and higher resistance to freezing. The role of the admixtures in the proprietary Monomix on the bond and compressive strength under microwave curing needs further research.

45 minutes of microwave curing to a temperature of about 40 °C of repairs applied at sub-zero ambient temperature have resulted in higher bond and compressive strength than the strength of control specimens which were not exposed to microwave curing. Microwave curing was applied to the fresh repair after 30 min of application. The increase in strength is due to the heat provided to early age repair by microwave curing. It is known that curing temperature of concrete before it is exposed to frost attack at an early age has a significant effect on its longer term strength [7]. Early age heating by microwave curing has accelerated the hydration of cement, resulting in a reduced amount of water available for freezing in the pore structure. It has also provided sufficient strength to the matrix to withstand subsequent exposure to freezing during 24 hours of sub-zero temperature. According to ACI 306R-10 [194] on cold weather

concreting, if concrete is able to achieve sufficient strength (approximately 3.5 MPa), it will resist damage caused by one cycle of freezing and thawing.

7.4.5 Relationship between bond strength and compressive strength

The graphs of bond strength versus compressive strength of the 100 x 100 x 50 mm prisms are shown in Figures 7.8 and 7.9 for repair materials applied at 20, 10, 2 °C and at -5 °C respectively. No relationship between bond strength and compressive strength is observed for both normally and microwave cured repairs applied at "repair temperatures" of 20, 10 and 2 °C (Series 1, 2 and 3 tests, Figure 7.8). The bond strength of the commercial repair materials Five Star, Monomix and Monopour PC6 remains reasonably constant at 1.90-2.75 MPa for the wide range of prism strengths 21-67 MPa. This is because repair materials are specially formulated by the manufactures to provide maximum bond strength while tailoring the compressive strength to specific applications for different classes of repair materials given in BS EN 1504-3 [42]. The bond strength of the CEM II mortar, for both normal and microwave curing, falls significantly below the data of the other repair materials in Figure 7.8.

The graphs for "repair temperature" of -5 °C, in Figure 7.9, show that under microwave curing, three of the four repair materials (Five Star, Monopour PC6 and CEM II, Table 7.3) develop bond strengths between 1.95 and 2.45 MPa while their compressive strength ranges between 32 and 50 MPa. The other microwave cured repair material (Monomix) develops a lower bond strength of 1.3 MPa at -5 °C of repair application. The corresponding bond strength of the normally cured repair materials Five Star, Monomix and Monopour PC6 for "repair temperature" of -5 °C fall in the significantly lower range of 0.7-0.8 MPa while their compressive strength ranges between 21.5 and

34 MPa. The normally cured CEM II mortar also falls in the low range bond strength of 1.15 MPa with a compressive strength of 31 MPa.

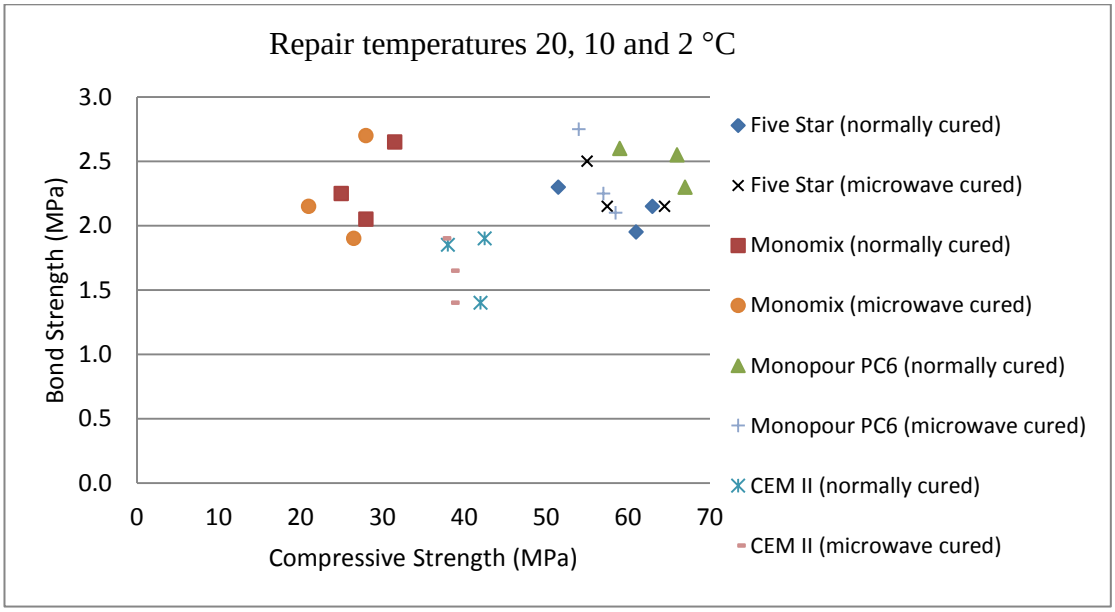

Figure 7.8: Bond strength versus compressive strength for repair temperatures 20, 10 and 2 °C

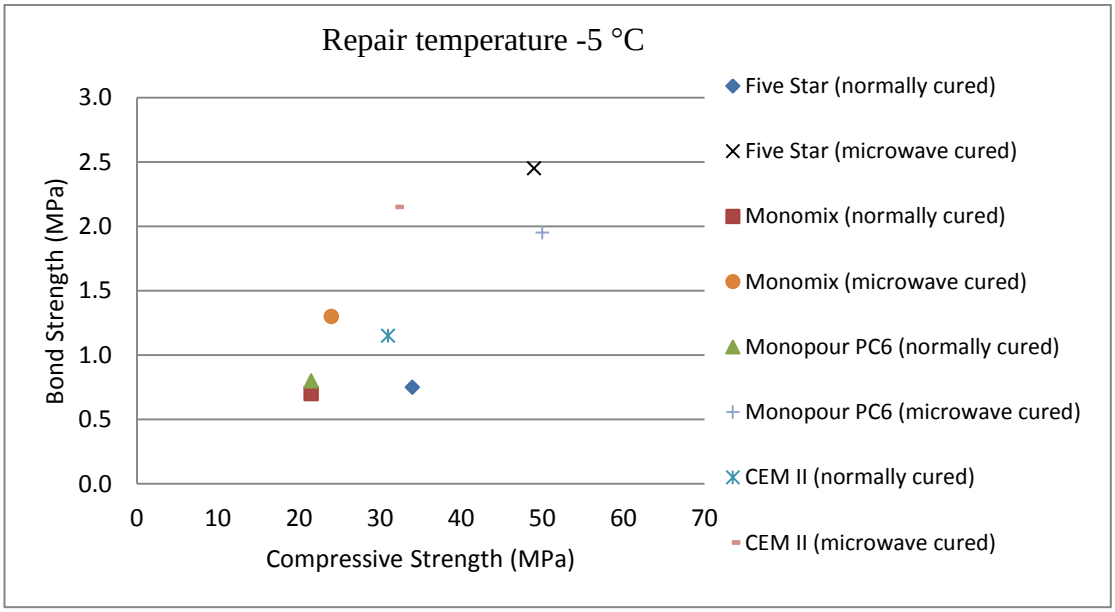

Figure 7.9: Bond strength versus compressive strength for repair temperature -5 °C

7.4.6 Effect of microwave exposure on strength of substrate concrete

After conducting a tensile split test on composite cubes, the substrate prisms were subjected to compression tests in order to determine the effect of microwave heating on the hardened substrate. Substrate prisms were 28 days old when they were exposed to 45 minutes of microwave heating after the repair patch was applied and 56 days old when compression tests were carried out.

Figure 7.10 and the data in Table 7.5 show the compressive strength for normally cured and microwave exposed concrete substrate prisms of the composite cubes obtained from the tensile split test. The difference between the compressive strength of normally cured and microwave heated concrete substrate varied between -11% and +11%. The average of all the substrate specimens for normal and microwave curing is 44.4 and 44.2 MPa respectively indicating no effect of microwave exposure on hardened concrete. This is due to the fact that a low microwave power was applied to achieve only about 40 °C for a short period. A temperature of 40 °C will accelerate the hydration of fresh concrete at an early age, however, this is not the case for 28 days old concrete substrate which has already hardened.

Table 7.5: Compressive strength of concrete substrate at 56 days age for the repair application at 20, 10, 2 and -5 °C

Series	Repair temperature (°C)	Repair material which applied on substrate	Normally cured		Microwave cured		Increase (%)
			Strength of Substrate* (MPa)	Standard Deviation (MPa)	Strength of Substrate* (MPa)	Standard Deviation (MPa)	
1	20	Five Star	39.3	6.0	43.0	2.5	-9%
		Monomix	41.8	4.4	41.9	4.1	0%
		Monopour PC6	39.5	4.3	44.0	0.8	-11%
		CEM II	43.7	1.7	43.3	6.0	1%
2	10	Five Star	45.3	2.9	45.2	3.7	0%
		Monomix	42.2	2.2	42.7	3.5	-1%
		Monopour PC6	41.7	0.9	40.5	5.4	3%
		CEM II	37.5	3.3	36.1	3.0	4%
3	2	Five Star	42.6	5.0	39.6	2.7	7%
		Monomix	45.2	1.1	42.0	1.9	7%
		Monopour PC6	46.5	3.1	45.1	3.7	3%
		CEM II	47.3	1.1	49.3	1.5	-4%
4	-5	Five Star	47.9	1.8	51.6	1.5	-8%
		Monomix	49.2	2.9	47.2	2.9	4%
		Monopour PC6	50.8	1.3	45.4	3.8	11%
		CEM II	49.5	3.6	49.8	2.0	-1%

*The average compressive strength of 4 prisms

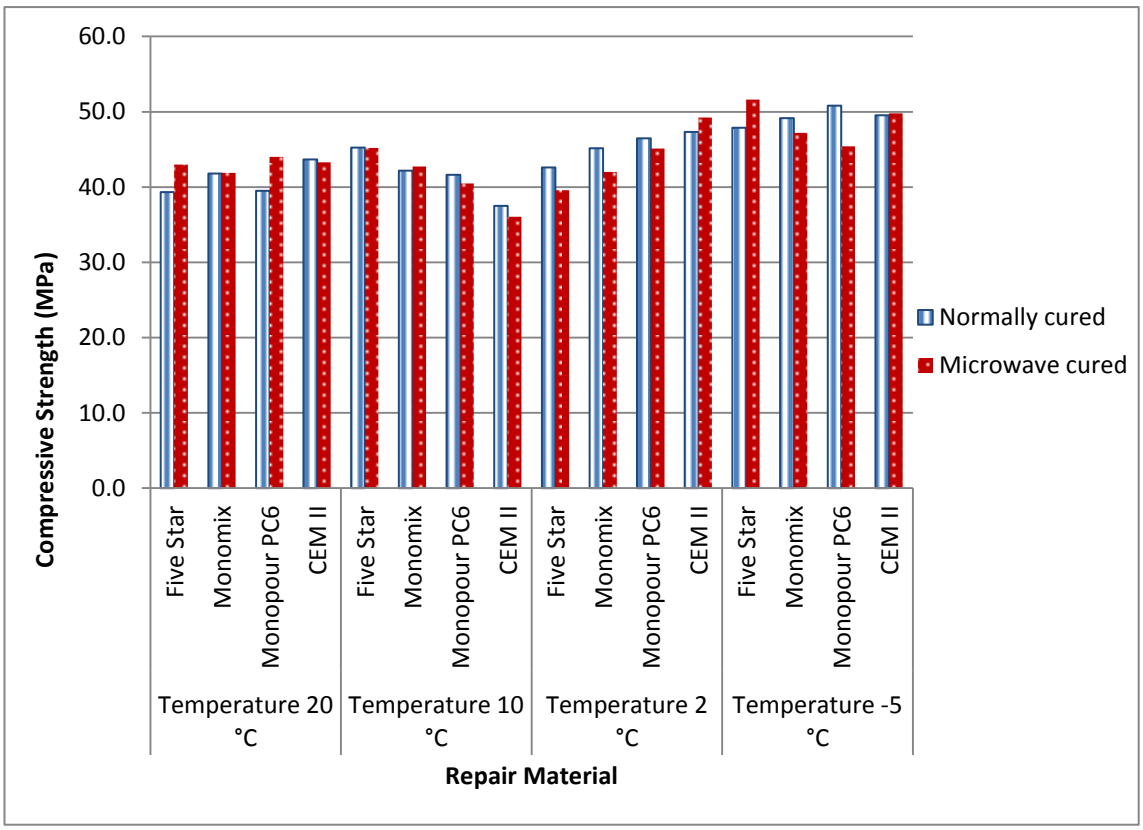

Figure 7.10: Compressive strength of substrate at 56 days age

7.5 Conclusions

The conclusions of this chapter are presented in two sections based on the repair temperature. The first section, presents the conclusions for results of repair temperatures 20, 10 and 2 °C and the second section, provides conclusions based on the results at repair temperature -5 °C.

7.5.1 Repair temperature 20, 10 and 2 °C

- Microwave curing of the fresh repair has no negative effect on the repair/substrate interfacial bond strength at 28 days age. In many cases, the bond strength of the microwave cured repair is slightly higher than normally cured repair.
- The bond strengths of repairs applied at these temperatures are similar and ranged from 1.9 to 2.45 MPa for three proprietary repair materials. The corresponding bond strength for CEM II is 1.4 to 1.9 MPa.
- The compressive strengths of the repair materials bear no relationship with their bond strengths with the substrate. The bond strength of the normally and microwave cured repair materials Five Star, Monomix and Monopour PC6 are between 1.9 and 2.75 MPa for the wide range of compressive strength (21-67 MPa).
- Microwave curing to about 40 °C reduces the 28 days compressive strength relative to the normally cured repair materials by an average of 6.75%.
- Microwave exposure of the concrete substrate during curing of the repair has no adverse effect on its compressive strength.

7.5.2 Repair temperature -5 °C

The following conclusions apply to microwave curing of repairs applied at -5 °C.

- A short period of microwave curing of the fresh repair followed by 24 hours sub-zero temperature exposure provides significantly higher bond strength at 28 days compared to control samples exposed to curing at -5 °C for 24 hours after casting followed by 27 days curing at 20 °C in water. For example, normally cured Monopour PC6 shows bond strength of 0.80 MPa compared to 1.95 MPa under microwave curing.
- Microwave cured commercial repair materials Five Star, Monopour PC6 and CEM II perform particularly well under freezing conditions. Microwave cured repair material Five Star applied at -5 °C has a bond strength of 2.45 MPa compared with (2.15-2.5) MPa for repairs applied at 20 to 2 °C. The corresponding values for Monopour PC6 are 1.95 MPa compared with 2.1-2.75 MPa. Microwave cured CEM II Mortar applied at -5 °C develops a bond strength of 2.15 MPa compared with (1.4-1.75) MPa for microwave cured repair application at (20 to 2 °C). These bond strengths of microwave cured repairs compare favourably with the "excellent" classification given to bond exceeding 2.1 MPa [184].
- Repair materials applied and cured at a "repair temperature of -5 °C for 24 hours followed by normal curing (20 °C, 60% RH) for 27 days suffer frost attack which results in bond strengths below 1.15 MPa.
- Microwave curing provides higher 28 days compressive strength than normal curing for repairs "applied" at -5 °C. The difference is very high for Repair material Five Star and Monopour PC6 (44 and 133% respectively) and fairly insignificant for Monomix and CEM II Mortar (12 and 3% respectively), indicating severity of frost attack on Monomix and CEM II. Monomix is a

lightweight material (density 1725 kg/m^3) and its constituents make it vulnerable to freezing temperature.

- The 28 day compressive strength of microwave cured repair materials applied at -5 ^{o}C is about 20% lower than the corresponding materials applied at (20 $^{\circ}$C to 2 $^{\circ}$C), thereby show some effect of damage due to freezing. For example, the strength of microwave cured Five Star decreased from the range (55.0-64.5) MPa to 49.0 MPa.
- The compressive strengths of the repair materials bear no relationship with their tensile bond strength with the substrate. The bond strengths of the microwave cured materials are between 1.95-2.45 MPa for the compressive strength range of (32-50) MPa. The corresponding bond strengths of normally cured materials are 0.7-1.15 MPa against a compressive strength range of 21.5-34 MPa.

Chapter 8

8. Bond of steel reinforcement with microwave cured concrete repair mortars

8.1 Introduction

This chapter aims to investigate the effect of microwave curing of patch repair when steel reinforcement is present. In the food industry, metals are normally not permitted for use inside the microwave oven as it results in the creation of sparks or arcing due to electrically charged metals. Therefore, laboratory experimental work has been carried out to determine any hazards related to microwave curing of steel reinforced concrete repair. In addition, the effect of microwave curing on bond strength between steel bar and repair materials is determined by conducting pull out tests on plain mild steel reinforcement bars embedded in repair materials. Furthermore, the effects of microwave curing on compressive strength, shrinkage and the pore structure of repair materials at the bond interface are determined and related to the bond strength.

8.2 Literature review

Concrete is the most widely used material in built infrastructure. The popularity of concrete is mainly due to its low production cost and high compressive strength. However, concrete is very weak in tension which is only about 10% of its compressive strength [194]. If a plain concrete structure is subjected to a tensile load or bending moment, reinforcement is required to withstand the tensile stresses. In addition reinforcement is added to the compression zone to reduce long term deflection due to shrinkage and creep. Reinforced concrete beams and slabs are structural elements which

are used in most structures to carry tensile and flexural loads. Therefore, any potential for using microwave curing for in situ concrete construction relies on the suitability of this technology to accommodate steel reinforcement.

Most of the research on microwave curing of concrete has focused on normal concrete materials [70, 72, 80] with hardly any attention to steel reinforced concrete and to in situ concrete repair which incorporates both proprietary repair mortars and steel reinforcement. Microwave curing of concrete with steel reinforcement raises two basic concerns. The first is safety relating to the electrically charged or reflected microwave energy causing sparks and overheating at the steel surface. The second concern is the effect of microwave curing on the bond between steel reinforcement and concrete, which is fundamental to the composite action of reinforced concrete. These two aspects are addressed in this chapter. Another aspect of bond strength which is of critical importance for the efficient performance of concrete repair is the interfacial bond between the substrate concrete and patch repair, which has been reported previously in Chapter 7.

The composite performance of reinforced concrete depends on the efficient interaction between the steel reinforcement and the concrete matrix, which relies on their bond strength. Plain steel bars provide a true bond failure mechanism with concrete, which includes chemical adhesion and frictional resistance. The pull out strength of deformed reinforcement bars overestimates the basic bond strength by including the mechanical interlock strength of the concrete [195]. The simple pull-out mechanism of the plain rebar embedded in concrete is made more complex in deformed bars by the bursting forces generated by the wedge action of ribs on the rebar which is confined to different degrees by the concrete cover and confining reinforcement [196, 197]. The bond behaviour is influenced by factors such as the rib geometry, their relative surface area

[198] and interlock with concrete lugs [199]. The fib model design code [200] provides a basic expression for rebar bond strength, relating it to the square root of concrete strength while also incorporating other empirical coefficients which depend on many parameters such as geometry of the section, strength, diameter and surface geometry of reinforcement, concrete cover, bar spacing and confinement of reinforcement [200]. However, the main aim of the research reported in this chapter is to isolate and determine the effect of microwave curing on reinforcement bond strength without introducing other factors which may interfere with the clarity of results. Therefore, plain reinforcement bars have been used in this experimental programme to provide a basic bond mechanism. In practice also, many reinforced concrete structures which have been constructed with plain steel bars in the past have reached their repair stage and the bond of this reinforcement in repair patches has become important.

The main parameters of microwave curing which are likely to affect the interfacial bond strength are the porosity and pore structure of the matrix at the steel interface, the shrinkage of the matrix and its compressive strength. These parameters are investigated in this chapter together with bond strength of reinforcement under microwave curing. The effect of microwave curing on the porosity and pore structure of the matrix by mercury intrusion has already been investigated in Chapter 6. The results of the bond strength are related to these parameters.

8.3 Test programme

8.3.1 Materials

The following repair materials were used for this investigation:

- Five Star

- Monomix
- HB40
- CEM II Mortar: (cement/sand ratio of 1:2 and water/cement ratio of 0.45).

A description of the above repair materials is presented in Chapter 3.

8.3.2 Microwave ovens

Microwave oven I (Logik L25MDM13) was used to observe the safety of microwave exposure of steel reinforced mortar specimens. Microwave oven II (Sharp R-2370) was used to microwave cure reinforced repair material specimens in order to determine the effect of microwave curing on the steel/mortar interface bond strength. In addition, it was also used to microwave cure specimens to investigate the effect of microwave curing on shrinkage and compressive strength. A 10% power level was used to generate actual microwave power of 132 W to microwave cure specimens. Lower powers of 92 and 60 W were also used for some tests.

8.3.3 Details of specimens, casting and curing

8.3.3.1 *Steel reinforced mortar for investigating safety of microwave curing*

Initially, preliminary tests were carried out to ensure the safety of microwave curing of reinforced concrete. A different number of steel bars (1, 2 or 3) were placed horizontally along the entire length of each 100 mm polystyrene cube mould by drilling two opposite vertical sides of the mould shown in Figure 8.1. The size of the steel bars was approximately 140 mm to cover the cube length (100 mm) and the thickness of two mould walls (20 mm each side). In addition, one polystyrene mould was cast with a steel bar with the length of 200 mm (30 mm protrusion from both sides) as shown in Figure 8.2. The steel bars used in this series were normal mild steel bars with diameters of 6 and 8 mm and galvanised mild steel with the diameter of 10 mm as shown in

Figure 8.3. In addition, to simulate steel bars with different top covers, specimens were cast with covers of 5, 15 and 25 mm as shown in Figure 8.4. Details of the steel reinforced specimens are given in Table 8.1. A mortar mix using CEM II cement (Cement/sand ratio of 1:2 and w/c ratio of 0.45) was prepared and the steel reinforced mortar specimens were cast in the laboratory and compacted on a vibrating table. 30 minutes after adding water to the mix (delay period), the specimens were exposed to the microwave energy for either of 15 or 45 minutes with powers ranging from 60 to 420 Watts as shown in Table 8.1. The top surface temperature of specimens was measured at the end of microwave curing using a Flir i7 thermal camera.

Figure 8.1: Polystyrene moulds with 1, 2 and 3 steel bars placed inside moulds

Figure 8.2: Polystyrene mould with three steel bars protruding from both sides

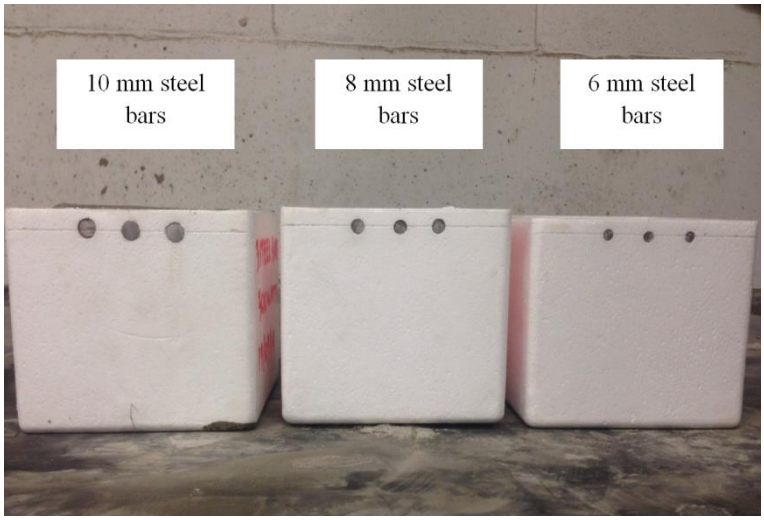

Figure 8.3: Specimens with different size of steel bars (10, 8 and 6 mm) and a 5 mm top cover

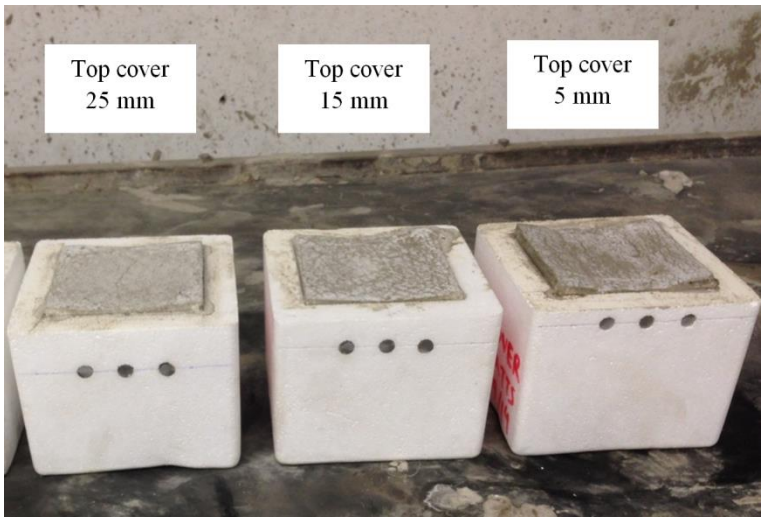

Figure 8.4: Specimens with different top covers after microwave curing

Table 8.1: Details of steel reinforced mortar specimens.

Cube size (mm)	Microwave power (W)	Microwave duration (min)	Number of Bars	Type of bars	Bar diameter (mm)	Top cover (mm)	Length of steel bars (mm)
100	60	45	1	GM steel*	10	25	140
	60	45	2	GM steel	10	25	140
	60	45	3	GM steel	10	25	140
	120	45	3	GM steel	10	25	140
	180	45	3	GM steel	10	25	140
	180	45	3	GM steel	10	15	140
	180	45	3	GM steel	10	5	140
	300	15	3	GM steel	10	5	140
	300	15	3	NM steel**	8	5	140
	300	15	3	NM steel	6	5	140
	420	15	3	NM steel	6	5	140
	420	15	3	NM steel	6	5	200

*GM-Galvanised mild steel
**NM-Normal mild steel

8.3.3.2 *Steel reinforced mortar specimens for pull out test*

The aim of these tests was to determine the effect of microwave curing on the bond strength between plain steel bar and various repair materials. Steel bars of diameter 10 mm and length 255 mm were used in the investigation. One end of each steel bar was machined on a lathe to create a threaded length up to 15 mm to connect the test specimen to a hinge joint which provided alignment of the specimen with the applied load during the pull out test. Prior to casting the specimens, each steel bar was cleaned with acetone and dried before it was placed horizontally across the entire length of a 100 mm polystyrene cube mould (wall thickness of 20 mm) by drilling two opposite vertical faces of the mould. The bar was located along the central axis of the cube and its threaded and un-threaded ends extended 85 and 30 mm respectively beyond the two opposite faces of the polystyrene mould. A plastic sleeve was inserted on the steel bar to provide a 50 mm unbonded length. Hence, the effective bond length between steel bar and the repair mortar was 50 mm as shown in Figure 8.5. 12 pull-out specimens were cast from three mixes for each repair material. Half of the specimens were cured

normally (20 °C, 60 % RH) and the other half were microwave cured. Figure 8.6 shows typical specimens after casting.

Immediately after casting and compacting on a vibrating table, the specimens were covered with a plastic sheet and cured at laboratory ambient temperature. Half of the specimens remained covered at room temperature (20 °C, 60 % RH) for 24 hours, and then demoulded. The other half of cubes were placed in microwave oven 30 minutes after commencing mixing and cured to reach approximately 40-45 °C. The pull out specimens made with the four different materials were subjected to microwave curing using powers of 132 (Series 1), 92 (Series 2) and 60 (Series 3) watts (Table 8.2). The temperature was measured at the centre of the top surface of each specimen at the start of microwave curing and then after every 10 minutes until the end of microwave curing using a Flir i7 thermal camera. The specimens were removed briefly from the microwave cavity to measure temperature at each time increment and then placed back for further microwave curing. The duration of microwave curing was 20-44 minutes for the different materials and applied powers (W) to achieve similar maximum top surface temperatures of 40-45 °C (Table 8.2). The ends of the steel bars protruding from the polystyrene mould of each repair were directly exposed to the microwaves during the curing period.

Figure 8.5: Preparation of moulds


Figure 8.6: Specimens after casting

Figure 8.7: Arrangement of specimens inside microwave oven

Table 8.2: Details of bond strength tests

Test Series	Repair material	Power (Watts)	Duration of microwave Curing (mins)
Series 1	Five Star	132	30
	Monomix	132	20
	HB40	132	20
	CEM II Mortar	132	30
Series 2	HB40	92	30
Series 3	HB40	60	44

8.3.3.3 *Specimens for compressive strength and shrinkage*

The effect of microwave curing on compressive strength was investigated by casting four 75 x 75 x 75 mm cube specimens in polystyrene moulds as described in the previous section. Two specimens were normally cured and the other two were microwave cured. Four shrinkage prism specimens of dimensions 75 x 75 x 300 mm were cast in polystyrene moulds. Two specimens were normally cured and the other two by microwave.

8.3.4 Testing

8.3.4.1 *Pull-out test*

Bond strength was determined at 42 days age by the pull-out test according to BS EN 10080 [201], as shown in Figure 8.8. Assuming a uniform bond stress distribution over the effective embedded length in the repair material, the average bond stress which is related to the pull-out tension force is calculated by the following formula:

$$\tau = \frac{F}{\pi d l} \qquad (8.1)$$

where τ is the average bond stress (MPa); F is the maximum pull-out tensile force (N); d is the diameter of the steel bar (10 mm) and l is the embedded length of the steel bar (50 mm, Figure 8.8).

The loading rate was determined according to BS EN 10080 [201], by the following formula:

$$\upsilon_p = 0.56 d^2 \qquad (8.2)$$

where υ_p is the loading rate (N/s) and d is the diameter of the steel bar (mm).

The pull-out specimens were tested in a computer controlled ESH Four Column Universal testing machine with maximum capacity of 250 KN. The tensile force was applied to the longer (threaded) end of the steel bar connected through a hinge to the jaws of the machine. A loading rate of 55 N/s was used. The load and slip at the loaded end of the bar were automatically recorded by the machine computer. No yielding of the steel bar was observed in any of the tests. The elongation of the un-bonded steel bar from the loaded end point, during the test, was negligible relative to the slip.

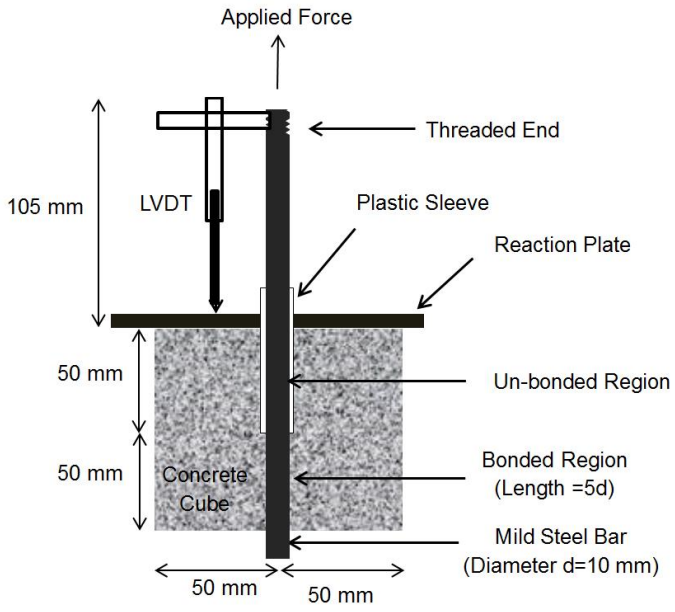

Figure 8.8: Schematic diagram of pull-out test

8.3.4.2 *Compressive strength*

Repair materials were cast in 75 x 75 x 75 mm polystyrene moulds and cured at a power of 132 Watts to achieve a temperature of 40-45 °C. Specimens were covered with a plastic sheet and kept in the laboratory for 24 hours. Then, they were demoulded and cured in air (20 °C, 60% RH) similar to the bond strength specimens. Specimens were tested for compressive strength according to the BS 12390-3:2009 [187] at 42 days. These results provided the compressive strength of pull out specimens at 42 days age.

8.3.4.3 *Shrinkage*

The effect of microwave curing on the drying shrinkage of the repair materials was determined by recording length change of the specimens up to 42 days. The 75 x 75 x 300 mm prism specimens were de-moulded and demec points were attached at the two

opposite faces to monitor shrinkage strain. The first (datum) demec reading was taken at 24 hours from commencing mixing. Subsequent readings were taken at regular intervals.

8.4 Results and discussion

8.4.1 Effect of steel reinforcement

No sparks or arcing was observed during microwave curing of all steel reinforced cube specimens. Typical temperature distributions of a plain concrete cube (control, microwave cured at 120 Watts), a mild steel reinforced cube (3 steel bars of 10 mm diameter, 25 mm cover cured at 120 Watts) and a mild steel reinforced cube (3 protruding steel bars of 6 mm diameter, 5 mm cover cured at 420 Watts) are shown in Figures 8.9 to 8.11, respectively. No significant changes in top surface temperature distribution and mid-point surface temperatures were observed by the presence of mild steel (galvanised or normal) bars or by varying the number of steel bars (1, 2 or 3), bar diameter (10, 8 or 6 mm) or top cover (25, 15 or 5 mm).

Figure 8.11 shows the extreme case of steel bars protruding from the cube moulds. The temperatures in the protruding parts of the steel bars are on the lower end of the recorded temperature scale and are much lower than the mortar specimen. There was no arcing observed in these tests.

The above results are provided to allay health and equipment safety concerns.

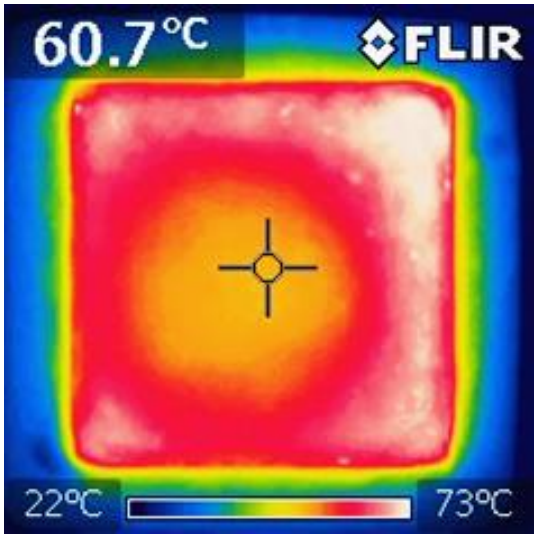

Figure 8.9 Temperature distribution of plain mortar specimen (control) after 45 minutes of microwave curing at 120 W.

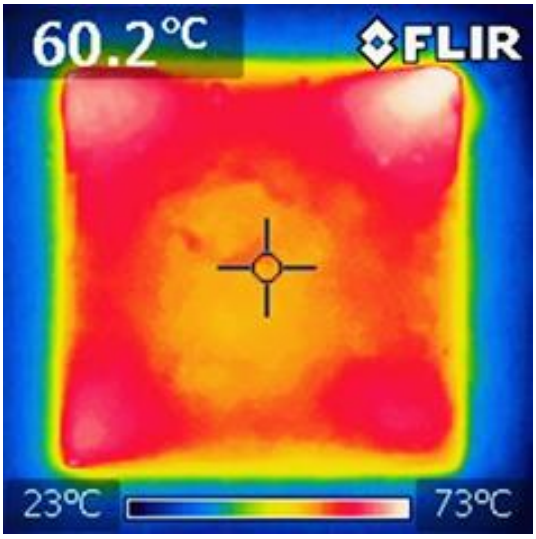

Figure 8.10 Temperature distribution of steel reinforced mortar specimen (3 steel bars, 10 mm diameter, 25 mm top cover) after 45 minutes of microwave curing at 120 W.

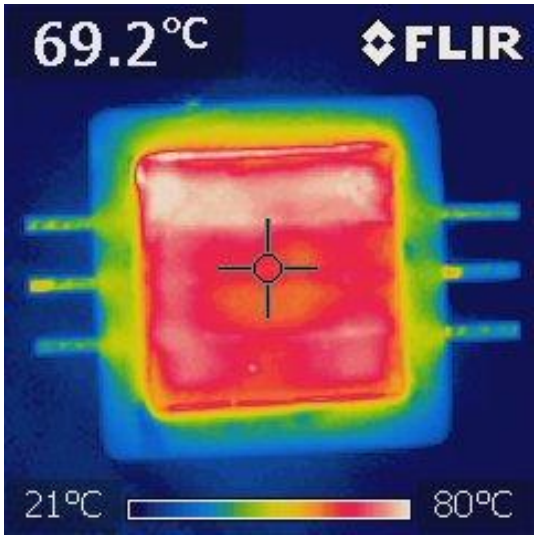

Figure 8.11 Temperature distribution of mortar specimen with 3 protruding steel bars after 15 minutes of microwave curing at 420 W.

8.4.2 Effect of microwave curing on the steel/mortar interface

8.4.2.1 *Top surface temperature*

Top surface temperature of specimens were recorded at the beginning and end of microwave curing by using Flir i7 thermal camera. Figure 8.12 shows a typical top surface temperature profile of Five Star repair material during 30 minutes of microwave curing. Significant temperature variations were observed between two cubes at the end of microwave curing, which are due to the different location of each specimen within

the microwave oven. In addition, the data in Table 8.3 show the midpoint top surface temperature of all specimens at the end of microwave curing. The average temperature of the 6 cubes is also presented for each material. Results show that specimens for each repair material achieved average temperature ranging between 41.5 and 48.2 °C.

HB40 repair material represents the highest average temperature of 48.2 °C under microwave curing at 60 Watts. The corresponding average temperature of HB40 at the end of microwave curing at 132 and 92 Watts are 41.8 °C and 41.7 °C respectively.

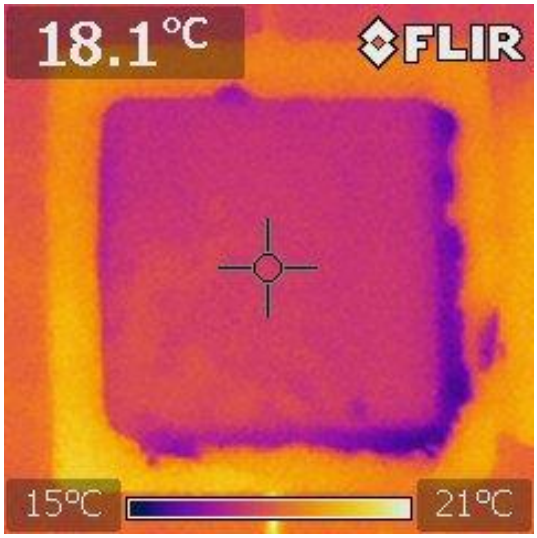

(a) At 0 minutes

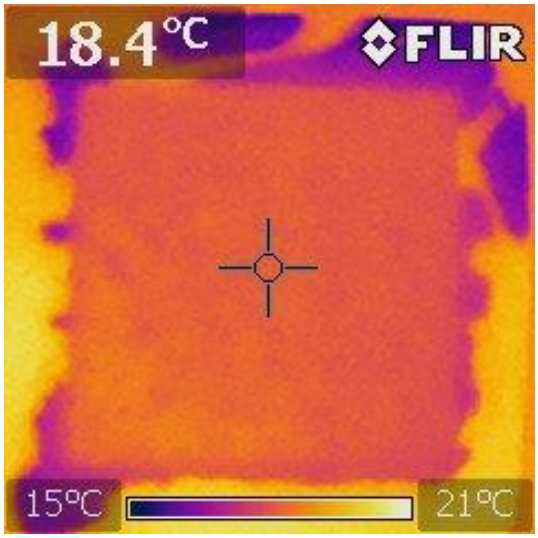

(b) At 0 minutes

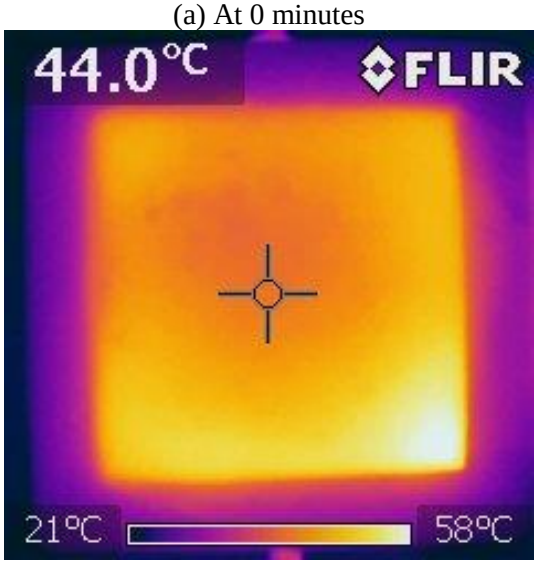

(c) At 30 minutes

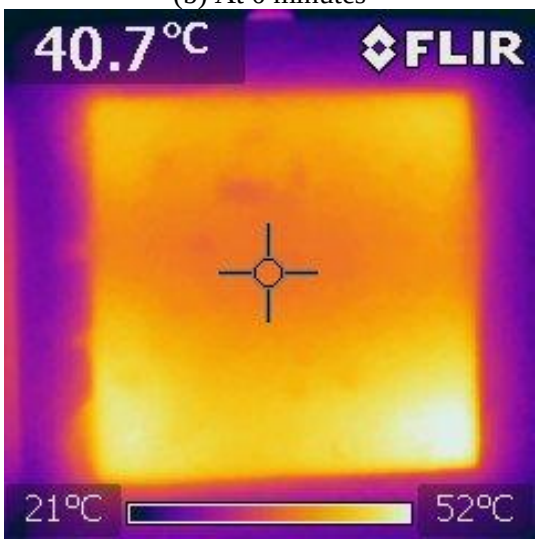

(d) At 30 minutes

Figure 8.12: Top surface temperature distribution of 2 cubes of Five Star repair material (cube 1 left and cube 2 right) subjected to 132 Watts output power.

Table 8.3: Midpoint top surface temperature at the end of microwave curing (powers 130, 92 and 60 W for Series I, II and III respectively)

Series	Material	Curing time (min)	Temperature at the end of microwave curing (°C)						Average temperature (°C)
			mix 1		mix 2		mix 3		
			Cube I	Cube II	Cube I	Cube II	Cube I	Cube II	
1	Five Star	30	45.4	43.9	44.0	40.7	44.8	39.5	43.1
	Monomix	20	42.3	41.2	42.9	42.7	37.5	42.3	41.5
	HB40	20	41.8	40.5	40.7	40.2	42.5	45.2	41.8
	CEM II	30	43.9	39.0	44.1	39.3	44.1	39.1	41.6
2	HB40	30	38.3	37.9	41.7	38.8	47.2	46.4	41.7
3	HB40	44	47.6	51.6	47.8	50.5	45.5	46.2	48.2

8.4.2.2 *Type of failure under pull out test*

Specimens subjected to the pull out test are likely to show three different types of failure. The most common failure when deformed steel bars are used is tensile splitting due to bursting forces generated at the ribs. The second type of failure is yielding of the steel when the bond length of the steel bar is higher than the yield length of the steel bar. The third type is bond failure accompanied by slip of the steel bar. This is a typical failure mode when plain steel bar of suitable embedment length is used. All pull-out specimens failed due to pull out of the bars without yielding of the steel and without any splitting or cracking of the matrix, which indicates that the maximum bond strength of reinforcement was achieved. Figure 8.13 shows a typical specimen after the pull out test.

Figure 8.13: A typical image of the specimen after the pull out test

8.4.2.3 *Bond stress-slip relationships*

The load and slip were measured at the loaded end of the bar and recorded by the computer. The load values were then, converted to bond strength by using Equation 8.1. Figure 8.14 (a-b) show the bond stress-slip curves for specimens of Five Star repair material (Series 1, Table 8.1). The slip values include the elongation of the un-bonded length of the reinforcement in the pull-out specimens. The elongation was below 10% of the slip at the maximum pull-out load. Both normally (Figure 8.14(a)) and microwave cured (Figure 8.14(b)) specimens show a similar rate of slip. Most test results in Figure 8.14 (a) show that after the peak load, bond stress starts decreasing gradually as slip increases. Tests reported in literature on normally cured pull-out specimens of plain rebar in concrete show that the slip increases with applied load until it reaches the maximum stress and then the bond stress drops and continues to decrease gradually as slip increases [202]. In the case of microwave curing (Figure 8.14 (b)), the bond stress starts decreasing immediately after the maximum stress in all samples, without an extended plateau on the bond-slip curve specimens in Figure 8.14 (a). The bond after

the peak bond stress is mainly maintained by mechanical friction for both curing methods.

(a)

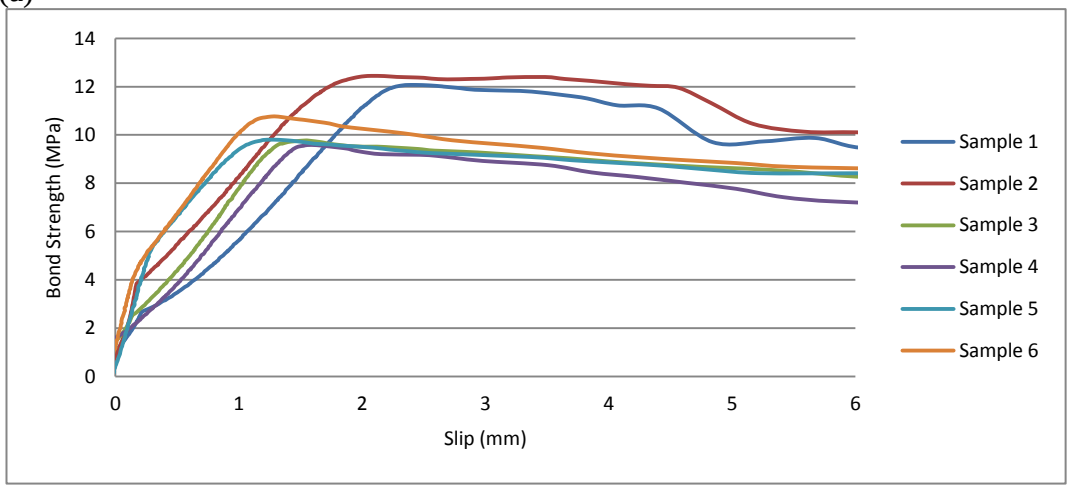

(b)

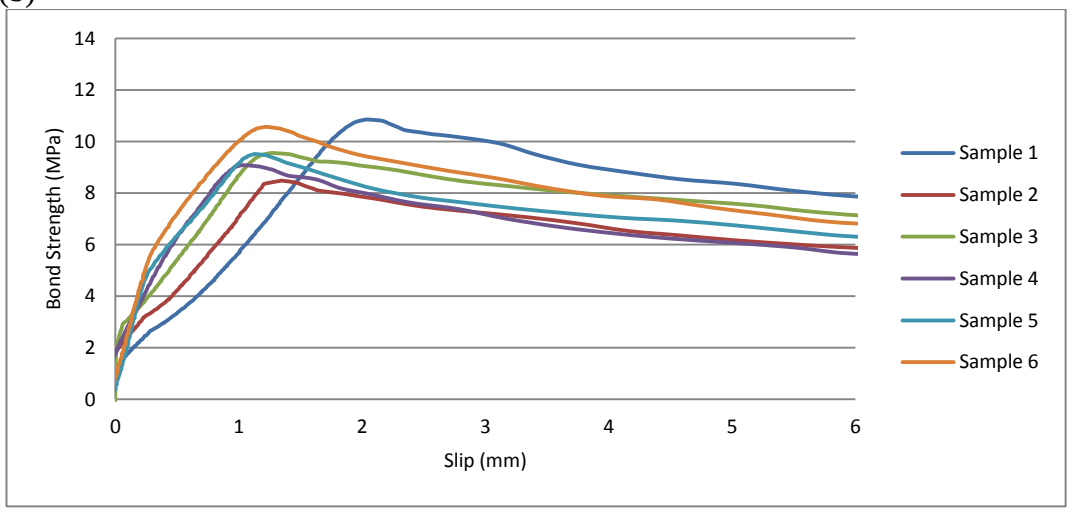

Figure 8.14: Bond stress-slip curves of (a) Normally cured; (b) Microwave cured specimens of Five Star (Series 1)

8.4.2.4 *Effect of microwave curing on bond strength*

The bond specimens for Series 1, 2 and 3 were cured at microwave powers of 132, 92 and 60 W, respectively (Table 8.4). The following sections provide pull-out results separately for Series 1 and in combination for Series 2 and 3. Each bond strength value given here is the average of 6 pull-out specimens.

8.4.2.4.1 Bond strength of specimens cured at 132 Watts

The average peak microwave curing temperature of the six bond specimens of repair materials Five Star, Monomix, HB40 and CEMII were 43.1, 41.5, 41.8 and 41.6 °C, respectively (Table 8.4). These were achieved after curing at microwave power of 132 Watts for 20 minutes (Monomix and HB40, Table 8.2) or 30 minutes (Five Star and CEM II, Table 8.2). Figure 8.15 and the data in Table 8.4 show that microwave curing significantly affects the mortar/steel interface bond strength at 42 days age. Figure 8.15 shows that from the four repair materials of Series 1, Monomix and HB40 experienced a significant reduction in bond strength with microwave curing. The normally cured HB40 shows an average bond strength of 6.95 MPa which reduced to 4.16 MPa due to microwave curing, resulting in a significant loss of 40%. The corresponding bond loss was less for Monomix, reducing from 6.74 MPa for normally cured specimens to 5.35 MPa for microwave cured specimens, showing a loss of 21%. Repair material Five Star shows a moderate reduction of 10 % under microwave curing. The bond strength of steel in the normally cured CEM II mortar was extrapolated from the relationship between bond and compressive strength in Figure 8.19 which is discussed in Section 8.4.3. It gives 11% lower bond with microwave curing.

Table 8.4: Series 1 bond strength results (132 Watts power for 20 or 30 minutes)

Repair material	Sample number	Normal Curing			Microwave Curing			Bond strength increase (%)	Average temperature at the end of microwave curing (°C)
		Bond strength (MPa)	Average bond strength (MPa)	SD* (MPa)	Bond strength (MPa)	Average bond strength (MPa)	SD* (MPa)		
Five Star	1	12.07	10.74	1.25	10.85	9.68	0.89	-10	43.1
	2	12.45			8.48				
	3	9.77			9.55				
	4	9.58			9.08				
	5	9.80			9.52				
	6	10.76			10.57				
Monomix	1	6.57	6.74	0.53	4.23	5.35	0.57	-21	41.5
	2	7.41			5.50				
	3	6.10			5.41				
	4	6.99			5.50				
	5	7.17			5.61				
	6	6.24			5.87				
HB40	1	6.62	6.95	0.48	4.06	4.16	0.49	-40	41.8
	2	6.85			4.49				
	3	7.34			4.85				
	4	7.53			4.30				
	5	7.12			3.59				
	6	6.22			3.65				
CEMII	1	-	-	-	8.68	8.64	0.51	-	41.6
	2	-			9.37				
	3	-			7.87				
	4	-			8.88				
	5	-			8.33				
	6	-			8.69				

*Standard deviation.

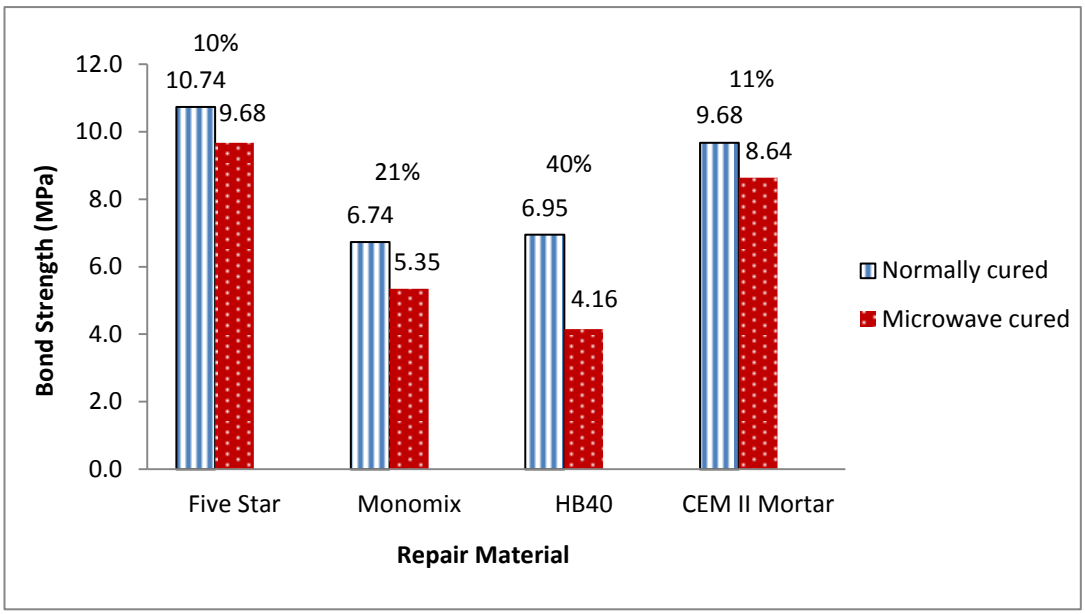

Figure 8.15: Bond strength of normally and microwave cured specimens (Series I, Power of 132 Watts)

8.4.2.4.2 Bond strength of HB 40 cured at 92 and 60 Watts

Figure 8.15 shows that the maximum reduction in bond strength with microwave curing occurred with repair material HB40 cured for 20 minutes to about 40 °C at 132 Watts. In order to investigate the effect of lower microwave heating rates on bond strength, Series 2 and 3 bond tests were performed on HB40 at reduced microwave power of 92 W and 60 W over a longer period of 30 and 44 minutes respectively to provide a temperature of 40-45 °C (Table 8.2). The results in Figure 8.16 and the corresponding data in Table 8.5 show that microwave curing at 132, 92 and 60 W similarly affected the interfacial bond strength at 42 days age. HB40 experienced a similar decrease in bond strength of 40, 42 and 36% at the three curing powers of 132, 92 and 60 W respectively, relative to the control specimens. It shows that a lower rate of heating at lower microwave power did not reduce the loss of bond strength relative to normal curing.

Reduction in bond strength reported in this chapter concurs with the reduction of bond strength of reinforced concrete due to autoclaving [7] or due to conventional curing at higher ambient temperatures [203]. The reduction of later age bond strength is due to

the higher early age curing temperature, which accelerates the hydration process. This results in higher early age bond strength, however, the later age bond strength is reduced due to the formation of hydration products of poorer physical structure [7].

In practice, however, the bond strength does not only depend on the properties of concrete but also on many other factors such as the geometry of the reinforcement, thickness of cover and confinement of reinforcement [200]. The reduction of bond strength observed on the plain steel bars with microwave curing may be less significant with deformed reinforcing bars which are normally used in modern concrete construction.

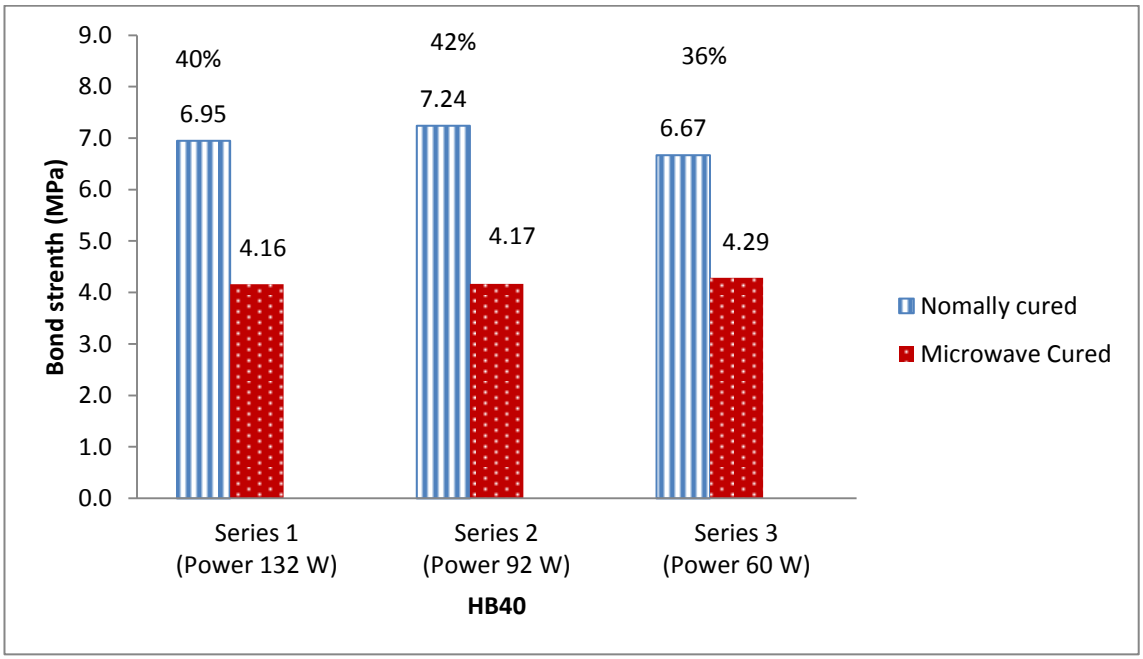

Figure 8.16: Comparison graphs of the average bond strength of HB40 for Series 1, 2 and 3

Table 8.5: Series 1, 2 and 3 bond strength results (132, 92 and 60 W)

Repair material	Sample number	Normal Curing				Microwave Curing			Bond strength increase (%)	Rate of temperature rise (°C/min)	Average temperature at the end of microwave curing (°C)
		Power (W)	Bond strength (MPa)	Average bond strength (MPa)	SD* (MPa)	Bond strength (MPa)	Average bond strength (MPa)	SD* (MPa)			
HB40	1	132	6.62	6.95	0.48	4.06	4.16	0.49	-40	1.2	41.8
	2		6.85			4.49					
	3		7.34			4.85					
	4		7.53			4.30					
	5		7.12			3.59					
	6		6.22			3.65					
HB40	1	92	6.99	7.24	0.68	5.36	4.17	0.63	-42	0.92	41.7
	2		7.93			4.27					
	3		7.42			3.60					
	4		6.02			4.11					
	5		7.71			3.87					
	6		7.39			3.81					
HB40	1	60	6.50	6.67	0.67	4.34	4.29	0.41	-36	0.73	48.2
	2		7.45			4.65					
	3		7.03			3.98					
	4		6.92			4.85					
	5		6.65			3.78					
	6		5.59			4.14					

*Standard deviation.

8.4.3 Effect of microwave curing on compressive strength of repair

Figure 8.17 shows the compressive strength of the four repair materials at 42 days age. It is clear that early age microwave curing (132 watts for 20 or 30 minutes) has reduced the 42 days compressive strength for all repair materials.

A comparison between Figures 8.18 and 8.17 shows that percentage of compressive strength and bond strength reduction with microwave curing are similar for each repair material. Reduction in long term compressive strength due to microwave curing is previously reported by other researchers [72, 204, 9]. It is due to the effect of the short period of high temperature exposure at early age on long-term strength development. A similar reduction of compressive strength also occurs due to conventional heat curing [7, 176, 205, 206]. The effect of curing temperature on early and later age strength also depends on the type of cementitious repair materials [172, 205]. For example, CEM I cured at 40 °C showed a reduction in its 28 days strength whereas CEM II shows an increase [205]. Both cements showed a reduction in the 28 days strength when cured at 85 °C [205]. Similar differences are likely in repair mortars which use different types of cements and additives.

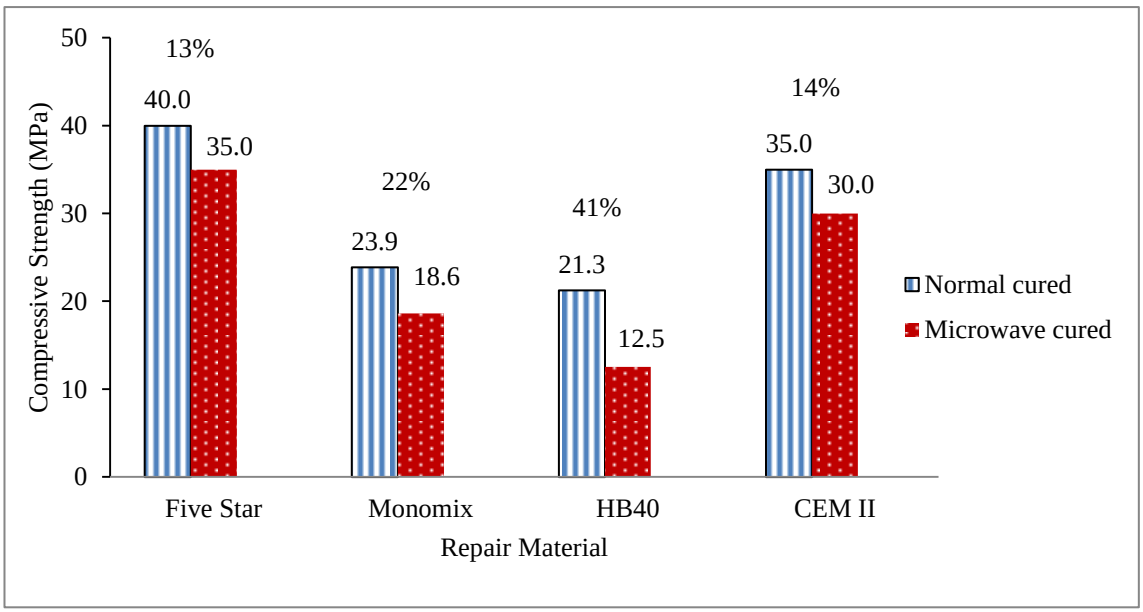

Figure 8.17: Compressive strength of repair materials at 42 days age

8.4.4 Effect of microwave curing on shrinkage

Cement based repair materials exhibit significant shrinkage during service life. The reduction is due to loss of free water in the form of vapour and it depends on the mix proportions, cement replacement materials and admixtures used in the proprietary repair formulations. Shrinkage is a detrimental property of repair materials and a major cause of patch repair failure in service life often due to bond failure at the repair interface. Manufactures often use shrinkage reducing admixtures or expansive cement as shrinkage compensators in repair materials.

Figure 8.18 and the corresponding data in Table 8.6 present the drying shrinkage results of microwave and normally cured repair materials. The results are the average of 4 readings for each repair material taken from 2 opposite faces of 2 prisms. The results show that microwave curing reduces the drying shrinkage of all four repair materials. This reduction ranges from 7% (CEM II) to 32% (HB40). Monomix exhibits the maximum drying shrinkage of 1035 microstrain at 42 days age under normal curing

which reduces to 940 microstrain under microwave curing (Table 8.6). Repair material HB40 exhibits the minimum drying shrinkage of 298 microstrain which reduces to 201 microstrain by microwave curing, resulting in 32% reduction. This reduction is due to the effect of microwave heating at early age which accelerates hydration and also leads to moisture loss by evaporation [207]. Reduction in shrinkage has also been reported under curing with conventional heating [208, 209].

A comparison of the bond strength and shrinkage of Monomix and HB40 repair materials shows the impact of shrinkage on bond strength. For example the 42 days shrinkage for the normally cured Monomix repair material is 1035 microstrain compared with 298 microstrain for HB40 repair material (Table 8.6). Monomix and HB40 repair materials represent the highest and lowest shrinkage curves respectively in Figure 8.18 for both normally and microwave cured specimens. The corresponding bond strengths of normally cured Monomix and HB40 are quite similar at 6.74 and 6.95 MPa respectively. This indicates that shrinkage itself has a modest effect on the bond strength. Other factors such as elastic modulus and density of the matrix also have an impact on the radial stresses induced on the embedded steel. The compressive strengths and, therefore, Elastic modulii [7] of Monomix and HB40 (normally cured) are similar (23.9 and 21.3 MPa respectively, Figure 8.17). The densities of the two materials are also similar.

Table 8.6: Shrinkage of normally and microwave cured specimens at 42 days age

Repair Material	Micro Strain (μm)		
	Normal	Microwave	Difference (%)
Five Star	841	642	24%
Monomix	1035	940	9%
HB40	298	201	32%
CEM II	685	640	7%

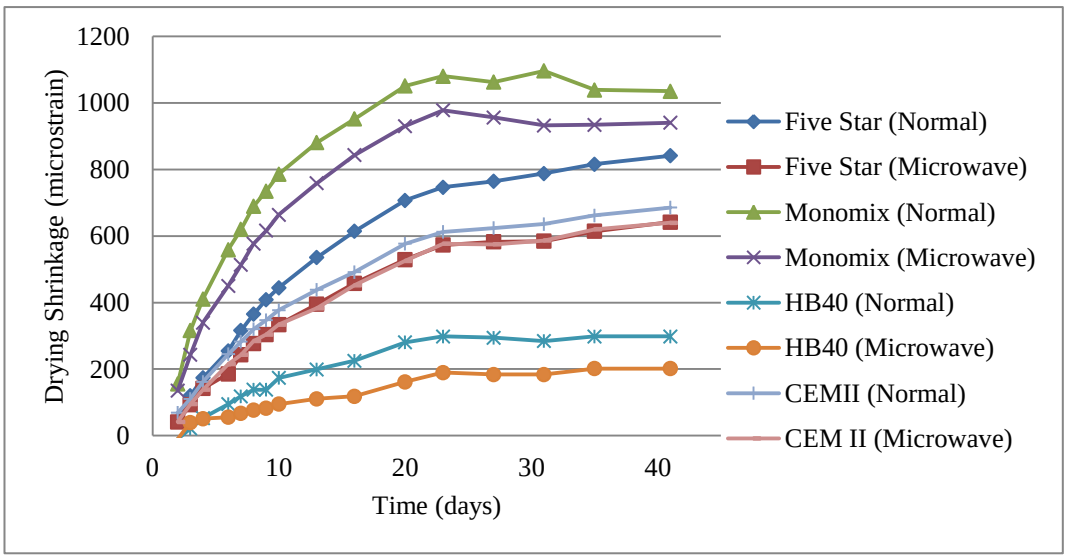

Figure 8.18: Drying shrinkage of normally and microwave cured repair materials as a function of time.

8.4.5 Interrelationships between properties

8.4.5.1 *Relationship between bond and compressive strength*

Figure 8.19 shows the relationship between bond strength and compressive strength for normally and microwave cured specimens at 42 days. There is a strong correlation between the bond strength of the 10 mm diameter plain steel bar and compressive strength for all repair materials, both under microwave and normal curing. Five Star repair material (normally cured) with a maximum bond strength of 10.74 MPa provides the highest compressive strength of 40 MPa while HB40 (microwave cured) shows both the lowest bond strength (4.16 MPa) and compressive strength of 12.5 MPa.

The relationship between bond strength and compressive strength of concrete is more complex with deformed reinforcement bars which are normally used in modern concrete. In this case, the strength of concrete provides additional bond through mechanical interlock of deformed bars [210] whereas bond strength of plain steel bars is composed of adhesive stress and friction [195]. A non-linear relationship of bond and compressive

strength is often used, with the fib code of practice [200] relating bond to the square root of strength. A regression analysis of the data in Figure 8.19 gives a similar non-linear equation of the form:

$$f_b = 0.55 f_c^{0.81} \qquad (8.3)$$

where f_b is the bond strength (MPa) and f_c is the compressive strength of the matrix (MPa). The coefficient of correlation is 0.98 which is similar to the strong correlation of the linear relationship in Figure 8.19. A wider range of data may have provided a distinction between the two relationships. The power coefficient of 0.81 in equation 2 is greater than the values of 0.5 and 0.67 given in literature [200] possibly because it pertains to the data on plain steel bars embedded in proprietary repair mortars.

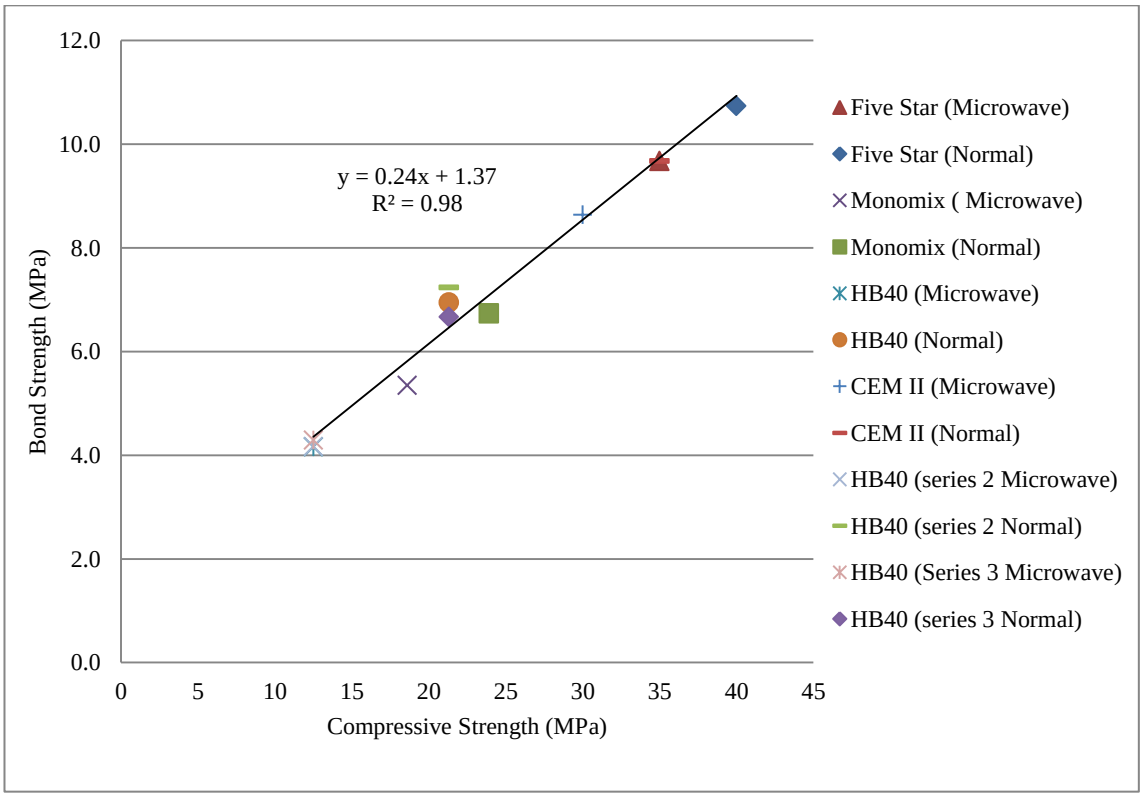

Figure 8.19: Relationship between compressive strength and bond strength of microwave repair materials

8.4.5.2 *Relationship between bond strength and total porosity*

Figure 8.20 shows the relationship between bond strength and effective porosity for both normally and microwave cured specimens at 42 days age. The total porosity data has been presented in Chapter 6 (Section 6.4.2). The bond strength decreases as porosity increases. For example, normally cured Five Star repair material shows the highest bond strength of 10.74 MPa and the lowest porosity of 10.37 %, while microwave cured HB40 repair material shows the lowest bond strength (4.16 MPa) and the highest total porosity (33.74%).

A non-linear equation between porosity and bond strength is also provided by the regression analysis of the data in Figure 8.20, which gives

$$f_b = 13.81 V_s^{2.58} \qquad (8.4)$$

where f_b is the bond strength; V_s is volume of solid matrix (1-p) with a coefficient of correlation of 0.89.

The strong relationship between bond and compressive strength (Figure 8.19 and equation 8.3) and between bond and porosity (Figure 8.20 and equation 8.4) implies a similar relationship between compressive strength and porosity, which conforms to existing knowledge on porosity-strength relationship of concrete [7].

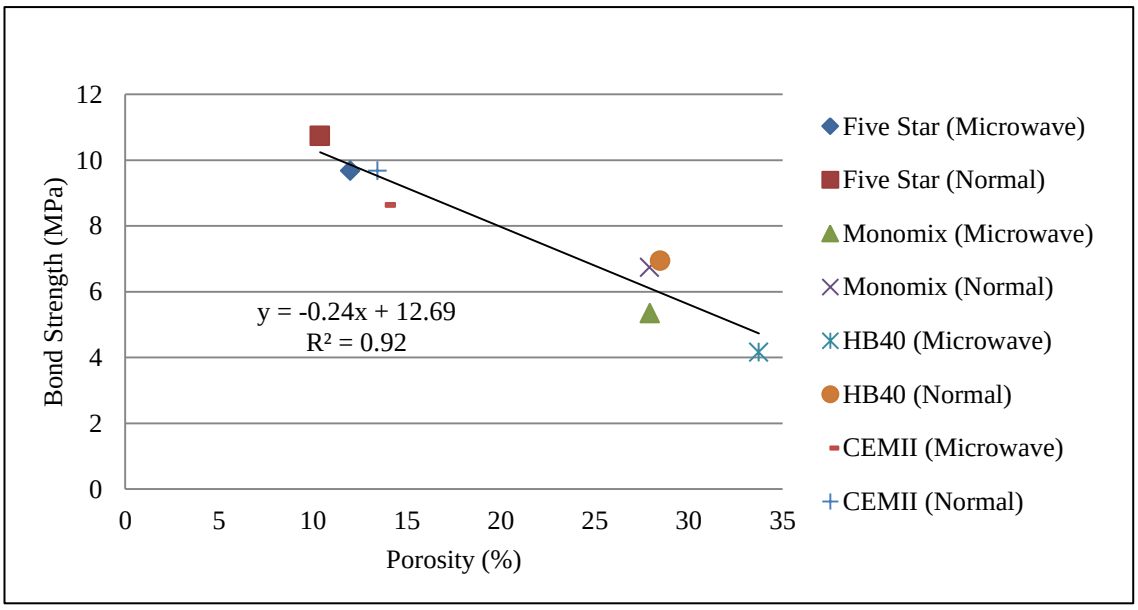

Figure 8.20: Linear relationship between bond and effective porosity for normally and microwave cured repair materials

8.5 Conclusions

Based on the results presented in this chapter the following conclusions can be drawn:

- The presence of steel reinforcement in repair mortar does not cause any arcing during microwave curing. This also applies to steel located at very low cover (5 mm) and to exposed steel bars protruding from the mortar substrate.

- Microwave curing reduces the bond strength between repair mortars and plain steel reinforcement by 10 to 40%.

- The change in a rate of temperature rise during microwave curing appears to have no effect on the bond strength for HB40 repair materials.

- Microwave curing reduces the drying shrinkage for all four repair materials used in the research. The reduction ranges from 7 % (CEM II) to 32 % (HB40). The reduction in shrinkage corresponds to the reduction in gel pore volume.

- The bond strength of steel reinforcement has a unique relationship with the matrix compressive strength and porosity under both normal and microwave curing. It increases both with an increase in the compressive strength and decrease in the porosity of matrix. Therefore, bond-compressive strength relationships used in design of reinforced concrete structures will be valid for microwave cured elements.

- Relationships between bond strength f_b and compressive strength f_c derived is of the form:

$$f_b=0.55f_c^{0.81}$$

- Relationships between bond strength f_b and porosity p derived is of the form:

$$f_b=13.81V_s^{2.58}$$

where $V_s=(1-p)$.

Chapter 9

9. Microwave Prototype System

9.1 Introduction

This chapter provides details of the prototype microwave system which was developed based on the laboratory results on microwave curing of repair materials presented in Chapter 4. In addition, it presents the results from field trials conducted with the prototype microwave system at the site of Jörg Heizmann Bauunternehmung GmbH contractor (Osterburken, Germany). The aim of the field trials was to validate the pre-industrial prototype system by testing elements of four commercial repair materials and CEM II concrete. Slabs of dimensions 1 m x 1 m and depth up to 80 mm were cast and microwave cured to a temperature up to 76.5 °C for a predetermined time. The internal temperature of the microwave cured slabs was recorded up to 24 hours.

9.2 Literature review and background

9.2.1 Microwave

Microwave heating refers to the heat generated by the frequency range 300 MHz to 300 GHz [211]. These ranges of waves have a variety of applications such as communication, radio detection, radar, navigation, spectroscopy and heating applications. The capability of microwave heating with this range was discovered accidentally by Percy Spencer an American engineer [212] and it lead to the manufacture of the first commercial microwave oven. There has been extensive research

since, to develop and improve the uniformity of the heat within the object as well as to increase the efficiency of microwave heating.

The primarily use of microwaves is to provide a source of heat energy. It provides a rapid uniform heating due to the penetration of microwave energy. Its largest market is the domestic microwave oven. However, the application of microwave heating is unbelievably extensive. For example, heating from microwaves can be used for drying paper, wood [213], photographic film and lather [50], oil extraction from tar sand, synthesis, crosslinking and processing of polymer materials [214], food industry for cooking, thawing, freeze drying, continuous cooking, pasteurisation and sterilization, etc. [50].

The popularity of microwave heating is due to the many advantages it has over conventional heating. This includes easy operation, quick start and stop process, rapid heating, energy saving, relatively uniform heating compared to conventional methods, eliminate warm-up time, high-temperature capabilities, portability of equipment and clean energy source compared to some conventional systems.

The industrial, scientific and medical (ISM) radio bands are frequencies reserved internationally for industrial, scientific and medical use. Several frequencies such as 0.915, 2.45, 10.6 and 18 GHz [215] have been allocated for these uses. Lower frequencies such as 0.915 or 2.45 GHz which are most commonly used, provide a higher penetration which exceeds the typical thickness of materials processed by most current microwave users. The higher microwave frequencies such as 10.6 or 18 GHz on the other hand, dissipate much faster in dielectric materials and, therefore, may lead to localised heating. Localised heating may not be beneficial in cases such as food industry

or microwave curing of concrete, however, it is desirable for other applications such as cutting, drilling and demolition of materials such as hard rock and concrete.

9.2.2 Applications of microwave technology in the concrete industry

The applications of microwave technology are limitless. These include demolition of concrete, recycling of concrete demolition waste [216], decommissioning of decontaminated concrete, cutting, drilling/ melting of concrete [217], non-destructive monitoring of concrete structures, concrete heating process [218], and microwave furnaces for cement manufacture [219]. There have been investigations aiming to develop a microwave curing system for concrete [220, 221]. For example, Morozov et al. [220] reported an experimental investigation of applying microwave energy to heat concrete while transferring the mixture into moulds. They have introduced a prototype and claimed that a microwave power of 50 KW increases the temperature of concrete by 6 °C for a plant with a capacity of 10 m^3.

9.2.3 Health and safety of microwave technology

There are two aspects related to the health and safety of microwave technology. One is the exposure to microwaves and second is the exposure to the high voltage of the microwave generator. Generally, microwave technology is operated with a high voltage of up to tens of thousands of volts. The high voltage may be present even while the microwave is not operating due to the capacitors that store high voltage electric charges. These high voltages can cause a serious health threat or even death in case of contact with the body. Therefore, manufacturers are required to enclose properly all microwave generating equipment and make them accessible only to the trained engineers. This is normally achieved by the use of door interlocks that shut the power down and discharge the stored charge automatically once the door is opened.

The other aspect is the radiation hazard. Recently there has been considerable public concern and legal proceedings about microwave oven [222] and cellular telephone systems which create the same frequency as a microwave. However, there is no available evidence confirming the relationship between exposure to the magnetic field waves related to the microwave frequencies and development of various cancers [223]. Unlike γ and x-ray frequencies, the photonic energy at various levels of microwave frequency is not sufficient to ionise the exposed materials. Nevertheless, microwave exposure provides thermal heating to the biological materials and therefore, the main concern is related to thermal injury which is the only confirmed health hazard associated with microwave heating. The level of the danger is related to the frequency, power and the period of exposure. The higher frequencies are capable of burning because the microwave penetration is low and microwave energy can concentrate in a smaller area. In addition, an increase in either the power or the duration of microwaves increases the level of the burning. Microwave systems are normally designed with a proper shielding to protect the operators against microwave heating. This is due to the fact that there are limitations set by the Federal Communication Commission (FCC), Occupational Safety and Health Administration and International Electrotechnical Commission (IEC) standard [224], which is applicable to equipment operating in the frequency range from 300 MHz to 300 GHz power. The power density on the human being should be limited to 50 W/m^2 from different sources such as medical devices, amateur radio, cellular phone base station, WiFi source, microwave ovens, traffic radar.

9.3 Description of the prototype microwave system

9.3.1 Microwave system

The prototype microwave system has been designed and manufactured by Fraunhofer IGB (Germany) [225] based on the results obtained from laboratory investigations which are reported in Chapter 4. In addition, ERS Control Technology GmbH & Co. KG [226] designed the control cabinet and software for the system. The microwave prototype system is operated by 3 phase electrical power, 400 Volts and frequency of 50 Hz. The microwave prototype system can be operated either manually through the touch screen panel or remotely from a connected computer. The magnetron used in this prototype can generate power at incremental levels of 5% from 10% up to 100% of its maximum power of 2000 Watts with a frequency of 2.45 GHz.

Microwaves emitted by the magnetron are guided by a slotted antenna of dimensions 500 x 100 mm. The slotted antenna is designed to guide microwave energy uniformly across the surface of the concrete. The face of the antenna which directs microwave energy to the test specimen has six slots, each of dimensions 58 mm x 6 mm.

The prototype system is shown in Figure 9.1. An external pump is used to run cooling oil through a reservoir and the magnetron with installed pipes in order to prevent overheating of the magnetron and electrical devices during operation. The slotted waveguide antenna was manufactured and placed inside the frame. Temperature sensors and a moisture sensor were also installed close to the slotted antenna. The slotted antenna along with sensors can remotely move through X, Y and Z directions controlled by 3 electrical motors, one for each direction. The movement ranges from 0 to 909 mm for both X and Y axes. The movement for Z-axis ranges from 406 to 607 mm (201 mm)

from the ground level. The external frame is attached to four wheels. It can move on the ground and adjust the position of the antenna above a patch repair.

Figure 9.1: Microwave prototype system

9.3.2 Temperature monitoring system

Temperature monitoring of microwave cured repair material is important to avoid excessive temperature while ensuring that sufficient heat has been provided to accelerate curing of cement based materials. Therefore, the prototype has been integrated with six non-contact infrared temperature sensors to measure spot temperatures ranging from -50 °C to 975 °C with an accuracy of ±1%. Figure 9.2 (a) shows the temperature sensors integrated on the top of the frame and showing live temperature and Figure 9.2 (b) shows a close view of the six sensors. Figure 9.3 shows the arrangement of the six sensors with the actual position related to the slotted wave antenna. The size of the spots is exaggerated in the drawing to assist the visibility of the location. Among these sensors, B221 and B220 come with laser markers indicating the location of the measurement on the top surface of the concrete. The arrangement of the

sensors provides the ability to determine the temperature at different locations of the concrete surface covered by the slotted antenna during microwave curing. The temperature recording system is capable of recording each location temperature, minimum, maximum and the average of the total temperatures.

(a) (b)

Figure 9.2: (a) microwave prototype system and (b) the location of the surface temperature sensors B220-B225

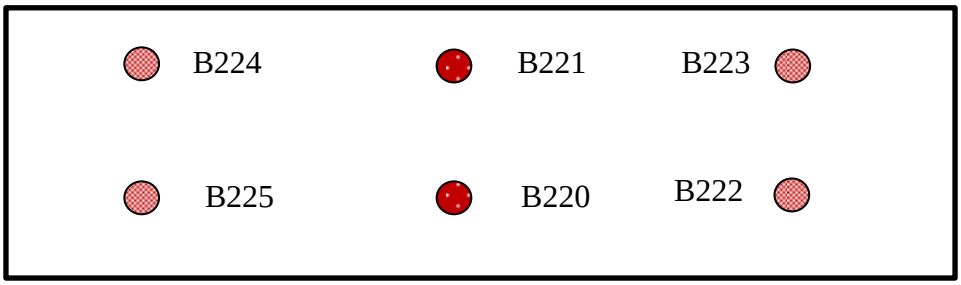

Figure 9.3: Pointed positions of non-contact infrared temperature sensors

9.3.3 Moisture monitoring system

Moisture content is another important parameter which provides concrete maturity and strength development [227]. It is very important to control moisture loss, as uncontrolled moisture loss during curing can cause detrimental effects on the quality of repair. A rapid moisture loss due to higher curing temperatures results in higher shrinkage and lower longer-term strength [228, 229].

The prototype is equipped with a moisture sensor to detect the moisture content of the fresh concrete. Figure 9.4 shows the moisture sensor which is located beside the slotted antenna. The moisture sensor measures the moisture content by detecting and measuring the reflected microwave energy from the concrete surface.

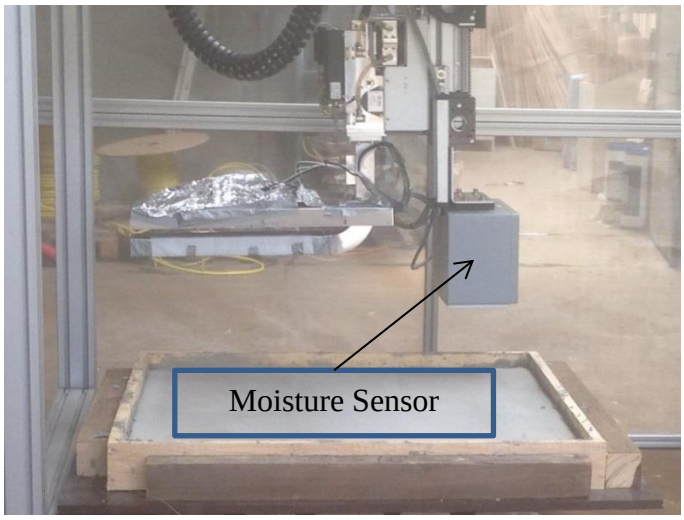

Figure 9.4: Location of the moisture sensor.

9.3.4 Microwave radiation safety system

Figure 9.5 (a) shows the microwave safety frame. Prototype has been designed to operate safely according to the International Standard IEC 60519-6 [224] by appropriately shielding any signal above the allowed limit of 50 W/m^2. This limitation in leakage is achieved by designing an aluminium frame with metallic fabric to cover the prototype system. The shield traps any reflected microwave energy during microwave curing. In addition, four microwave detector sensors installed at the top of each side of the frame were connected to a microwave leakage tester model MLT442. Each sensor was directly connected to the main control system and could individually shut down the whole system by detecting any leakage over 50 W/m^2 during operation. Furthermore, a manual microwave measuring instrument Votcraft model MWT - 2G

was used to monitor outside the frame while the prototype was operating. No leakage above the limit has observed throughout the trials.

(a) (b)

Figure 9.5: (a) Shield of the microwave prototype system and (b) microwave leakage sensor

9.3.5 Microwave operation software

The software to operate the microwave prototype is based on two different algorithms especially developed for the system. It gives the opportunity to the user to operate the system either manually or automatically. Parameters such as the movement pattern of the antenna over the microwave cured area, microwave power, target temperature and total heating time can be input before the start of operation by using the touch screen panel shown in Figure 9.6. The movement of the antenna is subdivided into step by step and continuous movement patterns. The step by step movement means that the antenna will move to the next position only when the target temperature of the current position is achieved. The continuous movement pattern means that the antenna will continuously move over the concrete surface at a constant speed/power. The algorithm to determine the time and the speed of the antenna based on the size of the slab for both step by step and continuous movement pattern are presented in Appendix 12.2.

The microwave prototype can microwave cure the elements in either manual or automatic mode.

(a) (b)

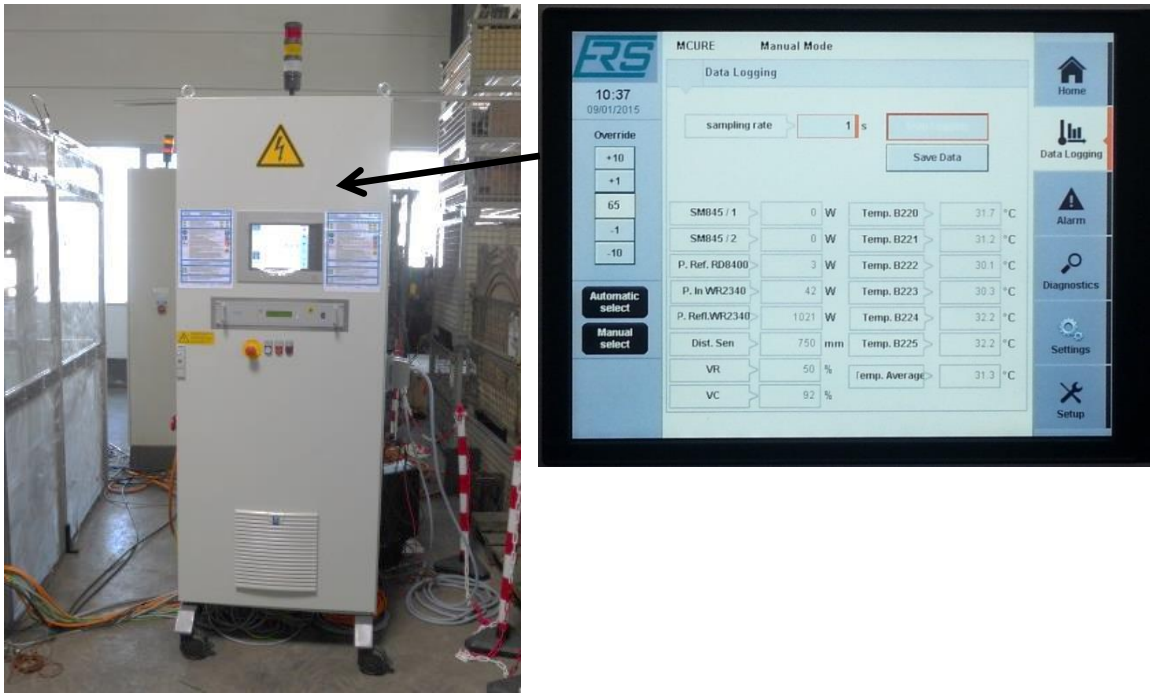

Figure 9.6: Control cabinet and the touch panel to operate the microwave system

9.3.5.1 ***Manual mode***

Microwave curing parameters such as the position of the antenna, microwave power and heating time should be determined by the operator in the manual mode of the machine. The target temperature can be reached using either continuous movement or a step by step approach. In the first case, the antenna moves at a constant speed along a pre-determined patch using fixed power and the temperature is recorded. This procedure can be repeated as many times as needed to achieve the target temperature. In the second case, the antenna is positioned above a pre-determined location and remains fixed until the area directly beneath the antenna has reached the target temperature. Once the target temperature is reached, the antenna is moved and positioned at the next area to be

microwave cured. By using this approach, it is possible each time to microwave cure an area slightly larger than the projected area of the antenna.

9.3.5.2 *Automatic mode*

When in automatic mode, only the movement pattern of the antenna is determined by the operator. The target temperature of the microwave cured patch repair is achieved by using either Proportional Integral Derivative (PID) algorithm or a Fixed Time Power Regulating (FTPR) algorithm specifically developed for this prototype system (see Chapter 4). The algorithm is used to regulate the required microwave power of the antenna at a specific position. Once the target temperature at this position is achieved, the antenna is moved and positioned over the next area to be microwave cured.

9.3.5.2.1 PID algorithm

The Proportional Integral Derivative (PID) controller is a control loop feedback mechanism [230]. It has become the most commonly used closed-loop controller in all types of industrial control systems due to its simplicity and excellent performance [231]. In a PID controller, its input signal is the error e(t) between a user defined setpoint r(t) and a measured plant/process variable y(t) as shown in Equation 9.1. The terms plant and process refer to the object or the process that is being controlled by the PID controller. In the case of Microwave prototype system, the process is the microwave heating of the repair patch and the error e(t) is the difference between the measured temperature y(t) and the target temperature r (t) (40 to 45 °C). The output signal u(t) of the PID controller in time t-domain is given by Equation 9.2.

$$e(t) = r(t) - y(t) \qquad (9.1)$$

$$u(t) = K_p e(t) + K_i \int_0^t e(t)dt + K_d \frac{de(t)}{dt} \qquad (9.2)$$

Where e(t) is the error signal; r(t) is the setpoint value for temperature; u(t) is PID output signal; K_p is proportional gain (a tuning parameter); K_i is integral gain (a tuning parameter) and K_d is derivative gain (a tuning parameter).

The PID controller in the microwave prototype system continuously measures the error and attempts to minimise it over time by only adjusting the microwave power supplied to the surface of the repair patch. Consequently, the required heating time to reach the target temperature cannot be controlled. Too much microwave power can lead to excessive rates of temperature increase, which in turn can result in plastic shrinkage and cracking, significantly reducing later age strength [228, 229]. In order to overcome the above limitation, a second algorithm called Fixed Time Power Regulating (FTPR) algorithm (presented in Chapter 4) has been developed for use with the microwave system. The FTPR algorithm achieves the target temperature at the end of microwave curing.

9.3.5.2.2 FTPR algorithm

The aim of this algorithm is to provide adequate microwave power for reaching the target temperature at the end of the fixed period of microwave curing. Prior to the application of microwave curing the rate of temperature increase for the entire curing cycle is determined based on the initial (ambient) temperature and the target temperature of curing. At the start of the curing cycle, an initial microwave power P_i is applied for an incremental period t_i and the temperature of the repair surface T_i is measured at the end of t_i. Next, the rate of temperature increase during period t_i is compared to that targeted for the entire curing cycle. If the rate of temperature increase during t_i is higher or lower than the rate of temperature increase required for the entire curing cycle the microwave power is either reduced or increased accordingly to a new

value P_1 according to the procedure given in Chapter 4, Section 4.4.10. The power is adjusted iteratively at regular intervals to reach the target temperature of curing.

9.4 Field trials

9.4.1 Test programme

Slab elements of 1 x 1 m dimensions were microwave cured using the microwave prototype system. Tests were carried out to validate the design, operating and control parameters of the microwave prototype system and to assess its reliability. The results were analysed to validate the microwave curing relationships developed for repair patches (Chapter 4).

9.4.2 Repair materials

The following repair materials were used to cast the slabs:

- Sika MonoTop 412 DE
- Sika MonoTop 613 DE
- StoCrete GM P
- StoCrete TG 204
- OPC concrete, a concrete mix with CEM II/A-LL 32.5 R cement conforming to BS EN 197-1, coarse sharp sand (50% passing a 600 mm sieve) and uncrushed river gravel (maximum size 20 mm) with w/c ratio of 0.50. The density of the fresh mix was 2350 kg/m^3. In addition, similar concrete mixes with w/c ratios of 0.40, 0.45, 0.50, 0.55 and 0.60 were used to test and calibrate the moisture detector of the prototype system.

The mix proportions of each repair material were based on the manufacturer's recommendations, which comprised of the bagged powder content and water at

water/powder ratios given in Table 9.1. A description of each repair material is given in Chapter 3.

9.4.3 Details of slabs

A total of 10 slabs were cast in timber moulds of 1000 x 1000 x 105 mm internal dimensions for the microwave curing trials of the repair materials. Details of all slabs are shown in Table 9.1.

Table 9.1: Details of slabs S1 to S10

Slab	Area (m^2)	Depth (mm)	Repair material	w/p*	Pre-curing time (minutes)	Substrate material
S1	1	62	Concrete	0.5 (w/c)**	45	N/A
S2		80			52	N/A
S3		34			35	N/A
S4		46			56	Concrete
S5		58			51	N/A
S6		58			43	N/A
S7		62	Sika Monotop 412 DE	0.14	40	N/A
S8		59	Sika Monotop 613 DE	0.13	46	N/A
S9		61	StoCrete TG 204	0.12	38	N/A
S10		64	StoCrete GMP	0.11	41	N/A

* water/powder ratio, ** water/cement ratio

9.4.4 Mixing and casting of slabs

The quantity of each repair material and water were mixed together in a concrete pan mixer to produce the volume required for the slab element. Each mix was cast in the timber mould and compacted by hand tamping and trowelled as shown in Figure 9.7 (a-b). The slab specimens were then placed inside the microwave prototype and microwave cured as shown in Figure 9.8. Microwave curing was started at 35 to 56 minutes (pre-curing time) after commencing mixing of the repair materials, to simulate the typical time taken on construction sites to apply a repair patch. Figure 9.9 shows 10 slabs (S1 to S10) at the end of microwave curing. Slab 4 was cast on top of substrate slab 1 to simulate repair applied on the substrate.

(a) (b)

Figure 9.7: (a) Compaction of newly cast mix and (b) surface finishing.

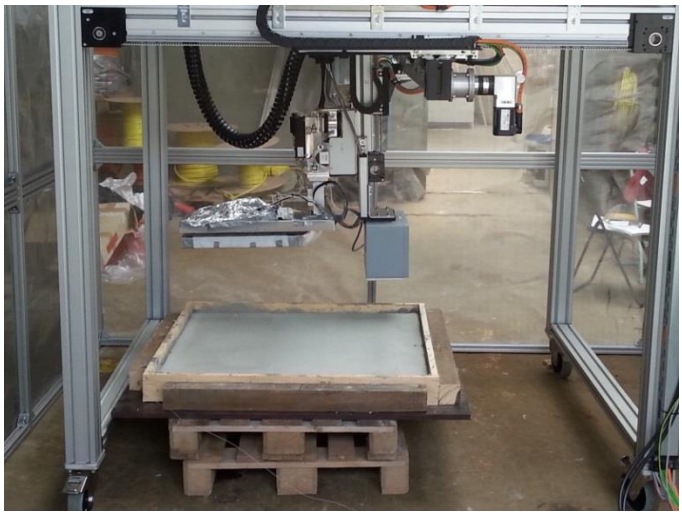

Figure 9.8: Slab placed inside microwave prototype for microwave curing

Figure 9.9: View of all microwave cured slabs

9.4.5 Microwave curing

The 1 m x 1 m surface area of slabs was exposed to microwave curing for nearly 1 hour. The surface of each slab was divided into 20 strip areas to heat as shown in Figure 9.10. The dimensions of each strip area were 0.5 x 0.1 m. The slab surface exposed to microwave power was not covered during curing. Each strip area was microwave cured for 5 minutes (Slabs S1 to S4) or 2.5 minutes (Slabs S5 to S10) at a power of either 1500 W (Slabs S1 to S4) or 1700 W (Slabs S5 to S10) by locating the microwave antenna above the strip. The projected area of the antenna on the slab, with some spread of the microwave energy due to the angle of the antenna slots, was heated at each location. After heating a strip, the antenna was moved to the next strip by operating the control system manually.

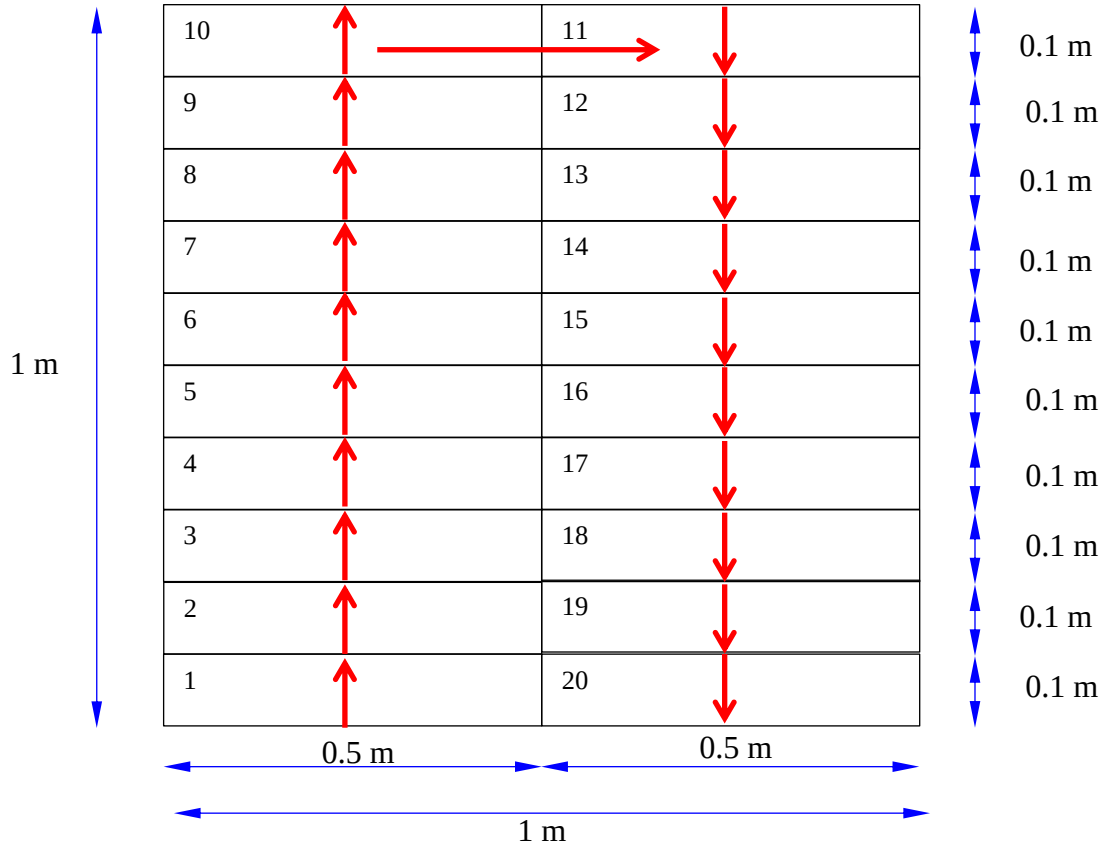

Figure 9.10 Schematic diagram of microwave curing sequence of strip areas.

9.4.6 Internal temperature

The internal temperature of each slab was measured by locating a single T type thermocouple at the base of the timber mould at the centre of Strip 2. Figure 9.11 (a) shows a typical timber mould with an installed thermocouple. In the case of slab S4, which was cast over previously cast hardened substrate slab (S1), a second thermocouple was installed at the interface between the hardened substrate and the repair material as shown in Figure 9.11 (b). The thermocouple was located at the top surface of the substrate directly above the first thermocouple applied at the base of the mould. Temperature measurements were taken every one-minute using a Data Taker DT85G digital logger.

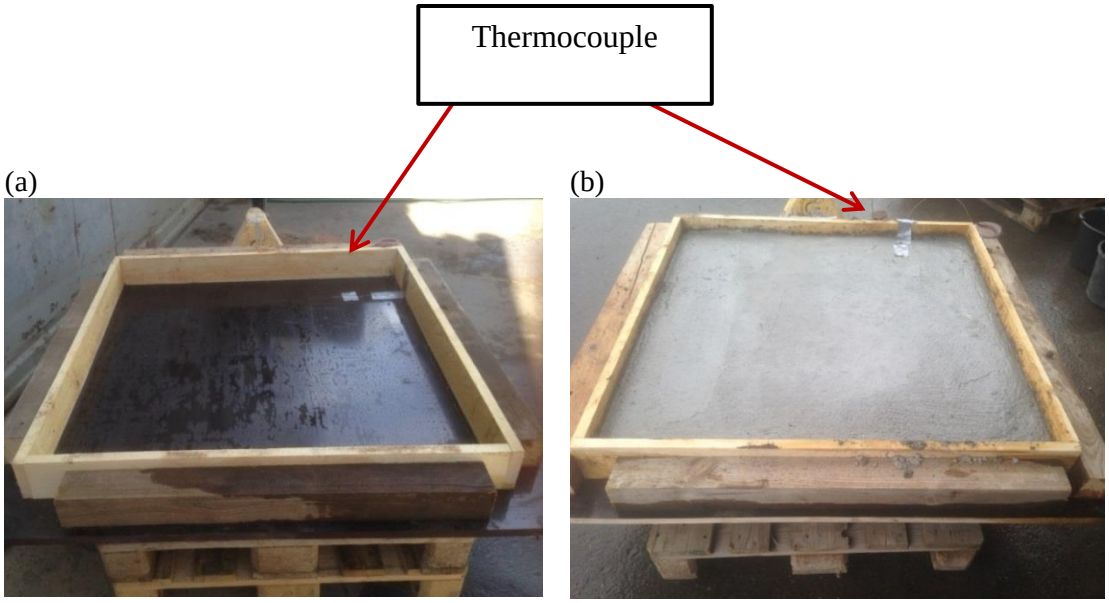

Figure 9.11: Location of type T thermocouple (a) on the base of the slab and (b) on top of the substrate surface of slab S4.

9.4.7 Surface temperature measurement

In addition to the temperature sensors within the microwave system, the surface temperatures of the slabs were measured using a Flir i7 thermal camera. The thermal camera specification is given Chapter 3.

9.4.8 Testing and calibration of the moisture sensor

Slabs of concrete mixes were prepared with different water/cement ratios of 0.4, 0.45, 0.50, 0.55 and 0.60 and placed inside the microwave prototype. The moisture detector of the prototype was used to determine the moisture content of each mix. The results from the prototype system were then compared to the actual moisture content of the mix and the relationship is determined to calibrate the moisture detector.

9.4.9 Effect of microwave curing on steel reinforced concrete

The effect of microwave curing on steel reinforcement has been previously studied based on a laboratory investigation and presented in Chapter 8. However, Field trials provided the opportunity to expose a reinforced concrete slab to the microwaves with a power up to 2 kW. One-quarter of a slab was reinforced with 2 steel links (diameter 10 mm) as shown in Figure 9.12 at a cover of approximately 30 mm from the top surface of the slab. The slab was microwave cured similar to the plain concrete slabs. The reinforced concrete area (strip 20) was microwave cured for an additional 5 minutes at 1.9 kW.

Figure 9.12: Placement of steel reinforcement links prior to casting.

9.5 Results and Discussion

9.5.1 Movement of the antenna along X, Y and Z directions

Figure 9.10 represents the surface of a cast slab, with the slotted wave antenna positioned above one corner. The slotted antenna was moved freely in the X, Y and Z directions. The movement range of the antenna along the X and Y axis was from 0 to approximately 909 mm. The range for the Z axis was from 406 to 607 mm from the ground level. The length and width of the slotted wave antenna are 500 x 100 mm which means that its slotted face projects over an area of 500 x 100 mm of the slab surface when the microwave operates. The result was that the microwave energy at each position of the antenna covered an area greater than 0.5 x 0.1 m^2 of slab strip area due to the angle of the antenna slots. Consequently, there was an overlapping effect of microwave heating when the antenna was moved from one strip position to the next as shown in Figure 9.13. There was also an overlap when the antenna was moved laterally to microwave cure strips 11-20 after curing strips 1-10. The central zone received a higher amount of microwave energy due to the overlapping effect (Figure 9.13).

Each strip area was microwave cured in succession starting from either strip 1 or 2 and moving upwards (Figure 9.13). The slotted waveguide antenna was positioned directly above each strip (Figure 9.13). For microwave curing strip areas 11 to 20 the antenna was positioned as far to the right as possible to minimise the overlap between the previously cured strips 1-10. The overlap area was approximately 0.11 x 0.10 mm over the centre of the slab as shown in Figure 9.13. This overlap was due to the restricted movement of the antenna in the X direction, caused by the antenna support system.

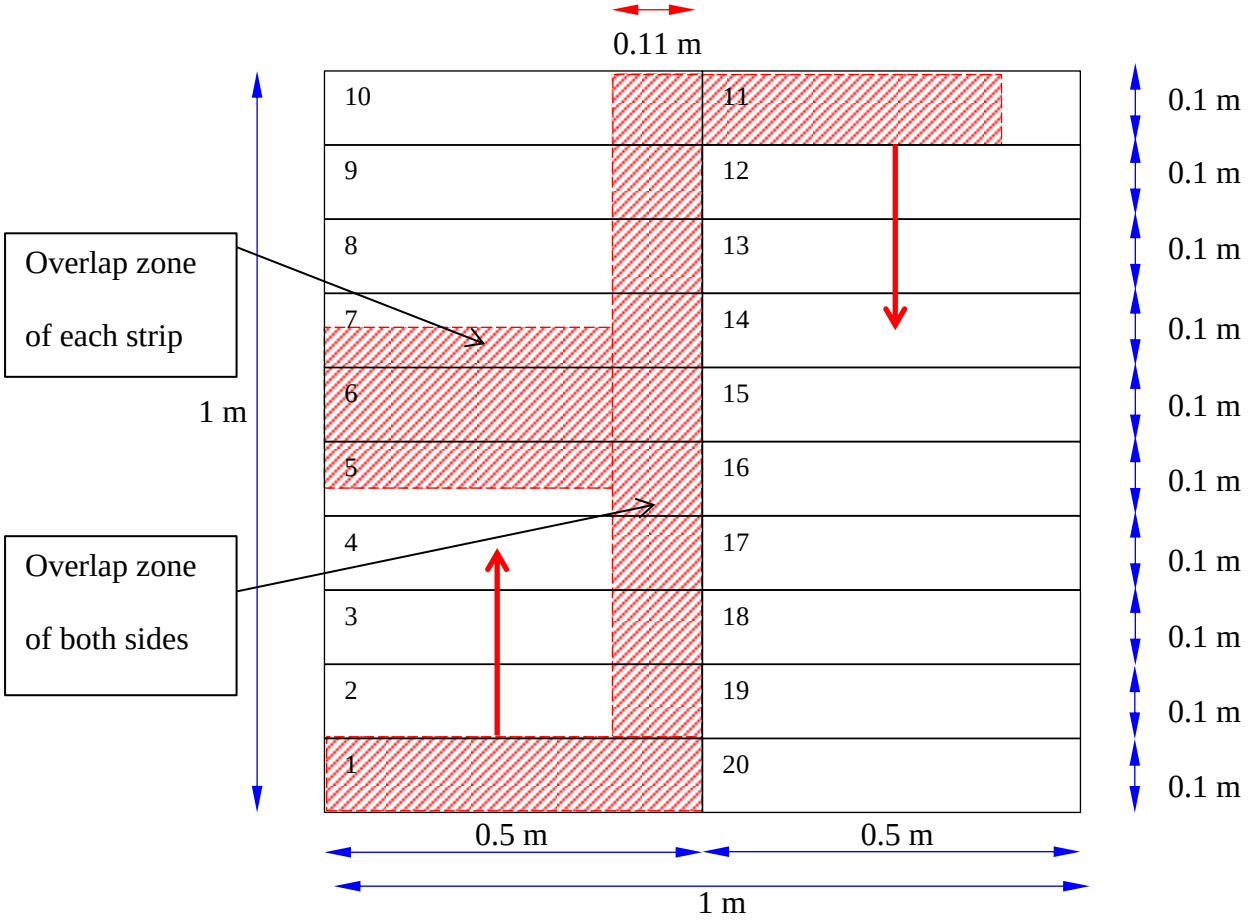

Figure 9.13: Schematic diagram of slotted wave guide antenna positioning over strip areas 1-10 and 11-20, showing the overlap zones.

9.5.2 Calibration of the moisture sensor

Table 9.2 shows the details of the concrete mixes with different water/cement ratios and their moisture content (actual and the moisture recorded by the microwave prototype sensors). The actual moisture content is calculated from the mix proportions (w/p). The relationship between the moisture sensor reading and the actual moisture content is presented in Figure 9.14. The results show that the moisture sensor reading decreases with an increase in moisture content. Mix 1 (w/c=0.4) gives the lowest actual moisture content of 7.4 % and the highest moisture sensor reading of 0.97%. The corresponding values for mix 5 (w/c=0.6) are 10.71% and 0.724 % for actual moisture content and the

moisture sensor reading respectively. The moisture sensor readings for mixes 2, 3 and 4 showed a range of variations which are given in Table 9.2 together with the average value. The reason for the inverse relationship between actual moisture content and the sensor reading is due to the fact that the sensor detects and measures the reflected microwaves from the mix. The higher moisture content of the mix results in higher microwave absorption and therefore, lower reflected microwaves to be detected by moisture sensor.

The moisture content from the sensor was also monitored while the microwave was operating. However, the readings obtained in the microwave environment were erratic, possibly due to interference of microwaves with the sensor. Therefore, microwave power was switched off when the moisture sensor readings were taken.

The results plotted in Figure 9.14 show a strong linear relationship between the actual moisture content and moisture sensor reading with R^2=0.84.

Table 9.2: Moisture content of concrete mixes

Mix number	Water Cement ratio (w/c)	Actual moisture content (%)	Moisture Sensor reading (%)
1	0.4	7.4	0.97
2	0.45	8.26	0.8195 (0.815-0.824)
3	0.5	9.09	0.8155 (0.813-0.818)
4	0.55	9.91	0.790 (0.789-0.791)
5	0.6	10.71	0.724

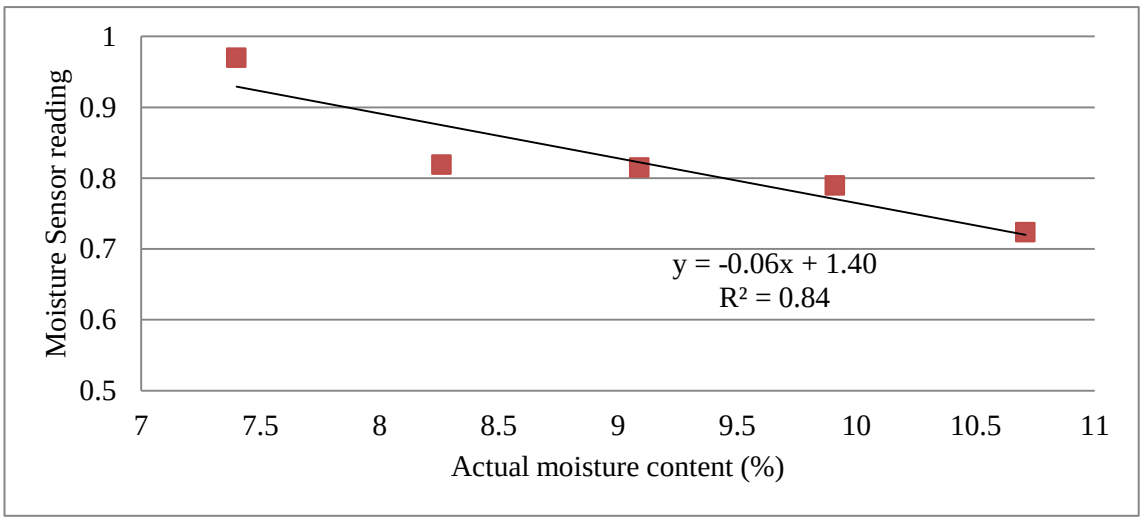

Figure 9.14: Relationship between moisture sensor reading and moisture content

9.5.3 Effective slab area heated by the antenna

Figure 9.15 (a-d) show the distribution of heat over the surface of the slab produced by microwave exposure from the antenna positioned at 135 mm above the slab. The microwave power was emitted from the slotted face of the antenna of dimensions 500 x 100 mm. The heated area of the slab shown by the thermal camera images in Figure 9.15 (a-b) is significantly larger than the strip area (500 x 100 mm) projected directly under the antenna. The images show a fairly uniformly heated zone of approximately 500 x (200 to 300) mm wide. This is a typical result which was also observed at other locations of the antenna on different slabs. This heated area indicates a significant spread of the microwave energy emitted from the antenna area (500 x 100 mm) when it reaches the slab surface. The effect of this spread of microwave energy is an overlap of heating provided by the antenna, as shown in Figure 9.13.

(a) (b)

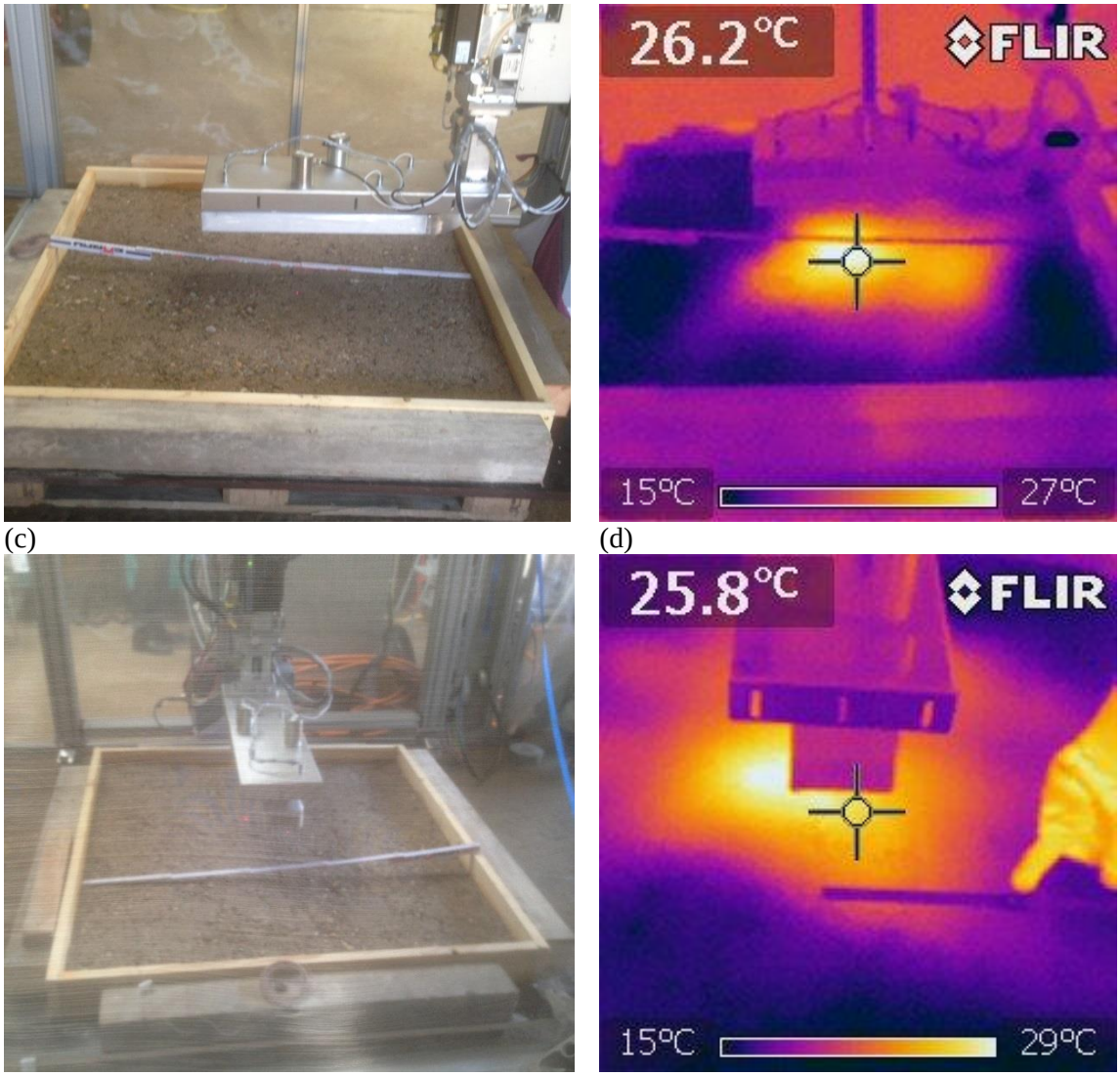

(c) (d)

Figure 9.15: (a) Front view of antenna positioned over a strip of slab (b) image of thermal camera at position (a) after microwave application (c) side view of antenna positioned over a strip of slab (d) image of thermal camera at position (c) after 5 minutes

9.5.4 Top surface temperature of microwave cured specimens

The temperature of the total slab top surface (at the middle) was measured at the start and at the end of microwave curing. Figure 9.16 shows a typical slab (slab 10) and Figures 9.17 (a-b) show the thermal images taken at the start and end of microwave curing of the whole slab top surface. Data in Table 9.3 present the temperature at start and end of microwave curing for all slabs. It also presents the total temperature increase during microwave curing. The results show that the top surface temperature of microwave cured slabs increased significantly from 24.1 to 48.5 °C within 50 minutes

of microwave curing. The range of temperature increase of slabs is from 12.6 to 49.2 °C, depending on thickness. Slab S3 shows the highest temperature increase of 49.2 °C and it is due to the fact that this slab has the lowest thickness (34 mm) compared to the other slabs.

At the end of microwave curing, all slabs were visually observed and they were free from plastic shrinkage cracking except slab S3. Figure 9.18 shows the slab S3 at the end of microwave curing showing cracks due to the high temperature at the end of microwave curing (76.5 ºC).

Slabs 1 to 10 are shown in Appendix 12.3 with their thermal images taken at the start and end of microwave heating.

Figure 9.16: Slab S10 at the end of microwave curing.

(a) (b)

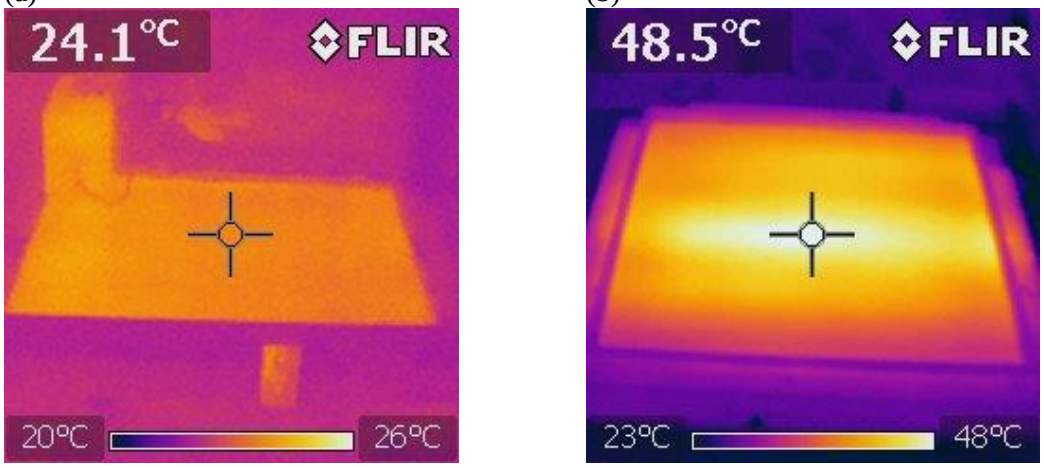

Figure 9.17: (a) Slab 10 temperature distribution before the start of microwave curing, and (b) after the end of microwave curing

Table 9.3: Temperature increase due to microwave heating for 50 minutes

Slab Number	Slab thickness (mm)	Power (W)	Temperature at beginning (°C)	Temperature at the end of microwave curing (°C)	Temperature increase (ΔT)
S1	62	1500	26.3	42.7	16.4
S2	80	1500*	22.0	42.2	20.2
S3	34	1500	27.3	76.5	49.2
S4	46	1500	19.6	44.5	24.9
S5	58	1700	25.2	41.8	16.6
S6	58	1700	27.8	40.4	12.6
S7	62	1700	22.8	41.9	19.1
S8	59	1700	26.7	43.3	16.6
S9	61	1700	27.9	42.5	14.6
S10	64	1700	24.1	48.5	24.4

*Strip 20 was also exposed to 1900 W for 5 minutes.

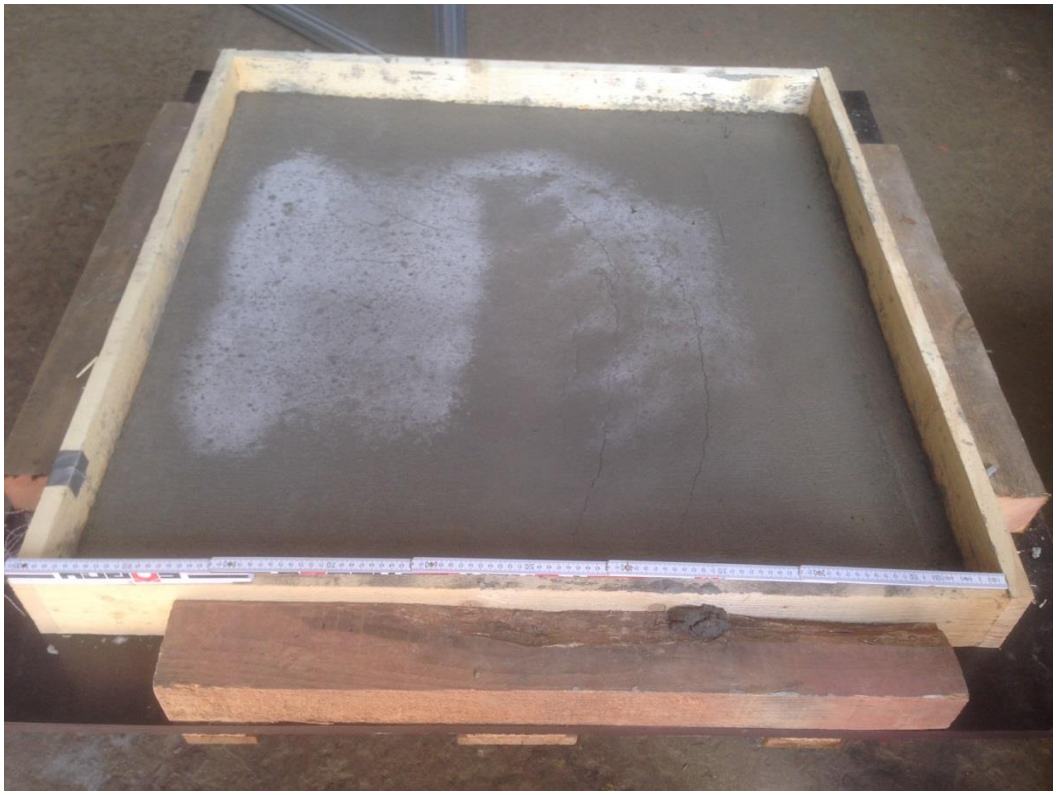

Figure 9.18: Slab S3 at the end of microwave curing showing plastic shrinkage cracking

9.5.5 Effect of microwave exposure on reinforcement

Figure 9.19 (a-b) shows the thermal images of slab 2 which was reinforced with steel links in one quarter. The slab was exposed to 1500 W for 50 minutes and at the end, the quarter of slab with reinforcement was exposed to 1900 W for an additional 5 minutes. The temperature increased from 22.0 to 42.2 ℃ at the end of microwave curing. Figure 9.20 shows the slab immediately after the end of microwave curing. No spark or arcing was observed during microwave curing of the steel reinforced slab.

(a) (b)

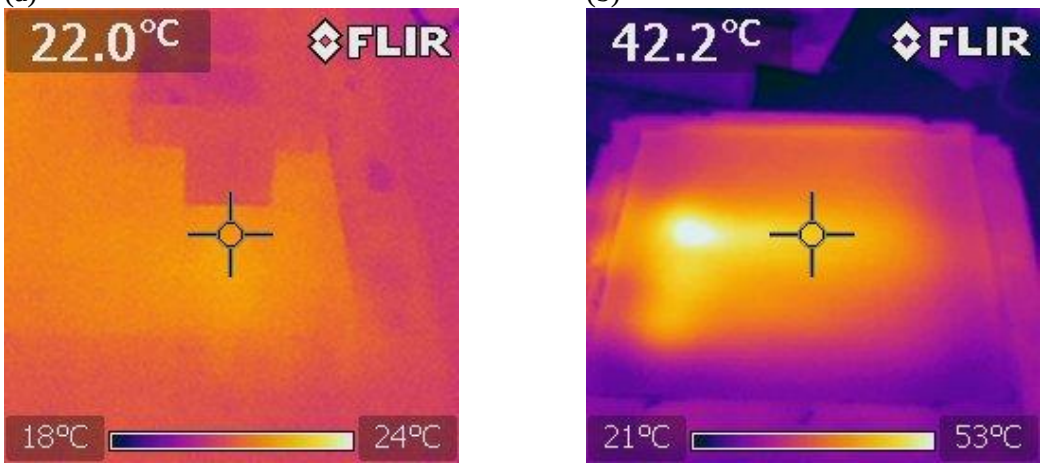

Figure 9.19: (a) Slab 2 temperature distribution before the start of microwave curing, and (b) after the end of microwave curing

Figure 9.20: Slab S2 at the end of microwave curing.

9.5.6 Internal temperature development during microwave curing

Internal temperature refers to the reading from the thermocouple applied at the base of the mould on the inside face. Figure 9.24 shows a typical internal temperature development graph of microwave cured slab S9. Results show an internal temperature of nearly 28.7 °C at the beginning of the microwave curing (38 minutes after adding water to the mix) which increases to 36.5 °C at 105 minutes (67 minutes after microwave curing) to reach the first peak. The temperature then decreased gradually

before it rose again at approximately 160 minutes and gradually reached a peak heat of 51.7 °C at 517 minutes. Similar internal temperatures were recorded for all slabs (Figures 9.21 to 9.24). The increase in temperature for the second peak is due to the heat of hydration.

A comparison of temperature profiles for slabs discussed here and the laboratory specimens (150 mm) reported in Chapter 5 shows that microwave cured 150 mm cubes show a higher value of the peak heat of of hydration and it occurs earlier compared to the slabs reported here. For example, the 150 mm cube of CEM II mortar shows a peak heat of hydration of 73.1 ºC occurring at 165 minutes whereas the microwave cured slab of CEM II (Figure 9.21) reached a maximum temperature of 46 ºC at 322 minutes.

Achieving a lower peak heat of hydration temperature and occurring at later time in slabs in field trials compared to the cube specimens in the laboratory can be due to several reasons. First, the thickness of the slabs is 58-64 mm whereas the thickness of the cube specimens is 150 mm. Second, the surface area and the surface/volume ratio (16.3 m^{-1}) of the slabs (1 m x 1 m) is much larger than 150 x 150 mm surface area of the cubes exposed to the ambient temperature. This results in greater heat loss. Third, the 150 mm cube is insulated by polystyrene walls (except the top) whereas the timber mould edges of the slabs are far apart (at 1 m) and provide negligible insulation to the concrete mass. Therefore, while the volume of the slabs (58 to 64 litres) is greater than the cube (3.4 litre), its effect on the heat of hydration is dominated by the above factors. In addition, the internal temperature of the 150 cubes reaches nearly 50 ºC at the base of the cube at end of microwave heating whereas the internal temperature of the slabs is about 40 ºC at the base.

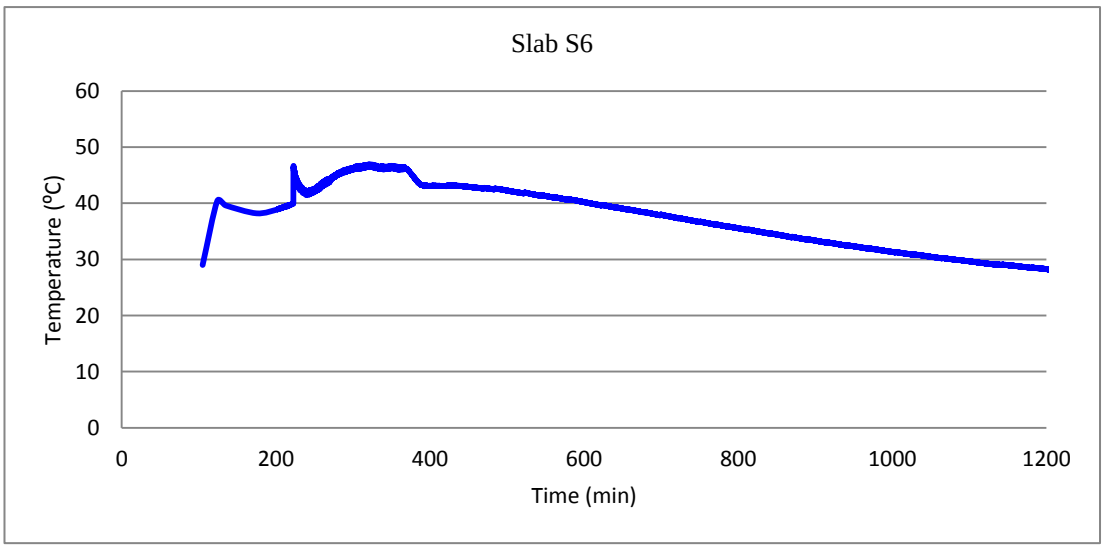

Figure 9.21: Thermocouple readings for a period of approximately 1260 minutes after the start of mixing the concrete.

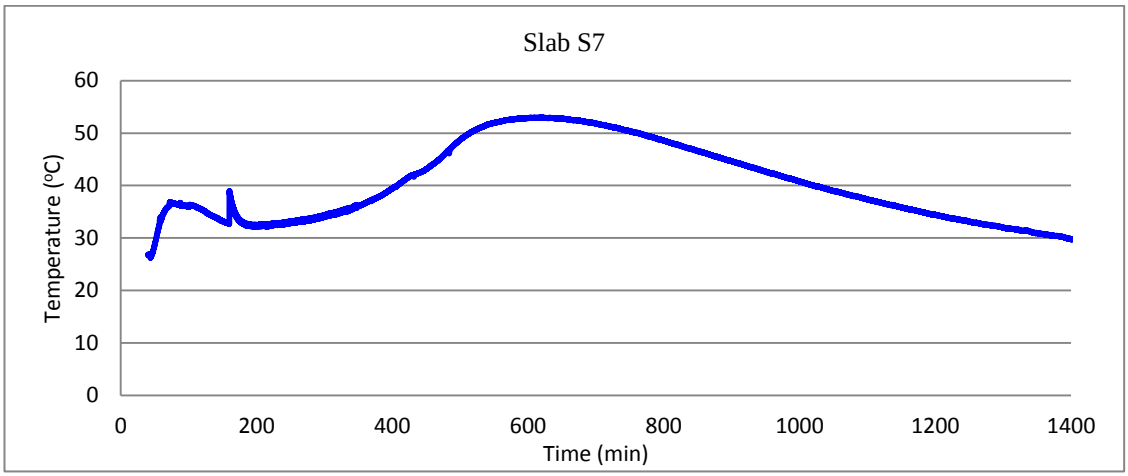

Figure 9.22: Thermocouple readings for a period of approximately 1400 minutes after the start of mixing the repair material.

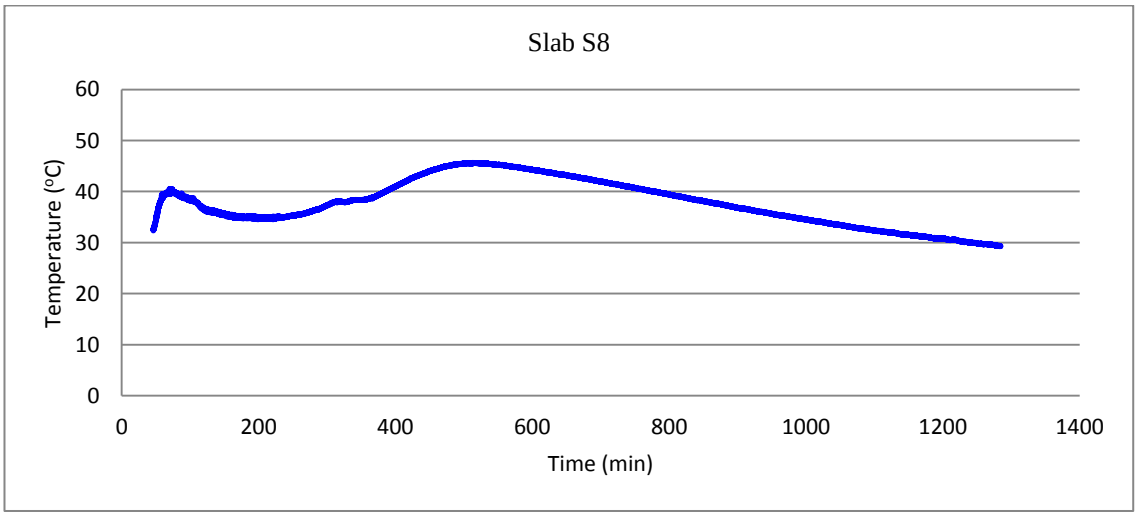

Figure 9.23: Thermocouple readings for a period of approximately 1200 minutes after the start of mixing the repair material.

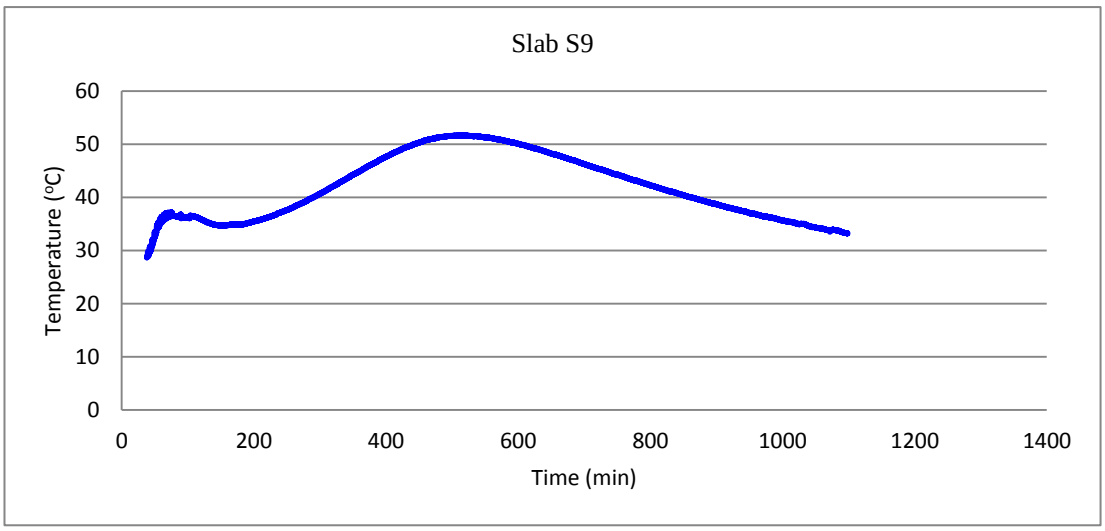

Figure 9.24: Thermocouple readings for a period of 1100 minutes after start of mixing the repair material.

9.5.7 Effect of repeated cycles of microwave heating

Concrete slabs S5 and S6 were exposed to microwave energy at 1700 Watts for a total of 2.5 minutes on each strip (50 minutes on whole slab). However, slab S5 (Figure 9.25) was cured in 2 cycles applying 1700 Watts for 1.25 minutes on each strip for each cycle covering the whole slab in 50 minutes. As a result the 2 cycles of curing for slab 5 were also completed in 50 minutes. The total microwave energy for both slabs was the same at 1700 watts over 50 minutes and, therefore, the temperature increase under microwave heating should be similar. However, slab S5 shows a temperature increase of 16.6 °C and slab S6 (Figure 9.26) shows a temperature increase of 12.6 °C (Table 9.3). The internal temperature peaked at 52.5 °C for slab S5 and nearly 47 °C for slab S6. This indicates that microwave curing of the concrete slab with two cycles provided a 32 % higher surface temperature than curing with one cycle over a constant period.

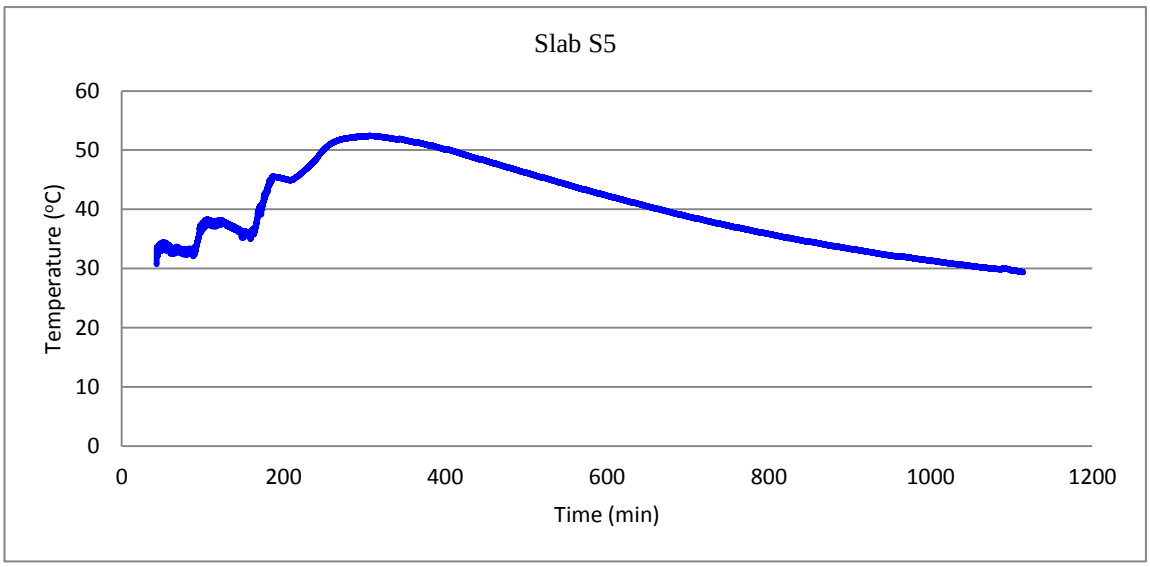

Figure 9.25: Thermocouple readings for a period of approximately 1100 minutes after the start of mixing the concrete

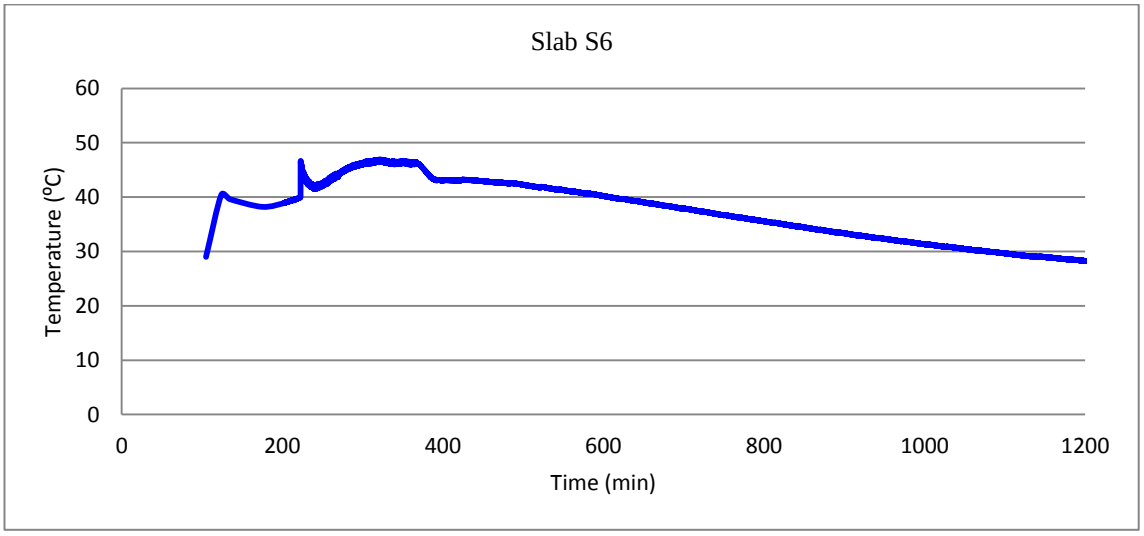

Figure 9.26: Thermocouple readings for a period of approximately 1260 minutes after the start of mixing the concrete.

9.5.8 Temperature development of slab cast over concrete substrate

Figure 9.27 shows the internal temperature of fresh concrete applied on top of hardened concrete substrate. Thermocouples were located at the base of the hardened concrete slab and at the top of the hardened concrete slab (base of the fresh concrete). The results show that the temperature at the base of the 58 mm deep freshly applied repair slab started increasing immediately on the application of microwave curing and reached its

maximum at the end of microwave curing. However, the temperature at the base of the 58 mm deep substrate (thermocouple located at the base of the substrate) started increasing gradually after the end of microwave curing. The temperature of the substrate increased due to convection of heat from its top surface rather than due to direct microwave heat reaching the bottom of the lower slab. This indicates that the temperature of the substrate at the interface starts increasing with the application of microwave curing which reduces the temperature differential at the interface. The wetting (and saturation) of the interface before the application of repair and with the mix water will also enable microwave heat penetration at the interface. These effects reduce the risk of cracking (cold joint) and bond failure at the interface. The effect of repair patch depth on reducing this temperature differential requires further investigations.

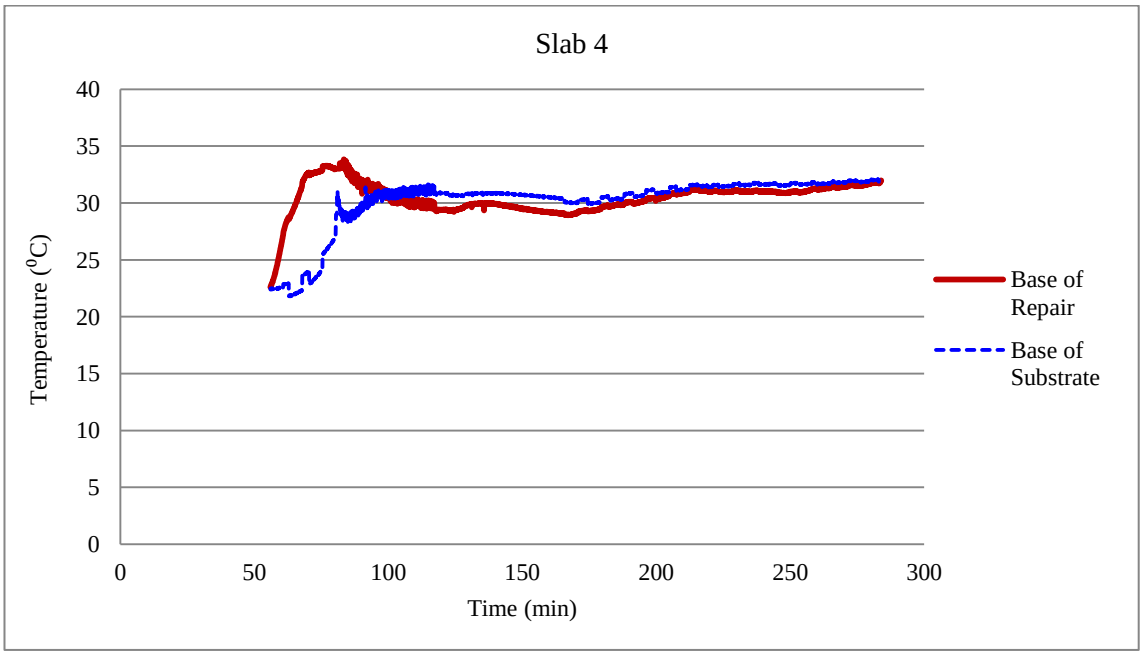

Figure 9.27: Thermocouple readings for a period of 284 minutes after the start of mixing the concrete.

9.6 Validation of results

Relationships of microwave curing temperature with power, time and volume of material have been derived based on laboratory test results in Chapter 4. A general relationship between these parameters and the temperature rise ΔT under microwave curing is shown in Equation 9.3. Figure 9.28 shows the application of this equation to laboratory test data (Chapter 4)

$$\Delta T = \frac{Pt}{\sqrt{V}} \qquad (9.3)$$

where ΔT is the temperature rise due to microwave curing ($^{\circ}$C); P is the microwave power (W); t is the duration of microwave curing (s) and V is the volume of the repair material (dm^3).

In the case of field trials, the microwave prototype cannot cure the whole surface of the slab under a single fixed position of the antenna. Therefore, the surface of the slab is divided into 20 strip areas (Figure 9.13). Each strip is exposed to a fixed microwave power and time. For example, for slab S10, each strip was exposed to microwave power of 1700 Watts for 2.5 minutes. Therefore, the total time taken to cover the whole surface of the slab was 50 minutes (2.5 minutes x 20 strips). However, the effective curing time for each strip is 2.5 minutes plus the heating time due to overlap of the antenna position as shown in Figure 9.13. As a result of the overlap, the effective curing time for each strip is greater than 2.5 minutes. It is calculated from equation 9.3 by substituting the values of ΔT, P and $\sqrt{V}$ for each trial slab S1 to S10.

Table 9.4 shows these calculated effective curing times of a strip based on Equation 9.3.

Slabs S5 to S10, in Table 9.4 were microwave cured at power 1700 W for 2.5 minutes over each strip. The depth of these slabs was similar at between 58 and 64 mm. Slabs S5 to S9 have an effective curing time per strip of 9.7, 6.5, 11.7, 10 and 8.9 (average 9.4) minutes and they can be reasonably assumed to validate the application of Equation 9.3 to the field data. In the case of slab S10, the temperature rise is due to a combination of microwave energy and the rapid setting chemistry of the repair material which achieved 48.0 ºC at the end of microwave curing compared with 40.4-44.5 for the materials (except S3) Table 9.3. This increases the effective curing time to 15.2 minutes.

Slabs S1-S4, in Table 9.4, were microwave cured at power 1500 W for 5 minutes over each strip. The depth of the slabs ranged between 34 mm for slab S3 and 46-80 mm for S1, S2 and S4. The effective curing time of slab S3 is high (25.3 minutes) compared to the other three slabs whose effective curing time is 11.6, 15.5 and 14.9 minutes.

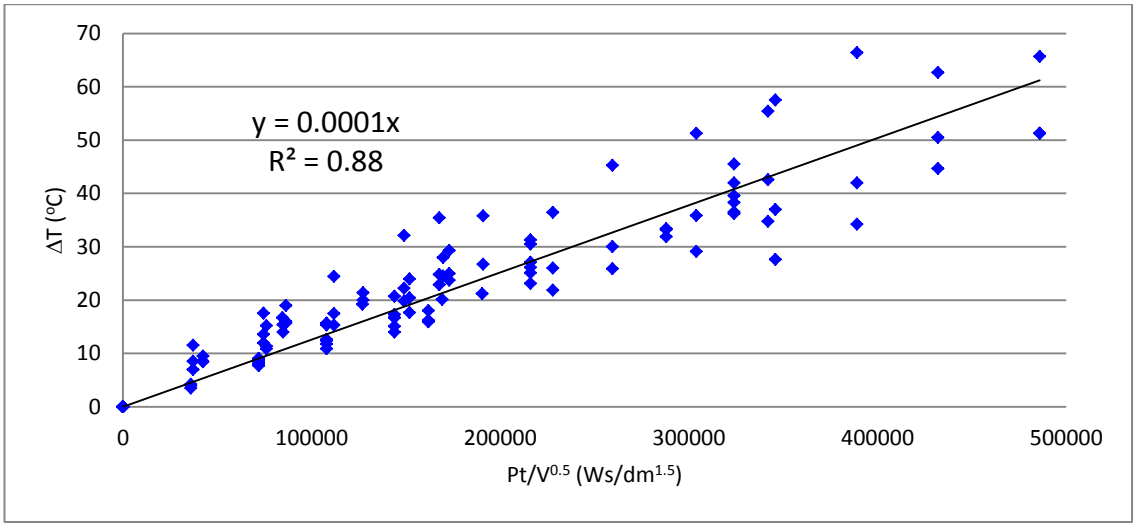

Figure 9.28: Relationship between microwave curing parameters and curing temperature ΔT of repair materials (Monomix, Monopour PC6 and Five Star).

Table 9.4: Calculation of effective curing time of a strip of slab

Slab Number	Material	Number of Curing Cycles	Actual Time of Curing (mins)	Effective Curing Time (mins)	ΔT (˚C)	Power (Watts)	Slab Depth (mm)	Volume (dm^3)
S 1	Concrete	1	5	11.6	16.4	1500	62	62
S 2	Concrete	1	5	15.5	20.2	1500	80	80
S 3	Concrete	1	5	25.3	49.2	1500	34	34
S 4	Concrete	1	5	14.9	24.9	1500	46	46
S 5	Concrete	2	2.5	9.7	16.6	1700	58	58
S 6	Concrete	1	2.5	6.5	12.6	1700	58	58
S 7	Sika Monotop 412 DE	1	2.5	11.7	19.1	1700	62	62
S 8	Sika Monotop 613 DE	1	2.5	10.0	16.6	1700	59	59
S 9	Stocrete TG 204	1	2.5	8.9	14.6	1700	61	61
S 10	Stocrete GMP	1	2.5	15.2	24.4	1700	64	64

9.7 Conclusions

The following conclusions can be made from the results of the field tests:

- The microwave curing parameters investigated in the laboratory investigation, which were incorporated in the design of the microwave prototype system, provided a satisfactory performance of the system. It validates the design equation ($\Delta T = \frac{Pt}{\sqrt{V}}$ (Equation 4.4)) derived in Chapter 4. The control system operated satisfactory on the FTRP algorithm and the PDI algorithm. However, further investigation is needed due to the time limit of the project.
- The moisture sensor which measures the reflected microwaves from the slab surface provides accurate measurement of moisture in the fresh concrete. The relationship between the actual moisture content and the sensor value is linear with a coefficient of correlation of 0.84.
- Microwave curing a concrete slab with two cycles provided a 32% higher temperature compared to one cycle over a constant time period.
- Test results on the scaled up slabs of repair materials validated the general relationship between the curing temperature ΔT and microwave curing parameters of power, time and volume, which was developed from laboratory tests.
- Microwave prototype operated successfully and safely. It provided accelerated curing of slabs. The slabs were free from plastic shrinkage cracking.

Chapter 10

10. Conclusions and Recommendations for future Work

10.1 General Conclusions

This research project investigated the effect of microwave curing on the properties of fresh and hardened concrete repair. The study shows that microwave energy can be used successfully to accelerate curing of concrete repair especially in cold weather. It also confirms the suitability of microwave curing for steel reinforced concrete repair which is commonly applied in construction practice. A summary of the conclusions and further research requirements are given in this chapter.

10.1.1 Microwave curing parameters of in-situ concrete repair

- Microwave curing is suitable for normal, non-rapid setting repair materials, avoiding excessively high temperatures.
- Considerable variation of temperature occurs on the surface of microwave cured cubes. The hot areas are at the edges of the mould, sometimes showing melting of the polystyrene mould. Elements with larger surface areas have more uniform temperature.
- Variation of temperature on the surface of microwave cured specimens should be taken into account in the cumulative total temperature of the microwave cured material when selecting the permissible microwave curing temperature.
- The following equations provide the limits for the permissible microwave curing temperature:

$$\boldsymbol{T_m + \Delta T_h \leq \frac{70}{\gamma_T}}$$

$$\boldsymbol{\Delta T_h = T_h - T_m}$$

where T_m is the permissible temperature at the end of microwave curing (^oC); T_h is the peak heat of hydration temperature ($T_h = T_m + \Delta T_h$) (^oC); ΔT_h is the increase in temperature after the end of microwave curing due to heat of hydration; γ_T is the factor of safety accounting for microwave curing temperature variations (hot spots).

- The temperature during microwave curing increases linearly with time and power input under the recommended limits of microwave curing temperature which is obtained from the above equation.
- The rate of temperature increase with microwave curing time (slope α=dT/dt) increases linearly with the applied power under the recommended limits of curing temperature (40-45 °C). The rapid setting materials are an exception unless the curing temperature T_m remains below the curing temperature limit.
- An empirical relationship between microwave power and the parameter *t*, *V* and temperature is proposed based on the experimental results as follows:

$$\Delta T = \frac{Pt}{\sqrt{V}} \qquad (4.4)$$

Where ΔT is the temperature rise due to microwave curing (°C); *P* is the microwave power (W); *t* is the microwave curing time (s); *V* is the volume of the repair material (dm^3).

- Fixed Time Power Regulating (FTPR) algorithm of microwave control system is developed to regulate power in order to achieve the target microwave curing

temperature in a fixed time period. The interval power input is given by the following equations:

$$P_1 = \left(\frac{T_1 - T_i}{t_1 - t_i}\right)\left(\frac{t_i P_i}{T_i - T_a}\right)$$

$$P_2 = \left(\frac{T_2 - T_1}{t_2 - t_1}\right)\left(\frac{t_i P_i}{T_i - T_a}\right)$$

$$P_3 = \left(\frac{T_t - T_2}{t_t - t_2}\right)\left(\frac{t_i P_i}{T_i - T_a}\right)$$

10.1.2 Temperature development of microwave cured repair materials

- Different durations of microwave curing at a constant power of 60 W are required for different repair materials to reach a common target temperature of curing (40-45 °C).
- Microwave curing accelerates the heat of hydration reactions and brings forward the time to reach the peak hydration temperature. For example, microwave cured HB40 repair material achieves a peak hydration temperature (combination of microwave heating and heat of hydration) of 71.1 °C at 60 minutes. The corresponding values are 34.0 °C at 600 minutes for normally cured HB40 repair material.
- Microwave curing of repair materials results in higher water loss than the normally cured specimens. For example, CEM II shows a water loss of 2.44 % at the end of 50 minutes microwave curing relative to 0.44 % under normal curing.

10.1.3 Pore structure of microwave cured repair materials

- Microwave curing increases the porosity of the bulk matrix and ITZ relative to normal curing under ambient conditions. For example, HB40 shows a porosity of 28.49 and 27.85 % in the bulk and ITZ respectively under normal curing. The

corresponding porosity increased to 33.74 % in the bulk and 35.05 % in the ITZ under microwave curing.

- Microwave curing reduces the intruded pore volume of small (gel) pores (<50 nm) of repair mortars relative to normal curing.
- Early age wet curing (after microwave curing) and prevention of moisture loss during microwave curing are the dominant factors for producing low porosity repairs.

10.1.4 Bond between microwave cured repair and concrete substrate

10.1.4.1 *Repair applied at ambient temperature 20, 10 and 2 °C*

- Microwave curing of the fresh repair has no negative effect on the repair/substrate interfacial bond strength at 28 days age.
- The bond strengths of repairs are similar and ranged from 1.9 to 2.45 MPa for three proprietary repair materials. The corresponding bond strength for CEM II is 1.4 to 1.9 MPa.
- The compressive strengths of the repair materials bear no relationship with their bond strengths with the substrate. The bond strength of the normally and microwave cured repair materials Five Star, Monomix and Monopour PC6 are between 1.9 and 2.75 MPa for the wide range of compressive strength (21-67 MPa).
- Microwave curing to about 40 °C reduces the 28 days compressive strength relative to the normally cured repair materials by an average of 6.75%.

10.1.4.2 *Repair applied at ambient temperature -5 °C*

- A short period of microwave curing of the fresh repair followed by 24 hours sub-zero temperature exposure provides significantly higher bond strength at 28

days compared to control samples exposed to curing at -5 ^{o}C for 24 hours after casting followed by 27 days curing at 20 ^{o}C in water.

- Microwave cured commercial Repair Materials Five Star, Monopour PC6 and CEM II perform particularly well under freezing conditions. The bond strengths of microwave cured repairs compare favourably with the "excellent" classification given to bond exceeding 2.1 MPa [184].
- Repair materials applied and cured at a "repair temperature of -5 ^{o}C for 24 hours followed by normal curing (20 ^{o}C, 60% RH) for 27 days suffer frost attack which results in bond strengths below 1.15 MPa.
- Microwave curing provides higher 28 days compressive strength than normal curing for repairs "applied" at -5 ^{o}C.
- The compressive strengths of the repair materials bear no relationship with their tensile bond strength with the substrate. The bond strengths of the microwave cured materials are between 1.95-2.45 MPa for the compressive strength range of (32-50) MPa. The corresponding bond strengths of normally cured materials are 0.7-1.15 MPa against a compressive strength range of 21.5-34 MPa.

10.1.5 Bond of steel reinforcement with microwave cured concrete repair mortars

- The presence of steel reinforcement in repair mortar does not cause any arcing during microwave curing.
- Microwave curing reduces the bond strength between repair mortars and plain steel reinforcement by 10 to 40%.
- The change in a rate of temperature rise during microwave curing has no effect on the bond strength for HB40 repair material.

- Microwave curing reduces the drying shrinkage for all four repair materials used in the research. The reduction ranges from 7 % (CEM II) to 32 % (HB40). The reduction in shrinkage corresponds to the reduction in gel pore volume.
- The bond strength of steel reinforcement has a unique relationship with the matrix compressive strength and porosity under both normal and microwave curing. Therefore, bond-compressive strength relationships used in design of reinforced concrete structures will be valid for microwave cured elements.
- Relationship between bond strength f_b and compressive strength f_c is of the form:

  $$f_b=0.55f_c^{0.81}$$

- Relationship between bond strength f_b and porosity p is of the form:

  $$f_b=13.81V_s^{2.58}$$

  where $V_s=(1-p)$.

10.1.6 Microwave system for situ curing of concrete repair

- The microwave curing parameters investigated in the laboratory investigation, which were incorporated in the design of the microwave prototype system, provided a satisfactory performance of the system. It validates the design equation ($\Delta T= \frac{Pt}{\sqrt{V}}$ (Equation 4.4)) derived in Chapter 4. The control system operated satisfactory on the FTRP algorithm and the PDI algorithm. However, further investigation is needed due to the time limit of the project.
- The moisture sensor which measures the reflected microwaves from the slab surface provides accurate measurement of moisture in the fresh concrete. The relationship between the actual moisture content and the sensor value is linear with a coefficient of correlation of 0.84.

- Microwave curing a concrete slab with two cycles provided a 32% higher temperature compared to one cycle over a constant time period.
- Test results on the scaled up slabs of repair materials validated the general relationship between the curing temperature ΔT and microwave curing parameters of power, time and volume, which was developed from laboratory tests.
- Microwave prototype operated successfully and safely. It provided accelerated curing of slabs. The slabs were free from plastic shrinkage cracking.

10.2 Originality and key findings for the research

The work presented in this thesis has introduced a novel technology to accelerate curing of concrete repair by using microwave energy. It has been the first time that the application of microwave energy has been investigated to cure concrete repair and has covered large subject area. The thesis provides new knowledge to microwave curing repair materials especially in cold weather where concreting is not allowed due to the risk of frost damage. It has developed basic relationships between the key properties of concrete repair and the parameters of microwave energy for curing. The project further determined the effect of microwave curing on the properties of repair such as internal temperature development, pore structure of microwave cured repair materials, the bond between substrate and repair and the bond between steel bar and microwave cured repair. The research has been conducted with microwave curing applied at ambient temperatures ranging between 20 °C and -5 °C. The thesis also provides the results from field trials conducted using the prototype microwave system which was developed in this project.

The manufacturers of cement based repair materials will benefit from this research by modifying their products to include additional specifications which satisfy microwave curing. In addition, it will benefit engineers to further develop the prototype and accelerate the commercialisation of the microwave system.

10.3 Recommendation for further research

The following areas have been identified for further research from this study:

- Long-term performance and stability of repair after a number of years need to be investigated.
- Computer modelling of microwave curing applied to different geometrical surfaces and different surface area to thickness ratios of the concrete repair by the use of finite element analysis (FEA).
- Investigate different methods to prevent moisture loss during microwave curing. Methods such as covering concrete repair with plastic sheet, sealing, internal moist curing and membrane-forming curing compounds can be investigated.
- Effect of microwave curing in cold weather needs to be investigated.

11. References

[1] P. H.Emmons, Concrete repair and maintenance illustrated, R.S. Means Company, Inc, 2002.

[2] M. Raupach, T. Büttner, Concrete repair to EN 1504, Diagnosis, Design, Principles and Practice, CRC Press, 2014.

[3] BENTZ, D.P. and STUTZMAN, P.E, "Curing, Hydration, and Microstructure of Cement Paste," *ACI Materials Journal,* pp. 348-356, 2006.

[4] "Cold Weather Concreting (ACI 306R) reported by ACI Committe 306-American," [Online].

[5] Kyung-Taek Koh, Chun-Jin Park, Gum-Sung Ryu, Jung-Jun Park, Do-Gyeum Kim, Jang-Hwa Lee, "An experimental investigation on minimum compressive strength of early age concrete to prevent frost damage for nuclear power plant structures in cold climates," *Nuclear Engineering and Technology*, vol. 45, no. 3, pp. 393-400, June 2013.

[6] "ASTM C150 Standard specification for Portland Cement," 2016.

[7] A. M. Neville, Properties of Concrete, Essex: Pearson Education Limited, 2011.

[8] L.Ming-Ju, L. Ming-Gin, W.Yung-Chin, H,Yishuo, W. Wei-Chein, "Study of steam and microwave curing of concrete containing slag, fly ash, or silica fume," *Journal of Testing and Evaluation,* vol. 43, no. 2, pp. 248-254, March 2015.

[9] Christopher K.Y, Leung, P. Thanakorn, "Determination of optimal process for microwave curing of concrete," *Cement and Concrete Research,* vol. 27, no. 3, pp. 463-472, 1997.

[10] B. T. Raupach. M, Concrete repair to EN 1504, Diagnosis, Design, Principles and Practice, CRC Press, 2014.

[11] W. G. Smoak, Guide to Concrete Repair, The Minerva Group,Inc, 2002.

[12] K. Grigoriadis, "Evaluation of concrete Patch Repairs," City University London, London, 2005.

[13] Bentz. D. P, Stutzman. P. E, "Curing, Hydration, and Microstructure of Cement Paste," *ACI Materials Journal,* vol. 103, no. 5, pp. 348-356, 2006.

[14] Whiting. NM, Snyder MB, "Effectiveness of Portland cement concrete curing compounds," *Transport Rec* , pp. 59-68, 2003.

[15] “Department for Transport, Specification for the reinstatement of openings in roads, Section 7. Third Eddition (Scotland),” January 2015.

[16] “Manual of Contract Documents for Highway Works. 2006. Volume 1: Specification for Highway Works, Series 1000: Road Pavements-Concrete Materials. Highways England.,” 2006.

[17] “Design Manual for Roads and Bridges: Volume 3, Highway structures: Inspection and Maintenance, Section 2, part 2, BD 27/86 Materials for the repair of concrte highway structures not applicable for use in Scotland”.

[18] J. W. J. Richard. R. Merritt, “Steam curing of portland cement concrete at atmospheric pressure,” Washington, D.C., 1962.

[19] William P. Odom, Hal Deatherage, “Steam cured concrete: varying the rate of temperature rise,” 1991.

[20] M. Shetty, Concrete Technology Therory and Practice, S. CHAND & COMPANY LTD., 2005.

[21] VicRoads, “Curing of concrete Technical Bulletin No 42,” Vic Roads, June 200.

[22] Ajay Goel, Jyoti Narwal, Vivek Verma, Devender Sharma, Bhuinder Singh, “A Comparative Study on the Effect of Curing on The Strengh Of Concrete,” *International Journal of Engineering and Advanced Technology (IJEAT),* vol. 2, no. 6, pp. 4001-406, August 2013.

[23] H. Kukko, “Use of heated fresh concrete,” in *Proceeding 3rd International Rilem Symposium on Winter Concreteing*, Espoo, Finland, 1985.

[24] J. Jonasson., “Early strength growth in concrete- preliminary test results concerning hardening at elevated temperature,” *3rd International Rilem Symposium on Winter concreting*, pp. 249-254, November 1985.

[25] A. D. Ross, “Some tests of electro-cured concrete,” pp. 282-284, 1954.

[26] Zuquan. Tang, Zhuoqiu. Li, Jueshi. Qian, Kejin. Wang, “Experimental study on deicing perfomrance of carbon fibre reinforced conductive concrete,” *Materials Science and Technology,* vol. 21, no. 1, pp. 113-117, 2005.

[27] Min Chen, Peiwei Gao, Fei Geng, Lifang Zhang, Hongwei Liu, “Mechanical and smart properties of carbon fiber and graphite conductive concrete for internal damage monitoring of structure,” *Construction and Building Materials,* vol. 142, pp. 320-327, 2017.

[28] E. M. Pajooh, “Snow and ice removal by smart parkinsg system using conductive concrete,” *International Journal of Advanced Technology in Civil Engineering,* vol. 1, no. 3, pp. 13-15, 2012.

[29] Peyman Maleki, Behnam Iranpour, Gholamali Shafabakhsh, “Investigation of de-icing of roads with conductive concrete pavement containing carbon fibre-reinforced polymer (CFRP),” *International Journal of Pavement Engineering,* pp. 1-9, 2017.

[30] Ernie Heymsfield, Adam Osweiler, Panneer Selvam, Mark Kuss, “Developing Anti-Icing Airfield Runways Using Conductive Concrete with Renewable Energy,” *Journal of Cold Regions Engineering* , vol. 28, no. 2, 2014.

[31] P. S. Mangat, G. Catley, “Low Voltage Accelerated Curing System for future Precast Concrete,” in *BIBM International Congress CONGRESS, International Bureau for Precast Concrete,* 2005.

[32] M. Leivo, “Radio wave heater for concrete,” *Cment and concrete research,* pp. 677-682, 1996.

[33] “BS EN 934-2:2009 Admixtures for concrete, mortar and grout Part 2: Concrete admixtures- Definitions, requirements, conformity, marking and labelling,” 2009. [Online].

[34] Fatma Karagöl, Ramazan Demirboğa, Mehmet Akif Kaygusuz, Mehrzad Mohabbi Yadollahi, Rıza Polat, “The influence of calcium nitrate as antifreeze admixture on the compressive strength of concrete exposed to low temperatures,” *Cold Region Science and Technology,* vol. 89, pp. 30-35, 2013.

[35] S. S. Wadhwa , L. K. Srivastava , D. K. Gautam & D. Chandra, “Direct electric curing of in situ concrete,” *Batiment International, Building Research and Practice,* pp. 97-101, 1987.

[36] C. J. Korhonen, “Antifreeze admixtures for cold region concreting: A litrature review,” U.S. Army Corps of Engineerng: Cold Regin Research & Engineering Laboratory, 1990.

[37] S. A. Mironov, V.D. Demidov, “Chohesion of new concrete with old under winter conditions.,” *Hydrotechnical Construction* , vol. 1, pp. 16-18, 1978.

[38] S. L. Matthews, J. R. Morlidge, “Performance based rehabilitation of reinforced concrete structures,” in *Concrete Repair, Rehabilitation and Retrofitting II – Alexander et al (eds),* London, 2009.

[39] Mladena Luković, Guang Ye, Klaas van Breugel, “Reliable concrete repair: a critical review,” in *International Conference Structural Fault and Repair,* 2012.

[40] BS EN 1504-10, “Products and systems for the production and repair of concrete structures definitions requirements qulaity control and evaluation of conformity,” 2003. [Online].

[41] L. Czarnecki, “Adhesion – A challenge for concrete repair,” in *Concrete Repair,*

Rehabilitation and Retrofitting II, 2009.

[42] "BS EN 1504-3:2005 Products and systems for the protection and repair of concrte structures-Definiations, requirments, quality control and evaluation fo concformity- Part 3: Structural and non-structural repair," 2005.

[43] Y. Pan, "Bond strength of concrete patch repairs: An evaluation of test methods and the influence of workmanship and environment," Loughborough University of Technology, 1995.

[44] R. V. Decareau, Microwaves in the food processing industry, London: Academic Press, INC, 1985.

[45] A. C. Metaxas, R. J. Meredith, Industrial microwave heating, 1983.

[46] H. Zhang, A.K. Datta, "Microwave Power Absorption in Single - and Multiple - Item Foods," *Food and Bioproducts Processing,* vol. 81, no. 3, pp. 257-265, 2003.

[47] M. R. Hossan, D.Y. Byun, P. Dutta, "Analysis of microwave heating for cylindrical shaped objects," *International Journal of Heat and Mas Transfer,* vol. 53, pp. 5129-5138, 2010.

[48] Narendra G. Patil, Evgeny V. Rebrov, Kari Eränen, Faysal Benaskar, Jan Meuldijk, Jyri-Pekka Mikkola, Volker Hessel, Lumbertus A. Hulshof, Dmitry Yu. Murzin, Jaap C. Schouten, "Effect of the load size on the efficiency of microwave heating under stop flow and continuous flow conditions," *Journal of Microwave Power and Electromagnetic Energy,* vol. 46, no. 2, pp. 83-92, 2012.

[49] J.L. Pedreño-Molina, J. Monzó-Cabrera, M. Pinzolas, "A new procedure for power efficiency optimization in microwave ovens based on thermographic measurments and load location search," *International Communications in Heat and Mass Transfer,* vol. 34, no. 5, pp. 564-569, 2007.

[50] K.G. Ayappa, H.T. Davis, G. Crapiste, E.A. Davis, J. Gordon, , "Microwave heating: an evaluation of power formulations," *Chemical Engineering Science,* vol. 46, no. 4, p. 1005–1016., 1991.

[51] H. Zhang, A. K. Datta, "Coupled electromagnetic and thermal modeling of microwave oven heating of foods," *Journal of Micorwave Power and electromagnetic Energy,* 2000.

[52] C. Persch, H. Schubert, "Characterisation of household microwave ovens by their efficiency and quality parameters," in *The 5th International Conference on Microwave and High Frequency Heating*, Cambridge University, uk, 1995.

[53] Ashim K. Data, Ramaswamy C. Anantheswaran, Handbook of micorwave technology for food applications, 2001.

[54] R. Vadivambal, D. S. Jayas, “Non-uniform temperature distribution during microwave heating of food materials - a review,” *Food Bioprocess Technol,* vol. 3, pp. 161-171, 2010.

[55] C. P. Teo, K. C. G. Ong, C. H. Shun, S. T. Tan, “Accelerated heating of precast ferrocement secondary roofing slabs using microwave energy,” in *Our World in Concrete & Structures*, Singapore, 2002.

[56] S.S.R. Geedipalli, V. Rakesh, A.K. Datta, “Modeling the heating uniformity contributed by a rotating turntable in microwave ovens,” *Journal of Food Engineering,* vol. 82, no. 3, pp. 359-368, 2007.

[57] C. R. Buffler, Microwave cooking and processing: Engineering Fundamentals for the Food Scientist, New York: Springer US, 1993.

[58] Sihai. Wen, D. D.L. Chung, “Effect of admixtures on the dielctric constant of cement paste,” *Cement and Concrete Research,* vol. 31, pp. 637-677, 2001.

[59] “BS 3999: Part 15 British Standard Method of meeasuring the performance of household electrical applicances. Part 15. Micorwave cooking appliancesmicorwave ovens for household and similar purposes,” 1983.

[60] “BS EN 60705:2015. Household mcirowave ovens. Methods for measuring performance.”.

[61] R. E. Mudget, “Microwave properties and heating characteristics of foods,” *Food Tehnol,* vol. 40, 1989.

[62] S.J. Maa, X.W. Zhoub, X.J. Sua, W. Moa, J.L. Yanga, P. Liua, “A new practical method to determine the microwave energy absorption ability of materials,” *Minerals Engineering,* vol. 22, no. 13, pp. 1154-1159, 2009.

[63] “Flexcrete,” [Online]. Available: http://flexcrete.com/. [Accessed 14 March 2016].

[64] “Webber,” [Online]. Available: http://www.netweber.co.uk/home.html. [Accessed 14 March 2016].

[65] “BS EN 197-1: Cement- Part 1: Composition, specification and conformity criteria for common cements,” *2011.*

[66] “BS EN 933-2;1996 Tests for geometrical properties of aggregated- Part 2: Determination of particle size distribtuion- Test sieves, nominal size of apertures,” 1996.

[67] “ASTM F1317-98 Standard Test Method for Calibration of Microwave Ovens, ASTM, USA,” Reaproved 2012.

[68] A. Waston, “Curing of concrete,” *Microwave Power Engineering,* vol. Volume 2, pp. 108-110, 1968.

[69] Wu Xuequan, Dong Jianbgo, Tang Mingshu, “Microwave curing technique in concrete manufacure,” *Cement and Concrete Research,* vol. 17, no. 2, pp. 205-210, 1987.

[70] R. G. Hutchinson, J.T. Chang, H. M. Jennings and M. E Brodwin, “Thermal acceleration of Portland Cement mortars with microwave energy,” *Cement and Concrete Research,* vol. 21, pp. 795-799, 1991.

[71] C. K. Y. Leung and T. Pheeraphan, “Microwave curing of Portland cement concrete: experimental results and feasibility for practical applications,” *Construction and Building Materials,* vol. 9, no. 2, pp. 67-73, 1995.

[72] D. Sohn, D. L. Johnson, “Microwave curing effects on the 28-day strength of cementitious materials,” *Cement and Concrete Research,* vol. 29, no. 2, pp. 241-247, 1999.

[73] Ming-Gin Lee, Yishuo Huang, Yu-Cheng Kan, “The strength and rapid chloride permeability of microwave cured concrete,” *International Journal of Applied Science and Engineering,* vol. 5, no. 1, pp. 53-63, 2007.

[74] K. C. Gary Ong, Ali. Akbarnezhad, Microwave-Assisted concrete technlology Production, Demolotion and Recycling, London: Taylor & Francis Group, 2015.

[75] Christopher K.Y. Leung, Thanakorn Pheeraphan, “Very high early strength of microwave cured concrete,” *Cement and Concrete Research,* vol. 25, no. 1, pp. 136-146, 1995.

[76] Phadungsak. Rattanadecho, Nattawut. Suwannapuma, Burachat. Chatveera, Duangduan. Atong, Narongsak. Makul, “Development of compressive strength of cement paste under accelerated curing by using a continuous microwave thermal processor,” *Materials Science and Engineering A,* vol. 472, p. 299–307, 2008.

[77] Jeevaka Somaratna, Deepak Ravikumar, Narayanan Neithalath, “Response of alkali activated fly ash mortars to microwave curing,” *Cement and Concrete Research,* vol. 40, pp. 1688-1696, 2010.

[78] Thanakorn Pheeraphan, Christopher K.Y. Leung , “Freeze-Thaw durability of microwave cured air-entrained concrete,” *Cement and Concrete Research,* vol. 27, no. 3, pp. 427-435, 1997.

[79] Li Dongxu, Wu Xuequan , “A study on the application of vacuum microwave composite dewatering technique in concrete engineering,” *Cement and Concrete Research,* vol. 24, pp. 159-164, 1994.

[80] Natt Makul, Phadungsak Rattanadecho, Dinesh K. Agrawal, “Microwave curing at an operating frequency of 2.45 GHz of Portland cement paste at early-stage

using a multi-mode cavity: Experimental and numerical analysis on heat transfer characteristics," *International Communications in Heat and Mass Transfer,* vol. 37, pp. 1487-1495, 2010.

[81] Zainab Hashim Abbasb, Hassen Shaker Majdi, "Study of heat of hydration of Portland cement used in Iraq," *Case Studies in Construction Materials,* vol. 7, pp. 154-162, 2017.

[82] Natt Makul, Phadungsak Rattanadecho, Amphol Pichaicherd b, "Accelerated microwave curing of concrete: A design and performance related experiments," *Cement and Concrete Composite,* vol. 83, pp. 415-426, 2017.

[83] N. Makul, D.K. Agrawal, "Influences of microwave-accelerated curing procedures on the microstructure and strength characteristics of type 1 Portland cement paste," *Journal of Ceramic Processing Research,* vol. 12, no. 4, pp. 376-381, 2011.

[84] Thanakorn Pheeraphan, Lilik Cayliani, Mario I. Dumangas Jr, Pichai Nimityongskul, "Prediction of later-age compressive strength of normal concrete based on the accelerated strength of concrete cured with microwave energy," *Cement and Concrete Research,* vol. 32, no. 4, pp. 521-527, 2002.

[85] M. G. Lee, "Preliminary study for strength and freeze-thaw durability of microwave and steam-cured concrete," *Journal of Materials in Civil Engineering,* vol. 19, no. 11, pp. 972-976, 2007.

[86] Natt Makul, Pornthip Keangin, Phadungsak Rattanadecho, Burachat Chatveera, Dinesh K. Agrawal, "Microwave-assisted heating of cementitious materials: Relative dielectric properties,mechanical property, and experimental and numerical heat transfer characteristics," *International Communications in Heat and Mass Transfer,* vol. 37, pp. 1096-1105, 2010.

[87] Ratthasak Prommas, Thaweesak Rungsakthaweekul, "Effect of microwave curing conditions on high strength concrete properties," *Energy Procedia,* vol. 56, pp. 26-34, 2014.

[88] Adam Buttress, Aled Jones, Sam Kingman, "Microwave processing of cement and concrete materials – towards an industrial reality?," *Cement and Concrete Research,* vol. 68, pp. 112-123, 2015.

[89] Baek-Joong. Kim, Chongku. Yi, Kyung-In. Kang, "Microwave curing of alkali-activated binder using hwangtoh without calcination," *Construction and Building Materials,* vol. 98, pp. 465-475, 2015.

[90] Yury Shamis, Alex Taube, Natasa Mitik-Dineva, Rodney Croft, Russell J. Crawford, Elena P. Ivanova, "Specific electromagnetic effects of micorwave radiation on escherichia coli," *Applied and Environmental Microbiology,* vol. 77, no. 9, pp. 3017-3023, 2011.

[91] A. M. Neville, J. J. Brooks, Concrete technology, London: 2nd, 2010.

[92] John Newman, Ban Seng Choo, Advanced concrete technology, Oxfore: Butterworth-Heinemann, 2003.

[93] J. Byfors, "Plain concrete at early ages Swedish Cement and Concrete Research Institute," 1980.

[94] Copeland. L.E, Kanto. D.L., "Chemistry of hydration of Portland cement at ordinary temperatures," *The Chemistry of cemtns,* vol. 1, pp. 313-370, 1972.

[95] Sidney Mindess, J. Francis Young, Concrete, Prentice-Hall International, Inc, London, 1981.

[96] W. Lerch, R.H. Bogue, "Heat of hydration of Portland cement pastes," *Bureau of Standards Journal of Research,* pp. 645-664, 1934.

[97] Jiong Hu, Zhi Ge, Kejin Wang, "Influence of cement fineness and water-to-cement ratio on mortar early-age heat of hydration and set times," *Construction and Building Materials,* vol. 50, pp. 657-663, 2014.

[98] S. Ahmad, "Effect of fineness of cement on properites of fresh and hardened concrete," in *Our World in Concrete & Structures*, Singapore, 2002.

[99] "RILEM Commission, 42-CEA, Properties of set concrete at early ages state-of-the- art- report," Material Construction, Dordrecht, 1981.

[100] Yunus Ballim, Peter C. Graham, "The effects of supplementary cementing materials in modifying the heat of hydration of concrete," *Materials and Structures,* vol. 42, no. 6, pp. 803-811, 2009.

[101] Maria Juenger, Moon Won, David Fowler, Chul Suh, Andre Edson, "Effects of supplementary cementing materials on the setting," 2008.

[102] Pailyn. Thongsanitgarn, Watcharapong. Wongkeo, Arnon. Chaipanich, Chi. Sun. Poon, "Heat of hydration of Portland high-calcium fly ash cement incorporating limestone powder: effect of limestone particle size," *Construction and Building Materials,* vol. 66, pp. 410-417, 2014.

[103] W. Nocuñ-Wczelik, "Heat evolution in hydrated cementitious systems admixtured with fly ash," *Journal of Thermal Analysis and Calorimetry,* pp. 613-619, 2001.

[104] R. D. Crow, E. R. Dunstan, "Properties of fly ash concrete. Effect of fly ash incorporation in cement and concrete," in *Proccedings of Sympusium Materials Research Society*, 1981.

[105] Mukesh Kumar, Sanjay K. Singh, N.P. Singh, "Heat evolution during the hydration of Portland cement in the presence of fly ash, calcium hydroxide and

super plasticizer," *Thermochimica Acta,* vol. 548, pp. 27-32, 2012.

[106] J Ivan Escalante-Garcia, J. H. Sharp, "The effect of temperature on the early hydration of portland cement and blended cements," *Advances in Cement Research,* vol. 12, no. 3, pp. 121-130, 2000.

[107] L. E. Copeland, D. L. Kantro, "Hydration of Portland cement," in *Proceedings of the 5th International Symposuim on the Chemistry of Cement*, Tokyo, Japan, 1968.

[108] Knut O. Kjellsen, Rachel J. Detwiler, "Reaction kinetics of portland cement mortars hydrated at different temperatures," *Cement and Concrete Research,* vol. 22, pp. 112- 120, 1992.

[109] H. F. W. Taylor, C. Famy, K. L. Scrivener, "Delayed ettringite formation," *Cement and Concrete Research,* vol. 31, no. 5, pp. 683-693, 2001.

[110] P. L. Ng, I. Y. T. Ng, A. K. H. Kwan, "Heat loss compensation in semi-adiabatic curing test of concrete," *ACI Materials Journal,* vol. 105, no. 1, pp. 52-61, 2008.

[111] RILEM, "Recommendations of TC 119-TCE: Avoidance of thermal cracking in concrete at early ages," *Materials and Structures,* vol. 30, no. 202, pp. 451-464, 1997.

[112] Methods of testing cement. Heat of hydration. Semi-adiabatic method, BS EN 196-9:2010.

[113] Hubert woods, Harold H. Steinour, Howard R. Starke, "Effect of composition of portland cement on heat evolved during hardening," *Industrial and Engineering Chemistry,* vol. 24, no. 11, pp. 1207-1214, 1932.

[114] Methods of testing cement. Heat of hydration. Solution method, BS EN 196-8:2010.

[115] ASTM C186-15a, "Standard test method for heat of hydration of hydraulic cement," 2015.

[116] Isothermal Conduction Calorimetry (ICC) for the determination of heat of hydration of cement: State of Art Report and Recommendations, PD CEN/TR 16632:2014.

[117] A. K. Schindler, K. J. Folliard, "Heat of hydration models for cementitious materials," *ACI Materials Journal,* vol. 102, no. 1, pp. 24-33, 2005.

[118] Attari Azadeh, McNally Ciaran, Richardson Mark G, "Numerical model for quantifying degree of hydration in concrete mixes with reduced CO2 footprint," in *Numerical Modeling Strategies for Sustainable Concrete Structures,* Aix-en-Provence, France, May 2015.

[119] L. E. Copeland, D. L. Kantro, George Verbeck, “Chemistry of hydration of Portland cement,” in *Proceedings of the Fonrth International Symposium Washington, D. C*, Washington, D. C, 1960.

[120] R. Springenschmid, Preventation of thermal cracking in concrete at early ages (RILEM Report), CRC Press, 1998.

[121] v. B. K, “Simulation of hydration and formation of structure in hardening cement based materials,” Delft University of Technology, Delft, Netherlands, 1991.

[122] B. J. H, “The chemistry of Portland cement,” *Reinhold Publishing corporation,* 1947.

[123] S.N. Kharkovsky, U.C. Hasar, C. D. Atis, S. Döver, “Electromagnetic properties of cement-based materials over time at microwave frequencies”.

[124] H. W. Yang, S. Gunaskearan, “Temperature profiles in a cylindrical model food during pulsed microwave heating,” *Journal of Food Science,* vol. 66, no. 7, pp. 998-1004, 2001.

[125] Laura A. Campañone, Carlos A. Paola, Rodolfo Horacio Mascheroni, “Modeling and simulation of microwave heating of foods under different process schedules,” *Food and Bioprocess Technology,* vol. 5, no. 2, pp. 738-749, 2012.

[126] G. Brodie, “The influence of load geometry on temperature distribution during microwave heating,” *Transactions of the ASABE (American Society of Agricultural and Biological Engineers),* vol. 51, no. 4, pp. 1401-1413, 2008.

[127] Jirina housova, Karel Hoke, “Temperature profiles in microwave heated solid foods of slab geometry: Influence of process parameters,” *Czech Journal of Food Sciences (CJFS),* vol. 19, no. 3, pp. 111-120.

[128] C.R. Cheeseman, S. Asavapisit, “Effect of calcium chloride on the hydration and leaching of lead-retarded cement,” *Cement and Concrete Research,* vol. 29, no. 6, pp. 885-892, 1999.

[129] J. Cheung, A. Jeknavorian, L. Roberts, D. Silva, “Impact of admixtures on the hydration kinetics of Portland cement,” *Cement and Concrete Research,* vol. 41, no. 12, pp. 1289-1309, 2011.

[130] J. Hill, B.R. Whittle, J.H. Sharp, M. Hayes, “Effect of elevated curing temperature on early hydration and microstructure of composites,” in *Proceedings of the Materials Research Society Symposium*, 2003.

[131] Byung Jae Lee, Jin Wook Bang, Kyung Joon Shin, Yun Yong Kim, “The effect of specimen size on the results of concrete adiabatic temperature rise test with commercially available equipment,” *Materials,* vol. 7, no. 12, pp. 7861-7874, 2014.

[132] Manal Al-Fadhala, Kenneth C. Hover, "Rapid evaporation from freshly cast concrete and the Gulf environment," *Construction and Building Materials,* vol. 15, no. 1, pp. 1-7, 2001.

[133] I. Odler and M. Robler, "Investigations on the relationship between porosity, structure and strength of hydrated portland cement pastes. II effect of pore structure and of degree of hydration," *Cement and Concrete Research,* vol. 15, pp. 401-410, 1985.

[134] Rakesh. Kumar, B. Bhattacharjee, "Porosity, pore size distribution and in situ strength of concrete," *Cement and Concrete Research,* vol. 33, pp. 155-164, 2003.

[135] Yudenfreund. M, Hanna. K M, Skalny. J, Odler. I, Brunauer. S, "Hardened portland cement pastes of low porosity part 5. Compressive strength," vol. 2, pp. 731-743, 1972.

[136] K. K. Aligizaki, Pore structure of cement-based materials: Testing, interpretation and requirements, Taylor & Francis, 2006.

[137] C. Andrade, P. Merino, X.R. Nóvoa, M.C. Pérez, L. Soler, "Passivation of Reinforcing Steel in Concrete," *Materials Science Forum,* Vols. 192-194, pp. 891-898, 1995.

[138] C. M. Hansson, "Comments on electrochemical measurements of the rate of corrosion of steel in concrete," *Cement and Concrete Research,* vol. 14, no. 4, pp. 574-584, 1984.

[139] S. Westermark, "Use of mercury porosimetry and nitrogen adsorption in characterisation of the pore structure of mannitol and microcrystalline cellulose powders, granules and tablets," Department of Pharmacy, Helsink, 2000.

[140] P. J. McDonald, V. Rodin, A. Valori, "Characterisation of intra- and inter-C–S–H gel pore water in white cement based on an analysis of NMR signal amplitudes as a function of water content," *Cement and Concrete Research,* vol. 40, no. 12, pp. 1656-1663, 2010.

[141] P. Kumar Mehta, Paulo J. M. Monteiro, Concrete microstructure, properties, and materials, 3rd ed., McGraw-Hill, 2005.

[142] E.J. Garboczi and D.P. Bentz , "The effect of statistical fluctuation, finite size error, and digital resolution on the phase percolation and transport properties of the NIST cement hydration model," *Cement and Concrete Research,* vol. 31, no. 10, pp. 1501-1514, 2001.

[143] D. P. Bentz, "Cement hydration: building bridges and dams at the microstructure level," *Materials and Structures,* vol. 40, pp. 397-404, 2007.

[144] Tiong Huan Wee, Yoshihisa Matsunaga, Ysohiharu Watanabe, Etsuo Sakai, "Production and properties of high strength concretes containing various mineral

admixtures," *Cement and Concrete Research,* vol. 25, no. 4, pp. 709-714, 1995.

[145] Z. Sawicz, S. S. Heng, "Durability of concrete with addition of limestone powder," *Magazine of Concrete Research,* vol. 48, no. 175, pp. 131-137, 1996.

[146] W. Zhongwei, "An approach to the recent trends of concrete science and technology," *Journal of Ceramic Society,* vol. 9, no. 1, pp. 262-267, 1979.

[147] Knut O. Kjellsen, Hamlin M. Jennings and Bjo Lagerblad, "Evidence of hollow shells in the microstructure of cement paste," *Cement and Concrete Research,,* pp. 593-599, 1996.

[148] K. Schiller, "Strength of porous materials," *Cement and Concrete Research,* vol. 1, no. 4, pp. 419-422, 1971.

[149] Xudong Chen, Shengxing Wu, Jikai Zhou, "Influence of porosity on compressive and tensile strength of cement mortar," *Construction and Building Materials,* vol. 40, pp. 869-874, 2013.

[150] Winslow. D. N and S. Diamond, "A mercury porosimetry study of the evolution of porosity in portland cement," vol. 5, pp. 564-585, 1970.

[151] H. Ma, "Mercury intrusion porosimetry in concrete technology: tips in measurement, pore structure parameter acquisition and application," *Journal of Porous Materials,* pp. 207-215, 2014.

[152] Y. Ma, J. Hu, G. Ye, "The pore structure and permeability of alkali activated fly ash," *Fuel,* vol. 104, pp. 771-780, 2013.

[153] A. B. Abell, K. L. Willis, & D. A. Lange, "Mercury intrusion porosimetry and image analysis of cement-based materials," *Journal of Colloid and Interface Science,* vol. 211, p. 39–44 , 1999.

[154] E. W. Washburn, "The dynamics of capillary flow," *The Physical Review,* p. 273–283, 1921.

[155] H. L. Ritter, L. C. Drake, "porosimeter and determination of complete macropore-size distributions. Pressure porosimeter and determination of complete macropore-size distributions," *Industrial and Engineering Chemistry,* vol. 17, no. 12, pp. 782-786, 1945.

[156] Dirch H. Bager, Erik J. Sellevold, "Mercury porosimetry of hardened cement paste: the influence of particle size," *Cement and Concrete Research,* vol. 5, no. 2, pp. 171-178, 1975.

[157] E. J. Sellevold, "Mercury porosimetry of hardened cement paste cured or stored at 97 °C," *Cement and Concrete Paste Research,* vol. 4, pp. 399-404, 1974.

[158] Seihi. Goto and Della M. Roy, "The effect of w/c ratio and curing temperature on the permeability of hardened cement paste," *Cement and Concrete Research,* vol. 11, pp. 575-579, 1981.

[159] T.C. Powers, T. L. Brownyard, "Studies of the physical properties of hardened Portland cement paste," *Journal of the American Concrete Institute,* vol. 22, no. 43, p. 101992, 1947.

[160] J. Khatib & P.S. Mangat, "Porosity of cement paste cured at 45 C as a function of location relative to casting position," *Cement and Concrete Composites,* pp. 97-108, 2003.

[161] R. Kumara, B. Bhattacharjee, "Assessment of permeation quality of concrete through mercury intrusion porosimetry," *Cement and Concrete Research,* pp. 231-328, 2004.

[162] S. Diamond, "Mercury porosimetry-an inappropriate method for measurement of pore size distributions in cement-based materials," *Cement and Concrete,* vol. 30, pp. 1517-1525, 2000.

[163] O. Knut, J. D. Rachel and E. G. Odd, "Pore structure of plain cement pastes hydrated at different temperatures," *Cement and Concrete Research,* vol. 20, pp. 927-933, 1990.

[164] J. M. Khatib, P.s. Mangat, "Influence of superplasticizer and curing on porosity and pore structure of cement paste," *Cement and Concrete Research,* vol. 21, pp. 431-437, 1999.

[165] P. Ballester, A. Hidalgo, I. Mármol, J. Morales, L. Sánchez, "Effect of brief heat-curing on microstructure and mechanical properties in fresh cement based mortars," *Cement and Concrete Research,* vol. 39, no. 7, pp. 573-579, 2009.

[166] M. Fall, J.C. Célestin, M. Pokharel, M. Touré, "A contribution to understanding the effects of curing temperature on the mechanical properties of mine cemented tailings backfill," *Engineering Geology,* vol. 114, pp. 397-413, 2010.

[167] "BS EN 60705:2012. Household microwave ovens. Methods for measuring performance.".

[168] "ASTM F1317-98 Standard Test Method for Calibration of Microwave Ovens, ASTM, USA," Reapproved 2012.

[169] V. Calderón, S. Gutiérrez-González, A. Rodriguez, M. Horgnies, "Study of the microstructure and pores distribution of lightweight mortar containing polymer waste aggregates," in *WIT Transactions on Engineering Sciences*, 2013.

[170] A. M. Alamri, "influence of curing on the properties of concretes and mortars in hot climates," The University of Leeds, 1988.

[171] Wu Xuequan, Dong Jianbgo, Tang Mingshu, "Microwave curing technique in concrete manufacture," *Cement and Concrete Research,* vol. 17, no. 2, pp. 205-210, 1987.

[172] Pei-ming. Wang, Xian-ping. Liu, "Effect of temperature on the hydration process and strength development in blends of Portland cement and activated coal gangue or fly ash," *Journal of Zhejiang University SCIENCE A,* vol. 12, no. 2, pp. 162-170, 2011.

[173] Lu Cui, Jong Herman Cahyadi, "Permeability and pore structure of OPC paste," *Cement and Concrete Research,* vol. 31, no. 2, pp. 277-282, 2001.

[174] Yaning Kong, Peiming Wang, Shuhua Liu, Zhiyang Gao, "Hydration and microstructure of cement-based materials under microwave curing," *Construction and Building Materials,* vol. 114, pp. 831-838, 2016.

[175] Abdurrahman A. Elgalhud, Ravindra K. Dhir, Gurmel Ghataora, "Limestone addition effects on concrete porosity," *Cement and Concrete Composites,* vol. 72, pp. 222-234, 2016.

[176] P. Ballester, A. Hidalgo, I. Mármol, J. Morales, L. Sánchez, "Effect of brief heat-curing on microstructure and mechanical properties in fresh cement based mortars," *Cement and Concrete Research,* vol. 39, no. 7, pp. 573-579, 2009.

[177] J. M. Khatib, P. S. Mangat, "Influence of superplasticizer and curing on porosity and pore structure of cement paste," *Cement and Concrete Research,* vol. 21, pp. 431-437, 1999.

[178] Knut O. Kjellsen, Rachel J. Detwiler, Odd E. Gjørv, "Pore structure of plain cement pastes hydrated at different temperatures," *Cement and Concrete Research,* vol. 20, pp. 927-933, 1990.

[179] Knut O. Kjellsen, Rachel J. Detwiler, Odd E. Gjørv, "Development of microstructure in plain cement pastes hydrated at different temperatures," *Cement and Concrete Research,* vol. 21, no. 1, pp. 179-189, 1991.

[180] A.T. Horne, I.G. Richardson, R.M.D. Brydson, "Quantitative analysis of the microstructure of interfaces in steel reinforced concrete," *Cement and Concrete Research,* vol. 37, no. 12, pp. 1613-1623, 2007.

[181] P. D, "Materials-what to specify?," *Construction maintenance & Repair,* vol. 5, no. 4, pp. 3-7, 1991.

[182] G Tilly, J Jacobs, "Concrete repairs: observations on performance in sevice and current practice, CON REP NET Project Report," IHS BRE Press, Watford, 2007.

[183] S. Matthews, "CONREPNET: Performance-based approach to the remediation of reinforced concrete structures: Achieving durable repaired concrete structures,"

Journal of Building Appraisal, vol. 3, no. 1, pp. 6-20, 2007.

[184] Michael M. Sprinkel, H. Celik Ozyildirim, "Evaluation of High Performance Concrete Overlays Placed on Route 60 Over Lynnhaven Inlet in Virginia," Virginia Transportation Research Council , Charlottesville, Virginia , 2000.

[185] "BS EN 12390-2:2009: Testing hardened concrete. Making and curing specimens for strength tests, British Standards Institute," 2009.

[186] "Design of normal concrete mixes," Building Research Establishment, Watford, 1998.

[187] "BS EN 12390-3:2009: Testing hardened concrete. Compressive strength of test specimens. British Standard Institute," 2009.

[188] "BS EN 12390-6:2009: Testing hardened concrete. Tensile splitting strength of test specimens, British Standard Institute," 2009.

[189] S. Nilsson, "The tensile strength of concrete determined by splitting tests on," *RILEM Bul,* vol. 11, pp. 63-67, 1961.

[190] Sergio Carmona, Antonio Aguado, "New model for the indirect determination of the tensile stress–strain curve of concrete by means of the Brazilian test," *Materials and Structures,* vol. 45, no. 10, pp. 1473-1485, 2012.

[191] Murdock JW, Kesler CE , "Effect of length to diameter ratio of specimen on the apparent compressive strength of concrete," *ASTM Bul,* pp. 68-73, 1957.

[192] M. A. Mansur, M. M. Islam, "Interpretation of concrete strength for nonstandard specimens," *Journal of Materials in Civil Engineering,* vol. 14, no. 2, pp. 151-155, 2002.

[193] Seong-Tae Yi, Eun-Ik Yang, Joong-Cheol Choi, " Effect of specimen sizes, specimen shapes, and placement directions on compressive strength of concrete," *Nuclear Engineering and Design,* vol. 236, no. 2, pp. 115-127, 2006.

[194] ACI Committee 306,, "ACI Committee 306,"Guide to cold weather concreting (306R-10)"," American Concrete Institute, 2010.

[195] Guohua Xing, Cheng Zhou, TaoWu, and Boquan Liu, "Experimental study on bond behavior between plain reinforcing bars and concrete," *Advances in Materials Science and Engineering,* vol. 2015, 2015.

[196] J. Cairns, K. Jones, "The splitting forces generated by bond," *Magazine of Concrete Research,* vol. 47, no. 171, pp. 153-165, 1995.

[197] G. A. Plizzari, M. A. Deldossi, S. Massimo, "Transverse reinforcement effects on anchored deformed bars," *Magazine of Concrete Research,* vol. 50, no. 2, pp.

161-177, 1998.

[198] Giovanni Metelli, Giovanni A. Plizzari, "Influence of the relative rib area on bond behaviour," *Magazine of Concrete Research,* vol. 66, no. 6, pp. 277-294, 2014.

[199] J. Cairns, R. Abdullah, "An evaluation of bond pullout tests and their relevance to structural performance," *The Structural Engineers,* vol. 73, no. 11, pp. 179-185, 1995.

[200] fib Model Code for concrete Structures 2010, Berlin, Germany: Ernst & Sohn, 2013.

[201] "BS EN 10080: Steel for the reinforcement of concrete. Weldable reinforcing steel-General. BSI, London," 2005.

[202] P.G. Gambarova,G.P. Rosati, B. Zasso,, "Steel-to-concrete bond after concrete splitting: test results," *Materials and Structures,* vol. 22, no. 35, pp. 347-356, 1989.

[203] Bappa Kumar Paul, Gopal Chandra Saha, Khokan Kumar Saha, Muhammad Harunur Rashid, "Effect of casting temperature on bond stress of reinforced concrete structure," *The Global Journal of Researches in Engineering,* vol. 13, no. 2-E, 2013.

[204] Christopher K Y Leung, Thanakorn Pheeraphan, "Microwave Curing of Portland Cement Concrete: experimental results and feasibility for practical applications," *Construction and Building Materials,* vol. 9, no. 2, pp. 67-73, 1995.

[205] I. Elkhadiri, M. Palacios, F. Puertas, "Effect of curing temperature on cement hydration," *Ceramics-Silikáty,* vol. 53, no. 2, pp. 65-75, 2009.

[206] Barbara Lothenbach, Frank Winnefeld, Corinne Alder, Erich Wieland, Peter Lunk, "Effect of temperature on the pore solution, microstructure and hydration products of Portland cement paste," *Cement and Concrete Research,* vol. 37, pp. 483-491, 2007.

[207] Benoît Bissonnette, Pascale Pierre, Michel Pigeon, "Influence of key parameters on drying shrinkage of cementitious materials," *Cement and Concrete Research,* vol. 29, no. 10, pp. 1655-1662, 1999.

[208] J. A. Hanson, "Prestress loss as affected by type of curing," *Journal of the American Concrete Institute ,* vol. 9, no. 2, pp. 69-93, 1964.

[209] T. Bakharev, J.G. Sanjayan, Y.-B. Cheng, "Effect of elevated temperature curing on properties of alkali-activated slag concrete," *Cement and Concrete Research,* vol. 29, pp. 1619-1625, 1999.

[210] How-Ji Chen, Chung-Hur Huang, Zhang-Yu Kao, "Experimental investigation on steel-concrete bond in lightweight and normal weight concrete," *Structural*

Engineering and Mechanics, vol. 17, no. 2, pp. 141-152, 2004.

[211] J. M. Osepchuk, "A history or microwave heating applications," *IEEE Transactions on microwave theory and techniques,* vol. 32, no. 9, pp. 1200-1224, 1984.

[212] J. B. Williams, The electronics revolution: Inventing the future, Chichester: Springer, 2017.

[213] P.Rattanadecho, "The simulation of microwave heating of wood using a rectangular wave guide: Influence of frequency and sample size," *Chemical Engineering Science,* vol. 61, no. 14, pp. 4798-4811, 2006.

[214] Darek Bogdal, Piotr Penczek, Jan Pielichowski, Aleksander Prociak, "Microwave assisted synthesis, crosslinking, and Processing of polymeric materials," in *Advances in Polymer Science* , vol. 163, 2003, pp. 51-58.

[215] K. C. Gary Ong, Ali. Akbarnezhad, Microwave-Assisted concrete technology Production, Demolition and Recycling, London: Taylor & Francis Group, 2015.

[216] R.V. Silva, J. de Brito, R.K. Dhir, "Properties and composition of recycled aggregates from construction and demolition waste suitable for concrete production," *Construction and Building Materials,* vol. 65, pp. 201-217, 2014.

[217] Eli Jerby, Yuri Nerovny, Yehuda Meir, Or Korin, Ron Peleg, and Yariv Shamir, "A silent microwave drill for deep holes in concrete," *IEEE Transactions on Microwave Theory and Techniques,* vol. PP, no. 99, pp. 1-8, 2017.

[218] A. Akbarnezhad, K. S. C. Kuang, K. C. G. Ong, "Temperature sensing in microwave heating of concrete using fibre Bragg grating sensors," *Magazine of Concrete Research,* vol. 63, no. 4, pp. 275-285, 2011.

[219] Dong Jianmiao,Long Shizong , "Effect of microwave processing on aluminate cement clinkering," *Journal of Wuhan University of Technology–Materials Science Edition,* vol. 20, no. 2, pp. 77-79, 2005.

[220] A. O. Morozov, O. A. Morozov, D. Z. Kalimullin, A. V. Prokopenko, V. P. Trebukh, "Research and development of installation for microwave heating of concrete before pouring into molds," in *Actual Problems of Electron Devices Engineering (APEDE),* 2016.

[221] Phadungsak Rattanadecho, Natt Makul, Aumpol Pichaicherd, Porncharoen Chanamai, Bunyong Rungroungdouyboon, "A novel rapid microwave-thermal process for accelerated curing of concrete: Prototype design, optimal process and experimental investigations," *Construction and Building Materials,* vol. 123, pp. 768-784, 2016.

[222] Lion Shahab, Jennifer A. McGowan, Jo Waller, Samuel G. Smith, "Prevalence of beliefs about actual and mythical causes of cancer and their association with

socio-demographic and health-related characteristics: Findings from a cross-sectional survey in England," *European Journal of Cancer,* vol. In Press, pp. 1-9, 2018.

[223] J. M. Elwood, "A critical review of epidemiologic studies of radiofrequency exposure and human cancers," *Environmental Health Perspectives,* vol. 1, pp. 155-168, 1999.

[224] "International Standard IEC 60519-6 - Safety in electroheat installations - Part 6: Specifications for safety in industrial microwave heating equipment," 2011.

[225] "Fraunhofer-Gesellschaft," Executing Institute: Fraunhofer Institute for Interfacial Engineering and Biotechnology IGB, [Online]. Available: http://www.igb.fraunhofer.de/en.html . [Accessed 24 April 2018].

[226] "E.R.S. Steuerungstechnik GmbH & Co. KG," [Online]. Available: http://www.ersgmbh.de . [Accessed 24 April 2018].

[227] N.J. Delatte, M.S. Williamson, D.W. Fowler, "Bond strength development with maturity of high-early-strength bonded concrete overlays," *Materials Journal,* vol. 97, no. 2, pp. 201-207, 2000.

[228] Dejian Shen, Xudong Wang, , Dabao Cheng, Jinyang Zhang, Guoqing Jiang, "Effect of internal curing with super absorbent polymers on autogenous shrinkage of concrete at early age," *Construction and Building Materials,* vol. 106, pp. 512-522, 2016.

[229] Ronaldo A. de Medeiros-Junior, Maryangela G. de Lima, Marcelo H. F. de Medeiros, "Service life of concrete structures considering the effects of temperature and relative humidity on chloride transport," *Environment, Development and Sustainability,* vol. 17, no. 5, pp. 1103-1119, 2015.

[230] N. Minorsky, "Directonal stablity of automatically steered bodies," *American Society of Naval Engineers* , vol. 34, no. 2, pp. 280-309, 1922.

[231] Karl Johan Aström, Richard M. Murray, Feedback Systems: An introduction for scientists and engineers, Princeton University Press, 2010.

12. Appendices

12.1 Appendix I: Cumulative intruded pore volume graphs of repair materials

12.1.1 Cumulative intruded pore volume graph of repair materials in Series I

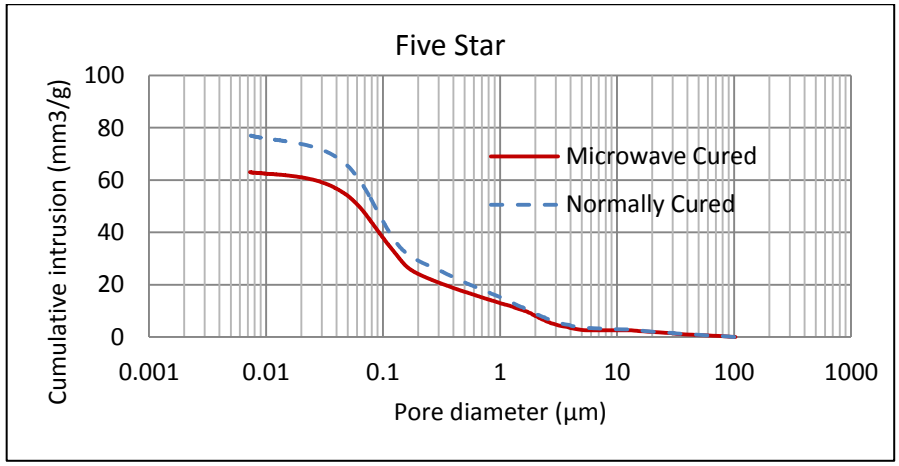

Figure 6.24: Cumulative intruded pore volume for Five Star repair material normal and microwave curing.

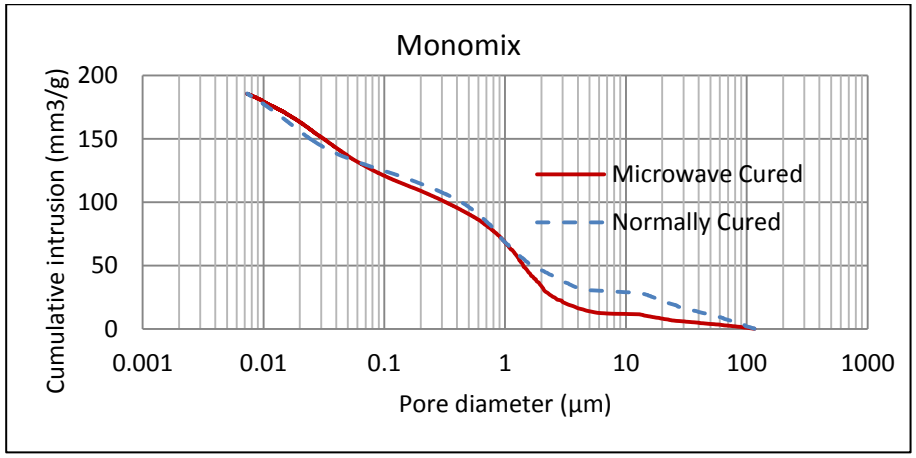

Figure 6.25: Cumulative intruded pore volume for Monomix material normal and microwave curing

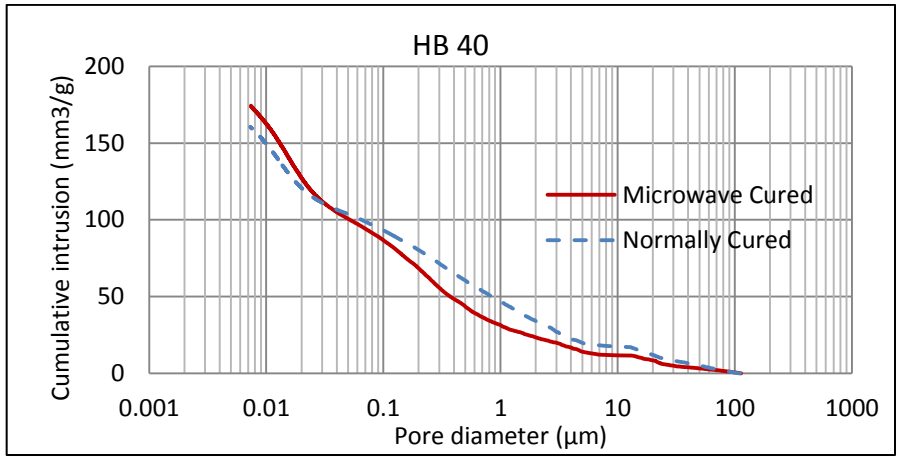

Figure 6.26: Cumulative intruded pore volume for HB 40 repair material normal and microwave curing.

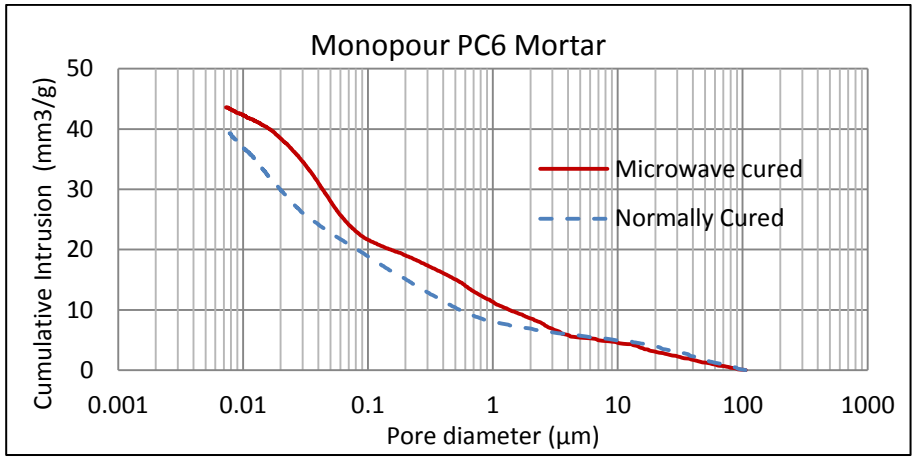

Figure 6.27: Cumulative intruded pore volume for Monopour PC6 Mortar normal and microwave curing.

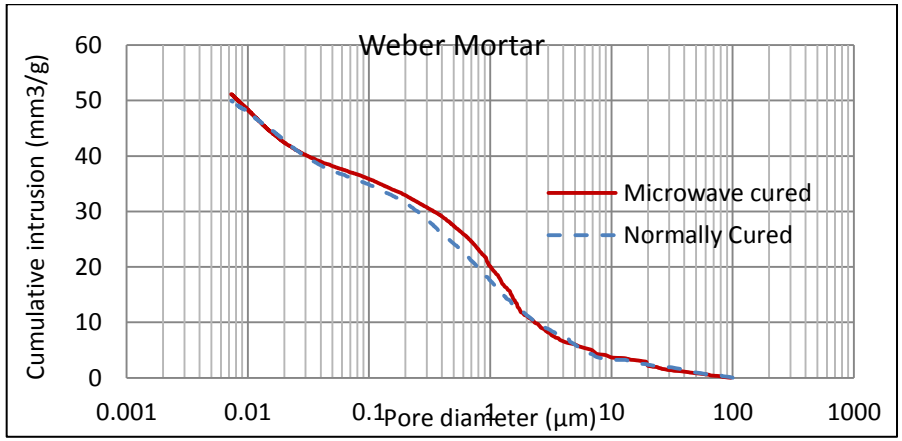

Figure 6.28: Cumulative intruded pore volume for Weber Mortar normal and microwave curing

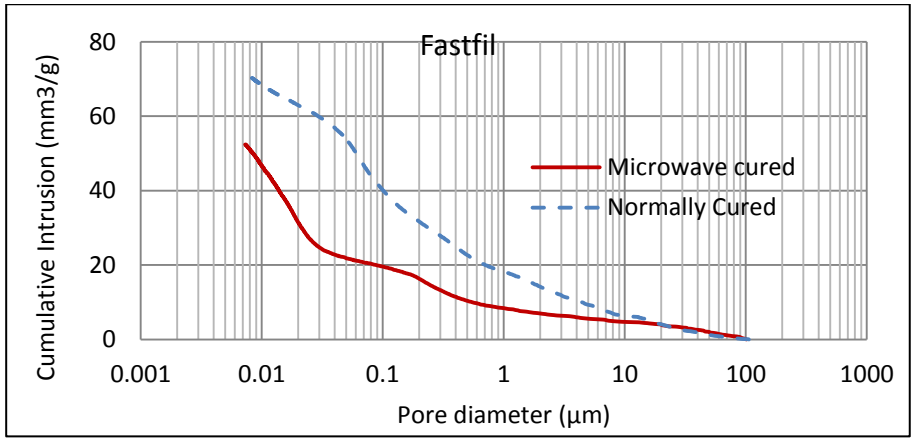

Figure 6.29: Cumulative intruded pore volume for Fastfill Mortar normal and microwave curing.

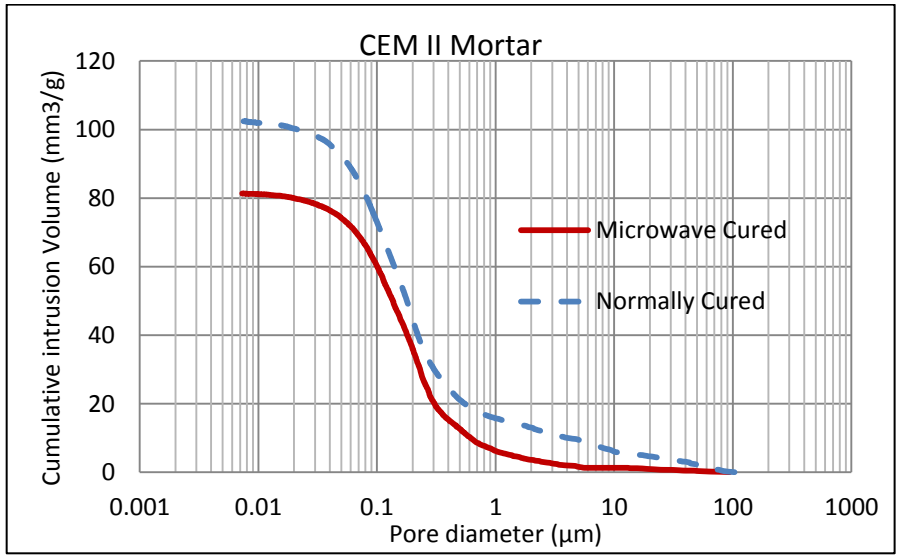

Figure 6.30: Cumulative intruded pore volume for CEM II Mortar normal and microwave curing.

12.1.2 Cumulative intruded pore volume graph of repair materials in Series II

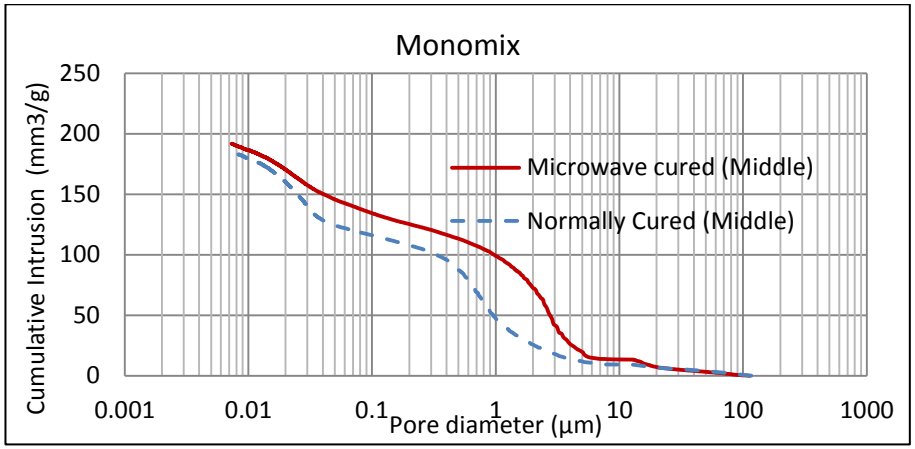

Figure 6.31: Cumulative intruded pore volume for normally and microwave cured Monomix taken from bulk

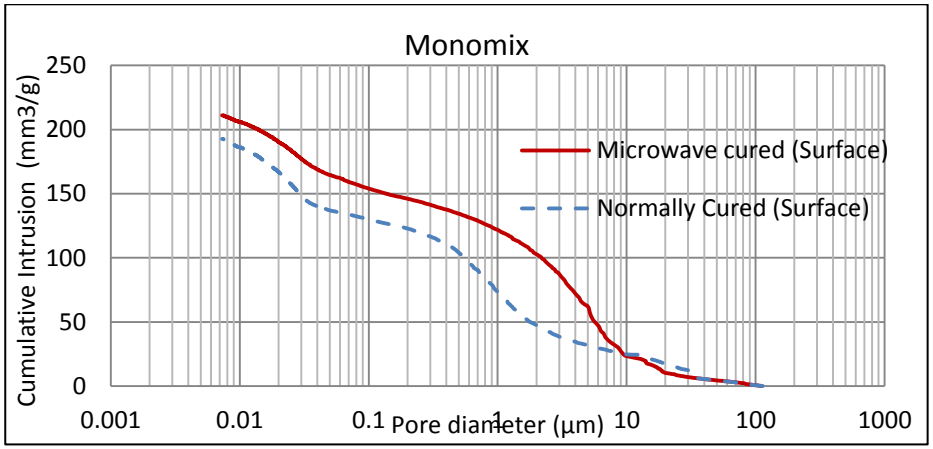

Figure 6.32: Cumulative intruded pore volume for normally and microwave cured Monomix taken from interface

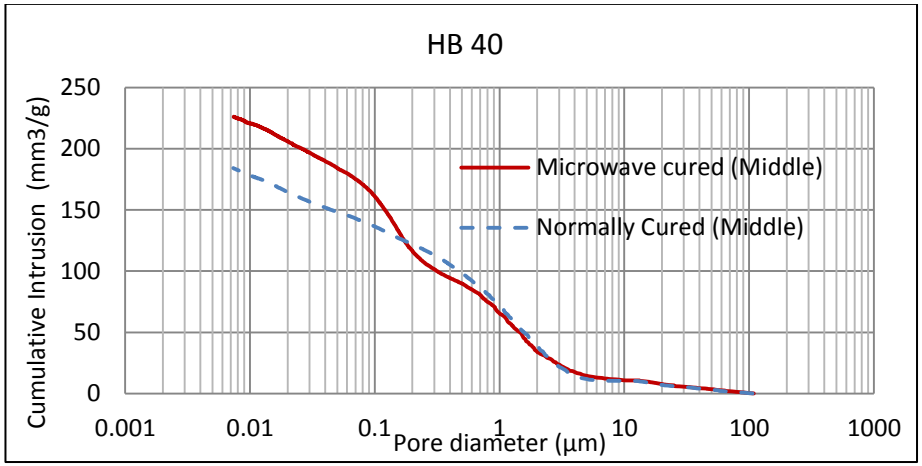

Figure 6.33: Cumulative intruded pore volume for normally and microwave cured HB40 taken from bulk

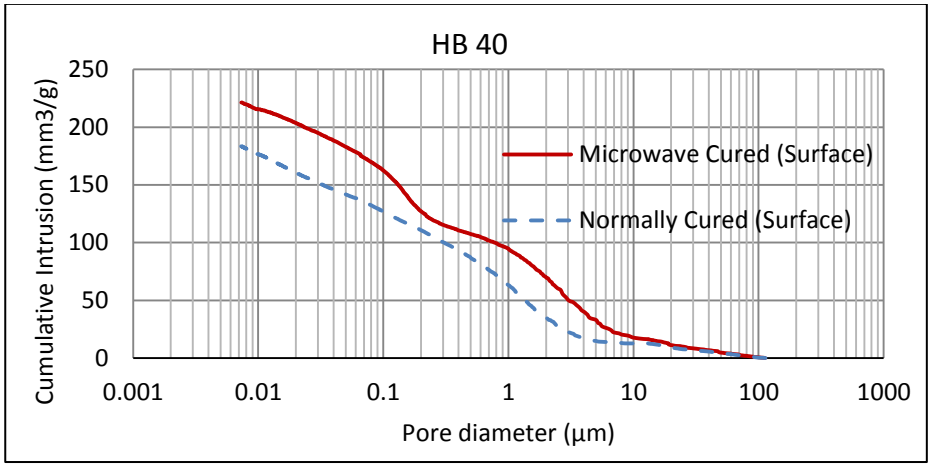

Figure 6.34: Cumulative intruded pore volume for normally and microwave cured HB40 taken from interface

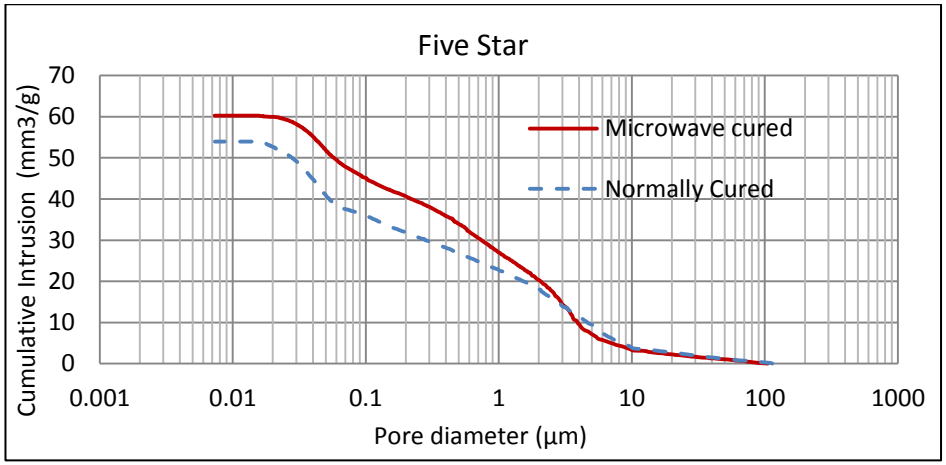

Figure 6.35: Cumulative intruded pore volume distribution curve for normally and microwave cured Five Star

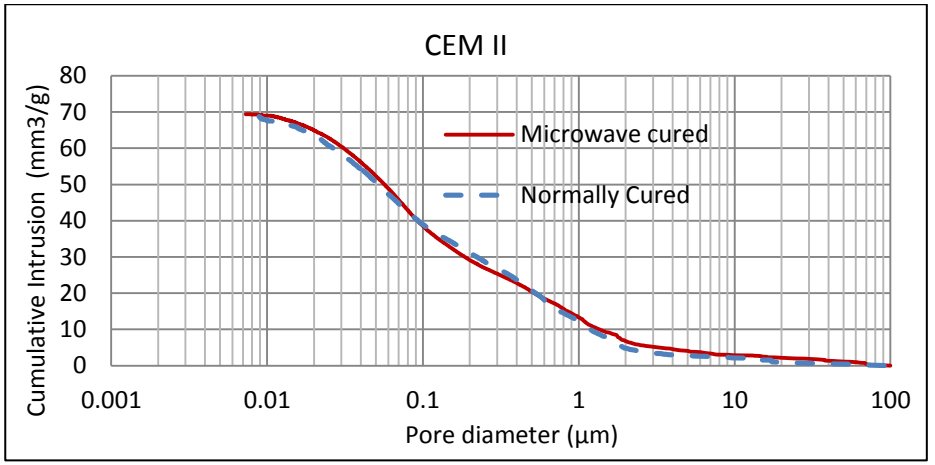

Figure 6.36: Cumulative intruded pore volume distribution curve for normally and microwave cured CEM II

12.2 Appendix II: Sequence of microwave curing with waveguide antenna under automated control mode

The surface area of the repair (slabs) is often larger relative to the size of the microwave antenna. Therefore, in order to cover the total surface of the repair, microwave antenna needs to move across the surface. Two methods can be used to microwave cure total surface of such slabs. Waveguide antenna can either continuously move across the slab surface or move step by step. In step by step movement pattern, antenna applies microwave energy while it is in a fixed position. After a certain time, it moves to the next position and applies microwave energy to the next position. In continuous movement pattern, the antenna applies microwave energy while it is moving with a constant velocity to cover the entire slab. For both methods, the total time of microwave curing is the same.

Assuming the repair slab is a rectangle with a surface area of n x m meter and the dimension of the antenna is a x b, the duration of the microwave curing to cover a total surface area of the slab can be calculated for both step by step and continuous movement pattern as follows:

12.2.1 Step by step movement pattern

Assume the microwave cured area (slab area) is a rectangle with length n and width m as shown in Figure 9. 29. The antenna is a rectangle with length a and width b.

The antenna starts by applying microwave energy to area 1 (unit area) for a specified time and then moves to area 2. The duration of each stop for each unit area is the same.

$$\text{The total number of unit areas for length n} = \frac{n}{a} \qquad (9.4)$$

The total number of unit areas for width m $= \frac{m}{b}$ (9.5)

The total number of unit areas for slab $\frac{n}{a} x \frac{m}{b}$ or $\frac{nm}{ab}$ (9.6)

Therefore, the antenna requires to apply microwave energy to the $\frac{nm}{ab}$ number of unit areas during microwave curing. (note: If $\frac{m}{b}$ or $\frac{m}{b}$ is a fraction, it needs to be rounded up to the full number as an approximation).

Now assume the total time required to cure the entire slab is t_t and the required time for each unit is t_i, therefore:

Total curing time = time required for each unit area x the number of unit area

$$t_t = t_i x \frac{nm}{ab}$$ (Equation 9.7)

$$t_i = t_t x \frac{ab}{nm}$$ (Equation 9.8)

Note: The values of *n* (length of slab), *m* (width of slab), *a* (length of the antenna), *b* (width of the antenna) and t_t (total time required to cure the slab) are known and only t_i (required time to cure each strip) is unknown.

This can be used to determine the time that required to cure each strip.

For larger slabs, each unit area needs to be heated rapidly to microwave cure the whole slabs whining 1 hour. To avoid rapid temperature increase, each unit can be heated in several passes of the antenna during the total microwave curing time. For instance, instead of curing each unit once for continuous 4 minutes, it can be cured in 2 cycles within the same total time. The unit area will be heated for 2 minutes in the first cycle

and for another 2 minutes in the second cycle. If the number of passes (cycles) is *D*, the time required for microwave curing each unit area during each pass is:

$$t_i = \frac{t_d}{D} \qquad (9.9)$$

Where t_d is the required time to complete *D* number of passes; t_i is the time required for each unit; *D* is the number of passes.

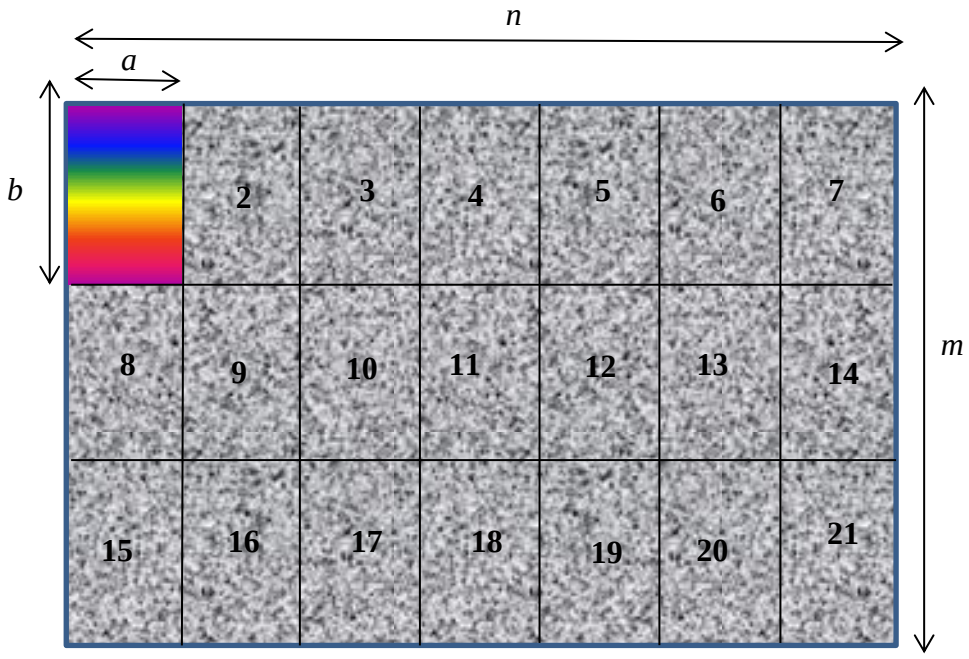

Figure 9. 29: Trial slab area cured with the microwave antenna in a fixed position (method 1)

12.2.2 Continuous movement pattern

Assume the microwave cured area (slab area) is a rectangle with length *n* and width *m* as shown in Figure 9. 30. The antenna is a rectangle box with a length of *a* and width *b*.

The antenna travels continuously across the width as shown in Figure 9. 30. For each trip across the width, the microwave antenna travels a distance *n* covering an area *na*. The number of trips of depth *b* by the antenna across the depth *m* the slabs is $\frac{m}{b}$. (Note: If $\frac{m}{b}$ is a fraction, it needs to be rounded up to the full number as an approximation).

Total distance traversed by the antenna = $\frac{nm}{ab}$ (9.10)

Velocity, V, of the antenna = distance traversed/curing time.

Hence:

$$V = (n\ \frac{m}{ab})/t \qquad (9.11)$$

$$V = \frac{n\ m}{abt} \qquad (9.12)$$

Where t = time of microwave curing

At the starting point, the antenna has already traversed a distance *a*. Therefore, the total distance traversed by the antenna is $(\frac{nm}{ab} - a)$ instead of $\frac{nm}{ab}$ as used in the above calculation therefore, actual velocity is:

$$\text{Velocity} = \frac{(\frac{n\ m}{ab} - a)}{T} \qquad (9.13)$$

If the microwave antenna only passes across the slab once, the temperature increase rate will be high. An alternative method, to lower the temperature increase rate, is to pass the antenna multiple times across the slab keeping the total exposure time the same in both cases. If the number of passes (cycles) is k, total distance traversed by the antenna is $k(\frac{nm}{ab} - a)$.

$$\text{Velocity} = k\ \frac{(\frac{n\ m}{ab} - a)}{T} \qquad (9.14)$$

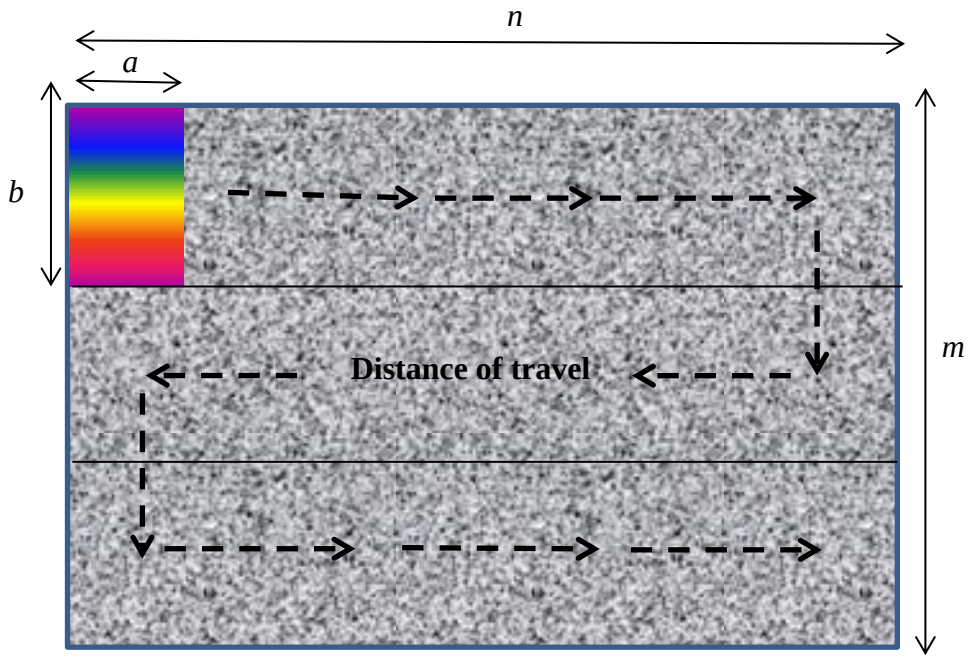

Figure 9. 30: Trial slab area cured with the moving microwave antenna

12.3 Appendix III: Top surface temperature of the slabs at the beginning and end of microwave curing

The following pictures show the slabs 1 to 10 and the thermal images taken at the beginning of microwave curing and also at the end of microwave curing.

Figure 9.31: Slab S1 at the end of microwave curing.

(a) (b)

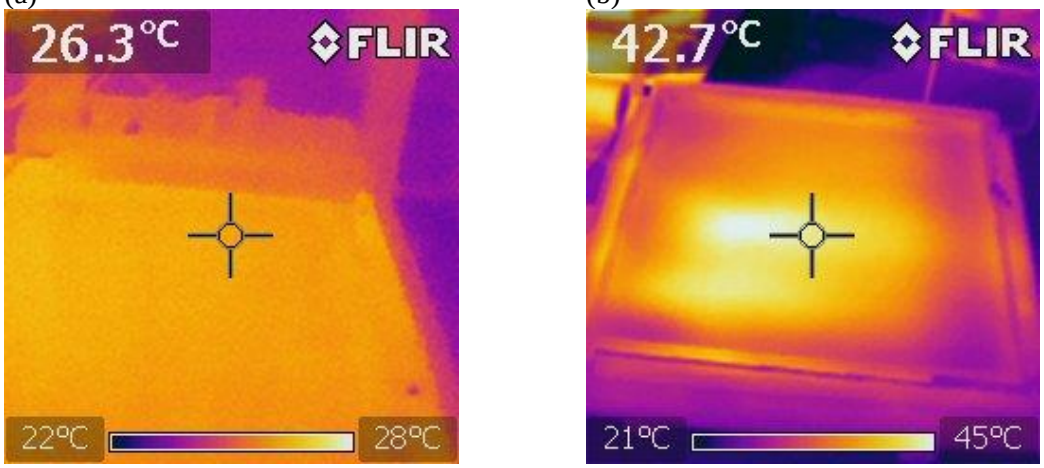

Figure 9.32: (a) Slab 1 temperature distribution before the start of microwave curing, and (b) at the end of microwave curing

Figure 9.33: Slab S2 at the end of microwave curing.

(a) (b)

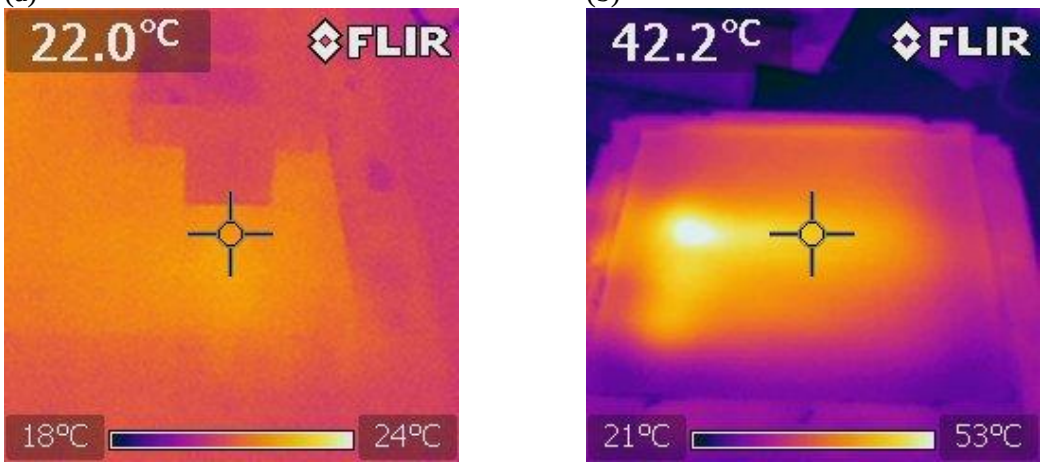

Figure 9.34: (a) Slab 2 temperature distribution before the start of microwave curing, and (b) at the end of microwave curing

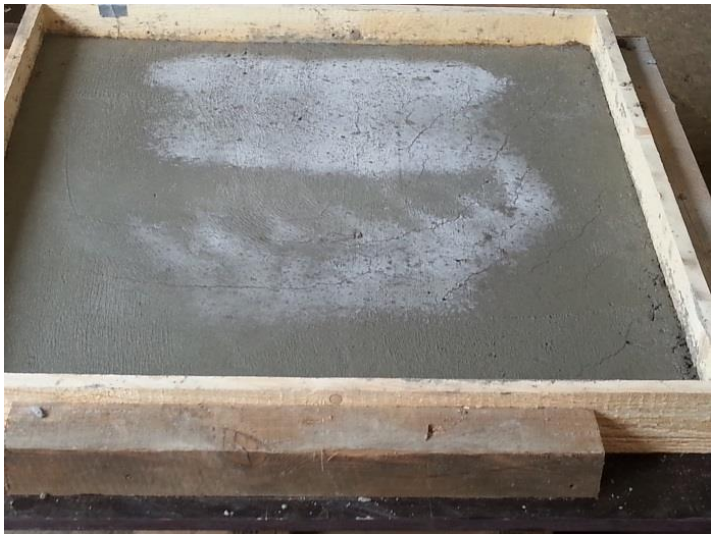

Figure 9.35: Slab S3 at the end of microwave curing.

(a) (b)

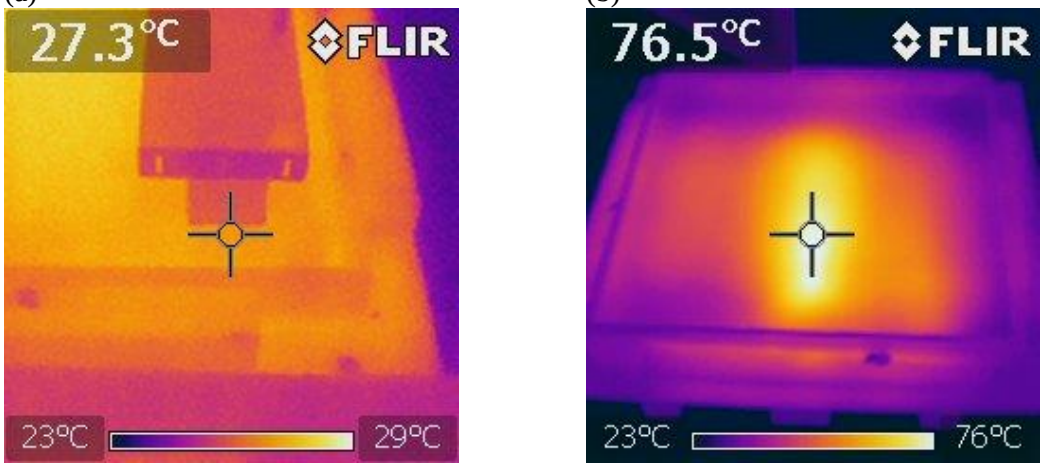

Figure 9.36: (a) Slab 3 temperature distribution before the start of microwave curing, and (b) at the end of microwave curing

Figure 9.37: Slab S4 at the end of microwave curing.

(b)

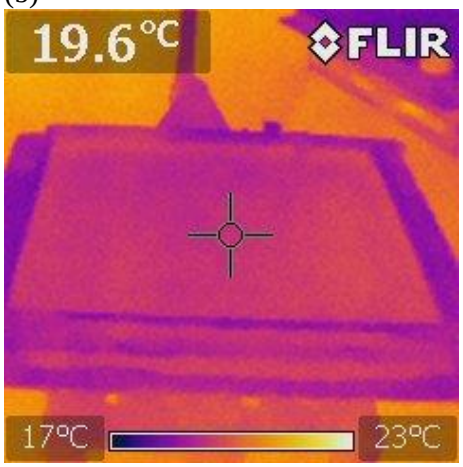

(b)

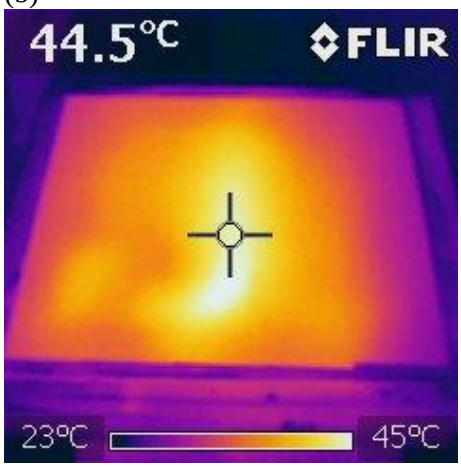

Figure 9.38: (a) Slab S4 temperature distribution before the start of microwave curing, and (b) at the end of microwave curing

Figure 9.39: Slab S5 at the end of two cycles of microwave curing.

(a) (b)

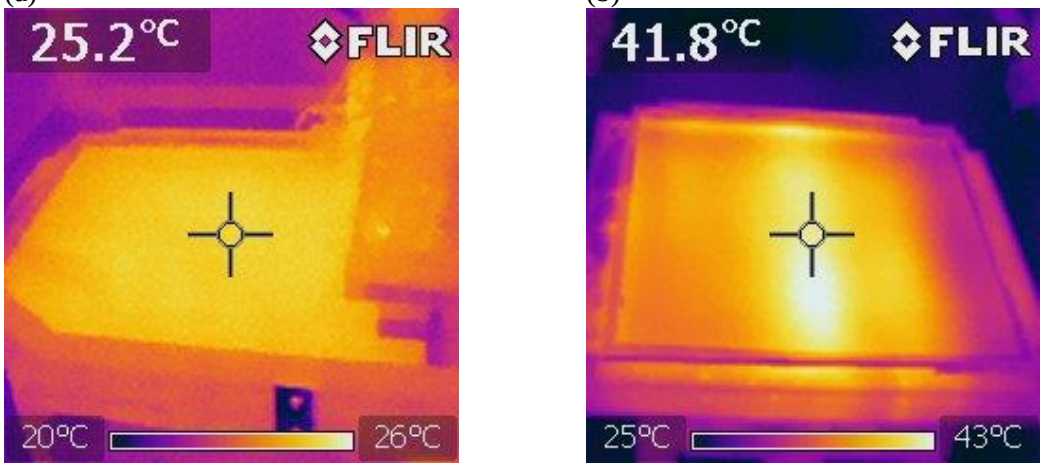

Figure 9.40: (a) Slab S5 temperature distribution before the start of microwave curing, and (b) at the end of two cycles (two passes) of microwave curing

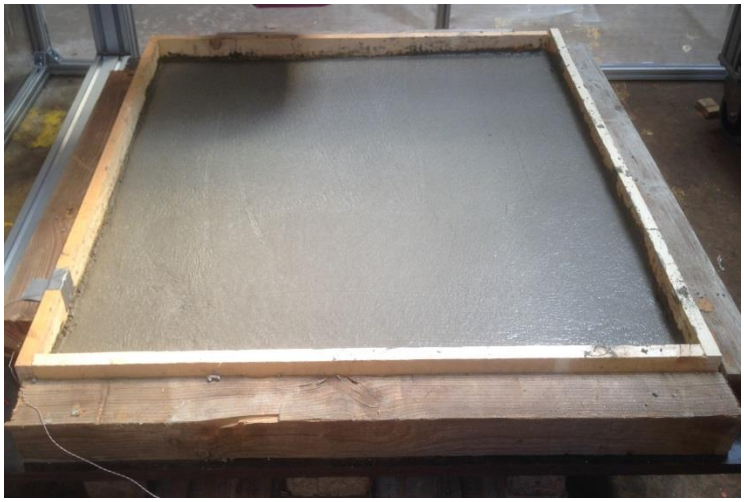

Figure 9.41: Slab S6 at the end of microwave curing.

(a) (b)

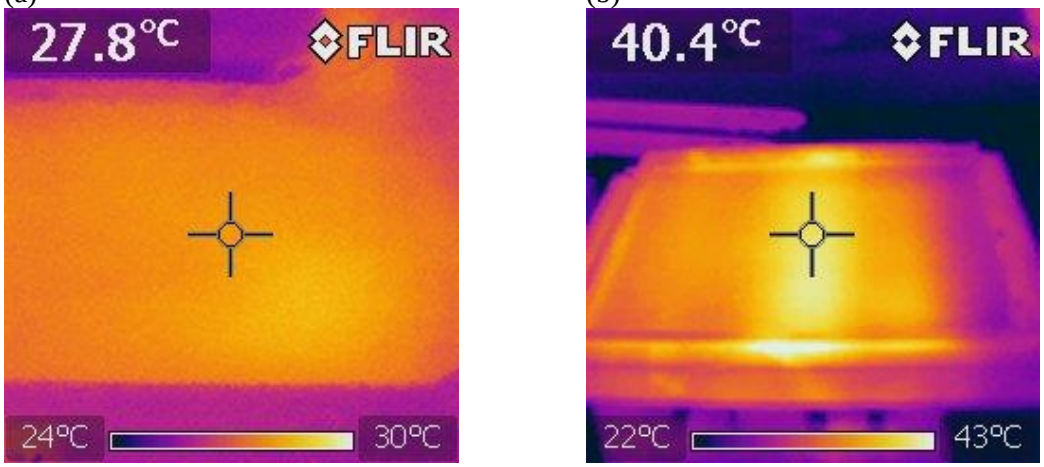

Figure 9.42: (a) Slab S6 temperature distribution before the start of microwave curing, and (b) at the end of microwave curing

Figure 9.43: Slab 7 at the end of microwave curing.

(a) (b)

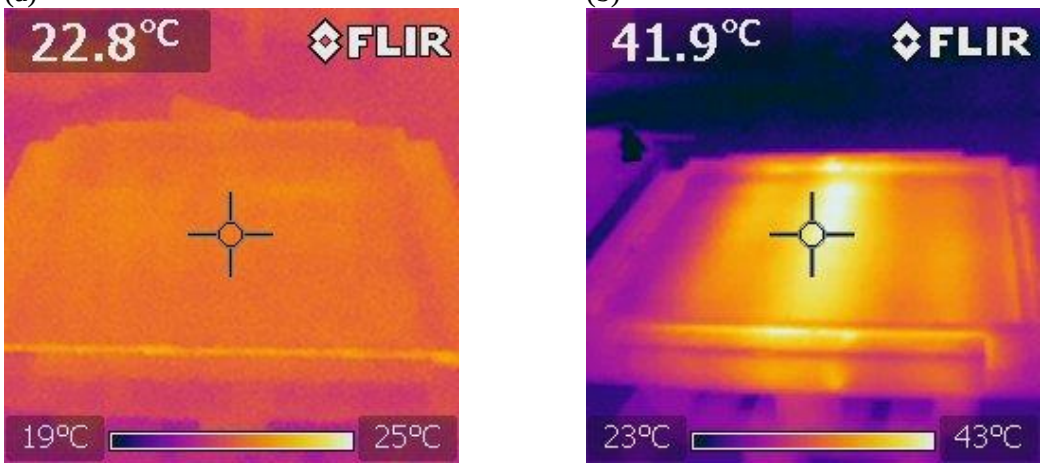

Figure 9.44: (a) Slab 7 temperature distribution before the start of microwave curing, and (b) at the end of microwave curing

Figure 9.45: Slab 8 at the end of microwave curing.

(a) (b)

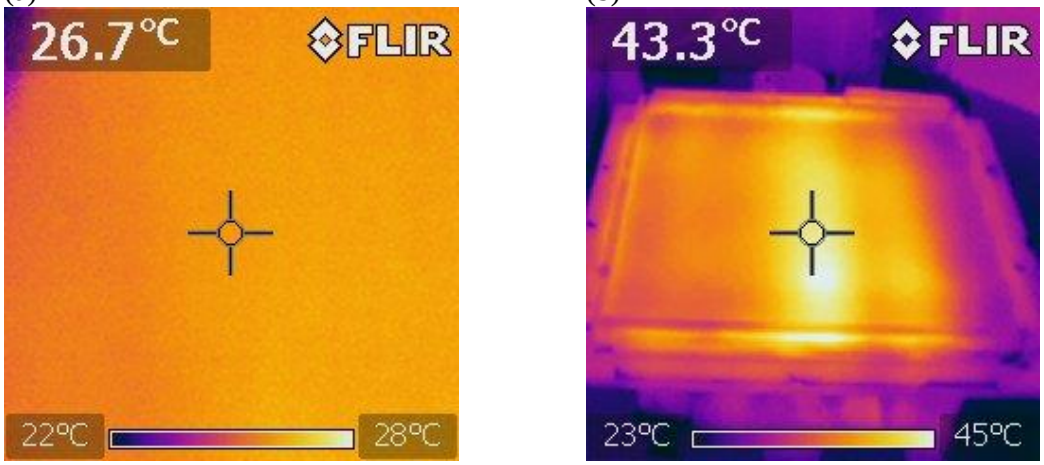

Figure 9.46: (a) Slab 8 temperature distribution before the start of microwave curing, and (b) at the end of microwave curing

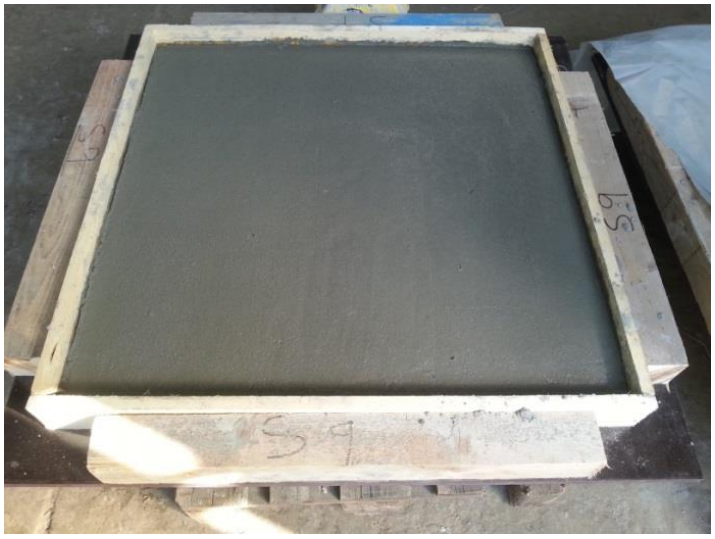

Figure 9.47: Slab S9 at the end of microwave curing.

(a) (b)

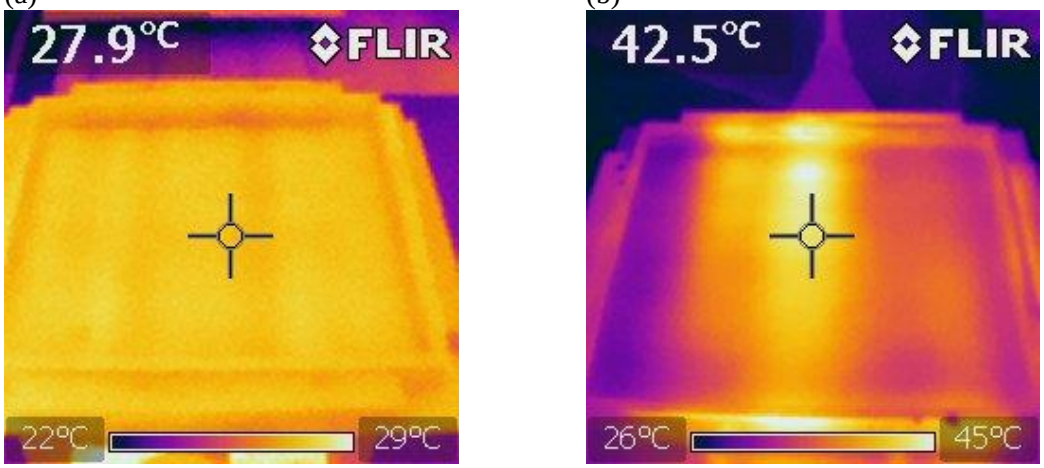

Figure 9.48: (a) Slab S9 temperature distribution before the start of microwave curing, and (b) at the end of microwave curing

Figure 9.49: Slab S10 at the end of microwave curing.

(a) (b)

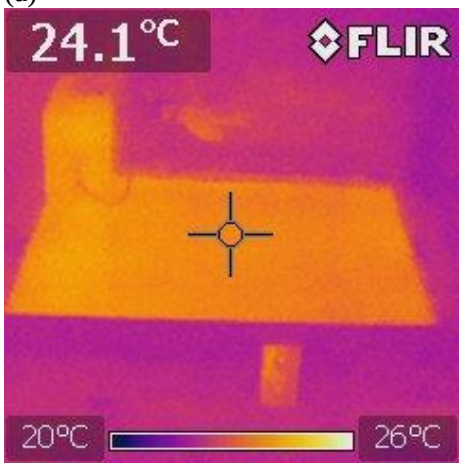

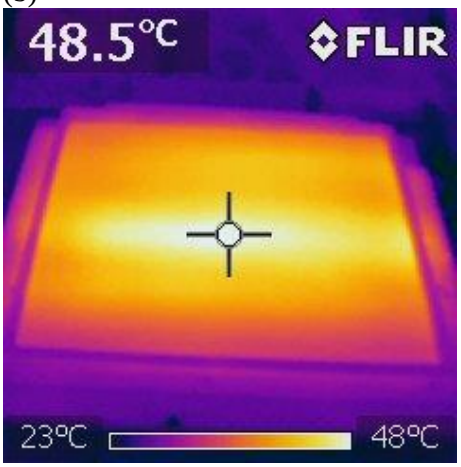

Figure 9.50: (a) Slab 10 temperature distribution before the start of microwave curing, and (b) at the end of microwave curing